Paolo Censi
Thomas H. Darrah
Yigal Erel *Editors*

Medical Geochemistry

Geological Materials and Health

Springer

Medical Geochemistry

Paolo Censi • Thomas H. Darrah • Yigal Erel
Editors

Medical Geochemistry

Geological Materials and Health

Springer

Editors
Paolo Censi
Department of Earth and Marine Sciences
University of Palermo
Palermo, Italy

Yigal Erel
Institute of Earth Sciences
The Hebrew University
Jerusalem, Israel

Thomas H. Darrah
Division of Earth and Ocean Sciences
Nicholas School of the Environment
Duke University
Durham, NC, USA

ISBN 978-94-007-4371-7 ISBN 978-94-007-4372-4 (eBook)
DOI 10.1007/978-94-007-4372-4
Springer Dordrecht Heidelberg New York London

Library of Congress Control Number: 2013932871

Printed on acid-free paper

Springer is part of Springer Science+Business Media (www.springer.com)

Preface

According to Goldschmidt, Geochemistry describes elemental distributions in geochemical spheres, assessing their abundances and rules driving element fractionations therein. Since dawn of civilization and more so since the Industrial Revolution, at the same time, the development of analytical techniques allow us to exposures can significant human health, especially interactions between solids (or products coming from their dissolutions) and different interfaces within the human body (respiratory, gastrointestinal, skin). These phenomena the recognition of this role. This solid-liquid processes between geogenic materials, dust or soils, and the human body in order to explain to the medical community. These contributed to the recognition of mechanisms responsible for several health maladies, the growth of a new geochemical branch, Medical Geochemistry.

This book is provided for students and researchers (chemists, geologists, geochemists, environmental scientists) Medical Geochemistry. The chapters in this lectures that the authors the Summer School on Medical Geochemistry at the Institute of the Coastal Marine Environment of Italian National Research Council (IAMC-CNR) in Capo Granitola (Italy) the University of Palermo and CNR with the aid of Regione Sicilia and contributions of Thermo Scientific and Bruker Corporation Italia.

Related to the human exposure interactions with geogenic solids, the structure of this book is based on eight chapters regarding the inhalation of suspended solids and their dissolution in contact with lung fluids; effects of the biological, geographical, dietary, and environmental exposure histories on the compositions of human bones; the origin of source materials of potentially inhaled atmospheric dust; biological effects on crystallization of newly formed minerals; mineralogical techniques exploited to investigate newly formed biominerals under physiological conditions; and trace element accumulations in hairs as a consequence of the human environmental exposure, rigorous assessment of the applied to data.

University of Palermo, Palermo, Italy — Paolo Censi
Duke University, Durham, USA — Thomas H. Darrah
The Hebrew University of Jerusalem, Jerusalem, Israel — Yigal Erel

Contents

Chapter 1
Using the Trace Element Contents in Bronchoalveolar Lavages to Probe the Human Exposure to Inhaled Particulates

Paolo Censi, E. Tamburo, L.A. Randazzo, Pierpaolo Zuddas, Angela Cuttitta, and Thomas H. Darrah

Abstract Explosive volcanic eruptions eject large volumes of high surface area, metal-rich dust and ash into the atmosphere. In areas near major volcanic eruptions, humans often interact with these materials and may bioaccumulate heavy and toxic metals. To evaluate these interactions, we examine bronchoalveolar lavage samples (BAL) collected from people exposed to the paroxysmal 2001 Etna eruption. BAL samples reveal a strong enrichment of many toxic heavy metals and the capacity for trace elements released from inhaled particles to induce crystallisation of phosphatic microcryst biominerals in intraaveolar spaces. BAL rare earth element (REE) concentration patterns normalised to shale reveal a 'V-shaped' feature caused by the depletion of elements from Nd to Tb (mid-REEs) as compared to the variable enrichments of heavy lanthanides, Y, La and Ce. This pattern is consistent with

P. Censi (✉)
Department of Earth and Marine Sciences, University of Palermo, Palermo, Italy

I.A.M.C. Consiglio Nazionale delle Ricerche, U.O.S. Capo Granitola, Via del Mare, 3, 91021 Torretta Granitola, Campobello di Mazara, Italy
e-mail: paolo.censi@unipa.it

E. Tamburo • L.A. Randazzo
Dipartimento D.I.S.T.E.M., Università di Palermo, via Archirafi, 36, 90123 Palermo, Italy

P. Zuddas
Paris-Sorbonne Institut des Sciences de la Terre de Paris 4, Université Pierre et Marie Curie, Place Jussieu Tour 46-00 (2étage), F75252 Paris Cédex05, France
e-mail: pierpaolo.zuddas@upmc.fr

A. Cuttitta
I.A.M.C. Consiglio Nazionale delle Ricerche, U.O.S. Capo Granitola, Via del Mare, 3, 91021 Torretta Granitola, Campobello di Mazara, Italy

T.H. Darrah
Division of Earth and Ocean Sciences, Nicholas School of the Environment, Duke University, 207A Old Chemistry Building, Box 90227, Durham, NC 27708, USA
e-mail: thomas.darrah@duke.edu

P. Censi et al. (eds.), *Medical Geochemistry: Geological Materials and Health*, DOI 10.1007/978-94-007-4372-4_1,

solutions that experience phosphate mineral crystallisation in laboratory conditions and suggests that phosphate precipitation occurs *in vivo* in the lungs through interactions between volcanic particles and lung fluids. The BAL trace element patterns allow us to reconstruct the source of inhaled materials and depict the fluid-mineral processes that occur between lung fluids and inhaled particles.

1.1 Introduction

The interaction between aquifer rocks and geological fluids (i.e., groundwaters) shapes the geochemical composition of the Earth's hydrosphere (Chapelle 2003), whereas fallout of atmospheric particulates strongly influences the chemistry of shallow seawater layers, specifically in coastal areas and epicontinental basins. Understanding the nature of these solid-liquid (i.e., water-rock) processes is a primary interest in the field of Geochemistry (Albarede 1995). The nature of solid-liquid interactions is investigated in the field and laboratory by geochemical analyses of the dissolved (aqueous) phases, residual 'weathered' solids or on newly formed mineral species (Tamburo et al. 2011 and references therein). These processes are also studied in the laboratory by simulating natural conditions in order to depict simplified features of the natural environment (Bowser and Jones 2002). Additionally, geochemical modelling of detailed analytical geochemical data of dissolved media and kinetic and thermodynamic parameters evaluates the physico-chemical processes that occur at the solid-liquid interface (see Merkel and Planer-Friedrich 2008 for a comprehensive review).

Explosive volcanic eruptions eject large volumes of high surface area, metal-rich dust and ash into the atmosphere, often subjecting nearby residents to potentially hazardous volcanic materials (including heavy metals). Despite the prevalence of this avenue of exposure to volcanic materials (e.g., Cuoco et al. 2012) and an extensive body of geochemical investigations on water-rock interaction processes described above, there is a limited amount of qualitative or quantitative data that evaluates how solid-liquid interactions occur *in vivo*. This paucity of data on the mineral-biofluid interactions that occur after the inhalation of atmospheric dust precludes an accurate risk assessment. A limited number of studies explore the chemical dissolution of atmospheric dust in presence of human bronchial fluids (e.g., Takaya et al. 2006; Forde et al. 2008; Dias Da Cunha et al. 2009), while the majority of prior work focuses on prominent examples including precursors of silicosis, asbestosis and cancers (e.g., Schuhmann et al. 2011; Leung et al. 2012 and references therein). An understanding of the basic mechanisms of mineral-biofluid interactions that occur in lung fluids is required to evaluate the potential health impacts related to the acute exposure and inhalation of atmospheric particulates and the physical mechanism by which they induce health maladies. To address these concerns, we evaluate these interactions by investigating the trace element composition of bronchoalveolar lavage samples (BAL) collected from people exposed to the paroxysmal 2001 Etna eruption.

The analysis of trace element geochemistry is routinely used in the geological sciences to investigate many processes including solid-liquid interactions. Similarly, trace element geochemistry is increasingly used to investigate the source of materials that form biominerals and the processes associated with biomineralisation (e.g., Censi et al. 2011a, b; Darrah 2009; Darrah et al. 2009; Hoogewerff 2008). Therefore, we suggest that the analysis of trace element geochemistry may allow us to evaluate the relationship between atmospheric particulate composition and the chemistry of pulmonary fluids (Censi et al. 2011a, b).

Because volcanic ash and dust have extremely high surface areas, they often adsorb high concentrations of metallic ions, including heavy metals, on their surfaces. If inhaled, these metals can release trace metals into biological fluids constituting significant sources of toxic metals *in vivo* (Hirano and Suzuki 1996; Yoon et al. 2005). The dose of toxic metals depends on (a) the flux of volcanic material that is inhaled and (b) the 'leachability' (or extractability) of metals that were adsorbed onto the surfaces of inhaled solids. Thus, bioavailability and potential toxicity depend on the geochemical composition and mineralogical nature of inhaled materials (Newman 2001; Sipes and Badger 2001; Hedberg et al. 2010) and the ambient geochemical conditions of biofluids (e.g., pH, Eh, temperature). At present, information about the potential impacts of volcanic particulate exposure on the pulmonary system is limited to select minor and trace elements and mineral phases (e.g., crystallisation of phosphate biominerals in lung tissues) (Hirano and Suzuki 1996; Pracyk et al. 1996; Yoon et al. 2005).

We attempt to investigate solid-fluid interactions that occur following inhalation of volcanic debris by evaluating the chemistry of volcanic particulates and BAL following a major pyroclastic eruption of volcanic ash (likely the most complex scenario for the potential mixtures of inhalable and respirable suspended particles) at Mount Etna (the largest European volcano) in July to August 2001. In order to accurately assess these factors, a suitable geochemical study that can distinguish between numerous sources of atmospheric particles must be developed. This factor is specifically difficult in urban areas (such as the present study), because the composition of respirable atmospheric particulates consists of a complex mixture of several source materials (including anthropogenic contributions). The complexity of this mixture drastically increases with increasing industrialisation and population density. Therefore, in populated industrial areas, the addition of anthropogenic components can obscure the contributions from natural materials even during times of major geological activity (i.e., volcanic eruption) (Kulkarni et al. 2007; Moreno et al. 2008; Cuoco et al. 2012) requiring the application of advanced geochemical approaches.

Herein, we investigate how the respiration of particles from atmospheric fall-out affects the composition of *sensu lato* pulmonary fluids using trace element geochemistry of bronchoalveolar lavages (BAL). Patients included residents of Catania who were treated at the University of Catania Hospital following acute exposure to the 2001 Mt. Etna eruptive materials in addition to prolonged subacute exposure to materials from local Catania anthropogenic activities. Previous work suggests that atmospheric particulates dissolve in simulated lung fluids (Luoto

et al. 1998; Forde et al. 2008; Dias Da Cunha et al. 2009). Similarly, our previous work evaluates the kinetics of trace element release and suggests that release from freshly erupted volcanic ashes begins within a few hours after deposition within a saline medium (Censi et al. 2007, 2010; Randazzo et al. 2012). Therefore, BAL solutions are potentially a representative model for trace element leaching of inhaled particles within bronchial pathways that can be interrogated using trace element geochemical approaches. We model the solid-liquid interactions that occur in the pulmonary system in an analogous fashion to simple water-rock interactions in groundwater hydrogeology. The current work focuses on the dissolved concentration of lanthanide (i.e., often termed rare earth elements) series elements and yttrium (hereafter named REE). Using these elements, we develop a systematic approach towards evaluating enrichment factors of REE in BAL to assess the processes of biomineralisation in the bronchial pathways. Evaluating this data allows us to determine (a) the fate of inhaled solids, (b) the processes leading to trace element leaching in the lungs, (c) the origin (i.e., anthropogenic vs. volcanic) of materials that interact in the lungs, and (d) the biomineralisation of phosphate minerals in the lungs.

1.2 Composition of Volcanic Materials

In addition to the naturally occurring atmospheric particles and anthropogenic contributions, the eruption of Mt. Etna led to the deposition of about 0.39 kg m^{-2} of ash between 21 and 24 July 2001 that continued until August (Scollo et al. 2007). The volcanic ash consists of a mixture of glass, aphanitic minerals and rock fragments. An extensive evaluation of the ash composition is available in Censi et al. (2010) and Randazzo et al. (2012).

In general, both optical and microscopic observations indicate that the majority of ejected material (∼70% by volume) consists of aphanitic volcanic glass. Optical and electron microscopy indicate that the remaining 30% include phenocrysts of olivine, clinopyroxene, spinel and plagioclase with a porphyritic texture. Additionally, we confirm the minor occurrence of green augite, Mg-rich olivine and Ti-rich magnetite phenocrysts. Glass fragments often show corroded surface textures (Fig. 1.1), which result from their interaction with volcanic fluids inside the plume during eruption. Scanning electron microscopy (SEM) observations reveal the presence of coated dust materials on grain surfaces with encrusting and deliquescent features, which confirm the occurrence of ash-leachate fraction consisting of sublimates of acids, metal salts and adsorbed fluids formed as a consequence of interactions between ash grains and volcanic fluids (Oskarsson 1980). Therefore, after inhalation of atmospheric particles, trace elements can be released from a soluble ash fraction (SAF), independent from breakdown of the solid (glassy and crystalline) fraction.

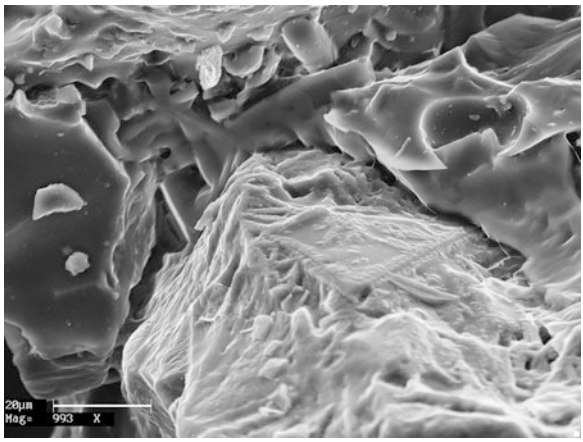

Fig. 1.1 SEM image illustrating the features of glass grains from erupted volcanic ash 'corroded' by reaction with plume fluids

1.3 Methodology

Bronchoalveolar lavage (BAL) samples were collected from six patients who underwent treatment in the Internal and Specialist Medicine Department of the University of Catania following the 2001 the pyroclastic eruption of Mount Etna between 19 July and 6 August 2001. All samples were collected immediately after admission following informed written consent. BAL collections were conducted according to standard procedures detailed previously in Censi et al. (2011a). All selected patients were residents of the city of Catania (Sicily).

BAL samples were obtained by instilling four 30 ml lavages of sterile solution consisting of 0.9% w/v NaCl, using a fibrobronchoscope (Bargagli et al. 2005). Each aliquot was immediately and gently aspirated. From each 20 ml lavage sample, only 10 ml was required for chemical investigations. After filtration through a 0.22 µm Nalgene™ membrane, each BAL sample was treated with 15 ml H_2O_2, 5 ml 30% nitric acid (HNO_3) solution, 30% hydrochloric (HCl) acid solution and 100 mg of solid NH_4F in a sealed, acid-washed reaction vessel. This was heated in a microwave oven (MARS 5™, CEM Corporation, UK) at 3×10^5 Pa and 200 °C for 30 min. Excess acid was removed to incipient dryness using a CEM MicroVap™ apparatus, and residual solution was rinsed with a 5% v/v of nitric acid solution to attain final solution volumes of 20 ml. Sample solutions were finally transferred to previously cleaned polycarbonate vials. The samples were treated under a clean laminar airflow to minimise potential contamination risks.

Trace element analyses were carried out using a sector field SF-ICP-MS Thermo Fisher Element 2 by external calibration approaches according to Censi et al. (2011a). The calibration for each element was based on seven standard solutions at known concentrations prepared by diluting 1 g/l of a single-element solution (Merck ICP standard), similar to the procedures used previously (Rodushkin and

Odman 2001; Darrah et al. 2009). Accuracy and precision for each investigated element was evaluated by analysing both standard reference materials (CASS-4 and NASS-5 from National Research Council of Canada; Ottawa, Ontario, Canada) and procedural blanks obtained from sterile BAL solution under analogous sample preparation conditions. The latter approach produces critical values (L_C) and detection limits (L_D) for used methods. More detailed information about analytical methods used to determine investigated elements and validations of carried out analyses are reported in Censi et al. (2011a, b).

1.4 Results

The magnitude of Etna's eruption during July–August 2001 was sufficient to expose all inhabitants of south-eastern Sicily to volcanic particles. Thus, although a comparative study of BAL composition between exposed people and control subjects outside of the area would be preferable, it was not possible. Therefore, the results of minor and trace element compositions in the BAL samples of people exposed to volcanic particle inhalation were compared with the few minor and trace element analyses carried out for BAL lavage samples in other studies (Baxter et al. 1999).

The amounts of minor and trace elements measured in this study range between 0.2 μg/L for uranium (U) and 229.36 mg/L for aluminium (Al). The latter (Al), together with iron (Fe), is the most abundant of the elements analysed in BAL solutions. REE cumulative concentrations span a range from 56.9 to 165.4 $\mu g\ l^{-1}$ (ppb). The relative abundances of the different REE were similar, with Y and light REE (LREE), La, Ce and Pr as the most abundant elements.

1.4.1 Thermodynamic Modelling

Low-temperature mineral reactions in equilibrium with aqueous media in subsurface environments can be investigated with geochemical modelling based on a knowledge of the compositions of interacting fluids and the thermodynamic conditions of the system. This approach was applied to a hypothetical fluid interacting with particles of volcanic ash under physiological conditions (pH = 7.4; $T = 37°C$). Starting composition of this simulated bronchial fluid (SBF) was consistent with Wood et al. (2006). When SBF interacted with freshly erupted volcanic particles in the lungs, it immediately dissolved the soluble ash fraction before interactions with glass and mineral ash fractions could occur. Therefore, SBF began to react with volcanic glass and minerals after dissolution of the soluble ash component. This process was simulated with the aid of the EQ3/6, version 7.2b, software package (Wolery 1979, 1992; Wolery and Daveler 1992) using the LLNL thermodynamic database from the Lawrence Livermore National Laboratory. The EQ3/6 algorithm

models the chemical evolution of geochemical systems using thermodynamic and kinetic constraints. In order to accurately model the release of major, minor and trace elements in a lung system consistent with water-rock interactions, the double solid reactant method (DSRM) was adopted according to Accornero and Marini (2008). In DSRM, each dissolving solid phase is considered as a double solid reactant, consisting of a pure mineral or a solid mixture (the solid reactant) and another reactant, defined as the special reactant according to EQ6 nomenclature. Thermodynamic and kinetic properties of the solid reactant are enclosed in the geochemical database and determine analogous properties (i.e., equilibrium constant of the hydrolysis reaction), whereas the same features are unknown for the special reactant. The saturation state of the aqueous solution with respect to the solid reactant is calculated during the progressive dissolution of rocks until solution saturation is attained. The speciation model for the investigated system can be carried out using a kinetic approach based on the transitional state theory (Eyring 1935a, b) using the EQ3NR computer code, taking into account the dissolution of basaltic glass particles in contact with lung fluids according to the reaction

$$SiAl_{0.36}O_2(OH)_{1.08} + 0.36H_2O \Leftrightarrow SiO_2 + 0.36Al(OH)_4^- + 0.36H^+ \qquad (1.1)$$

Thermodynamic properties were estimated from the stoichiometrically weighted sum of hydrolysis reactions for amorphous silica and gibbsite. They were recomputed using the temperature-pressure grid required by software package EQ3/6 and included in the thermodynamic database. The kinetic parameters used during model calculations are related to the Gislason and Oelkers (2003) estimations. Geometrical surface area was calculated assuming a spherical grain shape (with radius equal to 0.3 μm) with intra-grain porosity equal to 0.3. Trace element concentrations were used to define a special reactant associated with hydrated basaltic glass in DSRM. Model calculations were performed under open-system conditions (assuming the system is in contact with a large external gas reservoir) at 37 °C. The reaction path modelling leads to the crystallisation of several secondary minerals in agreement with physico-chemical conditions that occur during the alteration of a basaltic glass mixture assuming an instantaneous equilibrium between these minerals and lung fluids (Censi et al. 2011a). These results imply that REE co-precipitation with phosphates could be reached starting from an initial composition of lung fluids similar to the Gamble's solution, with 126 mg l^{-1} of dissolved phosphate (Midander et al. 2007). This possibility agrees with results reported by Wood et al. (2006) that recognise phosphates as newly formed solids in simulated lung fluids.

1.4.2 REE Behaviour as Geochemical Tool

The shale-normalised REE patterns found in BALs differ from those observed in the solid components of volcanic ejecta (Fig. 1.2). As a result, it is unlikely that the wide range of cumulative REE contents is caused by the presence of residual

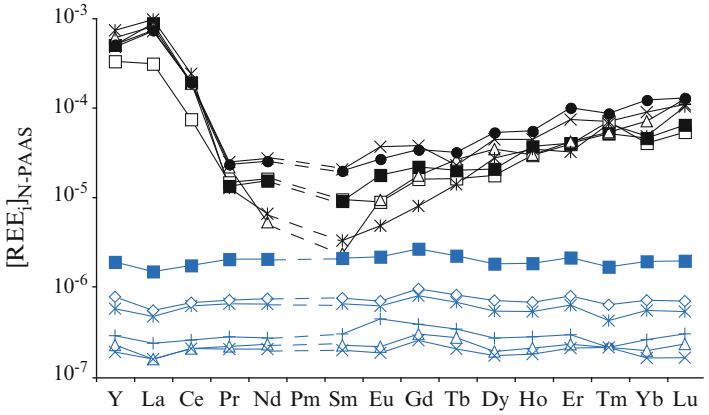

Fig. 1.2 Shale-normalised REE concentrations observed in BAL fluids (*black symbols*) compared with concentrations measured by Aiuppa et al. (2003) in soluble ash fractions ejected from Etna between 19 July and 6 August 2001 (*blue symbols*)

undissolved inhaled volcanic particles (<6.4 μm) that were mechanically removed from bronchial tissues during BAL lavages. Instead, REE patterns in BAL are characterised by LREE enrichment and intermediate REE (MREE) depletion that evolves towards a progressive increase of normalised REE concentrations along the series (i.e., V-shaped pattern). These features are very similar to those recognised in solutions that experience REE-phosphate co-precipitation (Byrne et al. 1996) and are related to the elemental fractionations that occur when phosphates precipitate from REE-bearing solutions. These results are consistent with experimental investigations that show that the removal of dissolved REE concentrations from aqueous media is controlled by co-precipitation of these elements with phosphates (Byrne and Kim 1993). REE fractionation in the dissolved (aqueous) phase with respect to the crystallising solid (biomineral) is represented by the expression

$$\log\left(\frac{[\mathrm{REE}_i]}{[\mathrm{REE}_i]_0}\right) = \lambda_{ij} \log\left(\frac{[\mathrm{REE}_j]}{[\mathrm{REE}_j]_0}\right) \tag{1.2}$$

where $[\mathrm{REE}_i]$ and $[\mathrm{REE}_j]$ are dissolved concentrations during co-precipitation, whereas $[\mathrm{REE}_i]_0$ and $[\mathrm{REE}_j]_0$ are the initial concentrations of the same elements. This relationship denotes that if $\lambda_{ij} \neq 1$ elements fractionate during precipitation.

By calculating the initial concentrations of lung fluids before any interactions with inhaled particles, the values of $\log([\mathrm{REE}_i]/[\mathrm{REE}_i]_0)$ ratios can be calculated from BAL analyses and reported for elements of interest (Fig. 1.3). The trace element patterns closely resemble the observed fractionations reported by Byrne et al. (1996) during phosphates co-precipitation from laboratory solutions at 25 °C and pH ≈ 4 between 24 and 49 hours (h). Patterns relative to BAL solutions are similar to the 49 h phosphate co-precipitation pattern, as compared to only 24 h. Figure 1.3 displays the discrepancies between the REE patterns of the 24 h time

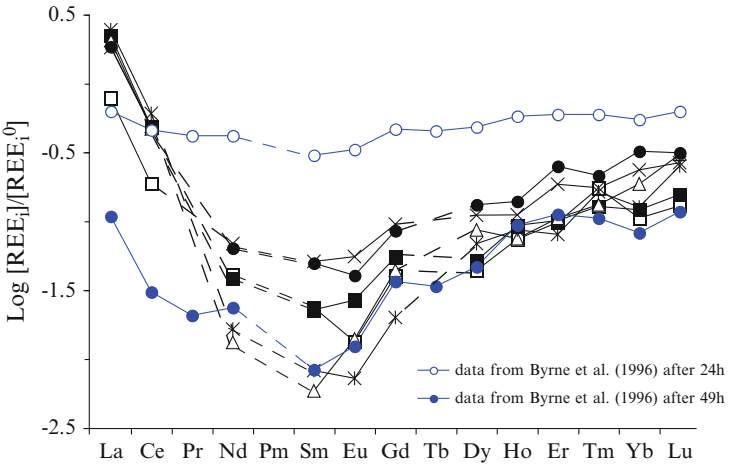

Fig. 1.3 REE fractionation induced by crystallisation of REE phosphates in lung fluids (*black symbols*). These values have been calculated starting from the initial modelled concentrations, represented by SBF and the BAL solutions. The observed REE patterns are compared with those measured by Byrne et al. (1996) during co-precipitations of REE phosphates under controlled laboratory conditions after 24 h and 49 h

period and the observed BAL solution values (i.e., $\log([REE_i]_0$ and $[REE_i]_0)$). Notice that Y, La and Ce concentrations are larger than those expected based on experimental fractionation patterns reported by Byrne et al. (1996). This data suggests the concurrent presence of an additional particulate source for these elements, potentially of anthropogenic origin, may lead to REE co-precipitation with phosphates. In order to evaluate these suggestions, the distribution of other trace elements in BAL has to be evaluated with respect to possible source materials of inhaled particulates.

1.4.3 Identifying Atmospheric Particulate Sources

The ability to uniquely identify the source of atmospheric particulates requires calculation of the enrichments or depletions of diagnostic elements for each potential inhaled particle source. Elemental enrichment factors in the BAL fluids were calculated with respect to Al concentration using the following equation (Puckett and Finegan 1980):

$$EF_{REF}^{Tr_i} = \frac{\frac{[Tr_i]_{BAL}}{[Al]_{BAL}}}{\frac{[Tr_i]_{REF}}{[Al]_{REF}}} \tag{1.3}$$

where $[Tr_i]$ is the concentration of a given trace element in the BAL solution or in a hypothetical source material used as the reference (McLennan 2001). In general, EF values smaller than 5 indicate that the element under consideration is not significantly enriched in the BAL fluid sample with respect to the hypothesised source, whereas EFs larger than 5 imply an enrichment of the element under investigation in the materials being studied with respect to the chosen source (Gao et al. 2002).

In the current case study, the possible sources of inhaled particles may include both soluble fraction of volcanic ash and parent magmatic products (Aiuppa et al. 2003). Additional sources may include automotive traffic or industrial particulates (Dongarrà et al. 2003). In our study area, geochemical characteristics of automotive traffic are difficult to investigate due to the concurrent occurrence of other suspended particulates. Moreover, Dongarrà et al. (2003) studied atmospheric pollution in Messina, a town characterised by a dense automotive traffic, located at about 60 km away from Catania with similar climatic conditions. As a result, we assumed that those results were representative of trace element compositions of particulate from automotive traffic in Catania.

The amplitude of enrichment factor (EF) values calculated with respect to the potential sources of inhaled atmospheric particulates (soluble ash fraction (SAF), parent magma (PM) and road dust (RD)) (Fig. 1.4) shows that Cr, Fe, As, Pb and U are leached from soluble fraction of ejected volcanic ash (SAF) when in contact with lung fluids. This observation is in agreement with EF values for these elements that are close to 1 or a bit lower as calculated with respect to this source, whereas the EF for Ni falls across a wide range between 1 and 10 (Fig. 1.4). These results suggest a contribution of Ni from a variety of sources with respect to SAF. We suggest that Cr, Fe, As, Pb and U could be released by dissolution of the soluble fraction of volcanic materials, while it is hard to imagine that soluble salt coatings persist in an undissolved form during interactions with lavage fluids. Therefore, leaching of V, Mn, Co, Ni, Cu and Cd from the parent magma (PM) or another source is likely. To test this hypothesis, we compare EF_{PM} values for the latter elements in Fig. 1.4. These EF_{PM} values are less than 1 for V, Mn and Co and close to 1 or slightly lower for Ni and Cu, while Cd shows ambiguous behaviour. When BAL fluids were compared to road dust (RD), EF values for V, Mn and Co were less than 1 and EF_{RD}^{Cd} close to 1 or slightly larger, in agreement with its origin from the automotive traffic source (Fig. 1.4). Together, this data suggests that both Ni and Cu were released during interactions between parent magma (PM) rock material and lung fluids, whereas V, Mn and Co are sourced from partially dissolved glass ash particles. Nonetheless, V, Mn and Co may have some anthropogenic sources.

Therefore, in order to differentiate anthropogenic vs. volcanic sources for Co, Mn, Ni, Cu and Cd, we compare the EF_{PM} and EF_{RD} values of labile trace element fractions in simulated atmospheric dust particle interactions with biological fluids. As reported in Fig. 1.5, EF_{PM} values for Co, Mn, Ni, Cu and Cd indicate an exponential range in the values of their bioavailability in PM_{10} atmospheric particles (Falta et al. 2008). By comparison, EF_{RD} values fall along a distinctly different exponential array calculated based on the bioavailability of these elements (apart from Cu) in $PM_{2.5}$ atmospheric dust fraction.

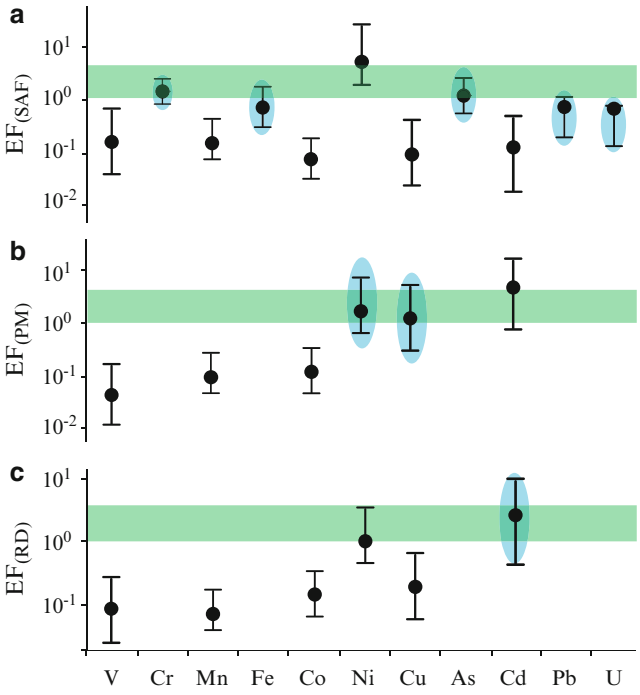

Fig. 1.4 Enrichment factors (*EF*) calculated for various elements with respect to different potential source materials. (**a**) Soluble fraction of erupted ash (*SAF*); (**b**) Etna's parent magma (*PM*) of the 2001 eruption; (**c**) road dust (*RD*). *Pale blue ellipses* highlight elements whose BAL composition is consistent with the investigated source composition. *Pale green* areas represent not significant EF values according to Gao et al. (2002). *Black dots* are medians and black segments link maximum to minimum EF values for each measured element. Data on Etna's parent magma and the soluble ash fraction (*SAF*) are reported in Aiuppa et al. (2003)

The exponential bioavailability trend of these elements agrees with the kinetic parameters calculated by Falta et al. (2008) and suggests that atmospheric dust produced from glass and rock fragments is enriched in the PM_{10} fraction, whereas atmospheric dust from anthropogenic sources related to automotive traffic is predominantly in the $PM_{2.5}$ particulate fraction. Conversely, the poor fit for Cu on these curves with respect to the other elements (i.e., Co, Ni, Mn and Cd) suggests a lithogenic source for this metal.

1.5 Discussion

The similarity between elemental enrichment factors for REE calculated with respect to SAF and PM, specifically for elements ranging between Nd and Tm, confirms that the distribution of these elements is controlled by similar processes. This similarity obfuscates the origin of trace element sources for these elements

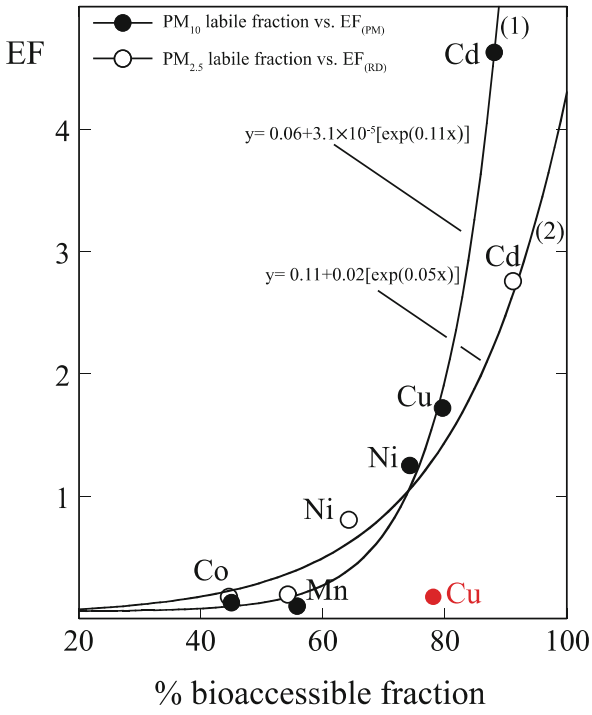

Fig. 1.5 Relationship between the EF values calculated with respect to the Etna's parent magma (*PM*) (*black dots*) and road dust reference composition (*RD*) (*circles*) for elements with EFs < 1 in Fig. 1.4. Mn, Co, Ni, Cu and Cd $EF_{(PM)}$ values reported in Fig. 1.4 were used to calculate curve (*1*), whereas Mn, Co, Ni and Cd $EF_{(RD)}$ values reported in Fig. 1.4 were used to calculate curve (*2*). Values of bioaccessible trace element fractions were reported in Falta et al. (2008). $EF_{(RD)}$ value for Cu, falling far from curve (*2*), suggests a non-anthropogenic Cu origin

(Fig. 1.6). Conversely, this similarity disappears for light REE (i.e., La, Y and Ce), which show higher EF_{PM} than EF_{SAF}. These differences suggest that the BAL fluid composition cannot simply be explained in terms of leaching from a singular inhaled product followed by fractionation in lung fluids during phosphate co-precipitation. As a result, the presence of another particulate source is required. The EF_{RD} assessment for those REE analysed in Dongarrà et al. (2003) confirms that atmospheric dust from automotive traffic is a suitable source for Ce, whereas La always shows $EF_{RD} > 10$, implying a different origin from highly enriched La sources (Fig. 1.6).

La-enriched anthropogenic sources are usually associated with materials coming from the petroleum industry where La-rich carbonates and zeolites are routinely employed as catalytic converters in hydrocarbon refinery practices. Therefore, La enrichments can be considered typical environmental signatures for the delivery of atmospheric particulates during hydrocarbon combustion in power stations (Kulkarni et al. 2007; Moreno et al. 2008). Similarly, the analyses of BAL fluid have La-Ce-Sm concentrations (i.e., La × 2-Ce-Sm × 10) consistent with particulate matter collected from refinery and oil power station emissions (Fig. 1.7) (Moreno et al. 2008). These results suggest that particulates emitted from oil refineries in the Augusta-Priolo area impact the air particulate and lung fluid chemistry of Catania. In fact, the compositions of BAL fluids in the La-Ce-V triangular diagram (Fig. 1.7) (i.e., La × 3.1-Ce × 1.54-V) cluster along a linear array between geological crustal

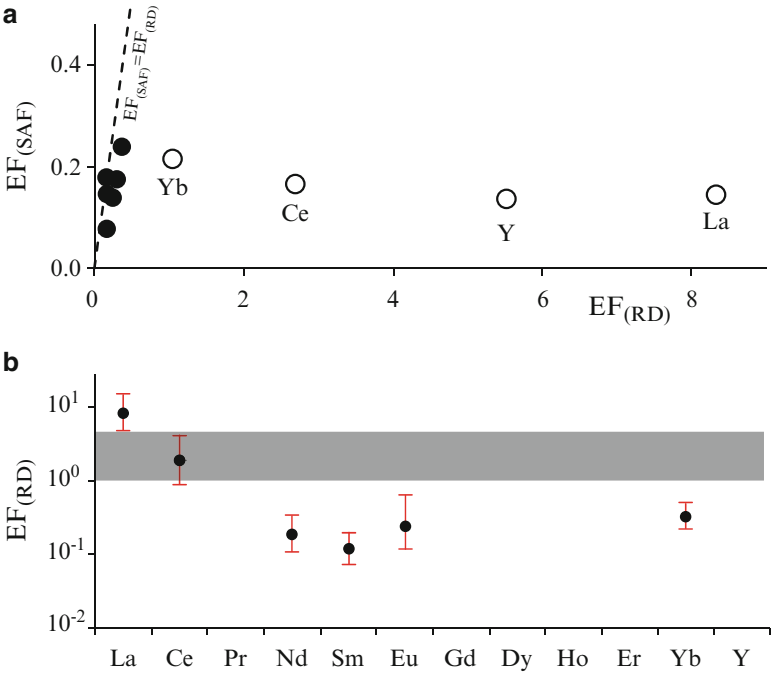

Fig. 1.6 (**a**) The relationship between $EF_{(SAF)}$ and $EF_{(RD)}$ values for REE. Only EFs for Yb, Ce, Y and La fall far from the line determined by relationship $EF_{(SAF)} = EF_{(RD)}$, indicating an anthropogenic origin of these elements from leaching of road dust particles. (**b**) $EF_{(RD)}$ values calculated for REE

materials and emissions from the oil refinery industry (as reported in Moreno et al. 2008). These observations confirm the important role of atmospheric particulates from oil refineries in determining the chemistry of lung fluids for people living in the Catania area.

The combination of REE and trace element distributions and model calculations based on the double solid reactant method leads to a viable explanation for the source of phosphate microcrysts in human lungs. During phosphate microcryst biomineralisation, variable MREE subtraction occurs in lung fluids. These observations strongly agree with alteration of the parent solution chemistry by the induction of phosphate co-precipitation in the lungs. These results are consistent with laboratory experiments and variable exposure to distinct sources of REE-rich dust (e.g., volcanic and anthropogenic). These features are characteristic of systems where low-grade dissolved REE complexation actively occurs, in comparison to variable REE dissolution induced by scavenging of pre-existing surfaces (Byrne and Kim 1990; Byrne et al. 1996). Therefore, based on the observed V-shaped REE fractionation pattern, the pre-existence of phosphate mineral solids in bronchial spaces appears unlikely. Instead, the observed REE fractionation indicates that primary crystallisation of REE-rich phosphates occurred in human lungs following the inhalation of REE-bearing particulates.

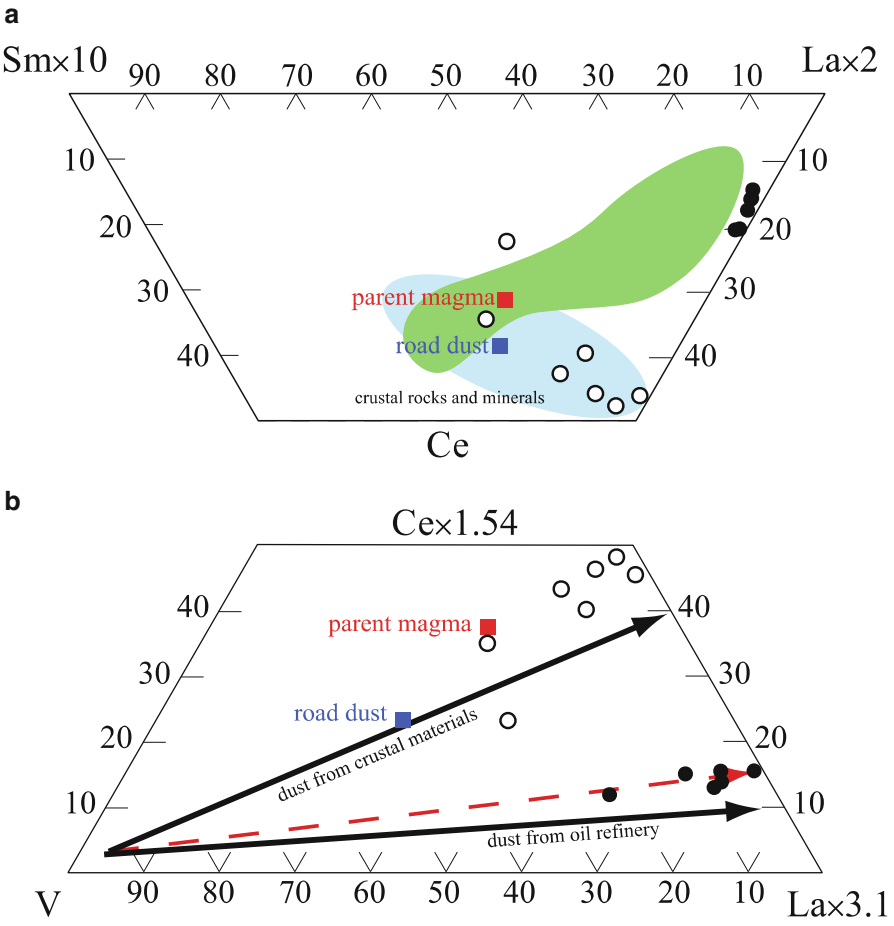

Fig. 1.7 Compositions of BAL (*black dots*) and SAF samples (*circles*) reported from Aiuppa et al. (2003) compared with typical crustal and anthropogenic products in terms of La-Sm-Ce (**a**) and La-Ce-V signatures (**b**). Compositions of the road dust (Dongarrà et al. 2003), the parent magma of Etna's 2001 eruption (Aiuppa et al. 2003), crustal materials (Taylor and McLennan 1995) and oil refinery products (Moreno et al. 2008) are given for reference

1.6 Conclusions

The trace element distribution of pulmonary fluids collected from people subjected to the inhalation of atmospheric dust particles represents a powerful tool for environmental and medical investigations. Trace element data provides information about source and geochemical nature of these inhaled materials and the processes of solid-biofluid interaction in the lungs. The REE pattern in BAL fluids can be used as a proxy to investigate the processes of pulmonary ossification. In this study, the

diagnostic V-shaped REE pattern indicates that active phosphate biomineralisation is occurring *in vivo*. These results suggest that the REE distribution in the dissolved phase can be a powerful environmental proxy for biomineralisation and metabolic reactions of solid-biofluid interaction.

The current geochemical approach is capable of distinguishing the source of trace elements in highly complex systems such as volcanic eruptions near highly industrialised urban areas. This approach is suitable for determining the origin of trace elements from prolonged subacute exposures to anthropogenic source materials and acute exposure to lithogenic solids that originated from short-term, major geological events (i.e., volcanic eruption). The occurrence of trace elements arising from both lithogenic and anthropogenic sources is an important component of trace metal burden in the human lungs. Our data indicates that Cr, Fe, As, Pb and U had a lithogenic origin that results from the dissolution of the soluble fraction of erupted ash. Ni and Cu were released from volcanic glass particles; however, Cd was probably leached from a road dust component of inhaled solids. The partial dissolution of both volcanic glass and road dust particles is responsible for the observed V, Mn and Co concentrations in BAL fluids in agreement with EF values for these elements and their bioavailability in presence of simulated biological fluids. Yttrium and other LREE enrichments provide diagnostic markers to differentiate exposure to anthropogenic activities (i.e., automobile exhaust, oil refinery and power production emission). Significant lanthanum (La) enrichments indicate anthropogenic (oil refinery) contributions to the budget of the atmospheric dust that interacts with biological fluids.

The concentrations of the trace elements analysed in bronchial fluids are sensitive to the partial and/or total dissolution of inhaled atmospheric particles. These observations demonstrate the power of using this geochemical approach for evaluating solid-liquid phase interactions, specifically in nonconventional environments such as the human body. Future analysis of the trace element content of biological fluids may allow us to recognise the origin and nature of inhaled solids if combined with geochemical modelling of trace element data.

Acknowledgments We are indebted to Drs. N. Crimi, C. Mastruzzo and P. Pistorio for sample collection of bronchoalveolar lavages.

References

Accornero M, Marini L (2008) The double solid reactant method for modeling the release of trace elements from dissolving solid phases: I. Outline and limitations. Environ Geol 55:1627–1635

Aiuppa A, Dongarrà G, Valenza M, Federico C, Pecoraino G (2003) Degassing of trace volatile metals during the 2001 eruption of Etna. Geophys Monogr 19:41–55

Albarede F (1995) Introduction to geochemical modeling. Cambridge University Press, Cambridge

Bargagli E, Bigliazzi C, Leonini A, Nikiforakis N, Perari MG, Rottoli P (2005) Tryptase concentrations in bronchoalveolar lavage from patients with chronic eosinophilic pneumonia. Clin Sci 108:273–276

Baxter PJ, Dupree R, Hards VL, Kohn SC, Murphy MD, Nichols A, Nicholson RA, Norton G, Searl A, Sparks RSJ, Vickers BP (1999) Cristobalite in volcanic ash of the Soufriere Hills Volcano, Montserrat, British West Indies. Science 283:1142–1145

Bowser CJ, Jones BF (2002) Mineralogic controls on the composition of natural waters dominated by silicate hydrolysis. Am J Sci 302:582–662

Byrne RH, Kim KH (1990) Rare earth element scavenging in seawater. Geochim Cosmochim Acta 54:2645–2656

Byrne RH, Kim K (1993) Rare earth precipitation and co-precipitation behavior: the limiting role of PO_4^{3-} on dissolved rare earth concentrations in seawater. Geochim Cosmochim Acta 57: 519–526

Byrne RH, Liu X, Schijf J (1996) The influence of phosphate co-precipitation on rare earth distributions in natural waters. Geochim Cosmochim Acta 60:3341–3346

Censi P, Larocca D, Aricò P, Sprovieri M, Saiano F, Mazzola S, Ferla P (2007) Effects of alteration of volcanic ashes in seawater. I. Anomalous Y/Ho ratios in coastal waters of the Central Mediterranean sea. Geochim Cosmochim Acta 71:5405–5422

Censi P, Randazzo LA, Zuddas P, Saiano F, Aricò P, Andò S, Mazzola S (2010) Trace element behaviour in seawater during pyroclastic etna's activity in 2001. Concurrent effects of nutrients and formation of alteration minerals. J Volcanol Geotherm Res 193:106–116

Censi P, Tamburo E, Speziale S, Zuddas P, Randazzo LA, Punturo R, Aricò P, Cuttitta A (2011a) Rare Earth elements and yttrium in human lung fluids probing the exposure to atmospheric fallout. J Hazard Mater 186:1103–1110

Censi P, Zuddas P, Randazzo LA, Tamburo E, Speziale S, Cuttitta A, Punturo R, Aricò P, Santagata R (2011b) Source and nature of inhaled atmospheric dust from trace element analyses of human bronchial fluids. Environ Sci Technol 45:6262–6267

Chapelle FH (2003) Geochemistry of groundwater. In: Holland DH, Turekian KK (eds) Treatise on geochemistry, vol 5. Elsevier, Amsterdam, pp 425–449

Cuoco E, Tedesco D, Poreda RJ, Williams JC, DeFrancesco S, Balagizi C, Darrah TH (2012) Impact of volcanic plume emissions on rain water chemistry during the January 2010 Nyamuragira eruptive event: implications for essential potable water resources. J Hazard Mater 244–245:570–584

Darrah TH (2009) Inorganic trace element composition of modern human bones: relation to bone pathology and geographical provenance. Doctoral thesis, University of Rochester, Rochester, NY, pp 1–183

Darrah TH, Prutsman-Pfeiffer JJ, Poreda RJ, Campbell ME, Hauschka PV, Hannigan RE (2009) Incorporation of excess gadolinium into human bone from medical contrast agents. Metallomics 1:479–488

Dias Da Cunha K, Santos M, Zouain F, Carneiro L, Pitassi G, Lima C, Barros Leite CV, Dália KCP (2009) Dissolution factors of Ta, Th, and U oxides present in pyrochlore. Water Air Soil Pollut 205:251–257

Dongarrà G, Sabatino G, Triscari M, Varrica D (2003) The effects of anthropogenic particulate emissions on roadway dust and *Nerium oleander* leaves in Messina (Sicily, Italy). J Environ Monit 5:766–773

Eyring H (1935a) The activated complex in chemical reactions. Chem Rev 17:65–77

Eyring H (1935b) The activated complex and the absolute rate of chemical reactions. J Chem Phys 33:107–115

Falta T, Limbeck A, Koellensperger G, Hann S (2008) Bioaccessibility of selected trace metals in urban PM2.5 and PM10 samples: a model study. Anal Bioanal Chem 390:1149–1157

Forde S, Hynes MJ, Jonson B (2008) Dissolution of glass compositions containing no added lead in simulated lung fluid. Int J Hygiene Environ Health 211:357–366

Gao Y, Nelson ED, Field MP, Ding Q, Li H, Sherrell RM, Gigliotti CL, Van Ry DA, Glenn TR, Eisenreich SJ (2002) Characterization of atmospheric trace elements on PM2.5 particulate matter over the New York-New Jersey harbor estuary. Atmos Environ 36:1077–1086

Gislason SR, Oelkers EH (2003) Mechanism, rates, and consequences of basaltic glass dissolution: II. An experimental study of the dissolution rates of basaltic glass as a function of pH and temperature. Geochim Cosmochim Acta 67:3817–3832

Hedberg Y, Gustafsson J, Karlsson HL, Möller L, Wallinder IO (2010) Bioaccessibility, bioavailability and toxicity of commercially relevant iron- and chromium-based particles: in vitro studies with an inhalation perspective. Part Fibre Toxicol 7 art. N° 23

Hirano S, Suzuki KT (1996) Exposure, metabolism, and toxicity of rare earths and related compounds. Environ Health Perspect 104:85–95

Hoogewerff J (2008) Introduction to the use and limits of elemental and isotopic analysis for the forensic provenancing of unidentified human remains. In: Proceedings of the American Academy of Forensic Science 60th annual scientific meeting, AAFS, Washington, DC

Kulkarni P, Chellam S, Fraser MP (2007) Tracking petroleum refinery emission events using lanthanum and lanthanides as elemental markers for PM2.5. Environ Sci Technol 41:6748–6754

Leung CC, Yu ITS, Chen W (2012) Silicosis. Lancet 379(9830):2008–2018

Luoto K, Holopainen M, Kangas J, Kalliokoski P, Savolainen K (1998) Dissolution of short and long rockwool and glasswool fibers by macrophages in flow through cell culture. Environ Res 78:25–37

McLennan SM (2001) Relationships between the trace element composition of sedimentary rocks and upper continental crust. Geochem Geophys Geosyst 2:1021

Merkel BJ, Planer-Friedrich B (2008) Groundwater geochemistry, 2nd edn. Springer, Berlin

Midander K, Wallinder IO, Leygraf C (2007) In vitro studies of copper release from powder particles in synthetic biological media. Environ Pollut 145:51–59

Moreno T, Querol X, Alastuey A, Gibbons W (2008) Identification of FCC refinery atmospheric pollution events using lanthanoid- and vanadium-bearing aerosols. Atmos Environ 42:7851–7861

Newman LS (2001) Clinical pulmonary toxicology. In: Sullivan JB Jr, Krieger G (eds) Clinical environmental health and exposures, 2nd edn. Lippincott Williams and Wilkins, Philadelphia

Oskarsson N (1980) The interaction between volcanic gases and tephra: fluorine adhering to tephra of the 1970 Hekla eruption. J Volcanol Geotherm Res 8:251–266

Pracyk JB, Simonson SG, Young SL, Ghio AJ, Roggli VL, Piantadosi CA (1996) Alveolar microlithiasis. Respiration 63:254–260

Puckett KJ, Finegan EJ (1980) An analysis of the element content of lichens from the Northwest Territories, Canada. Can J Bot 58:2073–2088

Randazzo LA, Saiano F, Zuddas P, Censi P (2012) The behaviour of Rare Earth Elements during the volcanic ash dissolution in seawater solution. Procedia Earth and Planetary Science (in press)

Rodushkin I, Odman F (2001) Assessment of the contamination from devices used for sampling and storage of whole blood and serum for element analysis. J Trace Elem Med Biol 15:40–45

Schuhmann M, Brims FJH, O'Reilly KMA (2011) Asbestos-related lung disease: an update. Clin Pulm Med 18(6):265–273

Scollo S, Delcarlo P, Coltelli M (2007) Tephra fallout of 2001 Etna flank eruption: analysis of the deposit and plume dispersion. J Volcanol Geotherm Res 160:147–164

Sipes IG, Badger D (2001) Principles of toxicology. In: Sullivan JB Jr, Krieger G (eds) Clinical environmental health and exposures, 2nd edn. Lippincott Williams and Wilkins, Philadelphia

Takaya M, Shinohara Y, Serita F, Ono-Ogasawara M, Otaki N, Toya T, Takata A, Yoshida K, Kohyama N (2006) Dissolution of functional materials and rare earth oxides into pseudo alveolar fluid. Ind Health 44:639–644

Tamburo E, Aiuppa A, Marini L, Valenza M (2011) Modelling groundwater processes in a carbonate catchment: a case study from the Madonie area (Northern Sicily). Appl Geochem 26:1274–1287

Taylor SR, McLennan SM (1995) The geochemical evolution of the continental-crust. Rev Geophys 33:241–265

Wolery TJ (1979) Calculation of chemical equilibrium between aqueous solutions and minerals: the EQ3/6 software package. Report UCRL-52658. Lawrence Livermore National Livermore, California

Wolery TJ (1992) A computer program for geochemical aqueous speciation-solubility calculations: theoretical manual, user's guide, and related documentation (version 7.0). Report UCRL-MA-110662 PT III. Lawrence Livermore National Laboratory, Livermore, California

Wolery TJ, Daveler SA (1992) EQ6, a computer program for reaction path modeling of aqueous geochemical systems: theoretical manual, user's guide, and related documentation (version 7.0). Report UCRL-MA-110662 pt IV. Lawrence Livermore National Laboratory, Livermore, California

Wood SA, Taunton AE, Normand C, Gunter ME (2006) Mineral-fluid interaction in the lungs: insights from reaction-path modeling. Inhal Toxicol 18:975–984

Yoon HK, Moon HS, Park SH, Song JS, Lim Y, Kohyama N (2005) Dendriform pulmonary ossification in patient with rare earth pneumoconiosis. Thorax 60:701–703

Chapter 2
Geochemistry and Biochemistry: Insights into the Fate and Transport of Pt-Based Chemotherapy Drugs

Robyn E. Hannigan and Thomas H. Darrah

Abstract Though some heavy metals, such as Pt, are considered toxic to humans, their toxic effects can be positively leveraged to treat diseases such as cancer. The use of Pt-based chemotherapies is, unfortunately, linked to severe side effects some occurring many years after treatment (late effects). Through the lens of geochemistry, it is possible to assess these late effects and associated biochemical interactions with other metals. This approach also presents a potential intervention/detection strategy for early detection and possible prevention of late effects.

Keywords Trace elements • Serum chemistry • Chemotherapy • Metal interactions • Platinum

2.1 Introduction

Metabolism of platinum (Pt)-based anticancer drugs (Fig. 2.1) begins as soon as it enters the bloodstream. Though doses, on average, range from 150 to 400 mg m^{-2}, only about 1% of the cisplatin that enters the cell actually binds to DNA (Reedijk 1999; Centerwall et al. 2006). In order to bind to the DNA, cisplatin (the most commonly used) undergoes hydration (aquation), wherein the chlorides on the molecule are replaced by water. The aquation half-life is approximately 2.4 h (Knox et al. 1986). Other Pt-based anticancer drugs undergo a similar process though

R.E. Hannigan (✉)
Department of Environmental, Earth, and Ocean Sciences, University of Massachusetts Boston, Boston, MA, USA
e-mail: Robyn.Hannigan@umb.edu

T.H. Darrah
Division of Earth and Ocean Sciences, Nicholas School of the Environment, Duke University, 207A Old Chemistry Building, Box 90227, Durham, NC 27708, USA
e-mail: thomas.darrah@duke.edu

P. Censi et al. (eds.), *Medical Geochemistry: Geological Materials and Health*, DOI 10.1007/978-94-007-4372-4_2,

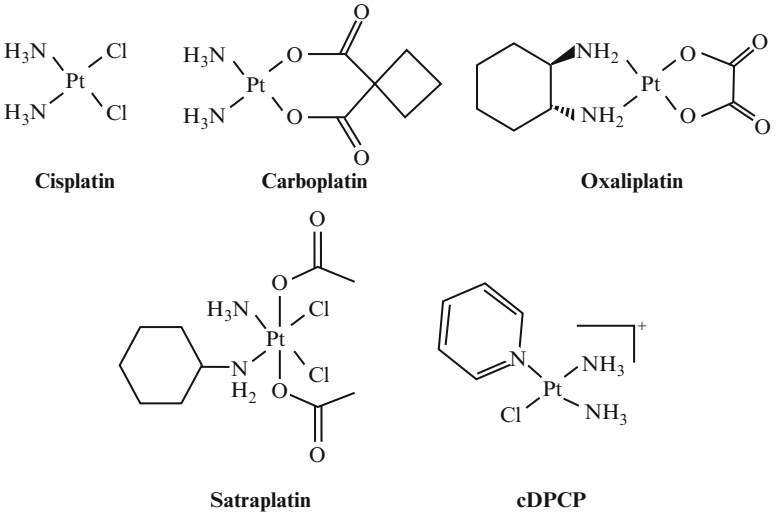

Fig. 2.1 Chemical structures of platinum anticancer drugs. Of these drugs, only cisplatin, carboplatin, and oxaliplatin are approved for use in the United States. Satraplatin has completed phase III trials but is not approved for use in the United States as of 2012. cDPCP inhibits transcription in vitro and is used for treatment of colorectal cancers

the aquation is slower, e.g., 268 h for carboplatin (Knox et al. 1986). The rate of aquation and preferential targeting of cancer cells is primarily due to the pH difference between cancerous and healthy cells (Centerwall et al. 2006). Ultimately, the aquated species will target the guanine residue of DNA. Platination of the DNA bends the double helix by 35–40° leading to antiproliferative effects including interruption of transcription and apoptosis (Todd and Lippard 2009).

The goal of this work was to evaluate, through a thorough literature review and analysis of serum (plasma after removal of clotting proteins) Pt and other metals in post-treatment patients, to explore the biochemical "behavior" of Pt. Ultimately, this work leverages geochemical approaches to understand Pt fate and transport, providing unique insights into the potential causes of late effects.

2.2 Methods

We performed a thorough literature review of Pt biochemistry and also leveraged our ongoing research on Pt anticancer agents and long-term Pt circulation in treated patients. Statistical analyses were performed using SPSS 20.0.

Elemental compositions of serum from treated patients (Sprauten et al. 2012) were measured by inductively coupled plasma mass spectrometry (ICP-MS). In brief, whole blood samples (300 μL) were centrifuged to remove cellular

components, acidified to pH < 2 with ultrapure HCl, diluted to 100 μL, and analyzed by solution-based ICP-MS using NIST 909b (human serum) and NIST 927c (bovine serum albumin) for calibration according to published methods (Darrah et al. 2009; McLaughlin et al. 2011).

2.3 Results and Discussion

2.3.1 Pt-Based Anticancer Drugs: Mode(s) of Action

The mode of action of cisplatin and other Pt-based anticancer drugs is well known as are the associated toxicologic impacts and long-term health impacts (late effects). These effects are strongly correlated with peak Pt concentrations in plasma (Polycarpe et al. 2004; Lanvers-Kaminsky et al. 2006). Recall that only 1% of cisplatin binds to DNA. The remaining cisplatin, carboplatin, oxaliplatin, and, presumably, satraplatin (Galanski and Keppler 2007; Reedijk 2009) can bind to a number of extra- and intercellular proteins (Mandal et al. 2003; Gabano et al. 2007). Whether as a free complex or partially aquated, the Pt acts as a soft Lewis acid with a high affinity for sulfhydryl (SH) groups on plasma proteins and enzymes. Cisplatin and carboplatin will react directly with sulfur-containing ligands such as methionine and cysteine (Barnham et al. 1996; Heudi et al. 1998; El-Khateeb et al. 1999). Recent research centered on the interaction between Pt and plasma proteins reveals a potential link between transferrin (an iron-transporting glycoprotein) and Pt (Gabano et al. 2007). Cisplatin binds to thiol-containing (sulfur, cysteine ligand) molecules such as glutathione (GSH) and metallothionein (MET). Cisplatin can displace zinc (Zn) and cadmium (Cd), and several Pt atoms can bind with a single metallothionein (Pattanaik et al. 1992; Zhang and Tang 1994; Hagrman et al. 2003; Mandal et al. 2003). Displacement of Zn and Cd as well as other metal-Pt interactions may lead to secondary toxic effects. In the case of Cd, though poorly mutagenic, it may act as an epigenetic or indirect genotoxic carcinogen (DHHS 2000).

Whether increases in plasma trace metal concentrations can be linked to Pt-based treatment and displacement of metals from plasma proteins is unknown. These potential interactions merit significant attention given the late effects associated with Pt-based treatments. Zinc plays a significant role in cell proliferation (Sun et al. 2007; Li and Maret 2009), and fluctuations in intercellular Zn concentrations are thought to be the regulatory mechanism for controlling the cell cycle. Imbalance in intercellular Zn may result in disruption of cell proliferation. Zn is a known environmental toxicant which, when occurring at high concentrations, has been found to impede mitochondrial function (Joseph et al. 2008). Zinc is also higher in the plasma of cancer patients (Pasha et al. 2008). Whether the displacement of Zn on metallothionein by Pt is directly related to late effects in Pt-based anticancer treatments remains unknown. Recent studies are clear, however, that the Pt from anticancer drugs that is bound to proteins may be causatively linked to

nephrotoxicity and ototoxicity (Aull et al. 1979; El-Khateeb et al. 1999; Rademaker-Lakhai et al. 2006).

Platinum toxicity resembles that of a number of other metals including mercury (Hg) (Gonzalez and Villasanta 1982), Cd (Huang et al. 2008), and, potentially, chromium (Cr) as it too forms DNA adducts (Shi et al. 2004; Zhitkovich 2004). Based on the relations between trace elements, including Pt, and plasma proteins, it is expected that significant changes in blood chemistry will occur as a result of Pt-based drug exposure. The feedback loops associated with Pt displacement of Zn as well as changes in cellular fluid pH during aquation of the compounds and subsequent changes in concentrations of other potentially toxic metals could all be potentially linked to toxic effects. The direct role of Pt itself and metal-Pt interactions needs to be established.

2.3.2 Pt in Biological Fluids and Tissues of Treated Patients

Pt concentrations in the plasma of patients treated with cisplatin and other Pt-based compounds are markedly different from those of unexposed patients (Tothill et al. 1992; Gietema et al. 2000; Brouwers et al. 2008a, b) as are concentrations of other potentially toxic trace metals (Vernie et al. 1988; Pasha et al. 2008). Pt concentrations in plasma and in tissues are dose dependent (Stewart et al. 1985; Tothill et al. 1992; Uozumi et al. 1993; Mandal et al. 2003; Rademaker-Lakhai et al. 2006; Brouwers et al. 2008a, b). Pretreatment hydration, patient fitness prior to treatment, and rest periods between treatments appear to ameliorate side effects including hypomagnesemia and hypocalcemia (Gonzalez and Villasanta 1982), nephrotoxicity (Hartmann et al. 1999; Hartmann 2002), and ototoxicity (Rademaker-Lakhai et al. 2006). Significant individual variation in therapeutic response has been seen despite commonalities in cancer histology and stage (Bokemeyer 1998; Fossa et al. 1999; Carrato et al. 2002; Hussain et al. 2008). Individual variations in side effects and urine/blood/tissue Pt concentrations have also been seen (Heydorn et al. 1998; Areberg et al. 1999; Hartmann et al. 1999; Gerl and Schierl 2000; Lykissa and Maharaj 2006; Brouwers et al. 2008a, b). Much of the variation in Pt concentrations in plasma can be related to dose as well as individual disease phenomena and individual metabolism. One thing is clear; however, despite individual variations, there are significant commonalities in late effects (Safirstein et al. 1987; Berger et al. 1996; Jakob et al. 1998; Hartmann et al. 1999; Kollmannsberger et al. 1999; Kintzel 2001; Maduro et al. 2003; Lanvers-Kaminsky et al. 2006; Rademaker-Lakhai et al. 2006). Post-treatment serum Pt concentrations suggest that Pt remains in the body long past treatment and can be linked, through protein interactions, to many of the late effects. Only 1% of the cisplatin is aquated and forms DNA adducts, and this process occurs within 2.4 h (longer for other Pt-based drugs).

The half-life of Pt in the body is between 4 and 6 years (Gietema et al. 2000; Rademaker-Lakhai et al. 2006; Brouwers et al. 2008a, b), and plasma Pt concentrations remain high long after treatment (>30 times control) (Tothill et al.

1992; Brouwers et al. 2008a, b; Sprauten et al. 2012). We also know that hematocrit declines during treatment (Getaz et al. 1980; Levi et al. 1981; Najarian et al. 1981) and that Fe concentrations in plasma in cancer patients are above that of healthy patients (Pasha et al. 2008). Both of these phenomena suggest that the heme molecule is impaired by Pt and further indicates that Pt, like other toxic metals (arsenic (As), Cd, Hg), interrupts the porphyrin metabolic pathway (Woods et al. 1991; Garcia-Vargas et al. 1994). Whether blood porphyrin levels or urine porphyrin profiles can be used as an early diagnostic of Pt-induced late effects remains to be seen. Regardless, there can be little doubt that the persistence of Pt in the body post-treatment and its interactions with plasma proteins is directly linked to late effects. The precise interactions that lead to the development of late effects remain to be discovered.

2.3.3 Pt Biochemistry and Metal-Metal Interactions

Platinum metal toxicity resembles that of a number of other metals including mercury (Hg) (Gonzalez and Villasanta 1982), Cd (Bokemeyer 1998), and, potentially, chromium (Cr) as it too forms DNA adducts (Shi et al. 2004). The currently available Pt-based chemotherapy drugs are toxic and carcinogenic *in vitro* and *in vivo* (DHHS 2000; Leonard et al. 2002; Polycarpe et al. 2004; Lanvers-Kaminsky et al. 2006) and are conclusively linked to the occurrence of secondary leukemia and solid tumors (Bokemeyer and Schmoll 1995; Travis et al. 1999; DHHS 2000; Travis et al. 2010) in patients treated for testicular and ovarian cancer. Residual Pt concentrations in serum have been associated with late effect symptoms as well (Sprauten et al. 2012).

Given that serum Pt levels, post-treatment, may represent a biomarker for late toxicity effects in combination with the known and potential interactions between Pt and other metals, we evaluated the levels of residual Pt in serum from 169 testicular cancer survivors (Sprauten et al. 2012). Cumulative cisplatin doses ranged from 191 to 1,565 mg m^{-2}, and median serum Pt concentrations ranged from 0.031 to 12.710 nmol L^{-1}. As expected, serum Pt and cisplatin dose were positively correlated ($p < 0.01$). Pt concentrations in patients who received high cumulative doses of cisplatin (>850 mg m^{-2}) are also statistically significantly different from those that received lower doses (<850 mg m^{-2}) (Fig. 2.2). There is no statistical difference in serum Pt concentrations between patients who received low doses of cisplatin and those who were not treated with cisplatin.

We evaluated relations between serum metal concentrations and chemotherapeutics using factor analysis with principal component extraction. Patients were coded based on the combination of chemotherapy treatments received as many of the patients received other drugs in addition to cisplatin. Of these compounds, the majority are sulfur bearing. Eight patients received variable doses of cisplatin as well as carboplatin ($C_6H_{12}N_2O_4Pt$). Though factor analysis reduced the data to five components accounting for 64% of the total variance in serum elemental

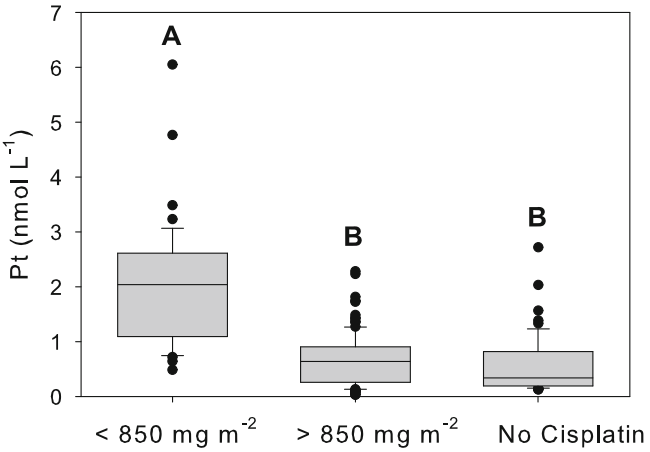

Fig. 2.2 Serum Pt concentrations across cisplatin dose groups. Concentrations are statistically distinct ($p < 0.000$) in serum from patients whose cumulative dose exceeded 850 mg m^{-2}

composition, few metals were strongly related to individual components. Factor loadings of metals on factors 1, 2, and 3 are shown in Fig. 2.3. Pt and Gd load low on factor 1 and variably on factors 2 and 3. Loading positively on factor 1 are the other metals. Factor 2 appears to discriminate between 2 groups of metals (Pb, Zn, Mo, Ce, La, Co, Mn and Cu, Sr, Fe, Se, Ti, Ca, Mg, Cr). The variance in metal concentration is best captured by factors 2 and 3 (Fig. 2.3). Based on the relations between factor loadings and coded groups, factor 1 appears to be related to treatment only. There appears to be a slight trend in loadings along factor 3 that may be related to Pt interactions with other metals such as Cu, Zn, Gd, and Pb ($R^2 = 0.823$) which is similar to the median loadings of coded groups ($R^2 = 0.803$).

Recall that Pt has the potential to displace Zn on metallothionein (Pattanaik et al. 1992; Zhang and Tang 1994; Hagrman et al. 2003; Mandal et al. 2003). Metallothioneins play an important role in transcription factor regulation, and their expression is often increased in some cancers, including testicular cancer. Given the mode of action of cisplatin, it is expected that the drug interacts with metallothioneins such as cysteine and methionine (Kelland 2007) leading to displacement of Zn and detoxification of Pt. That this interaction is not direct is also no surprise given that most patients also received S-bearing chemotherapy treatments that will also influence the relative abundances of metallothioneins. Interestingly, the relations presented by our factor analysis support the contention that the toxicity behavior of Pt is similar to that of Pb and other heavy metals.

To further evaluate the role of cisplatin in the long-term circulation of Pt, we performed a linear regression using loadings on factors 1 and 3 to predict Pt behavior. Factor 3 was most important in predicting serum Pt concentrations further supporting the supposition that Pt in serum is associated with interactions between metals and is indirectly associated with cisplatin dose. Both factor 1 and

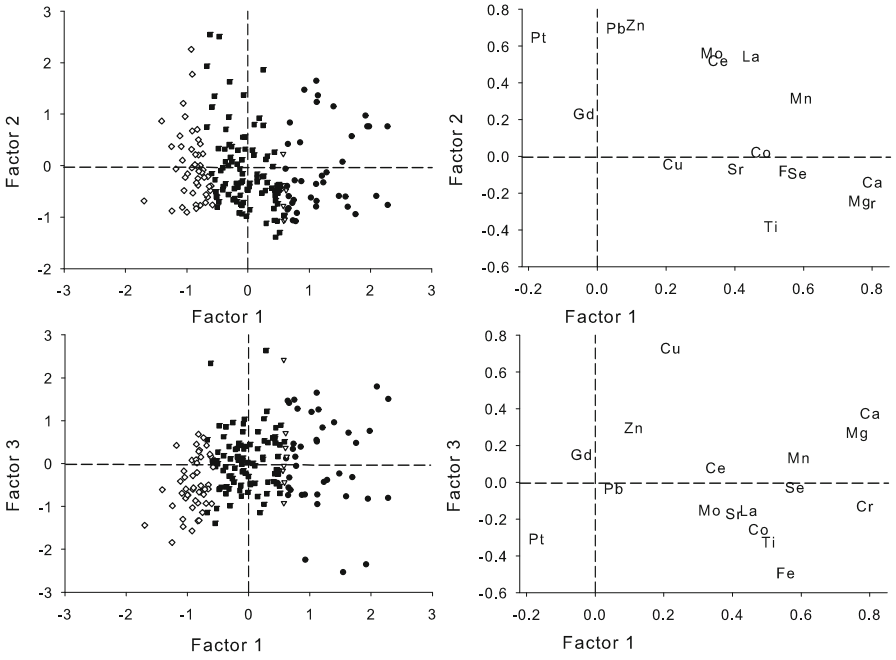

Fig. 2.3 Factor analysis results (principal component extraction) using serum metal concentrations. Samples are coded as follows: Patients who received >850 mg m^{-2} cisplatin and other combinations of nonmetallic agents (*full circles*); patients who received <850 mg m^{-2} cisplatin and other combinations of agents including Pt-bearing carboplatin (*open triangles*); patients who received <850 mg m^{-2} cisplatin and combinations of nonmetallic agents (*full squares*); and patients who received no chemotherapy (*open rhombs*)

factor 3 predict Pt concentrations ($R^2 = 0.237$); however, factor 1 appears to be the most important ($p < 0.001$). We attribute the variance captured by factor 1 to the chemotherapy treatment received by the patient. Factor 2 appears to isolate serum metals into 2 groups with major ions loading low on factor 2 and minor ions loading high. This suggests that the variance captured by factor 2 is associated with biochemical/physiological mediation of blood chemistry independent of chemotherapy drug exposure. Factor 3 further isolates the variance in blood metal chemistry and specifically isolated "redox" metals from major ions. Factor 3 is interpreted as that component associated with oxidative stress induced by the chemotherapy agents.

2.4 Conclusion

The literature is rife with evidence that there is significant individual variation in terms of toxic response to Pt-based anticancer drugs, variation in Pt concentrations in tissues, and variation in late effects. However, as we begin to link the interactions

of Pt at the molecular level with plasma proteins and associated impacts on trace element distributions in tissues with toxicity and late effects as well as begin to integrate epigenetics into the study of Pt-dose response, we begin to see that late effects may be attributed to differences between fast and slow regenerating tissues and associated release into the bloodstream of stored Pt possibly decades after treatment. Different tissues show variable half-lives, and the rate of regeneration of tissues decreases with age. Indeed, higher doses have been associated with longer Pt half-lives (Heydorn et al. 1998), which supports the contention that Pt levels in the plasma represent release of Pt during tissue regeneration (Brouwers et al. 2008a, b). The significant feedbacks between Pt – trace metal in plasma proteins – and potential for long-term storage and release of Pt long after treatment are only now beginning to reveal the necessity of large-scale integrative transdisciplinary research to fully understand late effects in patients treated with Pt-based anticancer therapies.

Acknowledgements We gratefully acknowledge Drs. Travis, Beard, and Fossa for providing the samples for this study and additional data regarding chemotherapy treatments. This work was funded, in part, by NIH 5U56CA118635 (Hannigan and Darrah) and S-E Norway Regional Health Authority #39247 (Sprauten). We also thank Ellen Campbell and Jenny Geldart for assistance in the lab and for Princess for being such a champion instrument.

References

Areberg J, Björkman S, Einarsson L, Frankenberg B, Lundqvist H et al (1999) Gamma camera imaging of platinum in tumours and tissues of patients after administration of ^{191}Pt-cisplatin. Acta Oncol 38:221–228

Aull JL, Allen RL, Bapat AR, Daron HH, Friedman ME et al (1979) The effects of platinum complexes on seven enzymes. Biochim Biophys Acta 571:352–358

Barnham KJ, Djuran MI, Murdoch PS, Ranford JD, Sadler PJ (1996) Ring-opened adducts of the anticancer drug carboplatin with sulfur amino acids. Inorg Chem 35:1065–1072

Berger CC, Bokemeyer C, Schuppert F, Schmoll HJ (1996) Endocrinological late effects after chemotherapy for testicular cancer. Br J Cancer 73:1108–1114

Bokemeyer C (1998) Current trends in chemotherapy for metastatic nonseminomatous testicular germ cell tumors. Oncology 55:177–188

Bokemeyer C, Schmoll HJ (1995) Treatment of testicular cancer and the development of secondary malignancies. J Clin Oncol 13:283–292

Brouwers EEM, Tibben MM, Pluim D, Rosing H, Boot H et al (2008a) Inductively coupled plasma mass spectrometric analysis of the total amount of platinum in DNA extracts from peripheral blood mononuclear cells and tissue from patients treated with cisplatin. Anal Bioanal Chem 391:577–585

Brouwers EEM, Huitema ADR, Beijnen JH, Schellens JHM (2008b) Long-term platinum retention after treatment with cisplatin and oxaliplatin. BMC Clin Pharmacol 8:1–10

Carrato A, Gallego J, Diaz-Rubio E (2002) Oxaliplatin: results in colorectal carcinoma. Crit Rev Oncol Hematol 44:29–44

Centerwall CR, Tacka KA, Kerwood DJ, Goodisman J, Toms BB et al (2006) Modification and uptake of a cisplatin carbonato complex by jurkat cells. Mol Pharmacol 70:348–355

Darrah TH, Prutsman-Pfeiffer JJ, Poreda RJ, Campbell ME, Hauschka PV, Hannigan RE (2009) Incorporation of excess gadolinium into human bone from medical contrast agents. Metallomics 1(6):479–488. doi:10.1039/b905145g

DHHS (2000) Tenth report on carcinogenesis. National Toxicology Program, Research Triangle Park, pp III 42–III 44

El-Khateeb M, Appleton TG, Gahan LR, Charles BG, Berners-Price SJ et al (1999) Reactions of cisplatin hydrolytes with methionine, cysteine, and plasma ultrafiltrate studied by a combination of HPLC and NMR techniques. J Inorg Biochem 77:13–21

Fossa SD, Stenning SP, Gerl A, Horwich A, Clark PI et al (1999) Prognostic factors in patients progressing after cisplatin based chemotherapy for malignant non-seminomatous germ cell tumours. Br J Cancer 80:1392–1399

Gabano E, Ravera M, Colangelo D, Osella D (2007) Bioinorganic chemistry: the study of the fate of platinum-based antitumour drugs. Curr Chem Biol 1:278–289

Galanski M, Keppler BK (2007) Searching for the magic bullet: anticancer platinum drugs which can be accumulated or activated in the tumor tissue. Anticancer Agents Med Chem 7:55–73

Garcia-Vargas GG, Del Razo LM, Cebrian ME, Albores A, Ostrosky-Wegman P et al (1994) Altered urinary porphyrin excretion in a human population chronically exposed to arsenic in Mexico. Hum Exp Toxicol 13:839–847

Gerl A, Schierl R (2000) Urinary excretion of platinum in chemotherapy-treated long-term survivors of testicular cancer. Acta Onocol 39:519–522

Getaz EP, Beckley S, Fitzpatrick J, Dozier A (1980) Cis-platin induced hemolysis. N Engl J Med 302:334–335

Gietema JA, Meinardi MT, Messerschmidt J, Gelevert T, Alt F et al (2000) Circulating plasma platinum more than 10 years after cisplatin treatment for testicular cancer. Lancet 355: 1075–1076

Gonzalez C, Villasanta U (1982) Life-threatening hypocalcemia and hypomagnesia associated with cisplatin chemotherapy. Obstet Gynecol 59:732–734

Hagrman D, Goodisman J, Dabrowiak JC, Souid A-K (2003) Kinetic study on the reaction of cisplatin with metallothionein. Drug Metab Dispos 31:916–923

Hartmann JT (2002) Long-term effects of platin and anthracycline derivatives and possible prevention strategies. Front Radiat Ther Oncol 37:92–100, Karger

Hartmann JT, Kollmannsberger C, Kanz L, Bokemeyer C (1999) Platinum organ toxicity and possible prevention in patients with testicular cancer. Int J Cancer 83:866–869

Heudi O, Cailleux A, Allain P (1998) Kinetic studies of the reactivity between cisplatin and its monoaquo species with methionine. J Inorg Biochem 71:61–69

Heydorn K, Rietz B, Krarup-Hansen A (1998) Distribution of platinum in patients treated with cisplatin determined by radiochemical neutron activation analysis. J Trace Elem Exp Med 11:37–43

Huang D, Zhang Y, Qi Y, Chen C, Ji W (2008) Global DNA hypomethylation, rather than reactive oxygen species (ROS), a potential facilitator of cadmium-stimulated k562 cell proliferation. Toxicol Lett 179:43–47

Hussain SA, Ma YT, Cullen MH (2008) Management of metastatic germ cell tumors. Expert Rev Anticancer Ther 8:771–784

Jakob A, Kollmannsberger C, Kanz L, Bokemeyer C (1998) Late toxicity after treatment for testicular germ cell cancer. Urologe A 37:635–647

Joseph L, Ryan M, Vasu DA (2008) Zinc toxicity alters mitochondrial metabolism and leads to decreased ATP production in hepatocytes. J Appl Toxicol 28:175–182

Kelland L (2007) The resurgence of platinum-based cancer chemotherapy. Nat Rev Cancer 7: 573–584

Kintzel PE (2001) Anticancer drug-induced kidney disorders – incidence, prevention and management. Drug Saf 24:19–38

Knox RJ, Friedlos F, Lydall DA, Roberts JJ (1986) Mechanism of cytotoxicity of anti-cancer platinum drugs: evidence that cis-diamminedichloroplatinum(ii) and cis-diammine-(1,1-cyclobutanedicarboxylato)platinum(ii) differ only in the kinetics of their interaction with DNA. Cancer Res 46:1972–1979

Kollmannsberger C, Kuzcyk M, Mayer F, Hartmann JT, Kanz L et al (1999) Late toxicity following curative treatment of testicular cancer. Semin Surg Oncol 17:275–281

Lanvers-Kaminsky C, Krefeld B, Dinnesen AG, Deuster D, Seifert E et al (2006) Continuous or repeated prolonged cisplatin infusions in children: a prospective study on ototoxicity, platinum concentrations, and standard serum parameters. Pediatr Blood Cancer 47:183–193

Leonard DGB, Travis LB, Addya K, Dores GM, Holowaty EJ et al (2002) P53 mutations in leukemia and myelodysplastic syndrome after ovarian cancer. Clin Cancer Res 8:973–985

Levi JA, Aroney RS, Dalley DN (1981) Haemolytic anaemia after cisplatin treatment. Br Med J 282:2003–2004

Li Y, Maret W (2009) Transient fluctuations of intracellular zinc ions in cell proliferation. Exp Cell Res 315:2463–2470

Lykissa ED, Maharaj SVM (2006) Total platinum concentration and platinum oxidation states in body fluids, tissue, and explants from women exposed to silicone and saline breast implants by IC-ICPMS. Anal Chem 78:2925–2933

Maduro JH, Pras E, Willemse PHB, de Vries EGE (2003) Acute and long-term toxicity following radiotherapy alone or in combination with chemotherapy for locally advanced cervical cancer. Cancer Treat Rev 29:471–488

Mandal R, Jiang GF, Li XF (2003) Direct evidence for co-binding of cisplatin and cadmium to a native zinc- and cadmium-containing metallothionein. Appl Organomet Chem 17:675–681

McLaughlin MP, Darrah TH, Holland PL (2011) Palladium and platinum derivatives of a blue copper protein. J Inorg Chem 50:11294–11296. doi:dx.doi.org/10.1021/ic2017648

Najarian T, Miller A, Zimelman AP, Hong WK (1981) Hematologic effect of cisplatinum-bleomycin therapy. Oncology 38:195–197

Pasha Q, Malik SA, Shah MH (2008) Statistical analysis of trace metals in the plasma of cancer patients versus controls. J Hazard Mater 153:1215–1221

Pattanaik A, Bachowski G, Laib J, Lemkuil D, Shaw CF et al (1992) Properties of the reaction of cis-dichlorodiammineplatinum(ii) with metallothionein. J Biol Chem 267:16121–16128

Polycarpe E, Arnould L, Schmitt E, Duvillard L, Ferrant E et al (2004) Low urine osmolarity as a determinant of cisplatin-induced nephrotoxicity. Int J Cancer 111:131–137

Rademaker-Lakhai JM, Crul M, Zuur L, Baas P, Beijnen JH et al (2006) Relationship between cisplatin administration and the development of ototoxicity. J Clin Oncol 24:918–924

Reedijk J (1999) Why does cisplatin reach guanine-n7 with competing s-donor ligands available in the cell? Chem Rev 99:2499–2510

Reedijk J (2009) Platinum anticancer coordination compounds: study of DNA binding inspires new drug design. Eur J Inorg Chem 10:1303–1312

Safirstein R, Winston J, Moel D, Dikman S, Guttenplan J (1987) Cisplatin nephrotoxicity: insights into mechanism. Int J Androl 10:325–346

Shi H, Hudson LG, Liu KJ (2004) Oxidative stress and apoptosis in metal ion-induced carcinogenesis. Free Radic Biol Med 37:582–593

Sprauten M, Darrah TH, Peterson DR, Campbell ME, Hannigan RE et al (2012) Impact of long-term serum platinum concentrations on neuro- and ototoxicity in cisplatin-treated survivors of testicular cancer. J Clin Oncol 30:300–307

Stewart DJ, Mikhael NZ, Nanji AA, Nair RC, Kacew S et al (1985) Renal and hepatic concentrations of platinum: relationship to cisplatin time, dose, and nephrotoxicity. J Clin Oncol 3:1251–1256

Sun L, Chai Y, Hannigan R, Bhogaraju VK, Machaca K (2007) Zinc regulates the ability of Cdc25C to activate MPF/cdk1. J Cell Physiol 213:98–104

Todd RC, Lippard SJ (2009) Inhibition of transcription by platinum antitumor compounds. Metallomics 1(4):280–291

Tothill P, Klys HS, Matheson LM, McKay K, Smyth JF (1992) The long-term retention of platinum in human tissues following the administration of cisplatin or carboplatin for cancer therapy. Eur J Cancer 28:1358–1361

Travis LB, Holowaty EJ, Bergfeldt K, Lynch CF, Kohler BA et al (1999) Risk of leukemia after platinum-based chemotherapy for ovarian cancer. N Engl J Med 340:351–357

Travis LB, Beard C, Allan JM, Dahl AA, Feldman DR et al (2010) Testicular cancer survivorship: research strategies and recommendations. J Natl Cancer Inst 102:1114–1130

Uozumi J, Ueda T, Yasumasu T, Koikawa Y, Naito S et al (1993) Platinum accumulation in the kidney and liver following chemotherapy with cisplatin in humans. Int Urol Nephrol 25: 215–220

Vernie LN, Goeij JJMD, Zegers C, Vries MD, Baldew GS et al (1988) Cisplatin-induced changes of selenium levels and glutathione peroxidase activities in blood of testis tumor patients. Cancer Lett 40:83–91

Woods JS, Bowers MA, Davis HA (1991) Urinary porphyrin profiles as biomarkers of trace metal exposure and toxicity: Studies on urinary porphyrin excretion patterns in rats during prolonged exposure to methyl mercury. Toxicol Appl Pharmacol 110:464–476

Zhang B, Tang W (1994) Kinetics of the reaction of platinum(ii) complexes with metallothionein. J Inorg Biochem 56:143–153

Zhitkovich A (2004) Importance of chromium DNA adducts in mutagenicity and toxicity of chromium(vi). Chem Res Toxicol 18:3–11

Chapter 3
Atmospheric Particulate Matter (PM) in the Middle East: Toxicity, Trans-boundary Transport, and Influence of Synoptic Conditions

Yigal Erel, O. Tirosh, N. Kessler, U. Dayan, S. Belkin, M. Stein, A. Sandler, and J.J. Schauer

Abstract The Middle East is one of the regions in the world where relatively high concentrations of atmospheric particulate matter (PM) have been detected frequently. It has been suggested that PM levels in the Middle East are present at levels that lead to adverse health effects and to poor visibility. In the current study, we summarize results published by our group over the last decade and introduce new data which demonstrate the extent of trans-boundary PM transport, and the fact that synoptic conditions control its chemical and mineralogical composition and might also affect its toxicity.

Keywords Atmospheric Particulate Matter (PM) • Toxicity • Trans-boundary transport • Trace metals • Genetically engineered bacterial reporter

Y. Erel (✉) • O. Tirosh • N. Kessler
Institute of Earth Sciences, The Hebrew University of Jerusalem, Edmond Safra Givat Ram Campus, Jerusalem 91904, Israel
e-mail: Yigal.Erel@mail.huji.ac.il

U. Dayan
Department of Geography, The Hebrew University of Jerusalem, Mount Scopus Campus, Jerusalem 91904, Israel

S. Belkin
Institute of Life Sciences, The Hebrew University of Jerusalem, Edmond Safra Givat Ram Campus, Jerusalem 91904, Israel

M. Stein • A. Sandler
The Geological Survey of Israel, 30 Malkhe Israel St, Jerusalem 95501, Israel

J.J. Schauer
Department of Civil and Environmental Engineering, 148 Water Science and Engineering Laboratory, University of Wisconsin, 660 North Park Street, Madison, WI 53706-1484, USA

P. Censi et al. (eds.), *Medical Geochemistry: Geological Materials and Health*, DOI 10.1007/978-94-007-4372-4_3,

3.1 Health Effect of Aerosols

The adverse effects of outdoor air pollution on human health, and in particular the harmful effect of high ambient concentrations of fine particles, have been demonstrated by a growing body of studies. The landmark Six Cities Study pointed out that air pollution was positively associated with death from lung cancer and cardiopulmonary disease, and that mortality was most strongly associated with fine particulates (Dockery et al. 1993). In another study conducted in 20 major cities in the USA from 1987 to 1994, it was assessed that the level of atmospheric particles (PM_{10}) is associated with the rate of death from all causes and from cardiovascular and respiratory illnesses (Samet et al. 2000). It was also reported that increases in ozone levels enhanced the relative death rates during the summer, when ozone levels are highest, but not during the winter; levels of the other pollutants (carbon monoxide, sulfur dioxide, and nitrogen dioxide) were not significantly related to the mortality rate. A third study, an 8-year follow-up to the Six Cities Study, reported a longer life span of people living in cities that reduced the amount of airborne fine particulate matter (Laden et al. 2006). More specifically, it was suggested that an average of 3% fewer people died (75,000 people per year in the USA) for every reduction of 1 $\mu g/m^3$ in the average levels of $PM_{2.5}$. These findings remained valid after controlling for the general increase in adult life expectancy in the USA during both the original and follow-up study periods. Numerous additional studies around the world have similarly reported excess morbidity and mortality associated with ambient particulate matter (e.g., Cohen 2005; Neubergera et al. 2007; Bell et al. 2009; Pope et al. 2009; Vedal et al. 2009; Brook et al. 2010 and references therein; Stanek et al. 2011). Furthermore, it has been demonstrated that elevated concentrations of suspended atmospheric particles (PM) are associated with oxidative stress, respiratory and cardiopulmonary diseases, and oxidative DNA damage; they have also been shown to have important impacts on the population, particularly on sensitive individuals including children, pregnant women, and elderly people (Laden et al. 2006; Brook et al. 2010; Delfino et al. 2010; Cao and Frey 2011; Lipfert and Murray 2012). Increasing evidence suggests that exposures to fine particles (less than 2.5 or even less than 1 μm) are associated with the largest health risk compared to coarse particles (Li et al. 2003; Vinzents et al. 2005; Brook et al. 2010). Likewise, the type of particles, their composition, and the amount of toxic components they contain have an important impact on the health of the exposed population (Xia et al. 2004; Brook et al. 2010). For example, Dockery et al. (1993) pointed out that "mortality was most strongly associated with air pollution with fine particulates, including sulfates." The link between PM composition and their health (and toxicity) effects will be discussed in more detail in the next section.

Given the need to reduce the public's risk due to PM exposure, an accurate assessment of the relative impact of different sources, including long-range transboundary transport, is greatly needed. Indeed, a comprehensive 3-year joint study

by the US EPA and the Israeli Ministry of Environmental Protection revealed that PM_{10}, considered to represent the breathable fraction of ambient particles, is responsible for the greatest portion of mortality and morbidity attributable to air pollution in greater Tel Aviv during 1995–1999 (Israel Ministry of Environment Protection 2003). The potential health problems were, in particular, attributed to particles containing organic carbon. Moreover, the Israeli Ministry of Environmental Protection published recently a literature review on the health effects of atmospheric particles, stressing the diverse nature of health problems caused by atmospheric particles, especially, fine and ultrafine particles (Karsenty 2007). Such information can serve as a foundation for the development of control strategies, and to design location-specific health studies that can quantify the spatial distributions of exposure and the relative risk associated with emissions from different sources.

3.2 Toxicity of Atmospheric Particulate Matter

Over the past few years, numerous studies have examined the toxicity of PM. Although mechanisms of PM cellular toxicity are still poorly understood, studies in cellular models suggest a variety of possible mechanisms (Salvi and Holgate 1999; Gonzalez-Flecha 2004; Nel 2005; Oberdorster et al. 2007; Turoczi et al. 2012). One of the main hypotheses under investigation is that PM cytotoxicity derives from oxidative stress, initiated by the formation of reactive oxygen species (ROS; Prahalad et al. 1999; Gonzalez-Flecha 2004; Cho et al. 2005; Cai et al. 2008; Cheung et al. 2010; Ren et al. 2010). Increased production of ROS after PM exposure is suggested by the finding that many of the proinflammatory genes induced upon exposure to PM are regulated by redox-sensitive transcription factors. Activation of these factors has been reported in alveolar and bronchial epithelial cell lines treated with PM (Jimenez et al. 2000; Kennedy et al. 1998; Shukla et al. 2000). As mentioned previously, particle size is thought to have a major effect on particle cytotoxicity. Li et al. (2003) showed that ultrafine particles (UFPs; <1.25 μm) have the highest oxidative activity in a DTT (dithiothreitol) assay in comparison with larger particles. Using electron microscopy, they demonstrated localization of UFPs in the mitochondria, where they induce major structural damage which may contribute to oxidative stress. PM composition also plays a significant role in their cytotoxicity. Organic pollutants, especially polycyclic aromatic hydrocarbons (PAHs), have been found to increase intracellular reactive oxygen species (ROS) (Klein et al. 1992; Penning 1993; Brook et al. 2010) and to be mutagenic in a variety of *in vitro* systems (Binkova et al. 1998; Topinka et al. 2000). Metals which are found in combustion-derived particulate matter, such as Cu, Ni, V, Fe, and Zn, have been studied and found toxic to exposed lung epithelial cells (Adamson et al. 2000; Riley et al. 2003). Special attention has been drawn to Fe, a common element found in atmospheric PM, originating from both natural and anthropogenic

Table 3.1 The nine reporter strains comprising the bioassay panel used by Kessler et al. (2012)

Responsive promoter	Indicated stress	Regulatory control
micF	Superoxide stress	SoxRS
sodA	Superoxide stress	SoxRs
katG	Peroxide stress	OxyR
grpE	Protein damage	"Heat Shock" (*rpoH*)
arsR	Excess As^{+5}/As^{+3}	ArsR
zntA	Excess $Pb^{+2}/Cd^{+2}/Zn^{+2}$	ZntR
recA	DNA damage	"SOS"
cydA	Respiratory inhibition	Arc
fhuF	Iron deficiency	Fur

sources. Iron has been shown to mediate the generation of free radical activity and peroxide formation on the particle's surface (Siefert et al. 1994; Donaldson et al. 1997) and to account for a major fraction of ROS activity of water extracts of PM (Shafer et al. 2010). Auffan et al. (2008) have shown that the redox state of Fe-based nanoparticles has a great influence on their toxicity to *Escherichia coli*, Fe^0 being highly cytotoxic, while the trivalent Fe nano-maghemite had no apparent effect. Hexavalent Cr, a known carcinogen (Dayan and Paine 2001), is also suspected to be a cytotoxic constituent of atmospheric PM. It was observed that yeast cells, defective in their Cu, Zn-superoxide dismutase, were hypersensitive to Cr(VI) under aerobic conditions (Sumner et al. 2005). They established an oxidative mode of Cr toxicity in yeast, which primarily involves oxidative damage to cellular proteins.

Kessler et al. (2012) utilized bioassay techniques to further investigate these aspects. For this purpose, a reporter panel of nine genetically engineered bacterial (*E. coli*) bioreporter strains was composed (Table 3.1). This was done by recombinant DNA technology, namely, fusion of two genetic elements inside the bacteria: (1) a sensing element, a promoter of a gene that is induced as a result of the relevant stress, and (2) a reporter element composed of bacterial bioluminescence genes, the combined expression of which results in light emission. Each panel member was designed to report on a different stress condition by a dose-dependent measurable light signal (Table 3.1). Toxic mechanisms and components were studied using six anthropogenic PM source samples, including two vehicle (gasoline and diesel) combustion particles, three coal fly ash (CFA) samples, and an urban dust sample collected in a parking lot. In addition, a few ambient aerosols collected under different atmospheric conditions were studied. The PM samples were extracted with deionized water and with deionized water + DMSO (dimethyl sulfoxide), and the genetically engineered bacterial strains were exposed to the extracts.

Like in previous studies (Van Maanen et al. 1999), broad panel responses of two of the CFA samples were detected. The activated panels indicate oxidative stress, respiration inhibition, and iron deficiency (Fig. 3.1). These responses were relieved

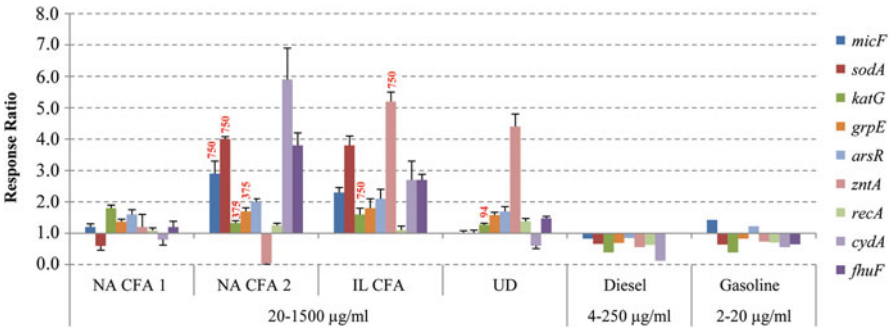

Fig. 3.1 The response ratios (light emission relative to a control) of the three types of coal fly ash sample, the car exhaust samples, and the urban dust (Modified after Kessler et al. (2012))

when the samples were treated with EDTA, suggesting the participation of metals in the observed effects. This was observed by the excess metal sensor as well as by the superoxide and respiratory stress sensors (Fig. 3.2). Indeed, water extracts of these two CFA samples had an order of magnitude higher concentration of Cr relative to all other samples (Table 3.2), suggesting that Cr was related to the toxic responses (Dayan and Paine 2001; Meng et al. 2011).

While the particles collected from the exhausts of the diesel and gasoline cars did not create any effect, the urban dust sample strongly suggested excess metal toxicity (Fig. 3.1). Since the car exhaust samples and the urban dust samples had a similar chemical composition, it was suggested that the difference in response was either related to the higher mass of the urban dust sample or to aging effects that rendered the toxic metals more bioavailable. Also, the urban dust sample had high concentrations (relative to the coal fly ash samples) of several metals including Cu, Co, Ni, Mn, Zn, Cd, Pb, and U. In contrast to all six PM source samples, ambient PM collected on four out of seven occasions caused peroxide stress and much lower superoxide stress (Fig. 3.3). Aerosol samples were collected by a $PM_{2.5}$ sampler located in western Jerusalem on the roof of the Earth Science building at the Safra Campus of the Hebrew University. It is also important to note that in all four occasions, when peroxide stress was detected, the prevailing air masses were arriving to Jerusalem from the Israeli coastal plain (where the major urban center is located); in the three occasions when no stress was detected, the wind directions were variable, and it was more difficult to determine the sources of the air masses. The reporter panel approach is capable of providing important insights with respect to the mechanisms of atmospheric PM toxicity. By combining the reporter panel's results with information obtained on elements released from the PM by aqueous extraction and with other types of sample manipulations (addition of EDTA, extraction with organic solvents), additional insights were gained regarding possible causes of PM toxicity.

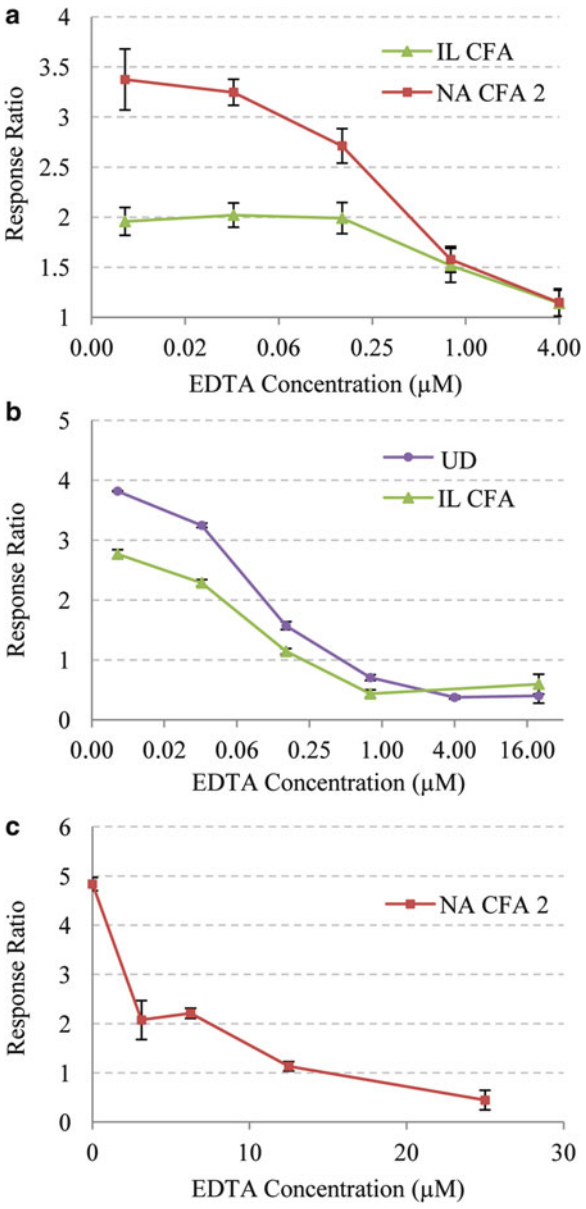

Fig. 3.2 The effect of added EDTA on the response of three reporters: (**a**) excess metal, (**b**) superoxide stress, and (**c**) respiratory stress (Modified after Kessler et al. (2012))

Table 3.2 Element composition of the aqueous extracts of the PM source samples in the bacterial reporters exposures

zntA			Oxidative & metal effect		Low cnc/ no aging	
Element	**Urban Dust**	**NA CFA 1**	**NA CFA 2**	**IL CFA**	**Diesel**	**Gasoline**
Na	4000 (500)	440 (40)	1130 (20)	54 (8)	78	180
Mg	1000 (100)	231 (10)	47 (3)	80 (6)	61	89
Al	55 (6)	740 (60)	10600 (400)	850 (30)	2	3
K	1500 (200)	960 (70)	130 (30)	21 (1)	31	54
Ca	16000 (2000)	8700 (600)	42000 (2000)	13900 (700)	580	860
Cr	0.62 (0.06)	1.12 (0.04)	12.6 (0.4)	9.7 (0.3)	0.17	0.13
Mn	21 (3)	0.04 (0.01)	0.06 (0.02)	0.22 (0.02)	1.05	1.42
Fe	17 (2)	6.4 (0.5)	29 (1)	12.7 (0.8)	1.89	1.83
Co	0.29 (0.04)	BDL	BDL	BDL	0.03	0.02
Ni	1.9 (0.2)	0.2 (0.1)	0.05 (0.04)	BDL	0.21	0.19
Cu	13 (1)	2 (1)	2 (3)	0.09 (0.06)	0.1	0.72
Zn	12 (2)	5 (2)	4 (3)	1.9 (0.5)	69	31
As	0.44 (0.03)	9.8 (0.5)	0.46 (0.04)	0.9 (0.05)	0.1	0.02
Rb	1.1 (0.1)	2.4 (0.2)	0.79 (0.03)	0.08 (0.01)	0.04	0.06
Sr	60 (7)	20 (2)	900 (30)	155 (9)	0.96	1.23
Cd	0.02 (0.01)	BDL	BDL	BDL	BDL	BDL
Pb	0.13 (0.03)	0.04 (0.01)	0.05 (0.01)	BDL	0.04	0.05
U	0.02 (0.01)	BDL	BDL	BDL	BDL	BDL

Adapted from Kessler et al. (2012)
Concentration in the maximal concentration of the exposure experiment (μg/l);
()- Standard deviation; BDL- Below detection limit.

3.3 The Role of Synoptic Classification and Reconstruction of Pollution Pathways

Many studies demonstrated that synoptic climatology is an efficient tool to explain the relationships between atmospheric circulation categories and environmental variables such as air pollutants in general (e.g., Dayan and Levy 2002; Dayan and Lamb 2007; Dayan et al. 2011; Drori et al. 2012) and ambient particulate matter concentration in particular (e.g., Triantafyllou 2001; Kassomenos et al. 2001; Alexandrova et al. 2003; Dayan and Levy 2005; Yang et al. 2007; Guzmán-Torres et al. 2009; Velders and Matthijsen 2009; Buchholz et al. 2010; Demuzere and van Lipzig 2010; Sfetsos and Vlachogiannis 2010; Tai et al. 2010; Tandon et al. 2010; Markovic et al. 2011; Fleming et al. 2011). The results of these circulation–particulate matter studies rely on fitting the spatiotemporal distribution of particulate matter to the spatiotemporal distribution of barometric systems on a synoptic scale.

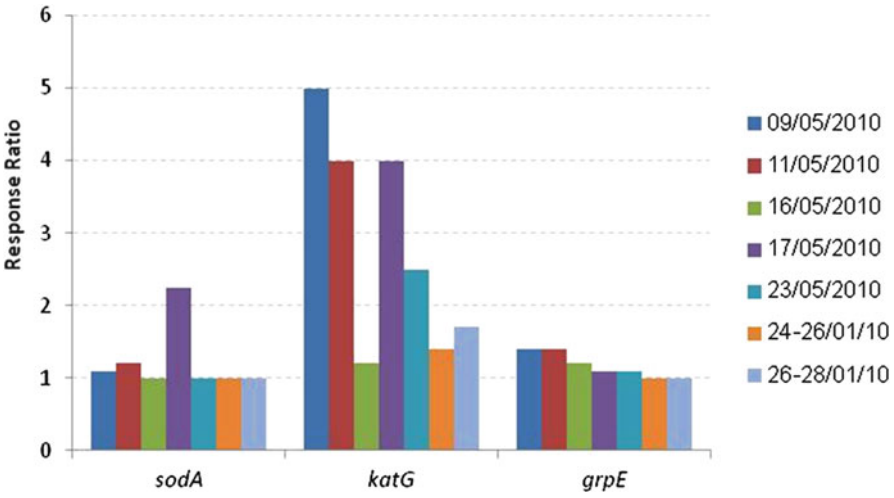

Fig. 3.3 Bacterial reporter responses to atmospheric PM. *sod-A* superoxide stress, *katG* peroxide stress, *grpE* protein damage. Dates indicate sampling periods of the atmospheric PM (Modified after Kessler et al. (2012))

This compatibility leads to distinctive seasonal and diurnal variations in ambient particulate matter concentrations obtained for any particular mode of atmospheric circulation (e.g., Dayan et al. 1991).

Synoptic climatology studies analyzing the associations between atmospheric circulation and PM have been performed over the Eastern Mediterranean and in Israel (Dayan et al. 1991; Moulin et al. 1997; Moulin et al. 1998; Dayan and Levy 2005; Erel et al. 2002, 2006, 2007; Dayan et al. 2007). For example, Moulin et al. (1998) have shown that the frequency of dust outbreaks is strongly related to the climatology of depressions affecting North Africa. Recently it was established that atmospheric particles emitted in two large urban areas affect the Eastern Mediterranean, including Israel. During winter and spring, pollution emitted in Cairo, Egypt, is transported toward Israel along with dust storms (Falkovich et al. 2004; Erel et al. 2006). During the summer, pollution originating in urban centers around the Black Sea is transported to the Eastern Mediterranean region (Erel et al. 2007; Kalderon-Asael et al. 2009). In all studies, it was shown that the concentrations of the aerosols in Israel were affected by the interactions of synoptic circulation types and regional wind flow pattern induced by mesoscale meteorological processes (i.e., land–sea breeze) (Levy et al. 2008, 2009a, b).

The nature of $PM_{2.5}$ in the Middle East (Jordan, the Palestinian Authority, and Israel) was examined by a multinational team led by one of us (JJS – Sarnat et al. 2010). Their findings are plotted in Fig. 3.4, which presents the generalized composition of $PM_{2.5}$ in the Middle East, indicating that the major constituents are organic and elemental carbon, with highly variable concentrations (both spatially and temporally). Terrestrial material is another important constituent, but it has a

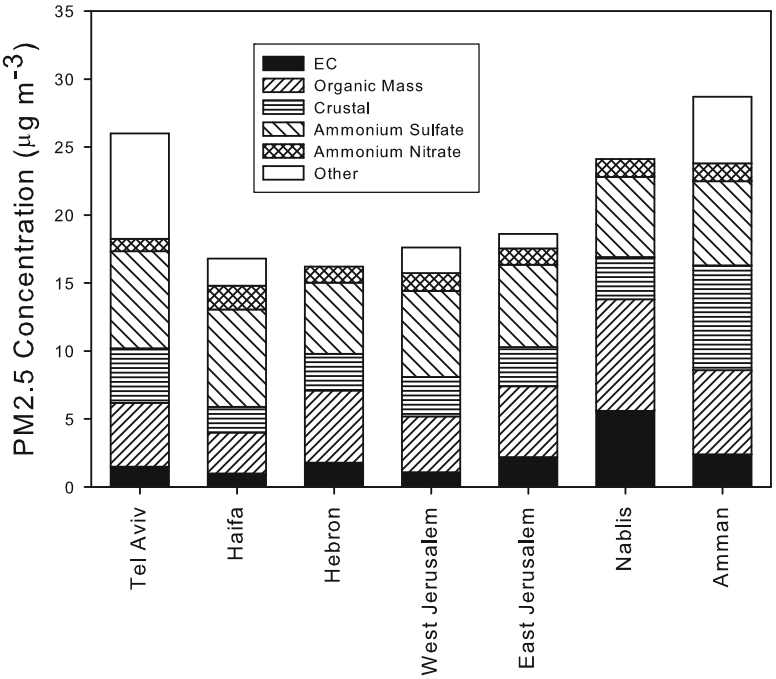

Fig. 3.4 The average composition of $PM_{2.5}$ in the Middle East (Modified after Sarnat et al. (2010))

more uniform distribution over the entire study area. Sulfates have very consistent levels on an annual basis but display seasonal differences across sites, suggesting strong influence of regional sources. Indeed, several studies have shown that the budget of sulfates in the atmosphere of the Middle East is governed by transport from Europe, both in the winter (southwestern Europe) and summer (southeastern Europe) (Luria et al. 1996; Wanger et al. 2000; Lelieveld et al. 2002; Dayan et al. 2002; Rudich et al. 2008). Based on a series of research flights, Matvev et al. (2002) estimated that approximately 15% of the sulfate aerosols emitted over Europe finally reach the Israeli Mediterranean coastline. Furthermore, Kalderon-Asael et al. (2009) demonstrated that the so-called terrestrial fraction of PM arriving to Israel from southeastern Europe in the summer contains approximately 50% anthropogenic phases.

By using a sequential dissolution scheme combined with measurements of Pb isotopic composition and Pb enrichment, Erel et al. (2006) showed that during dust storms, the desert dust arriving to Israel contains significant amounts of pollution, both attached to the desert dust surfaces and also polluted soil particles resuspended and carried by the strong winds generated in the forefront of advancing cyclones. Falkovich et al. (2004) who studied the same dust storms identified various anthropogenic organic compounds (Pesticides, PAH, oxy-PAH) that were attached to the dust particle surfaces. The issue of resuspension of polluted soils has gained

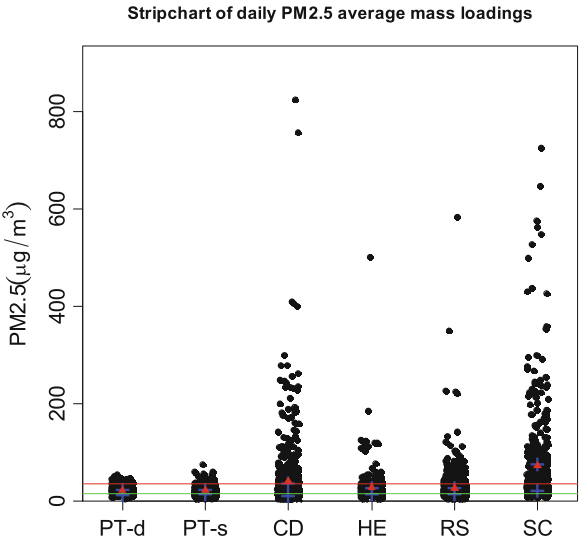

Fig. 3.5 24-h $PM_{2.5}$ load measured across Israel (in more than 20 stations) between 2000 and 2010 grouped according to synoptic conditions. *PT-d* deep Persian trough, *PT-s* shallow Persian trough, *CD* cold depression, *HE* high to the east, *RS* Red Sea trough, *SC* Sharav cyclone

interest in the last few years and was studied extensively in various parts of the world (e.g., Young et al. 2002; Filippelli et al. 2005; Laidlaw and Filippelli 2008; Tiea et al. 2009). A comprehensive summary of the resuspension of soils polluted with Pb may be found in http://www.urbanleadpoisoning.com/.

We have recently analyzed data of $PM_{2.5}$ and PM_{10} collected in more than 20 stations across Israel by the Ministry of Environmental Protection from 2000 to 2010. Samples were grouped according to six synoptic conditions: (1) deep Persian trough (PT-d), (2) shallow Persian trough (PT-s), (3) cold depression (CD), (4) high to the east (EH), (5) Red Sea trough (RS), and (6) Sharav cyclone (SC). The first two modes of PT prevail in the summer and carry mostly air masses from the Eastern part of the Mediterranean and from the region around the Black Sea (Dayan and Levy 2005). Cold depression prevails in the winter and is mostly associated with the arrival of cold fronts to Israel, bringing along with it moist air which produce most of the precipitation in the Middle East. When the cold depression has a southerly track, it carries with it desert dust from North Africa and the Sinai Peninsula. EH and Red Sea troughs carry air masses from Saudi Arabia, Jordan, and the Sinai Peninsula toward Israel that are sometimes associated with minor dust storms. Dayan et al. (1991) showed that transport of Saharan dust from North African sources has usually more intensive mass loading capacity and takes place in deeper atmospheric layers for a longer duration (approx. 2–4 days) than dust storms from the Arabian Desert. Sharav cyclone, which prevails in the spring, has similar air trajectories to the cold depression. A more detailed discussion of these synoptic conditions is given elsewhere (e.g., Dayan and Levy 2005).

Under all synoptic conditions, the $PM_{2.5}$ load (measured on a 24-h basis) exceeded the EPA daily standard of 35 $\mu g/m^3$ in all sampled stations (Fig. 3.5). While less than 10% of the days in the summer when PT condition prevail exceed that level, approximately 15% of the RS and EH days (air from Jordan and Saudi

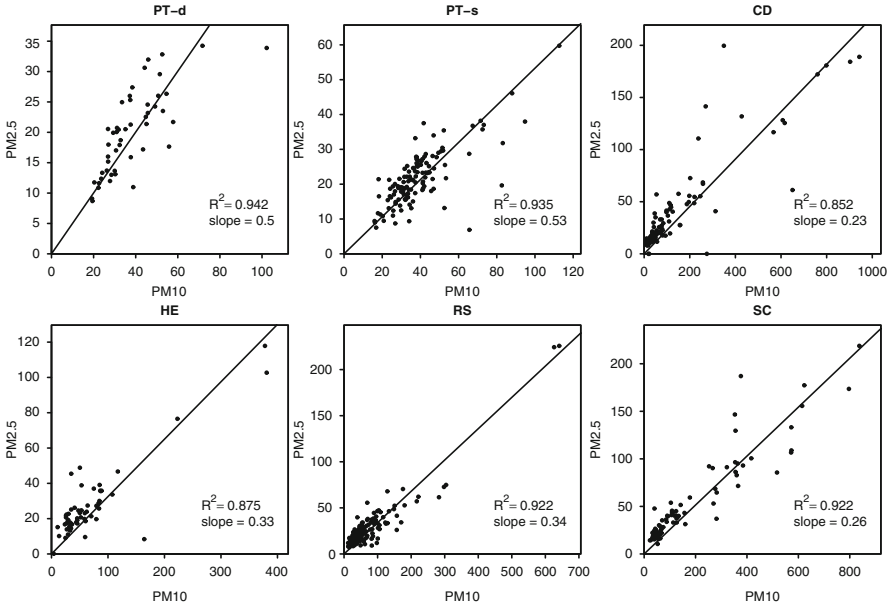

Fig. 3.6 $PM_{2.5}/PM_{10}$ ratio of samples collected across Israel from 2000 to 2010 grouped according to the six categories of synoptic conditions. *PT-d* deep Persian trough, *PT-s* shallow Persian trough, *CD* cold depression, *HE* high to the east, *RS* Red Sea trough, *SC* Sharav cyclone

Arabia), 25% of CD days (air North Africa and the Mediterranean), and 50% of SC days (air North Africa and the Mediterranean) exceeded the standard. Also, when comparing same-synoptic condition days with high and low $PM_{2.5}$ loads, it is generally observed that low $PM_{2.5}$ days occurred when the air masses spent extended period above the Mediterranean prior to their arrival to Israel. The six synoptic conditions also differ in their $PM_{2.5}/PM_{10}$ ratios. The PT samples which carry air from Eastern Europe with large anthropogenic contribution have $PM_{2.5}/PM_{10}$ of about 0.5, the EH and RS samples which contain PM from sources in Saudi Arabia and Jordan have $PM_{2.5}/PM_{10}$ of about 0.33, and the SC and CD samples which contain PM from North Africa have $PM_{2.5}/PM_{10}$ of about 0.25 (Fig. 3.6). These results demonstrate the strong influence of synoptic conditions on the properties of PM in the atmosphere of the Middle East. The use of meteorological data that is constrained by more limited measurements of PM load, composition, and toxicity can open a new paradigm for epidemiological studies and air pollution forecasting. This by no means is constrained to the Middle East, and studies carried out in other regions have yielded similar results which allow forecasting of air pollution episodes based on meteorological data (Dayan and Levy 2005; Guzmán-Torres et al. 2009; Velders and Matthijsen 2009; Buchholz et al. 2010; Demuzere and van Lipzig 2010; Sfetsos and Vlachogiannis 2010; Tai et al. 2010; Tandon et al. 2010; Markovic et al. 2011; Fleming et al. 2011).

3.4 Concluding Remarks

A few important conclusions can be made based on our observations:

- The major PM toxicity observed was oxidative stress related to the presence of transition metals.
- There is a strong effect of sources, and there is a possible effect of PM aging.
- In the Middle East, there is substantial trans-boundary component of particulate matter pollution and associated toxic components.
- There is strong evidence to resuspension of polluted soils.
- Some important PM properties are controlled by synoptic conditions.

Acknowledgments We thank our past students T. Axelrod, J. Jandorf, B. Kalderon, and R. Rabi. We also thank S. Bookman, R. Nissan, E. Refaeli, and D. Stern of the Hebrew University and L. Halitz, S. Ehrlich, O. Yoffe, I. Segal, and N. Teutsch of the Geological Survey of Israel for technical assistance. Financial support for this research was provided by the Israeli Science Foundation, the Israeli Ministry of Environmental Protection, and by the Environmental Health Fund.

References

Adamson IYR, Prieditis H, Hedgecock C, Vincent R (2000) Zinc is the toxic factor in the lung response to an atmospheric particulate sample. Toxicol Appl Pharmacol 166:111–119

Alexandrova OA, Boyer DL, Anderson JR, Fernando HJS (2003) The influence of thermally driven circulation on PM10 concentration in the Salt Lake Valley. Atmos Environ 37:421–437

Auffan M, Achouak W, Rose J, Roncato MA, Chane C, Waite DT, Masion A, Woicik JC, Wiesner MR, Bottero JY (2008) Relation between the redox state of iron-based nanoparticles and their cytotoxicity toward *Escherichia coli*. Environ Sci Technol 42:6730–6735

Bell ML, Ebisu K, Peng RD, Samet JM, Dominici F (2009) Hospital admissions and chemical composition of fine particle air pollution. Am J Respir Crit Care Med 179:1115–1120

Binkova B, Lenicek J, Benes I, Vidova P, Gajdo O, Fried M, Sram RJ (1998) Genotoxicity of coke-oven and urban air particulate matter *in vitro* cellular assays coupled with – postlabeling and HPLC analysis of DNA adducts. Mutat Res/Genet Toxicol Environ Mutagen 414:77–94

Brook RD, Rajagopalan S, Pope CA, Brook JR, Bhatnagar A, Diez-Roux AV, Holguin F, Hong Y, Luepker RV, Mittleman MA et al (2010) Particulate matter air pollution and cardiovascular disease. Circulation 121:2331–2378

Buchholz S, Junk J, Krein A, Heinemann G, Hoffmann L (2010) Air pollution characteristics associated with mesoscale atmospheric patterns in northwest continental Europe. Atmos Environ 44:5183–5190

Cai C, Hogrefe C, Katsafados P, Kallos G, Beauharnois M, Schwab JJ, Ren X, Brune WH, Zhou X, He Y, Demerjian KL (2008) Performance evaluation of an air quality forecast modeling system for a summer and winter season – photochemical oxidants and their precursors. Atmos Environ 42(37):8585–8599

Cao Y, Frey HC (2011) Geographic differences in inter-individual variability of human exposure to fine particulate matter. Atmos Environ 45:5684–5691

Cheung KL, Ntziachristos L, Tzamkiozis T, Schauer JJ, Samaras Z, Moore KF, Sioutas C (2010) Emissions of particulate trace elements, metals and organic species from gasoline, diesel, and biodiesel passenger vehicles and their relation to oxidative potential. Aerosol Sci Technol 44:500–513

Cho AK, Sioutas C, Miguel AH, Kumagai Y, Schmitz DA, Singh M, Eiguren-Fernandez A, Froines JR (2005) Redox activity of airborne particulate matter at different sites in the Los Angeles Basin. Environ Res 99:40–47

Cohen AJ (2005) The global burden of disease due to outdoor air pollution. J Toxicol Environ Health A 68:1301–1307

Dayan U, Lamb D (2007) Influences of atmospheric circulation on the variability of wet sulfate deposition. Int J Climatol. doi:10.1002/joc

Dayan U, Levy I (2002) Relationship between synoptic-scale atmospheric circulation and ozone concentrations over Israel. J Geophys Res 107(D24):4813. doi:2002JD00214

Dayan U, Levy I (2005) The influence of seasonal meteorological conditions and atmospheric circulation types on PM10 and visibility in Tel-Aviv, Israel. J Appl Meteorol 44:606–619

Dayan AD, Paine AJ (2001) Mechanisms of chromium toxicity, carcinogenicity and allergenicity: review of the literature from 1985 to 2000. Hum Exp Toxicol 20:439–451

Dayan U, Heffter J, Miller B, Gutman G (1991) Dust intrusion events into the Mediterranean basin. J Appl Meteorol 30(8):1185–1199

Dayan U, Lifshitz-Goldreich B, Pick K (2002) Spatial and structural variation of the atmospheric boundary layer during summer in Israel – profiler and Rawinsonde measurements. J Appl Meteorol 41:447–457

Dayan U, Ziv B, Shoop T, Enzel Y (2007) Suspended dust over South-Eastern Mediterranean and its relation to atmospheric circulations. Int J Climatol. doi:10.1002/joc.1587

Dayan U, Tubi A, Levy I (2011) On the importance of synoptic classification methods with respect to environmental phenomena. Int J Climatol. doi:10.1002/joc.2297

Delfino R, Staimer N, Tjoa T, Arhami M, Polidori A, Gillen DL, George SC, Shafer MM, Schauer JJ, Sioutas C (2010) Associations of primary and secondary organic aerosols with airway and systemic inflammation in an elderly panel cohort. Epidemiology 21:892–902

Demuzere M, van Lipzig NPM (2010) A new method to estimate air-quality levels using a synoptic-regression approach. Part I: present-day O3 and PM10 analysis. Atmos Environ 44:1341–1355

Dockery DW, Pope CA, Xu X, Spengler JD, Ware JH, Fay ME, Ferris BG, Speizer FE (1993) An association between air pollution and mortality in six US cities. N Engl J Med 329:1753–1759

Donaldson K, Brown DM, Mitchell C, Dineva M, Beswick PH, Gilmour P, MacNee W (1997) Free radical activity of PM10: iron-mediated generation of hydroxyl radicals. Environ Health Perspect 105:1285–1289

Drori R, Dayan U, Edwards DP, Emmons LK, Erlick C (2012) Attributing and quantifying carbon monoxide sources affecting the Eastern Mediterranean: a combined satellite, modelling, and synoptic analysis study. Atmos Chem Phys 12:1067–1082

Erel Y, Axelrod T, Veron A, Mahrer Y, Katsafados P, Dayan U (2002) Trans-boundary atmospheric lead pollution. Environ Sci Technol 36:3230–3233

Erel Y, Dayan U, Rabi R, Rudich Y, Stein M (2006) Trans boundary transport of pollutants by atmospheric mineral dust. Environ Sci Technol 40:2996–3005

Erel Y, Kalderon-Asael B, Dayan U, Sandler A (2007) European atmospheric pollution imported by cooler air masses to the Eastern Mediterranean during the summer. Environ Sci Technol 41:5198–5203

Falkovich AH, Schkolnik G, Ganor E, Rudich Y (2004) Adsorption of organic compounds pertinent to urban environments onto mineral dust particles. J Geophys Res-Atmos 109(D2): 1–19

Filippelli GM, Laidlaw MAS, Latimer JC, Raftis R (2005) Urban lead poisoning and medical geology: an unfinished story. GSA Today 15:4–11

Fleming ZL, Monks PS, Manning AJ (2011) Review: untangling the influence of air-mass history in interpreting observed atmospheric composition. Atmos Res 104–105:1–39

Gonzalez-Flecha B (2004) Oxidant mechanisms in response to ambient air particles. Mol Aspects Med 25:169–182

Guzmán-Torres D, Eiguren-Fernández A, Cicero-Fernández P, Maubert-Franco M, Retama-Hernández A, Ramos Villegas R, Miguel AH (2009) Effects of meteorology on diurnal and nocturnal levels of priority polycyclic aromatic hydrocarbons and elemental and organic carbon in PM10 at a source and a receptor area in Mexico City. Atmos Environ 43:2693

Israel Ministry of the Environment (2003) A comparative assessment of air pollution public health risks in two Israeli metropolitan areas: 1995–1999. Rep. 1222 in cooperation with Israel Union for Environmental Defense, Tel-Aviv Municipality, Ashdod-Yavne Regional Association of Towns for Environmental Protection, and US Environmental Protection Agency, 94 pp

Jimenez LA, Thompson J, Brown DA, Rahman I, Antonicelli F, Duffin R, Drost EM, Hay RT, Donaldson K, MacNee W (2000) Activation of NF-B by PM10 occurs via an iron-mediated mechanism in the absence of I B degradation. Toxicol Appl Pharmacol 166:101–110

Kalderon-Asael B, Erel Y, Sandler A, Dayan U (2009) Mineralogical and chemical characterization of suspended atmospheric particles over the east Mediterranean based on synoptic-scale circulation patterns. Atmos Environ 43(25):3963–3970

Karsenty E (2007) The health impact of atmospheric pollution of suspended particles – a literature review for the ministry for environmental protection (in Hebrew)

Kassomenos P, Gryparis A, Samoli E, Katsouyanni K, Lykoudis S, Flocas HA (2001) Atmospheric circulation types and daily mortality in Athens, Greece. Environ Health Perspect 109:591–596

Kennedy T, Ghio AJ, Reed W, Samet J, Zagorski J, Quay J, Carter J, Dailey L, Hoidal JR, Devlin RB (1998) Copper-dependent inflammation and nuclear factor-kappaB activation by particulate air pollution. Am J Respir Cell Mol Biol 19:366–378

Kessler N, Schauer JJ, Yagur-Kroll S, Melamed S, Tirosh O, Belkin S, Erel Y (2012) Development of a bacterial bioreporter panel to measure cytotoxicity of atmospheric particulate matter and related particulate matter emissions

Klein J, Post K, Seidel A, Frank H, Oesch F, Platt KL (1992) Quinone reduction and redox cycling catalysed by purified rat liver dihydrodiol/3 [alpha]-hydroxysteroid dehydrogenase. Biochem Pharmacol 44:341–349

Laden F, Schwartz J, Speizer FE, Dockery DW (2006) Reduction in fine particulate air pollution and mortality extended follow-up of the Harvard six cities study. Am J Respir Crit Care Med 173:667–672

Laidlaw MAS, Filippelli GM (2008) Resuspension of urban soils as a persistent source of lead poisoning in children: a review and new directions. Appl Geochem. doi:10.1016/j.apgeochem.2008.05.009

Lelieveld J, Berresheim H, Borrmann S, Crutzen PJ, Dentener FJ, Fischer H, Feichter J, Flatau PJ, Heland J, Holzinger R, Korrmann R, Lawrence MG, Levin Z, Markowicz KM, Mihalopoulos N, Minikin A, Ramanathan V, Reus MD, Roelofs GJ, Scheeren HA, Sciare J, Schlager H, Schultz M, Siegmund P, Steil B, Stephanou EG, Stier P, Traub M, Warneke C, Williams J, Ziereis H (2002) Global air pollution crossroads over the Mediterranean. Science 298:794–799

Levy I, Dayan U, Mahrer I (2008) A 5-yr study of the coastal recirculation and its effect on air pollutants over the East Mediterranean region. J Geophys Res 113. doi:10.1029/07JD009529

Levy I, Mahrer Y, Dayan U (2009a) Coastal and synoptic recirculation affecting air pollutants dispersion: a numerical study. Atmos Environ 43(12):1991–1999

Levy I, Dayan U, Mahrer I (2009b) Differing atmospheric scales of motion and their impact on air pollutants. Int J Climatol. doi:10.1002/joc.1905

Li N, Sioutas C, Cho A, Schmitz D, Misra C, Sempf J, Wang M, Oberley T, Froines J, Nel A (2003) Ultrafine particulate pollutants induce oxidative stress and mitochondrial damage. Environ Health Perspect 111:455–456

Lipfert FW, Murray CJ (2012) Air pollution and daily mortality: a new approach to an old problem. Atmos Environ 55:467–474

Luria M, Peleg M, Sharf G, Siman Tov-Alper D, Spitz N, Ben Ami Y, Gawii Z, Lifschitz B, Yitzchaki A, Seter I (1996) Atmospheric sulfur over the east Mediterranean region. J Geophys Res 101D:25,917–25,930

Markovic MZ, Hayden KL, Murphy JG, Makar PA, Ellis RA, Chang RYW, Slowik JG, Mihele C, Brook J (2011) The effect of meteorological and chemical factors on the agreement between observations and predictions of fine aerosol composition in southwestern Ontario during BAQS-Met. Atmos Chem Phys 11:3195–3210

Matvev V, Dayan U, Tass I, Peleg M (2002) Atmospheric sulfur flux rates to and from Israel. Sci Total Environ 291:143–154

Meng Q, Fan Z, Buckley B, Lin L, Huang L, Yu C-H, Stiles R, Bonanno L (2011) Development and evaluation of a method for hexavalent chromium in ambient air using IC-ICP-MS. Atmos Environ 45(12):2021–2027

Moulin C, Lambert CE, Dulac F, Dayan U (1997) Control of atmospheric export of dust from North Africa by the North Atlantic oscillation. Nature 387:691–694

Moulin C, Lamber CE, Dayan U, Masson V, Ramonet M, Bousquet P, Legrand M, Balkanski YJ, Guelle W, Marticorena B, Bergametti G, Dulac F (1998) Satellite climatology of African dust transport in the Mediterranean atmosphere. J Geophys Res 103(D11):13137–13144

Nel A (2005) Atmosphere enhanced: air pollution-related illness: effects of particles. Science 308:804–806

Neubergera M, Rabczenkob D, Moshammer H (2007) Extended effects of air pollution on cardiopulmonary mortality in Vienna. Atmos Environ 41:8549–8556

Oberdorster G, Stone V, Donaldson K (2007) Toxicology of nanoparticles: a historical perspective. Nanotoxicology 1:2–25

Penning TM (1993) Dihydrodiol dehydrogenase and its role in polycyclic aromatic hydrocarbon metabolism. Chem Biol Interact 89:1–34

Pope CA III, Ezzati M, Dockery DW (2009) Fine-particulate air pollution and life expectancy in the United States. N Engl J Med 360:376–386

Prahalad AK, Soukup JM, Inmon J, Willis R, Ghio AJ, Becker S, Gallagher JE (1999) Ambient air particles: effects on cellular oxidant radical generation in relation to particulate elemental chemistry. Toxicol Appl Pharmacol 158:81–91

Ren C, Park SK, Vokonas PS, Sparrow D, Wilker E, Baccarelli A, Suh HH, Tucker KL, Wright RO, Schwartz J (2010) Air pollution and homocysteine: more evidence that oxidative stress-related genes modify effects of particulate air pollution. Epidemiology 21:198–206

Riley MR, Boesewetter DE, Kim AM, Sirvent FP (2003) Effects of metals Cu, Fe, Ni, V, and Zn on rat lung epithelial cells. Toxicology 190:171–184

Rudich Y, Kaufman J, Dayan U, Hongbin Y, Kleidman RG (2008) Estimation of transboundary transport of pollution aerosols by remote sensing in the eastern Mediterranean. J Geophys Res Atmos 113(D14):D14S13

Salvi M, Holgate D (1999) Mechanisms of particulate matter toxicity. Clin Exp Allergy 29:1187–1194. doi:10.1046/j.1365-2222.1999.00576.x

Samet JM, Dominici F, Curriero FC, Coursac I, Zeger SL (2000) Fine particulate air pollution and mortality in 20 US cities, 1987–1994. N Engl J Med 343:1742–1749

Sarnat JA, Moise T, Shpund J, Liu Y, Pachon JE, Qasrawi R, Abdeen Z, Brenner S, Nassar K, Schauer JJ (2010) Assessing the spatial and temporal variability of fine particulate matter components in Israeli, Jordanian, and Palestinian cities. Atmos Environ 44:2383–2392

Sfetsos A, Vlachogiannis D (2010) A new approach to discovering the causal relationship between meteorological patterns and PM10 exceedances. Atmos Res 98:500–511

Shafer MM, Perkins DA, Antkiewicz DS, Stone EA, Quraishi TA, Schauer JJ (2010) Reactive oxygen species activity and chemical speciation of size-fractionated atmospheric particulate matter from Lahore, Pakistan: an important role for transition metals. J Environ Monit 12. doi:10.1039/b915008k

Shukla A, Timblin C, BeruBe K, Gordon T, McKinney W, Driscoll K, Vacek P, Mossman BT (2000) Inhaled particulate matter causes expression of nuclear factor (NF)-kappaB-related genes and oxidant-dependent NF-kappaB activation *in vitro*. Am J Respir Cell Mol Biol 23:182–187

Siefert R, Pehkonen S, Erel Y, Hoffmann MR (1994) Photoproduction of H_2O_2 in aqueous suspensions of ambient aerosol with oxalate. Geochim Cosmochim Acta 58:3271–3280

Stanek LW, Sacks JD, Dutton SJ, Dubois JJB (2011) Attributing health effects to apportioned components and sources of particulate matter: an evaluation of collective results. Atmos Environ 45(32):5655–5663

Sumner ER, Shanmuganathan A, Sideri TC, Willetts SA, Houghton JE, Avery SV (2005) Oxidative protein damage causes chromium toxicity in yeast. Microbiology 151:1939–1948

Tai APK, Mickley LJ, Jacob DJ (2010) Correlations between fine particulate matter (PM2.5) and meteorological variables in the United States: implications for the sensitivity of PM2.5 to climate change. Atmos Environ 44:3976–3984

Tandon A, Yadav S, Attri AK (2010) Coupling between meteorological factors and ambient aerosol load. Atmos Environ 44:1237–1243

Tiea X, Wub D, Brasseura G (2009) Lung cancer mortality and exposure to atmospheric aerosol particles in Guangzhou, China. Atmos Environ 43:2375–2377

Topinka J, Schwarz LR, Wiebel FJ, Cerna M, Wolff T (2000) Genotoxicity of urban air pollutants in the Czech Republic Part II. DNA adduct formation in mammalian cells by extractable organic matter. Mutat Res Genet Toxicol Environ Mutagen 469:83–93

Triantafyllou AG (2001) PM10 pollution episodes as a function of synoptic climatology in a mountainous industrial area. Environ Pollut 112:491–500

Turoczi B, Hoffer A, Toth A, Kovats N, Acs A, Ferincz A, Kovacs A, Gelencser A (2012) Comparative assessment of ecotoxicity of urban aerosol. Atmos Chem Phys Discuss 12: 8533–8546

Van Maanen JMS, Borm PJA, Knaapen A, van Herwijnen M, Schilderman PAEL, Smith KR, Aust AE, Tomatis M, Fubini B (1999) *In vitro* effects of coal fly ashes: hydroxyl radical generation, iron release, and DNA damage and toxicity in rat lung epithelial cells. Inhal Toxicol 11: 1123–1141

Vedal S, Hannigan MP, Dutton SJ, Miller SL, Milford JB, Rabinovitch N, Kim SY, Sheppard L (2009) The Denver Aerosol Sources and Health (DASH) study: overview and early findings. Atmos Environ 43(9):1666–1673

Velders GJM, Matthijsen J (2009) Meteorological variability in NO_2 and PM10 concentrations in the Netherlands and its relation with EU limit values. Atmos Environ 43:3858–3866

Vinzents PS, Moller P, Sorensen M, Knudsen LE, Hertel O, Jensen FP, Schibye B, Loft S (2005) Personal exposure to ultrafine particles and oxidative DNA damage. Environ Health Perspect 113:1485

Wanger A, Peleg M, Sharf G, Mahrer Y, Dayan U, Kallos G, Kotroni V, Lagouvardos K, Varinou M, Papadopoulos A, Luria M (2000) Some observational and modeling evidence of long range transport of air pollutants from Europe towards the Israeli coast. J Geophys Res 105(D6): 7177–7186

Xia T, Korge P, Weiss JN, Li N, Venkatesen MI, Sioutas C, Nel A (2004) Quinones and aromatic chemical compounds in particulate matter (PM) induce mitochondrial dysfunction: implications for ultrafine particle toxicity. Environ Health Perspect 112:1347–1358

Yang YQ, Hou Q, Zhou CH, Liu HL, Wang YQ, Niu T (2007) Sand/dust storms over Northeast Asia and associated large-scale circulations in spring 2006. Atmos Chem Phys Discuss 7: 9259–9281

Young TM, Heerman DA, Sirin G, Ashbaugh LL (2002) Resuspension of soil as a source of airborne lead near industrial facilities and highways. Environ Sci Technol 36:2484–2490

Chapter 4
Reaction Path Modeling: Theoretical Aspects and Applications

L. Marini

Abstract Reaction path modeling is an effective geochemical tool used by geochemists to predict water–rock interaction processes for approximately 45 years. In this chapter, theoretical aspects of reaction path modeling are presented and discussed together with some examples of application, taken from the available scientific literature and relating to the interaction of earth materials with simulated lung fluids. In two of these examples, on the dissolution of chrysotile and other common silicates in lung fluids, reaction path modeling highlights the importance of precipitation of secondary minerals, including hydroxyapatite. In the third example, yttrium and lanthanides are used to investigate the precipitation of phosphatic microcrystals in intra-alveolar areas of lungs, triggered by inhalation of volcanic dust and interactions with lung fluids. At present, geochemical modeling can be performed by referring to simplified systems due to the lack of a comprehensive thermodynamic database. Nevertheless, the experience gained by geochemists on water–rock interaction processes has great potential for collaborations between medical geochemists and biomedical experts.

Keywords Reaction path modeling • Water-rock interaction • Dissolution-precipitation reactions • Human lung fluids

4.1 Introduction

The adverse effects of several geological materials (e.g., asbestos, silica, coal dust, concrete, urban particulate, glass wool, mineral wool, edible soil, volcanic ash, wildfire smoke and ash) on human health has been the subject of recent

L. Marini (✉)
Consultant in Applied Geochemistry, via Fratti 253, I-55049 Viareggio (LU), Italy
e-mail: luigimarini@rocketmail.com

P. Censi et al. (eds.), *Medical Geochemistry: Geological Materials and Health*, DOI 10.1007/978-94-007-4372-4_4,

comprehensive reviews by Plumlee et al. (2006) and Plumlee and Ziegler (2007). As recognized by these authors, these effects result from complex pathways whose first necessary step is the interaction of geological materials with the human body through key interfaces, such as the respiratory tract, gastrointestinal tract, skin, and open wounds, where aqueous solutions are present: lung fluids, gastrointestinal fluids, sweat, and blood plasma, respectively.

Human body fluids are also involved in: (i) normal and pathological mineralization processes, including production of bones, teeth, otoconia, kidney stones, uric acid stones, gallstones, and development of calcified vasculature and (ii) reactions occurring upon implantation in the human body of biomaterials (Sahai 2007 and references therein).

From the geochemists' point of view, all the processes recalled above are similar to water–rock interaction processes, which can be studied using the analytical and numerical techniques developed and refined during the second half of the twentieth century. One of these numerical methodologies is reaction path modeling, which allows one to predict the evolution of multicomponent–multiphase systems, where several homogeneous and heterogeneous reactions may occur, based on the pillars of thermodynamics and chemical kinetics.

The main aim of this chapter is to provide an overview of reaction path modeling and to present some applicative examples, taken from the scientific literature, of this powerful tool on the interaction of geological materials with human body fluids (Wood et al. 2006; Taunton et al. 2010; Censi et al. 2011). Further details on reaction path modeling are given in Bethke (2008).

4.2 From Equilibrium Models to Reaction Path Modeling

Perhaps the first ever equilibrium model was developed by Garrels and Thompson (1962), who computed the distribution of aqueous species (also called speciation) in seawater starting from its bulk composition as determined emperically. To appreciate the difference between bulk composition and speciation, let us refer to dissolved magnesium in average seawater, whose total concentration is 1,290 mg/kg, which corresponds to 0.05501 mol/kg. Results of equilibrium models indicate that the prevailing species of dissolved magnesium is free ion Mg^{2+}, with a concentration of 0.03975 mol/kg, accounting for 72.3% of total Mg concentration. The remaining $0.05501 - 0.03975 = 0.01526$ mol/kg is contributed by aqueous complexes, mainly $MgCl^{+}$ (0.009126 mol/kg, 16.6%), $MgSO_4^{\circ}$ (0.005767 mol/kg, 10.5%), $MgHCO_3^{+}$ (0.0001981 mol/kg, 0.4%), and $MgCO_3^{\circ}$ (0.0001068 mol/kg, 0.2%).

How is aqueous speciation computed? The equilibrium state is defined by (a) a set of mass balance equations, one for each chemical component; (b) a set of mass action equations, or thermodynamic equilibrium constants, one for each aqueous complex; and (c) the charge balance equation, as required by the principle of electroneutrality. For instance, the total analytical molality of Mg, $m_{Mg,\,tot}$, is given

by the following mass balance:

$$m_{\mathrm{Mg,tot}} = m_{\mathrm{Mg^{2+}}} + m_{\mathrm{MgCl^{+}}} + m_{\mathrm{MgSO_4^{\circ}}} + m_{\mathrm{MgHCO_3^{+}}} + m_{\mathrm{MgCO_3^{\circ}}} + \cdots \tag{4.1}$$

where m_i is the molal concentration of the i-th aqueous species. The $MgCl^+$ aqueous complex, for an example, is related to free ions Mg^{2+} and Cl^- (both of which are component species) by the dissociation reaction:

$$\mathrm{MgCl^{+}} = \mathrm{Mg^{2+}} + \mathrm{Cl^{-}} \tag{4.2}$$

whose thermodynamic equilibrium constant is

$$K_{\mathrm{MgCl^{+}}} = \frac{a_{\mathrm{Mg^{2+}}} \cdot a_{\mathrm{Cl^{-}}}}{a_{\mathrm{MgCl^{+}}}} = \frac{m_{\mathrm{Mg^{2+}}} \cdot m_{\mathrm{Cl^{-}}} \cdot \gamma_{\mathrm{Mg^{2+}}} \cdot \gamma_{\mathrm{Cl^{-}}}}{m_{\mathrm{MgCl^{+}}} \cdot \gamma_{\mathrm{MgCl^{+}}}} \tag{4.3}$$

where a_i and γ_i are the activity and the activity coefficient of the i-th aqueous species, respectively.

Since activity coefficients are involved in mass action equations (e.g., Eq. 4.3), suitable relations to compute activity coefficients have also to be taken into account to solve the set of equations of interest. Activity coefficients of individual ionic solutes are generally computed by means of the extended Debye–Hückel equation:

$$\log \gamma_i = -\frac{A_\gamma \cdot Z_i^2 \cdot \sqrt{I}}{1 + \mathring{a}_i \cdot B_\gamma \cdot \sqrt{I}} + B^{\circ} \cdot I \tag{4.4}$$

where Z_i and $\mathring{a}_i$ are the charge and the temperature-independent ion-size parameter of the i-th ion, respectively; A_γ and B_γ are functions of temperature as well as density and the dielectric constant of the solvent; and I is the ionic strength of the aqueous solution. This is defined by the relation:

$$I = \frac{1}{2} \sum_i m_i \cdot Z_i^2 \tag{4.5}$$

Equation 4.4, also known as B-dot equation, was derived by Helgeson (1969) referring to the experimental data available for NaCl aqueous solutions up to temperature of 300°C and ionic strength of 3 mol/kg. The B-dot equation generally works satisfactorily up to ionic strengths close to 1 mol/kg, if the composition of the aqueous solution is dominated by Na and Cl. In fact, at higher ionic strengths, activity coefficients depend not only on the ionic strength of the aqueous solution but also on the concentrations of major solutes, as it was shown experimentally long ago (e.g., Harned and Owen 1958). Therefore, the use of the Pitzer's model (Pitzer 1979, 1987, 1992), involving suitable interaction parameters, is needed for concentrated electrolytes, especially for compositions different from NaCl. Considering that the inorganic part of blood plasma has ionic strength of 0.14 mol/kg (data from Plumlee and Ziegler 2007), the use of the B-dot equation should be acceptable in medical geochemistry.

Going back to the set of equations to be solved for computing the equilibrium state, it must be noted that activity coefficients are a function of ionic strength which, in turn, depends on the results of these calculations. Therefore, an iterative approach is needed to compute the equilibrium state. Today, this task is easily accomplished using different computer codes, the most popular of which are probably MINTEQA2 (Allison et al. 1991), WATEQ4F (Ball and Nordstrom 1991), PHREEQC (Parkhurst and Appelo 1996), and EQ3 (Wolery and Jarek 2003). However, amazingly, Garrels and Thompson (1962) computed the aqueous speciation of seawater by hand!

Why is aqueous speciation so important? Saturation states, one of the results of speciation models, indicate whether an aqueous solution has the potential to precipitate or dissolve a mineral or a gas phase. Moreover, the relative importance of individual aqueous complexes can be established. Today, equilibrium models are frequently used in fluid geochemistry and are applied to different targets including water management, mitigation of water pollution, acid mine drainage, radioactive waste storage, geological sequestration of CO_2, and exploration and exploitation of geothermal energy.

A different type of model was explored by Garrels and Mackenzie (1967), through the simulation of the reactions occurring during the progressive evaporation of spring water. First, they computed aqueous speciation in the initial spring water. Then, they removed step-by-step a given amount of water and recomputed the distribution of each aqueous species. In this way, geochemical modeling was extended from a single state to a number of states and a thus whole process was simulated.

4.3 Reaction Path Modeling: Generalities and Theoretical Aspects

Starting from the pioneering work of Garrels and Mackenzie (1967), the full-fledged methodology of reaction path modeling was proposed by Helgeson and coworkers at the end of the 1960s. The relationships needed to describe the irreversible water–rock mass transfer processes were presented and discussed by Helgeson (1968). Helgeson and coworkers wrote the first computer program for reaction path modeling, named PATHI ("path one"), and applied this technique to study several processes of geochemical interest, including weathering, hydrothermal alteration and ore deposition, sediment diagenesis, and evaporation (e.g., Helgeson et al. 1969, 1970). After a decade, two software packages for geochemical modeling were made available to the geochemical community: EQ3/6 by Wolery (1979) and SOLVEQ/CHILLER by Reed (1977, 1982).

Reaction path modeling allows one to compute the amounts of precipitated secondary phases (product solid phases) and the chemical composition of the aqueous solution during the progressive dissolution of one or more primary mineral phases (reactant solid phases). Through these geochemical models, it is possible

to predict the behavior and fate of the different chemical elements and species, in particular of the so-called potentially harmful elements and species (PHES) in the course of the considered process.

The system under investigation, comprised of one or more primary solid phases, an aqueous solution and possible secondary minerals, can be assumed to be in communication with one or more external gas reservoirs fixing the partial pressure of each considered gas at a constant value, specified at the beginning of each simulation. In this case, the system is said to be open with respect to the considered gas. The alternative situation, in which the gas is not provided to the system, is the so-called closed-system condition. Among gases, O_2 and CO_2 are very important in blood plasma, with arterial P_{O_2} of 0.132 atm, venous P_{O_2} of 0.02–0.053 atm, arterial P_{O_2} of 0.053 atm, and venous P_{CO_2} of 0.06 atm (Plumlee and Ziegler 2007). Moreover, the system of interest can be treated as open or closed with respect to secondary solid phases, whether they remain in the system or are removed from it. Unfortunately, application of the second approach by means of the EQ6 code (the so-called flow-through open system) is hindered by computation problems pertinent to the management of moles of secondary solid phases.

A complicated issue is the treatment of redox reactions. In general, redox reactions are slow or relatively slow and the condition of redox equilibrium is not attained. An example is represented by organic substances which are metastable with respect to either CO_2 or CH_4 or both, depending on the redox potential of the system. For instance, only CO_2 should be present in blood plasma, under the P_{O_2} values specified above, instead of the myriad of organic molecules which are actually present. Therefore, the condition of redox equilibrium cannot be used in geochemical modeling, at least for describing carbon speciation, and the concentrations of all relevant inorganic and organic component species have to be specified as input data in calculations.

Treatment dissolution reaction and trace elements release and fate are the subject of the next sections.

4.3.1 Description of Dissolution–Precipitation Reactions in Stoichiometric Mode or Time Mode

The advancement of chemical reactions can be described in terms of either thermodynamics only or in combination with chemical kinetics as well. Thermodynamics quantifies the energy differences controlling the evolution of the chemical reactions of interest. For example, focusing on a simple system comprising an aqueous solution and a single dissolving mineral, the decimal logarithm of the Q/K_{sp} ratio (where K_{sp} is the solubility product of the solid phase and Q is the corresponding activity product), known as saturation index, $SI = \log (Q/K_{sp})$, indicates the distance from the equilibrium condition. The dimensionless Q/K_{sp} ratio can be transposed in terms of energy taking its natural logarithm and multiplying it by R (the universal

gas constant, either 1.987165 cal mol^{-1} K^{-1} or 8.31441 J mol^{-1} K^{-1}) and T (the absolute temperature, in K). The obtained variable is known as thermodynamic affinity, A:

$$A = R \cdot T \cdot \ln \frac{Q}{K_{sp}} = R \cdot T \cdot \mathrm{SI} \cdot \ln(10) \tag{4.6}$$

Both the saturation index and thermodynamic affinity are negative numbers during the dissolution processes, as long as the aqueous solution is undersaturated with respect to the dissolving mineral, and zero at equilibrium, where the dissolution process ends.

Thermodynamic models are based on the hypothesis of attainment of equilibrium (either partial, metastable, or stable) and do not give any information on the time necessary for the advancement of chemical reactions. In general, fast and reversible reactions attaining chemical equilibrium can be satisfactorily treated from the thermodynamic point of view. In contrast, the treatment of irreversible and slow processes, such as the heterogeneous reactions involving an aqueous solution and one or more solid phases, cannot leave kinetics out of consideration. Coupling thermodynamics and chemical kinetics, the advancement of irreversible reactions toward the final equilibrium condition and the time needed to attain it can be suitably described.

Lung fluids interacting with inhaled silicate minerals constitute an example of a multiphase–multicomponent system, which is out of equilibrium in the beginning, particularly if primary solid phases are formed at high pressure and high temperature. Given enough time, chemical reactions between lung fluids and silicate minerals will take place, causing chemical and mineralogical changes (e.g., precipitation of secondary solid phases), which are governed by the progressive advancement toward the univocally defined final equilibrium state between primary solid phases and lung fluids. A number of chemical reactions may occur simultaneously, and different paths, comprising several intermediate steps of partial equilibrium, can be followed in this gradual progress toward the final equilibrium condition. Depending on the system, this final equilibrium might be attained or not.

The progressive advancement of the considered system toward the final equilibrium state is conveniently described by means of a variable known as *reaction progress* or *extent of reaction*, which is expressed in moles (e.g., De Donder 1920, 1927; Denbigh 1971). In fact, the number of moles of both destroyed primary solid phases and produced secondary minerals, as well as the molality of all solute species, can be calculated as a function of the reaction progress variable.

The reaction progress is used as pivotal variable to describe the evolution of the system in the so-called stoichiometric mode or reaction progress mode, which leaves kinetics out of consideration. Alternatively, reaction path modeling can be carried out with respect to time, taking into consideration reaction kinetics. The time-mode approach is more demanding than the stoichiometric-mode approach, as additional variables are needed, namely, surface areas and dissolution–precipitation rates of

solid phases (see below). In addition, it might be affected by larger uncertainties, related to possible errors on these parameters.

To understand the differences between the reaction progress mode and the time mode, let us consider a simple system in which a single solid phase is dissolving. In this case, the reaction progress variable, ξ, the change in the number of moles of the i-th species (either the dissolving primary solid phase or a solute), dn_i, and its stoichiometric coefficients, ν_i (adimensional), are related by the equation:

$$dn_i = \nu_i d\xi \tag{4.7}$$

Equation 4.7 can be easily integrated, by obtaining the following relationship:

$$n_i = n_i^\circ + \nu_i \Delta\xi \tag{4.8}$$

where n_i° represents the number of moles of the i-th species initially present in the considered system before the reaction starts. Let us now take the derivative with respect to time of Eq. 4.7:

$$\frac{dn_i}{dt} = \nu_i \cdot \frac{d\xi}{dt} \tag{4.9}$$

The ratio $d\xi/dt$ is the rate of the heterogeneous reaction, R, expressed in mol/s. Kinetics of dissolution–precipitation reactions of solid phases is usually described, referring to the specific reaction rate, r (mol m^{-2} s^{-1}), and to the surface area of the solid phase, A_S (m^2). These three variables are related by the simple equation:

$$R = r \cdot A_s \tag{4.10}$$

Therefore, Eq. 4.9 can be rewritten as follows:

$$\frac{dn_i}{dt} = \nu_i \cdot R = \nu_i \cdot r \cdot A_s \tag{4.11}$$

Assuming for simplicity that both the dissolution rate of the dissolving mineral and its surface area are constant, Eq. 4.11 can be integrated to obtain

$$n_i = n_i^\circ + \nu_i \cdot r \cdot A_S \cdot \Delta t \tag{4.12}$$

Equations 4.12 and 4.8 are the pivotal relations for reaction path modeling. Their comparison shows that there are two differences, in that (i) time is present in Eq. 4.12 instead of the reaction progress variable in Eq. 4.8 and (ii) both r and A_S appear in Eq. 4.12, whereas they are both absent in Eq. 4.8. It is evident that Eq. 4.8 is used to compute chemical changes in stoichiometric mode, whereas Eq. 4.12 is utilized to calculate chemical variations in time mode. It is also obvious that, in the second case, it is necessary to know both the dissolution rate of the considered mineral and its surface area.

4.3.2 The TST Rate Law

Different types of rate laws can be used to describe relevant dissolution–precipitation reactions. Among these rate laws, the transition state theory (TST) has the most robust theoretical foundations and is, therefore, the one most appropriate to describe dissolution–precipitation reactions. The general expression of the TST rate law for a dissolution (forward) reaction is (Wolery and Jarek 2003):

$$v_j = f_j \cdot A_{S,j} \cdot \sum_{i=1}^{i_{T+,j}} k_{+,ij} \cdot \left(\prod_{n=1}^{n_{T+,ij}} \cdot a_n^{-N_{+,ij}} \right) \cdot \left(1 - e^{-\frac{A_{+,j}}{\sigma_{+,ij} \cdot RT}} \right) \tag{4.13}$$

In Eq. 4.13, $A_{S,j}$ is the total surface area of the j-th mineral, that is, the surface of contact between the mineral and 1,000 g of the aqueous solution, and f_j is a factor (which is generally set equal to 1) representing the ratio between the effective surface area and the total surface area.

Equation 4.13 takes into consideration a total number $i_{T+,j}$ of parallel dissolution mechanisms, each one involving a rate constant ($k_{+,ij}$), a kinetic activity product (the first term in brackets on the right side of Eq. 4.13), and a term depending on thermodynamic affinity, $A_{+,j}$ (the second term in brackets on the right side of Eq. 4.13). The mechanism-specific kinetic activity product involves the activities of $n_{T+,ij}$ aqueous species, each one raised to a nonzero reaction order, $N_{+,ij}$. It must be recalled that, for most minerals, the main dissolution mechanisms are (a) the acidic mechanism, which is governed by the hydrogen ion and prevails at low pH values; (b) the basic mechanism, which is controlled by the hydroxyl ion and dominates at high pH values; and (c) the neutral mechanism, which is important in the circumneutral pH range. Dissolution rate of carbonate minerals, however, comprises also a mechanism controlled by aqueous CO_2 (or H_2CO_3). Several compilations and reviews of kinetic parameters are available (e.g., Palandri and Kharaka 2004; Marini 2007; Bandstra et al. 2008).

In addition to the absolute temperature, T, and the universal gas constant, R, the average stoichiometric number of Temkin, $\sigma_{+,ij}$, is also present in the affinity term. The stoichiometric number of Temkin is the ratio between the rate of decomposition of the activated complex and the overall dissolution rate. Therefore, it links the thermodynamic affinity of the macroscopic reaction, $A_{+,j}$, to that of the corresponding elementary or microscopic reaction, $A_{+,j}/\sigma_{+,ij}$. At equilibrium, the thermodynamic affinity, the affinity term, and the reaction rate become equal to zero.

Equation 4.13 can be used to describe the dissolution and precipitation rate of solid reactants whose thermodynamic and kinetic properties are known, such as pure minerals and solid solutions.

4.3.3 The Surface Area of Solid Reactants

The specific surface area of minerals, that is, the surface area exposed at the solid/liquid interface by the unit mass of the solid, can be obtained in two different ways. It can be measured by means of gas sorption/desorption isotherms (BET method), or it can be computed through a simple geometric approach, based on the ideal geometry of mineral grains.

The acronym BET is derived from the names of Brunauer, Emmett, and Teller, who proposed this widespread method long ago (Brunauer et al. 1938). The BET method consists of a preliminary heating step aimed at desorbing all gases from the solid surface at high temperature (typically 350°C) and under vacuum, which is obtained by the use of a rotary vane pump. After cooling the sample under vacuum, the isotherms of sorption and desorption are obtained based on gas pressure and the volume of gas sorbed onto the solid grains. Sorption and desorption isotherms are then used to compute the surface area of the sample, based on the assumption that only a monolayer of gas is sorbed. Either N_2 or Kr are used in the BET method, as their diameter (∼4 to 5 Å) is comparable with that of water (∼3 Å). Thus, the BET surface area is a reasonable evaluation of the wetted surface area. However, N_2 and Kr molecules cannot enter the pores where smaller ions may penetrate. In contrast, the surface area available for sorption of large organic biomolecules may be significantly lower than that available to gas sorption. Alternatively, by adopting this geometric approach, simple shapes can be assumed as analogues of mineral grains and surfaces of mineral grains can be obtained by simple computations (Oelkers 2002; Marini 2007).

The deviation of natural grains from ideal shapes may be taken into account through a parameter known as surface roughness, which is defined as the ratio between the true surface area and the corresponding geometric surface area of a hypothetical smooth surface encompassing the actual surface.

As indicated by both mineral grains from soils and those involved in laboratory experiments, dissolution processes affect, to different degrees, distinct portions of mineral surfaces, which evidently dissolve with different kinetics, resulting in the formation of etch pits. Further complications are caused by the formation of coatings, due to deposition of secondary phases on solid grains, which reduce the surface of contact between the aqueous solution and the mineral particles (e.g., White and Brantley 2003).

The description of mineral dissolution with respect to time is strongly dependent on the total surface of contact between the aqueous solution and the solid phase(s). In fact, as indicated by Eq. 4.12, a hyperbolic relation exists between the surface area and time corresponding to an inverse linear dependence between the logarithm of the surface area and the logarithm of time (Marini 2007).

4.3.4 The Double Solid Reactant Method: An Effective Approach to Model the Release of Trace Elements During Mineral Dissolution

As already recalled, TST-based rate laws can be used to describe the dissolution of solid phases whose thermodynamic and kinetic properties are known, that is, pure minerals and solid mixtures of idealized stoichiometry, such as those stored in the reference thermodynamic database of the EQ3/6 software package. The composition of real minerals, resulting from chemical analyses, differs from their idealized stoichiometry due to the presence of variable amounts of trace elements.

The double solid reactant method (DSRM) can be adopted to break this deadlock. The DSRM was proposed by Accornero and Marini (2008a) to model the release of trace elements from dissolving pure minerals or solid mixtures. In the DSRM, each dissolving solid phase is treated as a double solid reactant including both (1) an entity whose thermodynamic properties are known, either a pure mineral or a solid mixture, and (2) a special reactant *sensu* EQ6, that is, a material of known composition and unknown thermodynamic and kinetic properties.

The special reactant is used to take into considerations the contents of trace elements. Its composition has to be properly balanced in terms of either: (i) Oxygen atoms accompanying the considered trace elements, in oxides and complex oxides, including silicates, carbonates, phosphates, and sulfates; or (ii) sulfur atoms, in sulfides and sulfosalts; or (iii) Cl and/or F atoms, in halides; and so on.

In reaction path modeling, the relative dissolution rate of the special reactant is fixed equal to that of a companion solid phase. This can be readily done if either a single solid reactant is involved in the simulation (e.g., Marini 2007; Lelli et al. 2008) or if constant relative rates are assumed for all the considered solid reactants (which represent a strong simplification).

In contrast, reaction path modeling of the dissolution of several solid phases in a given time frame is a much more complicated exercise, as the reaction path has to be divided in a series of subsequent steps (small enough so that relative rates of all the solid reactants can be represented by approximately constant values) and the simulation has to be run twice for each step. In the first run, only pure minerals and solid mixtures are taken into account, thus obtaining the relative rates (mol/mol) for each solid reactant throughout the reaction path. In the second run, the relative rates are assigned to the special reactants accompanying each pure mineral or solid mixture. Examples are given by Accornero and Marini (2008b) and Apollaro et al. (2009, 2011). As a general indication, the special reactants should not contain component oxides (or sulfides) with molar fractions higher than 0.003.

4.4 Application of Equilibrium Models in Medical Geochemistry

4.4.1 Metal Speciation in Human Blood Plasma

As an example of application of equilibrium models in medical geochemistry, it is instructive to consider the speciation of metals in human blood plasma. This topic was reviewed by Shock (1998) on which this section is largely based. Considerable research in medical chemistry has established the bulk concentrations of metals in human blood plasma and the contents of the organic ligands forming complexes with each metal (Altman and Dittmer 1974; Ewers and Brockhaus 1991; Williams 1995). Chemical models of metal speciation in human blood plasma involve the association (formation) constants for thousands of complexes (May et al. 1977; Berthon et al. 1978, 1986; May 1995). Results of these models indicate that complexes with amino acids and proteins account for the majority of the speciation of metals in human blood plasma.

For example, the total concentration of copper is close to $1.8 \cdot 10^{-5}$ M on average, with 90% of it bound to ceruloplasmin, albumin, and amino acids like histidine dominating the rest of Cu speciation, and a computed concentration of free Cu^{2+} ion of $\sim 1.0 \cdot 10^{-18}$ M only (May et al. 1977). Organic complexes in human blood are important not only for Cu but also for other metals, with differences between total and free ion concentrations of five to eight orders of magnitude for Mn, Zn, and Pb and of 18 orders of magnitude for Fe (May et al. 1977).

The formation of metal complexes also has a large impact on the speciation of amino acids in human blood, with the concentration of free (uncomplexed) amino acids accounting for much less than 10% of their bulk concentrations and even much less than 1% in several cases.

Letkeman (1996) presented two computer programs, BEST and ECCLES, which generate distribution diagrams for various metal complexes in human blood plasma and applied this approach to investigate the speciation of lead and mercury. Results show that most metal complexes with organic ligands of low molecular weight, such as amino acids, become less important with decreasing pH (e.g., in the gastric fluids) due to the increased protonation of the organic ligands.

4.4.2 Solubility of Solid Particles in Lung Fluids

Solubility of solid particles in lung fluids was investigated by means of equilibrium models by several authors. Hume and Rimstidt (1992) showed that lung fluids should be strongly undersaturated with respect to chrysotile [$Mg_3Si_2O_5(OH)_4$], one of the fibrous minerals included in asbestos, which is considered to be the most powerful solid carcinogen (Fubini and Fenoglio 2007). Plumlee and Ziegler (2007)

computed the saturation state with respect to quartz and different asbestos-forming minerals of aqueous solutions having inorganic electrolyte compositions simulating those of lung fluids, intracellular fluids, and inferred lysosomal fluids. The adopted fluid compositions were probably too simple (as organic acids were not included in the equilibrium model) or incorrect (Al concentrations were possibly too high and inorganic phosphate is indistinguishable from organic phosphate based on available data), as recognized by the authors. Nevertheless, some useful indications were obtained. For instance, a general tendency to dissolve is observed for the asbestos-forming minerals, which are moderately undersaturated in the interstitial fluids, at pH 7.4, and strongly undersaturated in the acidic lysosomal fluid compositions. In contrast, sodic zeolites are only slightly undersaturated in the interstitial fluids, at pH 7.4. This might explain the biodurability of erionite [$Ca_3K_2Na_2(Al_{10}Si_{26}O_{72})\cdot 30H_2O$], a needle-shaped zeolite which is considered to be as toxic as asbestos (Fubini and Fenoglio 2007 and references therein).

4.5 Application of Reaction Path Modeling in Medical Geochemistry

Up to now, there are relatively few applications of reaction path modeling in medical geochemistry. Three examples are synthetically presented in the subsections of this section. The reader is referred to the original sources for further details.

4.5.1 Mineral–Fluid Interaction in the Lungs: Insights from Reaction Path Modeling by Wood et al. (2006)

Reaction path modeling was used by Wood et al. (2006) to predict the behavior of tremolite [$Ca_2Mg_5Si_8O_{22}(OH)_2$] and chrysotile in simulated lung fluids, again considering only electrolyte composition and neglecting organic ligands. As reported in the previous section, they found that simplified lung fluid is initially undersaturated with respect to tremolite and chrysotile and both minerals are therefore expected to dissolve. They also noted that, if Mg^{2+} and Ca^{2+} ions are complexed to a significant extent by organic species present in lung fluid, but not considered in calculations, then undersaturation with tremolite and chrysotile would be even more important.

Reaction path modeling, in both closed and open systems, shows that chrysotile starts to dissolve after a few days and it is completely destroyed after about 50–80 days. In contrast, significant tremolite removal begins after 1,000 days at pH 6.8 and after 100 days at pH 4.5, and its destruction is completed in 30,000 and 6,000 days, respectively. Although these times are approximated, due to uncertainties in dissolution rates and surface areas, there is no doubt on the distinct dissolution histories of the two considered solid phases. The larger persistence of tremolite

compared to chrysotile, as predicted by reaction path modeling, results from both the smaller dissolution rate constant for the neutral mechanism (by a factor of 60 to 300) and the smaller total surface area (by a factor of 24). These findings are consistent with the observation that the tremolite/chrysotile ratio in the lungs of humans exposed to asbestos minerals for long periods of time is significantly higher than the tremolite/chrysotile ratio in the initial asbestos material (Churg 1993). The reason for this finding is subject to some debate, in that it was attributed to either quicker dissolution of chrysotile than tremolite (see Hume and Rimstidt 1992) or faster removal of chrysotile than tremolite by macrophages (one of the cellular defenses to foreign particles present in the lungs), due to the different physical properties of the two minerals (Churg et al. 1989). For the second hypothesis, the dissolution rate of a minerals engulfed by a macrophage is expected to increase, since the intracellular pH of a macrophage is 4.5 whereas the pH of extracellular lung fluids is 7.4 (Plumlee et al. 2006). In addition to the two hypotheses mentioned above, results of reaction path model calculations indicate that asbestos minerals in the lungs might not only dissolve congruently but that precipitation of secondary minerals (e.g., talc or various Ca–Mg carbonates) might occur as asbestos minerals dissolve in lung fluids. This is an innovative conclusion, although several aspects were not taken into account in reaction path modeling, including kinetics of precipitation reactions and some dissolution reactions effects of dissolved organic species, the presence of other inorganic components in both minerals and lung fluids.

4.5.2 Geochemistry in the Lung: Reaction Path Modeling and Experimental Examination of Rock-Forming Minerals Under Physiologic Conditions by Taunton et al. (2010)

Taunton et al. (2010) explored the fate of selected rock-forming minerals (chrysotile, anorthite, K-feldspar, talc, muscovite, kaolinite, albite, and quartz) in simulated lung fluid by means of reaction path modeling. In addition, they investigated:

(a) The dissolution of a mineral mixture, mainly constituted by brucite and chrysotile, by means of aqueous batch experiments and X-ray diffraction (XRD) analysis of the mineral assemblage at the end of the runs.
(b) The precipitation of Ca-phosphate minerals in the lungs through SEM and energy dispersive X-ray analysis (EDS) of calcified pleural plaques.

The Gamble's solution (a solution similar to blood plasma) was used in aqueous batch experiments, which were carried out by placing the reaction vessels in a shaker bath at 37°C for 6 months. Then, the mineral assemblage was analyzed by XRD.

Reaction path modeling results show that rectangular particles of quartz, kaolinite, muscovite, and albite with a specific surface area of 10,000 cm^2/g do not dissolve

appreciably over a 50-year interval, whereas 99% of anorthite dissolves in 5 years, 99% of K-feldspar dissolves in 12 years, and 99% of talc dissolves in 35 years.

In addition, 99% of chrysotile particles with a specific surface area of 10,000 cm^2/g dissolve within 1 year approximately, and 99% of chrysotile particles with a specific surface area of 100,000 cm^2/g dissolve in approximately 1 month, irrespective of morphology (spheres vs. rectangular prisms) and mineral masses, corresponding to environmental (25,000 particles/mg dry lung), and occupational (300,000 particles/mg dry lung) exposure scenarios. These predicted dissolution times for chrysotile and talc are not significantly different from earlier results, such as those of Hume and Rimstidt (1992) and Jurinski and Rimstidt (2001), although they used a shrinking sphere model which does not take into account fluid composition.

Regardless of the total surface area of chrysotile, depending on mass and morphology, its dissolution appears to always be accompanied by precipitation of huntite [$CaMg_3(CO_3)_4$], talc [$Mg_3Si_4O_{10}(OH)_2$], and hydroxyapatite [$Ca_5(PO_4)_3(OH)$], with different timing and amounts of these secondary minerals. Both huntite and talc have ephemeral existence, in that they redissolve upon further dissolution of chrysotile, whereas hydroxyapatite persists through the entire time span of the simulations. It must be noted that the initial simulated lung fluid is strongly oversaturated with respect to hydroxyapatite, with a SI close to 7. Although this SI is probably overestimated, due to the presence of organic complexes involving Ca and P which are not considered in reaction path modeling, it is likely that lung fluids are slightly oversaturated with respect to hydroxyapatite (Plumlee and Ziegler 2007).

Interestingly, hydroxyapatite formed during the aqueous batch experiments and SEM analysis of calcified pleural plaques and associated tissues revealed the presence of various minerals, mostly calcium phosphates. The relatively large size of these mineral grains indicates that they were precipitated in the lung, as only inhaled particle of diameter <2 μm can reach the deepest parts of the lung (Plumlee et al. 2006) where the calcified pleural plaques were found. This finding is consistent with both the outcomes of reaction path modeling and the hypothesized slight supersaturation with respect to hydroxyapatite of lung fluids. Of course, it is difficult to understand the mechanisms controlling hydroxyapatite precipitation in different parts of the human body, as pointed out by Taunton et al. (2010).

Reaction path modeling also shows that dissolution of Al-silicate minerals, that is, anorthite [$CaAl_2(SiO_4)_2$] and K-feldspar [$KAlSi_3O_8$], is accompanied by precipitation of aluminum/aluminosilicate minerals such as mesolite [$Na_{0.667}Ca_{0.667}Al_2Si_3O_{10}{\cdot}2.667H_2O$], diaspore [AlO(OH)], and celadonite [$KMgAlSi_4O_{10}(OH)_2$]. This finding is of potential interest due to the association of Al^{3+} ion and aluminosilicate minerals with the Alzheimer's disease, as underscored by Taunton et al. (2010).

4.5.3 Yttrium and Lanthanides in Human Lung Fluids, Probing the Exposure to Atmospheric Fallout by Censi et al. (2011)

Precipitation of phosphate minerals in interstitial lung spaces was also investigated by Censi et al. (2011). They analyzed yttrium and lanthanides in bronchoalveolar lavages of people exposed to volcanic dust erupted from Mount Etna in 2001 and investigated dissolution of volcanic particulates in simulated lung fluids by means of reaction path modeling. Through comparison of analytical data and results of reaction path modeling, Censi et al. (2011) suggested that precipitation of phosphatic microcrystals may take place in intra-alveolar areas of lungs (sometimes leading to pulmonary fibrosis) due to inhalation of airborne particles and interactions with lung fluids.

Reaction path modeling calculations were performed using the simulated lung fluid composition of Wood et al. (2006) to which yttrium and lanthanides were added taking into account the fast dissolution of the soluble ash fraction. Basaltic glass was considered to be a mixture of amorphous silica and cryptocrystalline gibbsite [AlO(OH)], whereas the rock-to-water release of other chemical components of interest, in addition to Al and Si, was simulated adopting the DSRM (Accornero and Marini 2008a; see above). Reaction path modeling was carried out in time mode, using the kinetic parameters of basaltic glass (Gislason and Oelkers 2003) and computing the geometrical surface area of ash for a spherical grain shape of radius equal to 0.3 μm and an intra-grain porosity equal to 0.3.

Reaction path modeling indicates that dissolution of basaltic glass in simulated lung fluids is accompanied by early precipitation of poorly crystalline silica and a mechanical mixture of transition metal hydroxides [constituted by ferrihydrite, $Fe(OH)_2$, $Cr(OH)_3$, $Mn(OH)_3$, $Mn(OH)_2$, $Co(OH)_2$, $Ni(OH)_2$, $Cu(OH)_2$, and $Zn(OH)_2$], followed by late precipitation of AlOOH, a monazite of stoichiometry $Y_{0.15}La_{0.15}Ce_{0.31}Nd_{0.24}Sm_{0.10}Gd_{0.05}(PO_4)$, and hydroxyapatite.

Based on the results of this study, Censi et al. (2011) proposed the patterns of yttrium and lanthanides in bronchoalveolar lavages as a tool to identify the human exposure to heavy atmospheric particulate of volcanic provenance or caused by environmental pollution.

4.6 Conclusive Remarks

Although intuitive thinking is a prerogative of the human mind and the basis of all scientific progress, computer codes for chemical equilibrium and reaction path modeling (as well as reaction transport modeling) may be extremely useful to unravel the behavior of complex multicomponent, multiphase systems, such as the theoretical analogues corresponding to different parts of the human body. However,

the quality of the results of these codes is strictly related to the quality of their thermodynamic and kinetic databases.

Focusing on thermodynamic databases, their implementation has been made possible, thanks to the huge number of experimental data produced by chemists, biochemists, geochemists, and biogeochemists during the past century. Mineral data were compiled and reviewed by several scientists, and different internally consistent thermodynamic databases were proposed (e.g., Robie et al. 1979; Helgeson et al. 1978; Robie and Hemingway 1995; Holland and Powell 1985, 1990, 1998; Gottschalk 1997). Nevertheless, a lot of work has still to be done, with major problems concerning clay minerals, minerals of minor and trace elements, phosphate minerals, and sulfate minerals, as discussed by Oelkers et al. (2009).

Thermodynamic properties were determined experimentally for a limited number of aqueous species, whereas those of aqueous species not investigated through experimental work were obtained through correlations and empirical techniques (e.g., Martell and Motekaitis 1988; Martell and Hancock 1996; Grenthe et al. 1997), thus leading to the production of provisional estimates affected by varying uncertainties. In particular, formation constants of aqueous complex species may be expressed in terms of activity quotients or concentration quotients. Activity quotients are true *thermodynamic constants*, as they are referred to zero ionic strength. Nevertheless, they have to be extrapolated from experimental measurements, often performed at ionic strength very far from zero, adopting a suitable strategy for computing activity coefficients. This procedure is a possible source of uncertainty. In contrast, concentration quotients or *stoichiometric constants* can be determined directly, through suitable experiments in which a high and constant concentration of an inert background electrolyte is added to the aqueous solution. In this way, activity coefficients are kept constant and we do not have to worry about them. Of course, *stoichiometric constants* have limited applicability, whereas *thermodynamic constants* can be used universally. These or similar considerations have led chemists and biochemists to prefer stoichiometric constants and geochemists to choose thermodynamic constants.

It is evident that the creation of a comprehensive database, in which the data available in the thermodynamic databases used by geochemists are merged with the stability constants of aqueous complexes stored in the databases utilized by chemists and biochemists, is not a simple task. This is probably one of the major obstacles to be overcome for making equilibrium modeling and reaction path modeling a reliable tool which can be applied to complex biological systems, considering "all" the inorganic and organic dissolved species of interest.

At present, geochemical modeling can be performed by referring to simplified systems, as in the examples presented in the previous sections, with great success and encouraging results. In the present situation, geochemical models can be used to provide a qualitative or semiquantitative description of the processes occurring in different parts of the human body, where dissolution/precipitation processes occur. In spite of these limitations, the experience gained by geochemists on water–rock interaction processes can be very useful in collaborations with experts of biomedical disciplines.

References

Accornero M, Marini L (2008a) The Double Solid Reactant Method for modeling the release of trace elements from dissolving solid phases: I. Outline and limitations. Environ Geol 55: 1627–1635

Accornero M, Marini L (2008b) Contributo dell'alterazione meteorica del substrato roccioso alla formazione dei suoli: modellizzazione del percorso di reazione. In: Ottonello G (ed) GEOBASI, Il Foglio IGMI N°549: Muravera. Pacini Editore, Pisa, pp 201–249

Allison JD, Brown DS, Novo-Gradac KJ (1991) MINTEQA2/PRODEFA2, a geochemical assessment model for environmental systems: version 3.0 user's manual. Report EPA/600/3-91/021, U.S. Environmental Protection Agency, Office of Research and Development, Environmental Research Laboratory, Athens, p 106

Altman PL, Dittmer DS (1974) Biology data book, vol 3, 2nd edn. Federation of American Societies for Experimental Biology, Bethesda

Apollaro C, Accornero M, Marini L, Barca D, De Rosa R (2009) The impact of dolomite and plagioclase weathering on the chemistry of shallow groundwaters circulating in a granodiorite-dominated catchment of the Sila Massif (Calabria, Southern Italy). Appl Geochem 24:957–979

Apollaro C, Marini L, Critelli T, Barca D, Bloise A, De Rosa R, Liberi F, Miriello D (2011) Investigation of rock-to-water release and fate of major, minor, and trace elements in the metabasalt-serpentinite shallow aquifer of Mt. Reventino (CZ, Italy) by reaction path modelling. Appl Geochem 26:1722–1740

Ball JW, Nordstrom DK (1991) User's manual for WATEQ4F with revised thermodynamic data base and test cases for calculating speciation of major, trace, and redox elements in natural waters. U.S. Geological Survey Open File Report 91–183. Menlo Park, California, p 189

Bandstra JZ, Buss HL, Campen RK, Liermann LJ, Moore J, Hausrath EM, Navarre-Sitchler AK, Jang JH, Brantley SL (2008) Appendix: Compilation of mineral dissolution rates. In: Brantley SL, Kubicki JD, White AF (eds) Kinetics of water-rock interaction. Springer, New York, pp 737–823

Berthon G, May PM, Williams DR (1978) Computer simulation of metal-ion equilibria in biofluids. Part 2. Formation constants for zinc(II)–citrate–cysteinate binary and ternary complexes and improved models of low-molecular-weight zinc species in blood plasma. J Chem Soc Dalton Trans 1433–1438. doi:10.1039/DT9780001433

Berthon G, Hacht B, Blais MJ, May PM (1986) Copper-histidine ternary complex equilibria with glutamine, asparagine and serine: the implications for computer-simulated distributions of copper(II) in blood plasma. Inorg Chim Acta 125:219–227

Bethke CM (2008) Geochemical and biogeochemical reaction modeling, 2nd edn. Cambridge University Press, Cambridge, p 543

Brunauer S, Emmett PH, Teller E (1938) Adsorption of gases in multimolecular layers. J Am Chem Soc 60:309–319

Censi P, Tamburo E, Speziale S, Zuddas P, Randazzo LA, Punturo R, Cuttitta A, Aricò P (2011) Yttrium and lanthanides in human lung fluids, probing the exposure to atmospheric fallout. J Hazard Mater 186:1103–1110

Churg A (1993) Asbestos lung burden and disease patterns in man. In: Guthrie GD Jr, Mossman BT (eds) Health effects of mineral dusts: reviews in mineralogy, vol 28. Mineralogical Society of America, Washington, DC, pp 409–426

Churg A, Wright J, Gilks B, Depaoli L (1989) Rapid short term clearance of chrysotile compared to amosite asbestos in the Guinea pig. Am J Respir Crit Care Med 139:885–890

De Donder T (1920) Leçons de Thermodynamique et de Chimie-Physique. Gauthier-Villars, Paris

De Donder T (1927) L'Affinité. Gauthier-Villars, Paris

Denbigh K (1971) The principles of chemical equilibrium, 3rd edn. Cambridge University Press, Cambridge, 494

Ewers U, Brockhaus A (1991) Metal concentrations in human body fluids and tissues. In: Merian E (ed) Metals and their compounds in the environment: occurrence, analysis and biological relevance. VCH Publishers Weinheim, Germany, pp 207–220

Fubini B, Fenoglio I (2007) Toxic potential of mineral dusts. Elements 3:407–414

Garrels RM, Mackenzie FT (1967) Origin of the chemical composition of some springs and lakes. In: Stumm W (ed) Equilibrium concepts in natural water systems, advances in chemistry series. American Chemical Society, Washington, DC, pp 222–242

Garrels RM, Thompson ME (1962) A chemical model for sea water at 25°C and one atmosphere total pressure. Am J Sci 260:57–66

Gislason SR, Oelkers EH (2003) Mechanism, rates, and consequences of basaltic glass dissolution: II. An experimental study of the dissolution rates of basaltic glass as a function of pH and temperature. Geochim Cosmochim Acta 67:3817–3832

Gottschalk M (1997) Internally consistent thermodynamic data for rock forming minerals. Eur J Mineral 9:175–223

Grenthe I, Hummel W, Puigdomenech I (1997) Chemical background for the modelling of reactions in aqueous systems. In: Grenthe I, Puigdomenech I (eds) Modelling in aquatic chemistry. OECD Nuclear Energy Agency, Paris, pp 69–129

Harned HS, Owen BB (1958) The physical chemistry of electrolyte solutions, 3rd edn. Reinhold, New York

Helgeson HC (1968) Evaluation of irreversible reactions in geochemical processes involving minerals and aqueous solutions: I. Thermodynamic relations. Geochim Cosmochim Acta 32:853–877

Helgeson HC (1969) Thermodynamics of hydrothermal systems at elevated temperatures and pressures. Am J Sci 267:729–804

Helgeson HC, Garrels RM, Mackenzie FT (1969) Evaluation of irreversible reactions in geochemical processes involving minerals and aqueous solutions: II. Applications. Geochim Cosmochim Acta 33:455–481

Helgeson HC, Brown TH, Nigrini A, Jones TA (1970) Calculation of mass transfer in geochemical processes involving aqueous solutions. Geochim Cosmochim Acta 34:569–592

Helgeson HC, Delany JM, Nesbitt HW, Bird DK (1978) Summary and critique of the thermodynamic properties of rock-forming minerals. Am J Sci 278A:229

Holland TJB, Powell R (1985) An internally consistent thermodynamic dataset with uncertainties and correlations: 2. Data and results. J Metamorph Geol 3:343–370

Holland TJB, Powell R (1990) An enlarged and updated internally consistent thermodynamic dataset with uncertainties and correlations: the system K_2O–Na_2O–CaO–MgO–MnO–FeO–Fe_2O_3–Al_2O_3–TiO_2–SiO_2–C–H_2–O_2. J Metamorph Geol 8:89–124

Holland TJB, Powell R (1998) An internally consistent thermodynamic data set for phases of petrological interest. J Metamorph Geol 16:309–343

Hume LA, Rimstidt JD (1992) The biodurability of chrysotile asbestos. Am Mineral 77:1125–1128

Jurinski JB, Rimstidt JD (2001) Biodurability of talc. Am Mineral 86:392–399

Lelli M, Cioni R, Marini L (2008) The double solid reactant method: II. An application to the shallow groundwaters of the Porto Plain, Vulcano Island (Italy). Environ Geol 56:139–158

Letkeman P (1996) Computer-modelling of metal speciation in human blood serum. J Chem Educ 73:165–170

Marini L (2007) Geological sequestration of carbon dioxide: thermodynamics, kinetics, and reaction path modeling. Elsevier, Amsterdam, 470

Martell AE, Hancock RD (1996) Metal complexes in aqueous solutions. Plenum Press, New York, p 253

Martell AE, Motekaitis RJ (1988) The determination and use of stability constants. VHC, New York

May PM (1995) Modelling metal-ligand equilibria in blood plasma. In: Berthon G (ed) Handbook of metal-ligand interactions in biological fluids, bioinorganic chemistry. Marcel Dekker, New York, pp 1184–1194

May PM, Linder PW, Williams DR (1977) Computer simulation of metal-ion equilibria in biofluids: models for the low-molecular-weight complex distribution of calcium(II), magnesium(II), manganese(II), iron(III), copper(II), zinc(II), and lead(II) ions in human blood plasma. J Chem Soc Dalton Trans 588–595. doi:10.1039/DT9770000588

Oelkers EH (2002) The surface areas of rocks and minerals. In: Buccianti A, Marini L, Ottonello G, Vaselli O (eds) Proceedings of the Arezzo seminar on fluid geochemistry, Arezzo, 29 Aug–1 Sept 2000, Pacini Editore, Pisa, pp 18–30

Oelkers EH, Bénézeth P, Pokrovski GS (2009) Thermodynamic databases for water–rock interaction. In: Oelkers EH, Schott J (eds) Thermodynamic and kinetics of water—rock interaction, reviews in mineralogy and geochemistry, vol 70. Mineralogical Society of America, Washington, DC, pp 1–46

Palandri JL, Kharaka YK (2004) A compilation of rate parameters of water–mineral interaction kinetics for application to geochemical modeling. U.S. Geological Survey, Open File Report 2004-1068. U.S. Geological Survey, Menlo Park

Parkhurst DL, Appelo CAJ (1996) User's guide to PHREEQC (version 2) – a computer program for speciation, batch-reaction, one-dimensional transport, and inverse geochemical calculations. U.S.G.S. Water-Resources Investigations Report 99-4259. U.S. Geological Survey, Menlo Park, p 312

Pitzer KS (1979) Theory: ion interaction approach. In: Pytkowicz RM (ed) Activity coefficients in electrolyte solutions. CRC Press, Boca Raton, pp 157–208

Pitzer KS (1987) Thermodynamic model for aqueous solutions of liquid-like density. In: Carmichael ISE, Eugster HP (eds) Thermodynamic modeling of geological materials: minerals, fluids and melts, reviews in mineralogy, vol 17. Mineralogical Society of America, Washington, DC, pp 97–142

Pitzer KS (1992) Ion interaction approach: theory and data correlation. In: Pitzer KS (ed) Activity coefficients in electrolyte solutions, 2nd edn. CRC Press, Boca Raton, pp 75–153

Plumlee GS, Ziegler TL (2007) The medical geochemistry of dusts, soils, and other earth materials. In: Lollar BS (ed) Treatise on Geochemistry, vol 9. Elsevier, Amsterdam, pp 263–310

Plumlee GS, Morman SA, Ziegler TL (2006) The toxicological geochemistry of earth materials: an overview of processes and the interdisciplinary methods used to understand them. Rev Mineral Geochem 64:5–57

Reed MH (1977) Calculation of hydrothermal metasomatism and ore deposition in submarine volcanic rocks with special reference to the West Shasta district, California. Ph.D. thesis, University of California, Berkeley

Reed MH (1982) Calculation of multicomponent chemical equilibria and reaction processes in systems involving minerals, gases, and aqueous phase. Geochim Cosmochim Acta 46:513–528

Robie RA, Hemingway BS (1995) Thermodynamic properties of minerals and related substances at 298.15 K and 1 bar (10^5 pascals) pressure and at higher temperatures. US Geol Surv Bull 2131:461

Robie RA, Hemingway BS, Fisher JR (1979) Thermodynamic properties of minerals and related substances at 298.15 K and 1 bar (10^5 pascals) pressure and at higher temperatures. US Geol Surv Bul 1452, p 456

Sahai N (2007) Medical mineralogy and geochemistry: an interfacial science. Elements 3:381–384

Shock E (1998) Co-transport of metals and organic compounds in geochemical, biochemical and environmental processes. In: Marini L, Ottonello G (eds) Proceedings of the Rome seminar on environmental geochemistry, Castelnuovo di Porto, 22–26 May 1996, Pacini Editore, Pisa, pp 73–102

Taunton AE, Gunter ME, Druschel GK, Wood SA (2010) Geochemistry in the lung: reaction-path modeling and experimental examination of rock-forming minerals under physiologic conditions. Am Mineral 95:1624–1635

White AF, Brantley SL (2003) The effect of time on the weathering of silicate minerals: why do weathering rates differ in the laboratory and field? Chem Geol 202:479–506

Williams RJP (1995) Introduction to bioinorganic chemistry. In: Berthon G (ed) Handbook of metal-ligand interactions in biological fluids, bioinorganic chemistry. Marcel Dekker, New York, pp 1–20

Wolery TJ (1979) Calculation of chemical equilibrium between aqueous solutions and minerals: the EQ3/6 software package. Report UCRL-52658. Lawrence Livermore National Laboratory, Livermore

Wolery TJ, Jarek RL (2003) Software user's manual, EQ3/6, version 8.0. Civilian radioactive waste management system management and operating contractor. 10813-UM-8.0-00. Prepared for U.S. Department of Energy, Office of Civilian Radioactive Waste Management, Las Vegas

Wood SA, Taunton AE, Normand C, Gunter ME (2006) Mineral–fluid interaction in the lungs: insights from reaction-path modeling. Inhal Toxicol 18:975–984

Chapter 5
An Observation on the Composition of Urinary Calculi: Environmental Influence

Maria Luigia Giannossi and Vito Summa

Abstract Urinary stones exist throughout the world and are considered among the most painful medical conditions. Primary causal factors for the formation of these stones include both biological and environmental factors. Environmental factors are suspected to have a direct relationship to the composition of urine, which is governed mainly by diet and drinking water composition. This is a brief review on the influence of the environment on urinary stones formation: prevalence, geographical distribution and composition. A pilot case study on urinary stones in southern Italy is reported.

Keywords Urinary stones • Environmental influence • Epidemiology

5.1 Introduction

People experience their environment through a combination of physical, chemical, biological, social, cultural and economic conditions that differ according to the local geography, infrastructure, season, time of day and type of activity undertaken. Clearly, the relation between human health and the environment includes numerous complex interactions. The extent that the environment creates a hazard to human health depends on many factors, including the degree of human exposure. Exposure requires that people are present both at the place and at the time when the environment changes became hazardous. Exposure thus refers to the intersection between people and environmental hazards. Levels of exposure may range from harmless and acceptable to dangerous and unacceptable, depending on the potential for physical harm. Environmental hazards can lead to a wide range of health effects.

M.L. Giannossi (✉) • V. Summa
Laboratory of Environmental and Medical Geology, IMAA-CNR, Tito Scalo (PZ) 85050, Italy
e-mail: marialuigia.giannossi@imaa.cnr.it; vito.summa@imaa.cnr.it

P. Censi et al. (eds.), *Medical Geochemistry: Geological Materials and Health*, DOI 10.1007/978-94-007-4372-4_5,

Most important diseases are associated with more than one type of exposure, and environmental hazards interact with genetic factors, nutrition, lifestyle hazards and other factors in causing disease. Exposures to chemicals (and physical agents) are typically unevenly distributed geographically and temporally. Therefore, not surprisingly, disease occurrence also shows geographically varying patterns. Disease maps can be valuable tools in risk assessment to explore changes in disease patterns potentially associated with changes in environmental exposures.

The environmental epidemiology has an important role in the recognition of health threats from environmental exposures and in verifying the effectiveness of environmental remediation programmes (Nielsen and Jensen 2005). The goal of an environmental epidemiological study is to provide assessment tools to identify the spread of environmental health risk factors. Furthermore, such studies are essential for providing insight into prevention and rehabilitation as well as provide additional information on the disease. The correlations between geo-environmental factors and some diseases are not always known or sufficiently thorough; it is the case of urolithiasis (urinary stone formation).

5.2 Urolithiasis

Urolithiasis is a pathology of the formation of biominerals in the urinary tract and is commonly used to refer to the formation of biominerals in the human kidney, called kidney stones. Urinary calculi disease is one of the most common and most painful medical problems encountered throughout the world. Studies on the mineralogy of urinary stones and the crystallisation processes are particularly important in order to understand the possible environmental and metabolic factors that cause stone formation. Early studies on the urinary calculi problem have highlighted discoveries on composition, mineralogy, structure, processes of formation and geo-environmental factors that influence the formation of calculi (Ackermann et al. 1988; Bellizzi et al. 1999; Kohri et al. 1989).

5.2.1 Urinary Stone Types

Major chemical constituents of calculi are calcium phosphate (hydroxyapatite), calcium oxalates (whewellite and weddellite) and urates (Table 5.1) (Nasir et al. 2004).

There are 11 main groups of urinary stone (Fig. 5.1). Classification takes into consideration mineralogy, the presence of trace substances, location as well as the etiologic factors that could be deduced from the stones' macro- and microstructure (Daudon et al. 1993; Giannossi and Summa 2012; Giannossi et al. 2012; Grases et al. 1998, 2002).

Table 5.1 Mineral components of urinary calculi

Chemical name	Mineral name	Chemical formula	Abbreviation
Oxalates			
Calcium oxalate monohydrate	Whewellite	$CaC_2O_4 \cdot H_2O$	COM
Calcium oxalate dihydrate	Weddellite	$CaC_2O_4 \cdot 2H_2O$	COD
Phosphates			
Calcium phosphate	Hydroxyapatite	$Ca_5(PO_4)_3(OH)$	HA
Calcium hydrogen phosphate	Brushite	$CaHPO_4 \cdot 2H_2O$	BR
Magnesium ammonium phosphate hexahydrate	Struvite	$(NH_4)Mg(PO_4) \cdot 6H_2O$	STR
Purines			
Uric acid		$C_5H_4N_4O_3$	UA
Monosodium urate monohydrate		$N_aC_5H_3N_4O_3 \cdot H_2O$	MSU
Other			
Cystine		$C_6H_{12}N_2O_4S_2$	CY

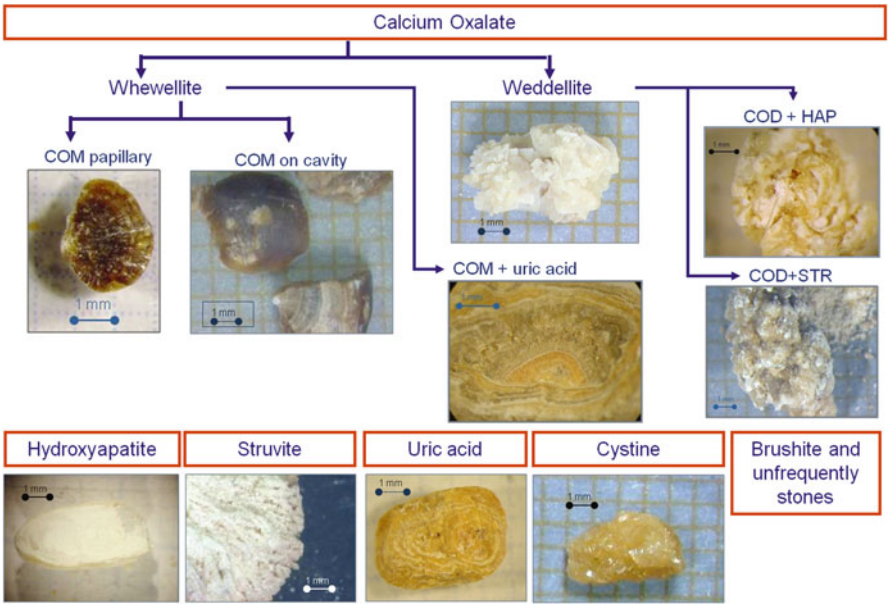

Fig. 5.1 Urinary stone classification scheme

5.2.2 *Environmental Influence on the Urinary Stone Formation*

Local environment influences human health. Environmental factors that can promote urolithiasis include the following: number of hot days in summer months (Baker et al. 1993); extra sunlight exposure, which induces extra vitamin D formation that can increase blood Ca absorption (Gunes et al. 2006); semiarid conditions (Pendse and Singh 1986); droughts (Bond et al. 2008); water hardness (Sierakowski et al. 1979); fluoride in groundwater (Singh et al. 2001); and elevated sodium intake (Massey 2005). In recent decades, the cause of increased incidence of this disease has been closely tied to changes in lifestyle, industrialisation and changes in diet patterns. These recent changes in environmental factors have been related to the deficiency of fibre in diet; excessive intake of animal protein, calcium and salt; hot and dry weather; alcohol consumption (Holmes et al. 2001); lack of physical activity and exercise; and low-potassium diet (Gupta and Kesarwani 2002). These changes have been found to be most pronounced in people between the ages of 20 and 50 years old, males and people with family history of this disease (Holmes et al. 2001).

Among the public perceptions about environmental causative factors, hardness of water is strongly thought to be related. Previous studies show negative as well as positive correlations to stone formation with hardness of drinking water. The ratio of Mg and Ca has also shown contrasting relations to urolithiasis (Kohri et al. 1989, 1993). Negative correlations have revealed the importance of intake of Ca for the excretion of excess oxalates (Ackermann et al. 1988; Candarella et al. 1998; Guttenbrunner et al. 1989; Marangella et al. 1996; Rodgers 1997, 1998; Sommariva et al. 1987). Ingestion of excess fluoride seems to facilitate stone formation. This has been shown in studies on calcium oxalate crystalluria and formation of bladder stones in rats (Anasuya 1982). Influence of other elements apart from Ca, Mg, phosphates and oxalates has not been extensively studied, though determination of element impurities in stones has shown that Cr, Fe and Zn collect in oxalates and Sr, Rb, I and Pb in phosphate stones (Kadurin 1998).

Many epidemiological studies have recorded a geographic variability in the prevalence of stone disease (Chen et al. 2000; Hesse et al. 2003; Komatina 2004; Lee et al. 2002). It has been postulated that this variability may be due to variations in climate and sun exposure, although others have questioned the role of diet and water quality as well. The most convincing evidence to date has demonstrated that temperature and sun exposure play important roles in the geographic variability of stone disease. It is verified that individuals living in hot climates have an increased lifetime prevalence of stone disease. The only factor that has a greater effect on stone disease is dehydration. Further, individuals living in areas with increased sun exposure are likely to have absorptive hypercalciuria secondary to elevated vitamin D synthesis (Curhan and Curhan 1994; Parry and Lister 1975; Robertson et al. 1974, 1975).

Similar to geographical location, a person's occupation may influence their risk for urolithiasis (Borghi et al. 1993; Ferrie and Scott 1984; Zheng et al. 2002). As warm climates seem to predispose a person to stone formation, so do occupations involved with warm working environments. However, the situation of occupation is independent of the effects of sun exposure and vitamin D synthesis.

Nutritional factors may cause stone formation or exaggerate metabolic risk factors (Borghi et al. 2002; Curhan et al. 1993, 1997b; Goldfarb et al. 2005). Strenuous physical exercise or excessive sweating in a hot climate may enhance stone formation altering urine composition, including changed urinary pH and hypocitraturia. A high sodium intake can increase hypercalciuria and lower urinary citrate concentrations (Kleeman et al. 1964; McCarron et al. 1981; Phillips and Cooke 1967). A diet rich in animal protein may result in increased urinary uric acid and calcium concentrations and lower citrate concentrations (Breslau et al. 1988; Robertson et al. 1979). The stone-forming risk of dietary calcium is dependent of the disease condition and the dietary oxalate intake. Idiopathic hypercalciuria is an important and common risk factor for the formation of stones, and uncontrolled hypercalciuria is a cause of recurrences. Thiazides can reduce urinary calcium excretion, but since calcium excretion depends in part on diet, initial attempts to decrease hypercalciuria should involve dietary modification. Since most patients with hypercalciuria have intestinal hyperabsorption of calcium, it is common clinical practice to recommend a low-calcium diet. However, there are no long-term data on the efficacy of this approach (Broadus et al. 1984; Coe and Kavalach 1974; Coe et al. 1992; Pak et al. 1980; Strauss et al. 1982; Yendt and Cohanim 1978). Short-term studies have shown that a low calcium intake significantly reduces urinary calcium excretion but can cause a deficiency of calcium and an increase in urinary oxalate (Epstein 1968; Marshall et al. 1972).

5.3 Urolithiasis Project in Southern Italy

5.3.1 Background of the Study

Urinary stone disease varies in frequency and stone type between different climates and geological features. Understanding the epidemiology of stone disease is important to determine the significance of the disease at a community level, the associations and risk factors for individuals and the likelihood of stone recurrence. This section attempts to describe the epidemiology of urinary stone disease including its association and risk factors. Most previous studies have focused on the country scale; however, this present study focuses on a much smaller study area in the Basilicata region in southern Italy. The intent of this study is to account for the various environmental factors and conditions responsible for genesis of urolithiasis among the local population (Giannossi 2010a, b).

5.3.2 Materials and Methods

Data from 3 years between 2003 and 2005 were collected to relate temporal changes in urolithiasis to gender and age group. Urinary stones data was provided by the main hospital of the region, whereas climatic data, water/soil quality data and urolithiasis data were acquired from different regional agencies. Analyses performed in this study were made by use of logistic and multinomial logistic regression. For assessing the prevalence of urolithiasis across demographic characteristics, we performed logistic regressions for each potential risk factor. This approach produced odds ratios (ORs), which indicate the odds that members of a given social group (e.g. exposed to a potential risk factor) would report urolithiasis, relative to a reference group (e.g. nonexposed).

5.3.2.1 Epidemiological Data Collection

The data referred to for the epidemiological analysis were taken from the Basilicata Regional Authority, more specifically from the Department for Health, Safety and Social Solidarity (Basilicata web site). The privacy of the patients was maintained. This study included Basilicata residents (population $\approx$ 597,000) that were hospitalised for urolithiasis both in the region and in hospitals outside the area between 2003 and 2005. When using the regional dataset, a variety of surrogate markers were used to estimate stone prevalence, including hospital discharges, physician office visits, emergency room visits, procedures related to a primary diagnosis of stone disease or a self-reported history of stones (Pearle et al. 2007; Saigal et al. 2005). All of these surrogates are compromised in that they likely underestimate the prevalence of disease either because a patient may pass a stone without requiring any health-care resources, because a patient may report a history of stones based on unsubstantiated symptoms or not report a history of stones because a stone was never collected despite classic symptoms of renal colic. We assumed that hospitalisation rates tally with stone incidence rates; the prompt character of this study underestimates the real kidney disease prevalence because only the hospitalised cases of urinary stones were included, which does not influence the distribution prevalence. The records of the Basilicata resident patients hospitalised for urolithiasis in the region and outside the area between 1 January 2003 and 31 December 2005 were taken as targets. The data obtained included patients' personal details such as age, gender and address. Population affected by stones was also compared to a control population; that is to say, the Basilicata resident population (293,220 men and 303,569 women) was grouped together according to the age.

In Basilicata, there are 131 municipal areas; the main towns are Potenza and Matera, with 69,295 and 57,075 residents, respectively. Data on the number of Basilicata resident patients could only be obtained from specific databases of the regional population (ISTAT website). A "resident" was defined as a person who was registered as having lived within the regional boundaries during the year preceding the stone episode. The cases were separated according to their town residence, year

of hospitalisation, gender and age group (0–19, 20–29, 30–39, 40–49, 50–59, 60–69, ≥70 years old).

The numerical data were manipulated and analysed with standard statistical methods (Mendenhall 1967) and a software for epidemiologic statistics (OPENEPI 2.2.1). The annual incidence was calculated as the estimated number of new lithiasis cases out of 100 inhabitants for each annual survey. Urolithiasis prevalence percentage was age-adjusted through direct standardisation, using a standard town population.

5.3.2.2 Urinary Stone Data Collection

All the patients hospitalised for urolithiasis at the San Carlo Hospital (the main medical facility in Basilicata) during the study period were selected as donors and involved in this study. We collected more than 200 urinary stones either expelled or extracted surgically. In order to avoid a selection bias, more than one stone from the same patient was studied, and an average composition was assigned. The stones were first fragmented and then observed to establish their original form and internal structure.

All the urinary stones collected were dried in a desiccator at room temperature for 2 weeks; then, the dry samples were photographed. Optical observations were carried out with a stereomicroscope to determine colour, shape, overall appearance, surface features and any possible occurrence of crystalline layer and/or organic matter on the surface. Attention was directed at identifying the site on the kidney wall where the stone is attached. Half of the sample was used for X-ray diffraction (XRD) analysis. Urinary stones were crushed in an agate mortar in order to obtain a fine mesh powder for X-ray diffraction, so as to obtain the crystalline phase composition of the urinary stones.

5.3.2.3 Climatic Data

Surface weather station data (Fig. 5.2) for each municipality was procured from ALSIA Agency – agro-climatic automatic stations belonging to the project "Analysis of climatological and implementation of a system for returning meteorological data in a grid format for Basilicata" (Stelluti and Rana 2004). The weather station provided major climate parameters, including as mean annual temperature data, sunlight index and altitude.

5.3.2.4 Soil/Water Data

The chemical analysis data of groundwater samples from the study area was obtained from the Groundwater Survey Authority (*Acquedotto Lucano spa*). These data were used to estimate correlations between urolithiasis and groundwater hardness. Because people residing in the study area also drink bottled water, the

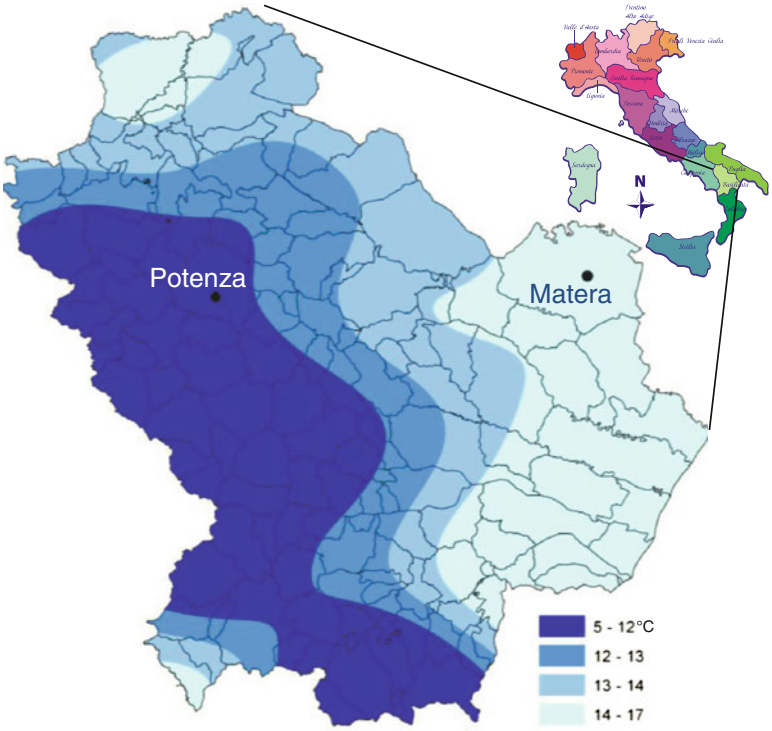

Fig. 5.2 Distribution of the average annual temperatures

chemistry of the major types of bottled water was also considered in the analysis. The calcium and magnesium content of the water was used to estimate the hardness of the water, expressed in units of milligrams of calcium carbonate $CaCO_3$ in a litre of water. The unit of measure more used is the French degree (°f), which corresponds to 10 mg/L of $CaCO_3$. Based on the most common classification of hardness, the classes of water were soft water (hardness <15°f), average hardness (hardness between 15° and 30°f) and hard (with hardness >30°f) (Limits of law D.Lgs. 31/2001). The hardness values of the waters are presented in Fig. 5.3.

Basilicata is divided into areas with different soil properties, classified on macroscale and named soil regions (DASREM 2006). There are five different classes of soil types (Fig. 5.4) accounting for differences in geology and lithology. It was anticipated that different soil properties would influence the tendency for the development of urinary stones. In addition to being aware of regional soil properties, it is also important to understand the relationship between soils that through agriculture produce foods that are consumed locally. This information may also be useful to justify the origin of some chemical elements that could reach the humans (food and water), causing various kinds of diseases (Barberis 1996; Felici 2005).

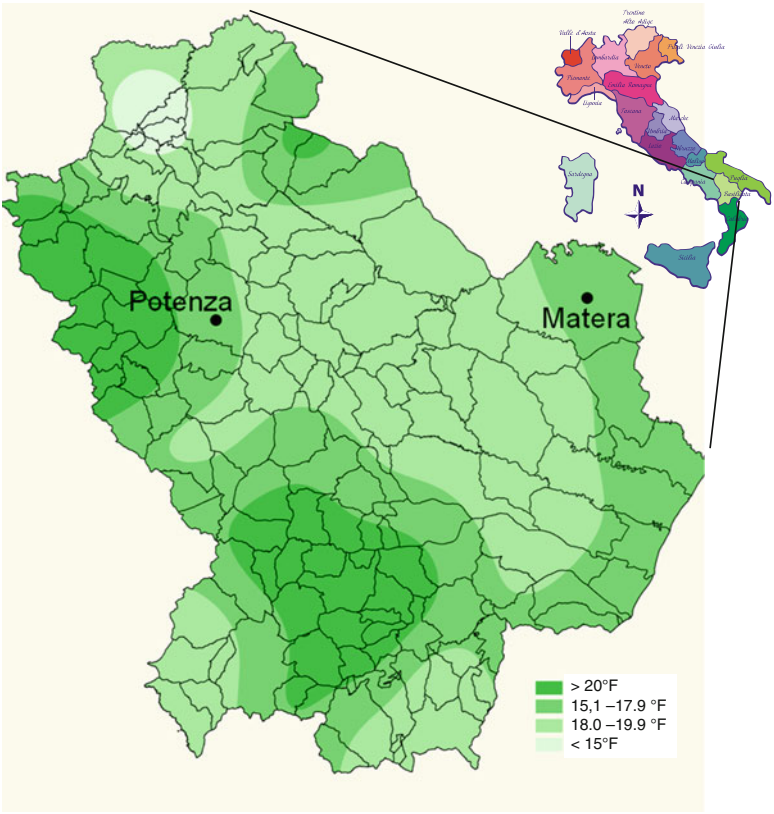

Fig. 5.3 Distribution of drinking water hardness

5.4 Results and Discussion

After processing the climatic and geochemical data with respect to urolithiasis epidemics observed in study area, it is understood that there is a correlation between the environment and urolithiasis epidemics. Prior to that, in the study of epidemiological parameters of urolithiasis, it was demonstrated that year, gender distribution and age group distribution were correlated to prevalence of this disease.

5.4.1 Prevalence of Urolithiasis and Impact of Age and Gender

The data indicated that 3,876 persons out of the total Basilicata resident population (≈597,000) reported urinary stones. The lifetime prevalence of urolithiasis among

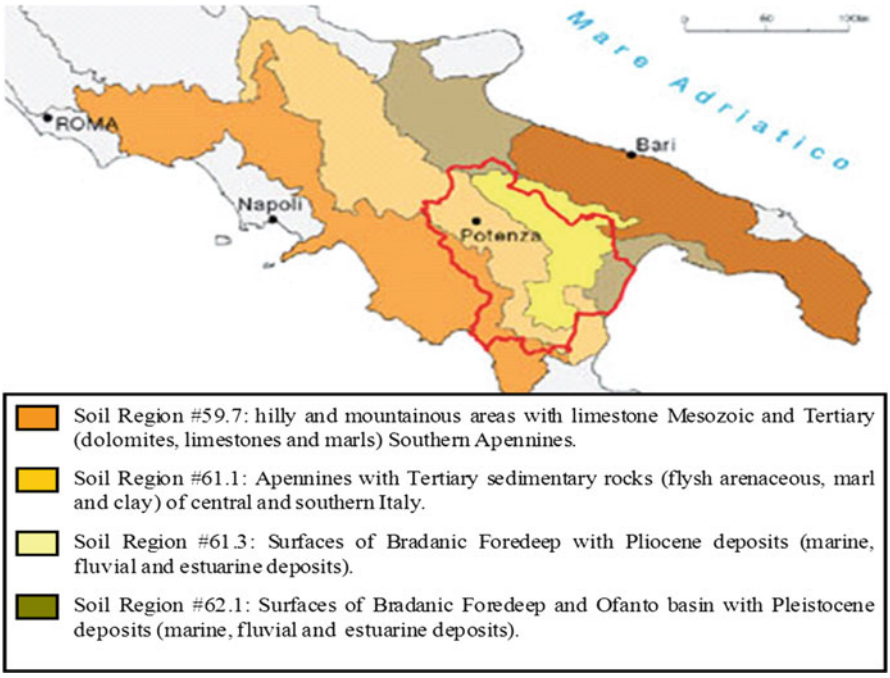

Fig. 5.4 Pedological areas in Basilicata

Table 5.2 Urolithiasis prevalence in Basilicata

Group	Control population (%)	Prevalence *n* (‰)
Male	293,220(49.13)	2,089 (7.12)
Female	303,569 (50.87)	1,787 (5.89)
Age group		
0–19	126,319 (21.17)	152 (1.20)
20–29	82,212 (13.78)	385 (4.68)
30–39	91,023 (15.25)	619 (6.80)
40–49	83,982 (14.07)	758 (9.03)
50–59	69,044 (11.57)	691 (10.01)
60–69	61,820 (10.36)	598 (9.67)
>70	82,389 (13.81)	673 (8.17)
	596,789 (100)	*3,876 (6.49)*

them (Table 5.2) was 6.49% (SD ± 3). The prevalence of urolithiasis increased with age. Table 5.2 lists the distribution of the prevalence of urolithiasis according to age groups.

Unfortunately, very few databases on the prevalence of urolithiasis in Italy have been published up to now (Baggio 1999; Bellizzi et al. 1999; Borghi et al. 1990, 2006; Ramello et al. 2000; Serio and Fraioli 1999). To our knowledge, this is the first epidemiological study of urolithiasis prevalence in Basilicata.

Table 5.3 Annual prevalence of urinary stone for 1,000 inhabitants: age and gender difference

	2003			2004			2005		
Age	n. tot '03	Men	Women	n. tot '04	Men	Women	n. tot '05	Men	Women
0–19	0.47	0.41	0.52	0.33	0.26	0.41	0.40	0.29	0.52
20–29	1.73	1.86	1.59	1.63	1.50	1.76	1.33	0.98	1.69
30–39	2.34	2.56	2.12	2.24	2.12	2.36	2.22	2.43	2.01
40–49	2.93	3.34	2.52	3.11	3.87	2.35	2.99	3.46	2.52
50–59	3.48	3.89	3.07	3.36	3.92	2.81	3.17	4.06	2.30
60–69	3.49	4.00	3.04	3.35	4.00	2.76	2.83	3.35	2.37
>70	2.95	3.54	2.51	2.35	2.85	1.99	2.86	3.14	2.66
	2.28	*2.51*	*2.05*	*2.13*	*2.35*	*1.92*	*2.08*	*2.26*	*1.91*

The lifetime prevalence of urolithiasis in the inhabitants of Basilicata was 6.49% with a higher rate in men (7.12%) than in women (5.89%). This difference is statistically significant ($p < 0.01$). The relative risk for men was 1.2 times the relative risk for women, which means that the probability of developing lithiasis is 20% greater in men. This result is consistent with that reported by Serio and Fraioli 1999, who calculated this ratio to be 1.25, and Borghi et al. 1990, who calculated this ratio to be 1.5, but it was significantly lower than what the proceedings of the Consensus Conference 4 (1988), which was a ratio of 4.0. Given the different features of the population involved, the large number of assessment methods and the many definitions of urolithiasis, the studies were difficult to compare. In light of these inconsistent definitions, varying populations and varying assessment methods, it is understandable that many problems exist in epidemiological studies.

In 2003, the annual incidence of urolithiasis was higher than in any other year studied. The distribution of urolithiasis was 54% for men and 46% for women between 2003 and 2005. The average annual incidence of new stone formations was 2.16 per 1,000 inhabitants. This rate was calculated for new cases occurring between January 2003 and December 2005.

The frequency of new stone formations was found to be higher among men than women in the three-year survey. The average annual incidence was 2.37 out of 1,000 inhabitants in the male group and 1.96 per 1,000 inhabitants in the female one (Table 5.3). The incidence was found to be lower in small boys than small girls (<19) but 1.2 times higher among 19- to 59-year-old adults and 1.5 times higher in men than women among the elderly (>60). These are large differences, given that the male to female population ratio in those age groups is 1:1.

The correlations between urolithiasis and age and male to female ratio were calculated. The test was performed with several different age groups (greater than 40 years, 30–59 years and 40–59 years) based on the results of urolithiasis prevalence, especially among adults. The two determinants (male gender and age at risk) were then combined (Table 5.3).

The disease prevalence rate found in subjects over the age of 19 was 7.91‰; this did not match Borghi's findings (Borghi et al. 1990) (5.3 up to 6.1% in northern

Italy). This inconsistency was due to a problem of standardisation given that the distribution of age in southern Italy differed from the north.

From all the studies made, it can be inferred that urinary stone disease is relatively rare in children from developed countries where the prevalence ranges from 2 up to 2.7% (Borghi et al. 1990; Vahlensieck et al. 1982). It is therefore easy to understand why authors have studied subjects over the age of 19 only (Borghi et al. 1990; Serio and Fraioli 1999; Stamatelou et al. 2003; Trinchieri et al. 2000). The prevalence of urolithiasis in Basilicata children was very low (1.2‰). The prevalence of urolithiasis increased with age both in men and women, which was consistent with the findings reported by other authors (Ljunghall and Hedstrand 1975; Robertson et al. 1984).

Table 5.4 shows the odds ratios obtained by the association and the probability as a value *p*, which indicates how likely is it that the association seen is due to chance. There is a positive association between factor and disease, which becomes significant when combined with multiple parameters. In all cases, the regression or multiple regressions were significant, indicating that there is a low chance that the observed results were due to chance.

5.4.2 Prevalence of Urolithiasis

The Basilicata region was divided into five local health centres (ASL) to which municipal areas were assigned according to territorial principles. After a direct standardisation, prevalence was found to be higher in the ASL n. 2, 1 e 5, in decreasing order, also considering a high standard deviation (SD ± 3) (Fig. 5.5). Prevalence ratio of male to female occurrence, at this detailed scale, is remarkably increased compared to the average regional prevalence ratio (6.49‰).

For each town, the standardised prevalence rate was calculated (Fig. 5.6). The values of the rates calculated exceeded the average regional index up to >12‰. The towns with a higher prevalence appeared to be distributed especially in the north-western area of the region.

Whether there is a correlation between the size of the town residence and the prevalence of stone disease was considered. The prevalence in towns with less than 5,000 inhabitants was 2.3‰, in those with more than 5,000 was 2.11‰, in Potenza 3.25‰ and in Matera 1.10‰. When the results were standardised to account for age, the larger towns appeared to have more stone diseases.

The correlation between the size of the town residence and the prevalence of stone disease is important. Bigger towns had a higher prevalence; this implies a close connection with the higher prevalence of urolithiasis found in the 40–60 age group to which commuters belonged. There is a higher occurrence of females and elderly in small villages. Moreover, it is here that the traditional lifestyles are handed down.

The population involved was divided into two areas (the northern Apennine Basilicata zone and the southern Basilicata Bradanic Foredeep) on the basis of

Table 5.4 Relation between some potential risk factors and urolithiasis

Risk factors	Total no.	No. of cases	Odds ratio (95% confidence interval)	*p* value
Age group (*years*)				
30–59	241,982	2,068	1.67	0.01
40–59	151,577	1,449	1.74	0.01
30–59 years + male gender	120,564	1,175	1.84	0.01
30–59 years + female gender	121,417	893	1.48	0.01
40–59 years + male gender	75,238	850	1.98	0.01
40–59 years + female gender	76,340	599	1.49	0.01
Mean annual temperature (°*C*)				
>13	326,661	1,826	0.73	0.01
>13 + male gender	160,805	974	0.71	0.01
>13 + female gender	165,856	852	0.74	0.01
>13 + 40–59 years	41,006	410	0.78	0.01
>13 + 40–59 years + male gender	21,156	225	0.78	0.01
High altitude (*m a.s.l.*)				
>600	191,694	1,600	1.51	0.01
>600 + male gender	93,493	866	1.53	0.01
>600 + female gender	98,200	734	1.49	0.01
>600 + 40–59 years	69,787	787	1.39	0.01
>600 + 40–59 years + male gender	34,767	465	1.41	0.01
Water hardness (°*f*)				
>22.5	32,422	240	1.27	0.01
>30	8,430	67	1.60	0.05
>30 + male gender	9,294	108	1.80	0.01
>30 + female gender	9,987	90	1.29	0.01
>30 + 40–59 years	8,026	64	0.99	1
>30 + 40–59 years + male gender	4,001	40	1.22	0.6

geological environmental and climatic features. Municipal areas were assigned to the above-mentioned areas according to geographic-geological proximity and climatic similarity. The prevalence of urolithiasis varied considerably depending on geographic and geological characteristics. The prevalence rate of urolithiasis was significantly higher in the northern Apennine Basilicata zone and tended to decrease in the southern Basilicata Bradanic Foredeep. This observation may be explained by differences in local environmental features, such as temperature, altitude, solar radiation, water, soil quality and residents' lifestyle (Ackermann et al. 1988; Borghi et al. 1996; Candarella et al. 1998; Curhan et al. 1993, 1994, 1997a, b; Felici 2005; Goldfarb et al. 2005; Hesse et al. 2003; Komatina 2004; Parry and Lister 1975; Rodgers 1997; Shuster et al. 1985; Strauss et al. 1982).

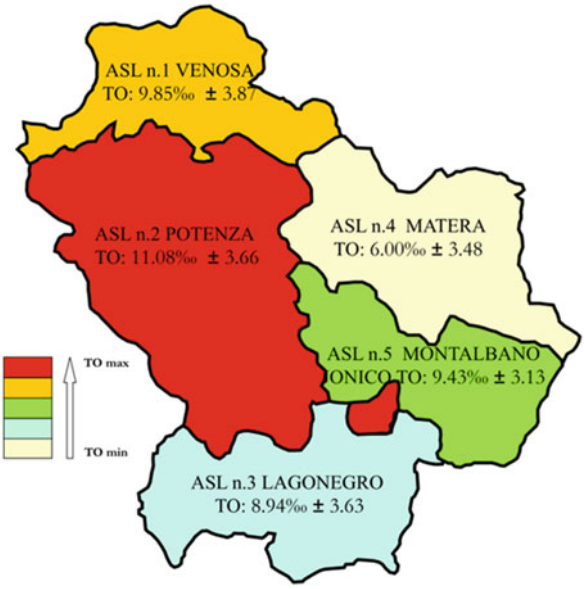

Fig. 5.5 Average hospitalisation rate (TO) in 5 Basilicata local health centres (ASL)

5.4.3 Typical Types of Uroliths and Their Geographical Distribution

The results in Table 5.5 show that 66% of the urinary stones studied were composed of calcium oxalates (38% formed by calcium oxalate monohydrate ($CaC_2O_4 \cdot H_2O$), whewellite, and 28% present in major quantity the dihydrate form of calcium oxalate ($CaC_2O_4 \cdot 2H_2O$), weddellite). The calcium oxalates were not pure since trace quantity of other components (organic and inorganic) could be observed. The other 34% was composed of different phases, such as uric acid ($C_5H_4N_4O_3$) (15%), magnesium phosphates (struvite ($MgNH_4 \cdot PO_4 \cdot 6H_2O$) 6%), hydroxyapatite (13%) and cystine ($C_6H_{12}N_2O_4S_2$) (1%).

Thirty-two percent of the stones were found to be multi-composed: weddellite plus hydroxyapatite, weddellite plus struvite and whewellite plus uric acid. During the mineralogical analysis, we recognised in 6% of the total stones analysed the presence of a new mineralogical assemblage, consisting of weddellite plus struvite (Giannossi and Summa 2012; Giannossi et al. 2012), which was not included in the classification presented by Grases et al. (1998, 2002).

The distribution of the eight groups of stones is different if we compare the urinary stones expelled by men and women. The latter are more likely to form struvite and whewellite. Men are more prone to uric acid and weddellite. The whewellite papillary stones have a similar frequency in both groups. The new

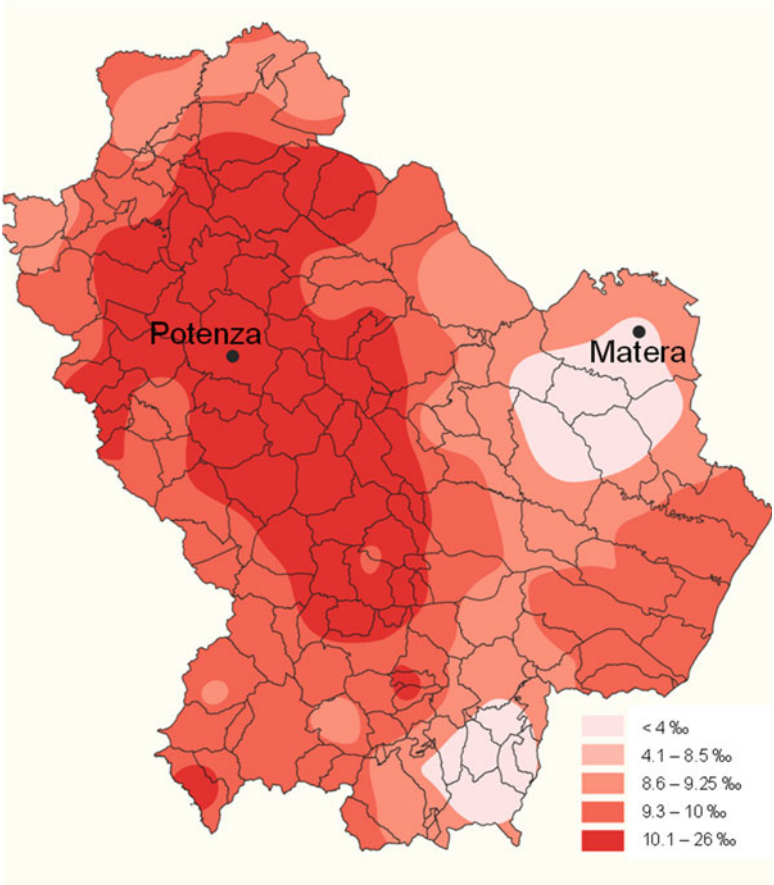

Fig. 5.6 Distribution of the specific prevalence rate between 2003 and 2005

type – COD + STR – is more common in men. Age also influences the stone type. Young people aged under 30 years are much more frequently COD stones, whereas the population with an age greater than 60 had uric acid. The whewellite papillary stones are more common in adulthood.

Each sample was associated with the patient's residence in one of the 131 municipalities in the Basilicata territory. To identify possible areas of increased production of urinary stones, the samples were mapped by assimilating the sampling point with the residence of patients. The stones composed primarily of oxalates had a wide distribution. Stones composed of struvite were concentrated in southern Basilicata. The uric acid stones, which are plentiful in the region, were especially concentrated in the Apennine northern part of the region.

Table 5.5 Urinary stones percentage distribution in Basilicata

Type of urinary stone	Basilicata region (Italy) (%)
Calcium oxalates	59
COM papillary	11
COM on cavity	19
COD	29
COD + HAP	6
Pure calcium phosphates	0
Hydroxyapatite	0
Brushite	0
Struvite	4
Uric acid	18
COM + uric acid	6
Cystine	1
New types (COD + STR)	6

5.4.4 Prevalence of Urolithiasis and Risk Factors

5.4.4.1 Climate and Season

Among the environmental risk factors, the first to be evaluated is the average annual temperatures. Based on the distribution of average annual temperatures, it is possible to assert that the oriented distribution is obvious, from the north-west towards south-east, of the Basilicata Apennines, characterised by low average annual temperatures, especially near the highest mountains, like Mt. Volturino, Mt. Stringi and Pollino (9–11°C). The warmer zones are, instead, those at sea level, above the Metaponto plain, overlooking the Ionian Sea (15.5–15.8°C). The zones with intermediate temperatures correspond to the Fossa Pre-Murgiana, neighbour with the Puglia, and that one to north of the Mt. Vulture, with the initial portion of the basin Ofanto (14.0–15.0°C).

To our knowledge, there does not exist in the literature a critical regional temperature that identifies geographical regions that are at risk for promoting dehydration. On the basis of regional values, the range of higher temperature was taken into account, and on this data, the calculation of the association between urolithiasis prevalence and high temperatures has been imprinted. The calculation was then repeated for other temperature ranges gradually lower. In light of these examinations, the range of $T > 13$°C has been taken into account which is the temperature that exposes to a greater risk of developing urinary stones, including in the calculation all the moderated zones at sea level and areas intermediate. The calculations of odds ratio yielded the following results (Table 5.4). It is observed that for up to a temperature of 13°C, there is no association between the exposure and the disease, even when they are evaluated together with other risk factors. Since the value of odds ratio is less than 1, the exposure in question is not to be considered as a risk factor but rather as a protective factor.

The highest mountains of the region recorded the lowest average annual temperatures. The elevation, and the temperatures can be related to the development of urinary stones. Also in this case, there does not exist a bibliographic reference about the maximum altitude beyond which a greater risk is recorded. The correlation was therefore calculated for different intervals, until we find a positive association with urolithiasis and altitudes above 600 m a.s.l. (Table 5.4).

Season is an important factor in the disease. In this study, spring is the season that most patients are referred to the hospital with symptoms related to urinary stones. In a review conducted by Borghi et al. (1999), instead, most patients had been referred to therapeutic centres during or immediately after a hot season. This result confirms the previous data on the need to consider the high temperatures of the summer months a protective factor rather than risk. In this case, the number of disease increases during the winter.

5.4.4.2 Dietary Habits and Lifestyle

By analysing the patients' personal information, the physical predisposition to urolithiasis could also be assessed, and it was seen that both obese people and those who are overweight (based on the value of body mass index) are more affected by urolithiasis.

The most significant socio-economic information given by the patients (type of work, sport activity) and their medical histories (personal and family medical history, dietary habits) showed no clear evidence for heredity as a factor of the disease or a clear link with other diseases. Excessive sweating and insufficient physical activity are common features among patients, and most patients had already suffered from stones (high percentage of recidivism). This is statistically significant ($p < 0.01$).

Struvite stones were expelled exclusively by females (age > 55 years), who are historically speaking more susceptible to this type of stones. The only cystine stone found belongs to a 47-year-old woman. The development of these stones is mainly related to hypercystinuria which is due to genetic features, as in this case, which shows a genetic predisposition to the disease.

An abundance of uric acid stones could be observed only in male patients (86% of cases). The most determinant risk factor for the crystallisation of uric acid is the presence of a strongly acidic environment (pH < 5.5) in which uric acid crystals cannot dissolve (Ferrari and Bonny 2004). In fact, acidic urinary pH decreases uric acid solubility and consequently favours crystallisation of uric acid.

All these factors, together with hyperuricosuria are strictly connected to dietary habits and the type of water ingested. An excessive intake of animal proteins (Anderson 1972; Drach 1978; Park and Coe 1994; Robertson and Peacaock 1982) was found in overweight patients who also showed high alcohol consumption (Schlesinger 2005). The lack of soft drink intake as well as the use of weakly bicarbonate water (bottled or not) does not promote sufficient urine alkalinisation that is necessary to dissolve uric acid crystals, which are the easiest type of stones to prevent and treat because they are easily soluble *in vivo*.

For calcium oxalate stones, the focus has been placed on the potential sources of oxalate. Some of these are produced directly by the human body, and the amount produced is directly proportional to body weight (Massey 2003). A direct relation between diets rich in oxalates and hyperoxaluria is well known (Brinkley et al. 1990; De Mendonca et al. 2003).

An increased intake of mineral waters causing an increases of pH seems to be associated with oxalate stones mixed with percentages of phosphates. For all the cases reported, there is a low consumption of liquid, which does not reach 2 L/day, to ensure a high urinary volume (Chang and Goldfarb 2004; Goldfarb 1988, 1990; Siener and Hesse 2003; Tucak et al. 2000; Vitale et al. 1996). Among people with calcium oxalate stones, there is an average excess body mass especially in cases of whewellite stones formed in kidney cavities.

5.4.4.3 Water Quality

Among the risk factors related to eating habits, the assumption of the liquids and in particular of the water re-enters. From the literature, data showed that there is a dispute between those who suggest the use of water rich in calcium and who advise against it in the urolithiasis cases.

Assuming that the consumption of soft water just helps prevent the development of urinary stones, the hardness of water was evaluated as a risk factor.

For the calculation at the regional level we assume a risk from a hardness greater than 30°f, but the association has been evaluated also for a risk equal to a hardness greater at 22.5°f, intermediate between the values corresponding to medium hardness.

In Basilicata, in the light of these data, it is possible to hypothesise that consumption of this water rich in calcium helps the further development of urolithiasis. Unfortunately, as can be seen from the Table 5.4, some values of odds ratio are not statistically significant due to the small number of cases registered.

5.4.4.4 Soil Quality

Based on the distribution of prevalence rates in the region, which indicate a greater spread of the disease in Apennines areas, the calculation of odds ratio was made considering at risk the residence in pedological regions with Apennines soil.

For the study, the prevalence of urolithiasis in Apennines soil, areas located at altitudes above 1,000 m, was compared to other areas, in the south-western part, divided by climatic aspects. The values of odds ratios showed a positive association between the prevalence of urolithiasis and Apennine soil; however, the values obtained are not considered statistically significant ($p < 0.1$).

The association is in any case present but not directly related to the different types of soil but related to the boundary variables such as climate, morphology and

altitude, which regulate the pedogenetic processes. It is these factors that determine the power of the association. Our hypothesis was that some chemical elements of the soil, through plants, could enter in the food chain and then in the human body by influencing the development of kidney stones. This does not occur because residents said they did not consume crops grown on these soils.

5.5 Conclusion

The geographic epidemiological survey showed the regional urolithiasis distribution (6.49% on average) and the areas particularly at risk due to demographic, environmental and behavioural factors. The municipalities with a prevalence of urinary stones are distributed in the central north-western region (Apennine area). Low temperatures, high altitude, low solar radiation and some soil characteristics are some of the risk factors which could explain the prevalence found, all of them influencing the Basilicata inhabitants' lifestyle.

This study underestimated real urinary disease prevalence, but for the aim of the study it was only necessary to verify a difference in the prevalence index of urolithiasis and also verify the environmental impact on the distribution of the pathology in the Basilicata towns. This simple study was meant to gain more information about the prevalence of lithiasis in a particular region of southern Italy such as Basilicata. This epidemiological survey helps to extend our knowledge of the distribution of this disease in our population, facilitating an estimation of its impact on society so as to improve prevention projects.

5.6 Concluding Remark

Geochemical and mineralogical investigations are providing important contributions to help understand the nature of the environmental risk factors to which affected populations have been exposed.

Rapid growth in the field of medical geochemistry is predicted, as it is a discipline that will continue to make valuable contributions to the study of epidemiology and public health, providing a dialogue among geochemists, mineralogists, epidemiologists, clinicians and medical doctors.

Acknowledgments Financial support came from POR Basilicata 2000/2006 – FONDO FESR – misura 1.5 – azione A – "MASPONE-FAECAB Project".

The authors gratefully acknowledge the Nephrology Unit, San Carlo Hospital (Potenza, Italy) and the Department for Health, Safety and Social Solidarity of the Basilicata Regional Authority.

References

Ackermann D, Baumann JM, Futterlieb A, Zingg EJ (1988) Influence of calcium content in mineral water on chemistry and crystallization conditions in urine of calcium stone formers. Eur Urol 14:305–308

Anasuya A (1982) Role of fluoride in formation of urinary calculi: studies in rats. J Nutr 112(9):1787–95

Anderson DA (1972) Environmental factors in the aetiology of urolithiasis. In: Proceedings of international symposium on renal stone research, Madrid, 1972, Karger, Basel, pp 130–144

Baggio B (1999) Genetic and dietary factors in idiopathic calcium nephrolithiasis. What do we have, what do we need? J Nephrol 12(6):371–374

Baker PW, Coyle P, Bais R, Rofe AM (1993) Influence of season, age and sex on the renal stone formation in south Australia. Med J Aust 159:390–392

Barberis E (1996) Il suolo inquinato: una possibile bomba chimica ad orologeria. Argille Minerali Argille III:249–260

Basilicata web site. http://www.sanita.basilicata.it. Accessed 1 June 2007

Bellizzi V, De Nicola L, Minutolo R (1999) Effects of water hardness on urinary risk factors for kidney stones in patients with idiopathic nephrolithiasis. Nephron 81(suppl 1):66–70

Bond NR, Lake PS, Arthington AH (2008) The impacts of drought on freshwater ecosystems: an Australian perspective. Hydrobiologia 600:3–16

Borghi L, Ferretti PP, Elia GF, Amato F, Melloni E, Trapasi MR, Novarini A (1990) Epidemiological study of urinary tract stones in a Northern Italian City. Br J Urol 65:231–235

Borghi L, Meschi T, Amato F, Novarini A, Romanelli A, Cigala F (1993) Hot occupation and nephrolithiasis. J Urol 150:1757–1760

Borghi L, Meschi T, Amato F, Briganti A, Novarini A, Giannini A (1996) Urinary volume, water and recurrences in idiopathic calcium nephrolithiasis: a 5-year randomized prospective study. J Urol 155:839–843

Borghi L, Meschi T, Schianchi T, Briganti A, Guerra A, Allegri F, Novarini A (1999) Urine volume: stone risk factor and preventive measure. Nephron 81(suppl 1):31–37

Borghi L, Schianchi T, Meschi T, Guerra A, Allegri F, Maggiore U, Novarini A (2002) Comparison of two diets for the prevention of recurrent stones in idiopathic hypercalciuria. N Engl J Med 346:77–84

Borghi L, Meschi T, Maggiore U, Prati B (2006) Dietary therapy in idiopathic nephrolithiasis. Nutr Rev 64(7):301–312

Breslau NA, Brinkley L, Hill KD, Pak CYC (1988) Relationship of animal protein-rich diet to kidney stone formation and calcium metabolism. J Clin Endocrinol Metab 66:140–6

Brinkley LJ, Gregory J, Pak CYC (1990) A further study of oxalate bioavailability in foods. J Urol 144:94–96

Broadus AE, Insogna KL, Lang R, Ellison AF, Dreyer BE (1984) Evidence for disordered control of 1,25-dihydroxyvitamin D production in absorptive hypercalciuria. N Engl J Med 311:73–80

Candarella R, Rizzoli E, Buffa A, Bottura A, Stefoni S (1998) Comparative study of the influence of 3 types of mineral water in patients with idiopathic calcium lithiasis. J Urol 159:658–663

Chang MA, Goldfarb DS (2004) Occupational risk for nephrolithiasis and bladder dysfunction in a chauffeur. Urol Res 32(1):41–43

Chen Y, Roseman JM, Devivo MJ, Huang C (2000) Geographic variation and environmental risk factors for the incidence of initial kidney stones in patients with spinal cord injury. J Urol 164:21–26

Coe FL, Kavalach AG (1974) Hypercalciuria and hyperuricosuria in patients with calcium nephrolithiasis. N Engl J Med 291:1344–50

Coe FL, Parks JH, Asplin JR (1992) The pathogenesis and treatment of kidney stones. N Engl J Med 327:1141–52

Conference C (1988) Prevention and treatment of kidney stones. JAMA 260:977

Curhan GC, Curhan SG (1994) Dietary factors and kidney stone formation. Compr Ther 20: 485–489
Curhan GC, Willett WC, Rimm EB, Stampfer MJ (1993) A prospective study of dietary calcium and other nutrients and the risk of symptomatic kidney stones. N Engl J Med 328:833–838
Curhan GC, Rimm EB, Willett WC, Stampfer MJ (1994) Regional variation in nephrolithiasis incidence and prevalence among United States men. J Urol 151:838–841
Curhan GC, Willett WC, Rimm EB, Stampfer MJ (1997a) Family history and risk of kidney stones. J Am Soc Nephrol l8:1568–1573
Curhan GC, Willet WC, Speizer FE, Spiegelman D, Stampfer MJ (1997b) Comparison of dietary calcium with supplemental calcium and other nutrients as factors affecting the risk for kidney stones in women. Ann Intern Med 126:497–504
DASREM (2006) AA.VV. I suoli della Basilicata. Carta pedologica della Regione Basilicata in scala 1:250000. Dipartimento Agricoltura, Sviluppo Rurale, Economia Montana, Regione Basilicata
Daudon M, Bader CA, Jungers P (1993) Urinary calculi: review of classification methods and correlations with etiology. Scanning Microsc 7:1081–1104
De Mendonca OGC, Martini LA, Baxmann AC (2003) Effects of an oxalate load on urinary excretion in calcium stone formers. J Ren Nutr 13:39–46
Decreto 31 maggio 2001. G U della Repubblica Italiana del 27.06.2001, Serie Generale N. 147, concernente il regolamento recante i criteri di valutazione delle caratteristiche delle acque minerali naturali
Drach GW (1978) Urinary lithiasis. In: Harrison JH, Gittes RF, Perlmutter AD, Stamey TA, Walsh PC (eds) Compbell's urology, vol 1. W.B. Saunders, Eastbourne, pp 779–878
Epstein FH (1968) Calcium and the kidney. Am J Med 45:700–714
Felici ML (2005) Fattori ambientali e salute: il ruolo degli elementi in traccia nella salute umana. Periodico Trimestrale della Società Italiana di Geologia Ambientale. Anno XIII 3:8–15
Ferrari P, Bonny O (2004) Diagnostik und prevention des harnsauresteins. Ther Umsch 61:571–574
Ferrie BG, Scott R (1984) Occupation and urinary tract stone disease. Urology 24:443–445
Giannossi ML (2010a). Studio di biominerali patologici presenti nel corpo umano: caratteri composizionali ed influenza ambientale nel caso studio della Basilicata [The study of pathological biominerals in humans: compositional features and environmental influence on Basilicata (southern Italy) case study]. Ph.D. thesis, Basilicata University, Potenza, 200 pp
Giannossi ML (2010b) The study of pathological biominerals in humans: compositional features and environmental influence on Basilicata (southern Italy): case study. Plinius. Supplemento italiano all'European J Mineral PLINIUS 36:100–104, ISSN 1972-1366
Giannossi ML, Summa V (2012) New mixed urinary stone: review of classification scheme. The Urologist 1(2) online publication
Giannossi ML, Mongelli G, Tateo F, Summa V (2012) Mineralogical and morphological compositions of kidney stones of a pilot case of a mediterranean region (Basilicata, Italy). Journal of X-ray science and technology 20:175–186. doi:10.3233/XST-2012-0327
Goldfarb S (1988) Dietary factors in the pathogenesis and prophylaxis of calcium nephrolithiasis. Kidney Int 34:544–555
Goldfarb S (1990) The role of diet in the pathogenesis and therapy of nephrolithiasis. Endocrinol Metab Clin North Am 19:805–820
Goldfarb DS, Fischer ME, Keich Y, Goldberg J (2005) A twin study of genetic and dietary influences of nephrolithiasis: a report from the Vietnam Era Twin (VET) Registry. Kidney Int 67:1053–1061
Grases F, Costa-Bauzá A, García-Ferragut L (1998) Biopathological crystallization: a general view about the mechanisms of renal stone formation. Adv Colloid Interface Sci 74:169–194
Grases F, Costa-Bauzá A, Ramis M, Montesinos V, Conte A (2002) Simple classification of renal calculi closely related to their micromorphology and etiology. Clin Chim Acta 322:29–36
Gunes S, Bilen CY, Kara N, Asci R, Bagci H, Yilmaz AF (2006) Vitamin D receptor gene polymorphisms in patients with urolithiasis. Urol Res 34:47–52

Gupta NP, Kesarwani P (2002) Current approaches in the medical management of urolithiasis; a review article. Indian J Urol 19:20–28
Guttenbrunner C, Gildsdrof K, Hildebrandt G (1989) The effect of mineral water containing calcium on supersaturation of urine with calcium oxalate. Urology 28:15–19
Hesse A, Brandle E, Wilbert D, Kohrmann KU, Alken P (2003) Study on the prevalence and incidence of urolithiasis in Germany comparing the years 1979 vs. 2000. Eur Urol 44(6): 709–713
Holmes RP, Goodman HO, Assimis DG (2001) Contribution of dietary oxalate to urinary oxalate excretion. Kidney Int 59:270–276
ISTAT website. http://demo.istat.it/. Accessed 1 June 2007
Kadurin S (1998) Minerals in human kidneys. In: Proceedings of the European crystallographic meeting, Praha, Czech Republic, 16–20 Aug 1998
Kleeman CR, Bohannan J, Bernstein D, Ling S, Maxwell MH (1964) Effect of variations in sodium intake on calcium excretion in normal humans. Proc Soc Exp Biol Med 115:29–32
Kohri K, Kodama M, Ishikawa Y, Katayama Y, Takada M, Katoh Y, Kataoka K, Iguchi M, Kurita T (1989) Magnesium-to-calcium ratio in tap water, and its relation to geological features and the incidence of calcium-containing urinary stones. J Urol 142:1272–1275
Kohri K, Ishikawa Y, Iguchi M, Kurita T, Okada Y, Yoshida O (1993) Relationship between the incidence infection stones and the magnesium–calcium ratio of tap water. Urol Res 21:269–72
Komatina MM (2004) Medical geology: effects of geological environments on human health. Elsevier, Amsterdam, p 488
Lee YH, Huang WC, Tsai JY, Lu CM, Chen WC, Lee MH, Hsu HS, Huang JK, Chang LS (2002) Epidemiological studies on the prevalence of upper urinary calculi in Taiwan. Urol Int 68(3):172–177
Ljunghall S, Hedstrand H (1975) Epidemiology of renal stones in a middle-aged male population. Acta Med Scand 197(6):439
Marangella M, Vitale C, Petrarulo M, Rovera L, Dutto F (1996) Effects of mineral composition in drinking water on risk for stone formation and bone metabolism in idiopathic calcium nephrolithiasis. Clin Sci 91:313–318
Marshall RW, Cochran M, Hodgkinson A (1972) Relationships between calcium and oxalic acid intake in the diet and their excretion in the urine of normal and renal-stone-forming subjects. Clin Sci 43:91–99
Massey LK (2003) Dietary influences on urinary oxalate and risk of kidney stones. Front Biosci 8:584–594
Massey LK (2005) Effect of dietary salt intake on circadian calcium metabolism, bone turnover, and calcium oxalate kidney stone risk in postmenopausal women. Nutr Res 25(10):891–903
McCarron DA, Rankin LI, Bennett WM, Krutzik S, McClung MR, Luft FC (1981) Urinary calcium excretion at extremes of sodium intake in normal man. Am J Nephrol 1:84–90
Mendenhall W (1967) Introduction to probability and statistics, 2nd edn. Wadsworth Publishing Company, Inc., Belmont, Chap. 10
Nasir S, Kassem ME, El-Sherif A, Fattah T (2004) Physical investigation of urinary calculi: example from the Arabian Gulf (State of Qatar). http://www.oxfordresearchforum.i12.com/articles/article%205.htm. Accessed 22 May 2012
Nielsen JB, Jensen TK (2005) Environmental epidemiology. In: Selinus O, Alloway B, Centeno JA, Finkelam RB, Fuge R, Lindh P, Smedley P (eds) Essential of medical geology, vol 21. Elsevier Academic Press, Amsterdam, pp 529–540
Pak CYC, Britton F, Peterson R et al (1980) Ambulatory evaluation of nephrolithiasis: classification, clinical presentation and diagnostic criteria. Am J Med 69:19–30
Park SJ, Coe FL (1994) An increasing number of calcium oxalate stone events worsens treatment out com. Kidney Int 45:1722–1730
Parry ES, Lister IS (1975) Sunlight and hypercalciuria. Lancet I:1063–1065
Pearle MS, Calhoun EA, Curhan GC (2004) In: Litwin MS, Saigal CS (eds) Urologic diseases in America. National Institute of Health, Bethesda, pp 3–42

Pearle MS, Calhoun EA, Curhan GC (2007) Urolithiasis. In: Litwin MS, Saigal CS (eds) Urologic diseases in America. US department of health and human services, public health service, national institutes of health, national institute of diabetes and digestive and kidney diseases. Washington, DC: US Government Printing Office, 2007; NIH Publication No. 07–5512, pp 281–320

Pendse AK, Singh PP (1986) The etiology of urolithiasis in Udaipur 562 (Western Part of India). Urol Res 14:59–62

Phillips MJ, Cooke JNC (1967) Relation between urinary calcium and sodium in patients with idiopathic hypercalciuria. Lancet 1:1354–7

Ramello A, Vitale C, Marangella M et al (2000) Epidemiology of nephrolithiasis. J Nephrol 13(3 Suppl):S45–S50

Robertson WG, Peacaock M (1982) The pattern of urinary stone disease in Leeds and in the United Kingdom in relation to animal protein intake during the period 1960–1980. Urol Int 73: 394–399

Robertson WG, Gallagher JC, Marshall DH, Peacock M, Nordin BEC (1974) Seasonal variations in urinary excretion of calcium. BMJ IV:436–437

Robertson WG, Peacock M, Marshall RW, Speed R, Nordin BEC (1975) Seasonal variations in the composition of urine in relation to calcium stone-formation. Clin Sci Mol Med 49:597–602

Robertson WG, Heyburn PJ, Peacock M, Hanes FA, Swaminathan R (1979) The effect of high animal protein intake on the risk of calcium stone formation in the urinary tract. Clin Sci (Colch) 57:285–8

Robertson WG, Peacock M, Baker M, Marshal DH, Pearlman B, Speed R, Sergeant V, Spith A (1984) Epidemiological studies on the prevalence of urinary stone disease in Leeds. In: Ryall RL et al (eds) Urinary stone. Churchill and Livingston, Melbourne, p 6

Rodgers AL (1997) Effect of mineral water containing calcium and magnesium on calcium oxalate urolithiasis risk factors. Urol Int 58:92–99

Rodgers AL (1998) The influence of South African mineral water on reduction of risk of calcium oxalate kidney stone formation. S Afr Med J 8:448–451

Saigal CS, Joyce G, Timilsina AR (2005) Urologic diseases in America project. Direct and indirect costs of nephrolithiasis in an employed population: opportunity for disease management? Kidney Int 68:1808–1814

Schlesinger N (2005) Dietary factors and hyperuricaemia. Curr Pharm Des 11:4133–4138

Serio A, Fraioli A (1999) Epidemiology of nephrolithiasis. Nephron 81(suppl 1):26–30

Shuster J, Finlayson B, Scheaffer RL, Sierakowski R, Zoltek J, Dzegede S (1985) Primary liquid intake and urinary stone disease. J Chron Dis 38:907–914

Siener R, Hesse A (2003) Fluid intake and epidemiology of urolithiasis. Eur J Clin Nutr 57(suppl 2):S47–S51

Sierakowski R, Finlayson B, Landes R (1979) Stone incidences as related to water hardness indifferent geological regions of the United States. Urol Res 7:157–160

Singh SP, Khare P, Satsangi GS, Lakhani A, Kumari KM, Srivastava SS (2001) Rainwater composition at a regional representative site of a semi-arid region of India. Water Air Soil Poll 127:93–108

Sommariva M, Rigatti P, Viola MR (1987) Prevention of the recurrence of urinary lithiasis: mineral waters with high or low calcium content? Minerva Med 78:1823–1829

Stamatelou KK, Francis ME, Jones CA, Nyberg LM, Curhan GC (2003) Time trends in reported prevalence of kidney stones in the United States: 1976–1994. Kidney Int 63:1817

Stelluti M, Rana G (2004) Caratterizzazione climatologia della Basilicata. Istituto Sperimentale Agronomico, Bari, 55 pp, ISSN 0304 – 0615

Strauss AL, Coe FL, Deutsch L, Parks JH (1982) Factors that predict relapse of calcium nephrolithiasis during treatment: a prospective study. Am J Med 72:17–24

Trinchieri A, Coppi F, Montanari E, Del Nero A, Zanetti G, Pisani E (2000) Increase in the prevalence of symptomatic upper urinary tract stones during the last ten years. Eur Urol 37: 23–25

Tucak A, Kalem T, Cvijetić S, Galić J, Prlić D, Zorić I, Dekanić Ožegović D (2000) The incidence and risk factor of urolithiasis in active working population of the Osijek community: an epidemiological study. Period Biol 102(4):431–435

Vahlensieck EW, Bach D, Hesse A (1982) Incidence, prevalence and mortality of urolithiasis in the German Federal Republic. Urol Res 10:161–164

Vitale C, Marangella M, Petrarulo M, Rovera L, Dutto F (1996) Effects of mineral composition of drinking water on risk for stone formation and bone metabolism in idiopathic calcium nephrolithiasis. In: Pak CYC, Resnick MI, Preminger GM (eds) Urolithiasis 1996. Miller, Dallas, pp 173–174

Yendt ER, Cohanim M (1978) Prevention of calcium stones with thiazides. Kidney Int 13:397–409

Zheng W, Beiko DT, Segura JW, Preminger GM, Albala DM, Denstedt JD (2002) Urinary calculi in aviation pilots: what is the best therapeutic approach? J Urol 168:1341–1343

Chapter 6
Magnetite Minerals in the Human Brain: What Is Their Role?

Pierpaolo Zuddas, D. Faivre, and J.R. Duhamel

Abstract Although it has long been known that magnetite (Fe_3O_4) can be formed biochemically by bacteria, protists, and a variety of living organisms, it is only in the past 20 years that magnetite has discovered to be present in the human brain. Researchers have documented the presence of magnetite nanocrystals in the human brain using magnetometric methods and transmission electron microscopy.

To understand the mechanism behind the formation of magnetite nanocrystals in the human brain, we have chosen to take a transdisciplinary approach associating studies of magnetite biomineralization in other species and geochemical research.

Although the exact role of magnetite nanocrystals on human cerebral physiology has yet to be determined, we suspect that it plays a significant role in the nervous system.

Keywords Brain magnetic nanominerals • Human nervous system • Biomagnetite

6.1 Introduction

Throughout the past 30 years, biologists and geochemists have carried out extensive research on organisms that have the ability to produce the ferromagnetic mineral magnetite. Magnetite is a mix of iron (II, III) oxide, Fe_3O_4, and is one of the

P. Zuddas (✉)
Institut des Sciences de la Terre de Paris, Université Pierre et Marie Curie – Paris Sorbonne, 4, place Jussieu, 75005 Paris, France
e-mail: pierpaolo.zuddas@upmc.fr

D. Faivre
Department of Biomaterials, Max Planck Institute of Colloids and Interfaces, Research Campus Golm, G14424 Potsdam, Germany

J.R. Duhamel
Centre de Neuroscience Cognitive, CNRS Université Claude Bernard Lyon1, 67 Bld Pinel, 69675 Bron Cedex, France

P. Censi et al. (eds.), *Medical Geochemistry: Geological Materials and Health*, DOI 10.1007/978-94-007-4372-4_6,

principal magnetic iron ores. Known since antiquity, magnetite was believed to have a purely inorganic origin resulting from magmatic or metamorphic events. The discovery of minerals formed by biological organisms (biominerals) with ferromagnetic properties and identification of biological magnetite was the first breakthrough toward an understanding of why some animals have the ability to detect the Earth's magnetic field. Small magnetite crystals are indeed found in many living organisms: bacteria, mollusks, arthropods, etc. All these organisms have evolved the ability to capture iron from their surroundings and convert it to magnetite.

The search for biogenic magnetite in human tissue was inconclusive until the early 1990s when magnetite crystals were found in human brain tissue extracted from the cerebral cortex, cerebellum, and meninges (membranes surrounding the brain and spinal cord), thanks to high-resolution transmission electron microscopy and electron diffraction (Kirschvink et al. 1992). We do not know how or why nanometer size crystals of magnetite form in the human brain, but formation mechanisms can be tentatively deduced using our knowledge on magnetite nanocrystals formed by magnetotactic bacteria (MTB).

MTB, also called biological magnets, are bacteria capable of moving along a magnetic field, including the Earth's magnetic field. Prokaryotic organelles present in magnetotactic bacteria are called magnetosomes. They are specialized organelles synthesized by MTB for geomagnetic navigation in their aquatic habitats. Recent studies suggest that these bacteria possess at least 30 genes involved in this process. We also know that fish, birds, and other species such as bats accumulate iron present in their environment and convert it into magnetite. Magnetite magnetosomes present in animal brains orient themselves according to the magnetic field and are responsible for the animal's capacity to locate itself spatially.

In this chapter, we documented the presence of magnetite crystals in the human brain and analyzed the possible reasons for their formation. Magnetite crystal formation is of interest for neurobiologists as it could be implicated in neurodegenerative and neoplastic diseases (Dobson and Grassi 1996; Dobson 2001; Hautot et al. 2007; Kobayashi et al. 1997). Sensitivity to magnetic fields is probably not the only role played by magnetite, which may also be responsible for transmitting magnetosome polarity in species over their long evolutionary path (Nanney 1985; Hedges 1985). This is the first evidence of nongenetically transmitted heredity. We could hypothesize that information fixation may be possible in biomagnetite in the absence of DNA (Banaclocha et al. 2010). Magnetite crystals present in the brain could be a component of evolutionary mechanisms designed to detect and transduce magnetic fields generated inside the cerebral neocortex.

6.2 Presence of Magnetite in the Human Brain

Biomagnetite has long been observed in bacteria, insects, birds, and marine fish, but it is only in the past 20 years that we have discovered biomagnetite in the human brain. Twenty years ago, Kirschvink et al. (1992) observed the presence of magnetite in human brain tissue when they analyzed postmortem human tissue samples from

patients between 48 and 88 years of age. Out of a total of 48 patients, 4 were suspected to have Alzheimer disease. Kirschvink et al. (1992) initially measured the emitted magnetic field using SQUID (superconducting quantum interference device), a magnetometer able to detect very weak magnetic fields. Brain tissue was sampled either by frozen fracture or dissection and put in a sterile vessel. Kirschvink and his team found that all the samples presented remnant isothermal magnetization (IRMs), saturating at about 300 mT, i.e., the characteristic value for magnetite. They estimated an equivalent of 4 ng of magnetite per gram of tissue, while the average values for the meninges from three of the sampled brains were 20 times higher. No significant differences were found between "normal brain" tissue and tissue from patients with suspected or confirmed Alzheimer disease. Using IRM (isothermal remnant magnetization), they found that magnetite particles were concentrated in small areas. Magnetite crystals were found in human brain tissue extracts from the cerebral cortex, cerebellum, and meninges (membranes surrounding the brain and spinal cord). Using high-resolution transmission electron microscopy (TEM) and electron diffraction, they indentified the presence of magnetite-maghemite crystals with an average size of 30 nm.

Observations showed that magnetite crystals were organized into linear, membrane-bound chains of a few micrometers in length, with up to 80 crystals per chain. Furthermore, each individual crystal's {111} was aligned along the length of the chain axis. This particular crystallographic direction corresponds to the "easiest" direction of magnetization. The {111} crystal alignment has been interpreted as a biological mechanism for maximizing the magnetic momentum per particle, as the {111} direction yields approximately 3% higher saturation magnetization than do other crystallographic directions of magnetite crystals. The shape of magnetite particles found in the human brain does not correspond to the usual octahedral morphological habitus of common crystals formed under geological conditions.

Magnetite crystals in the human brain appear to have a single magnetic domain, which means that they are uniformly and stably magnetized with the maximum magnetic momentum per unit volume possible for magnetite. Elemental analysis, by energy-dispersive X-ray analysis, electron diffraction patterns, and high-resolution transmission electron microscopy lattice images indicate that many of the particles were structurally well ordered and single domain, suggesting a precise biological control mechanism in the formation of this biomagnetite (Fig. 6.1).

6.3 Magnetite Nanocrystals Under Earth Surface Conditions

If in the past magnetite was believed to form under magmatic conditions at high temperatures and pressure, we now know that nanometer size magnetite crystals may form both inorganically under low-temperature conditions and/or in biological-controlled media. Inorganic magnetite crystals can be formed under natural sedimentary conditions and may resemble the biogenic ones formed by bacteria. In fact, inorganic magnetite nanocrystals can form at low temperatures

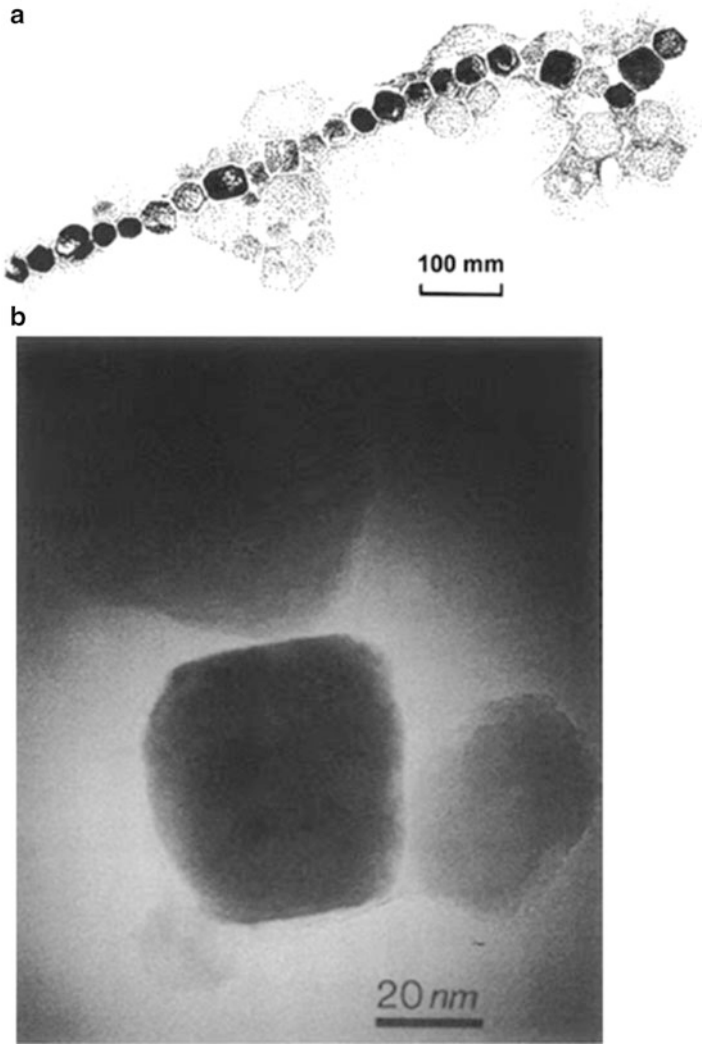

Fig. 6.1 (**a**) Magnetite crystals under low magnification, (**b**) transmission electron microscope image of a magnetite crystal from a human brain (From Kirschvink et al. 1992)

in aqueous media under relatively high iron concentrations and pH, i.e., total iron concentration exceeds 10 mM and pH is between 9 and 10 (Faivre and Zuddas 2006). These conditions are characteristic of anoxic conditions in continental and marine interstitial waters and are different when compared to the assumed physiological pH and extracellular iron concentrations typically between 1 and 100 μM.

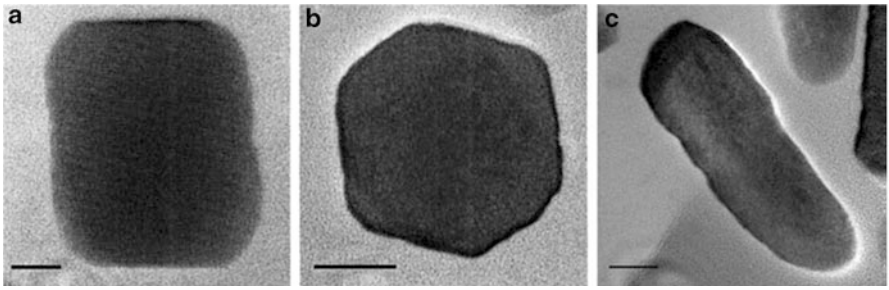

Fig. 6.2 Possible morphologies observed for magnetosomes based on high-resolution TEM images: (**a**) parallelepiped projection of a possibly peudohexagonal prismatic morphology, (**b**) hexagonal projection of a possibly cuboctahedral crystal, and (**c**) tooth-shaped (anisotropic) magnetosomes (the *scale bar* represents 20 nm). Note that the tooth-shaped magnetosomes are usually the larger ones and the cuboctahedral the smaller ones (From Faivre et al. 2005)

The most intriguing example of the biological formation of magnetite is biomineralization in bacteria magnetosomes. The magnetosomes comprise membrane-enveloped, nanosized crystals of magnetic iron oxide magnetite. The magnetosomes are arranged in intracellular chains that enable the cell to align itself with and swim along external magnetic fields, a behavior known as "magnetotaxis" (Blakemore 1975). Magnetotaxis facilitates the dwelling of bacteria in growth-favoring microoxic zones on the bottom of chemically stratified natural waters (Frankel and Blakemore 1991).

The morphology of magnetosome crystals is not constant but rather varies in combinations of cubic {100}, octahedral {111}, and dodecahedral {110} with possible distortions and elongations (Devouard et al. 1998). Same-species magnetite crystals possess a nearly equidimensional cubo-octahedra ({100} + {111}) morphology (Mann et al. 1984). Little to no biological intervention is required to explain the formation of isometric cubo-octahedral crystals in the *Magnetospirillum* strains, since identical morphologies are obtained through inorganic synthesis (Faivre et al. 2005) (Fig. 6.2).

We propose that since the morphology of the magnetosome crystals is very species specific, with sizes always within the SD range, magnetic crystal growth must be regulated. Unfortunately, this regulation mechanism is as yet undetermined (Faivre and Zuddas 2007). Recent studies have shown that several proteins in MAI genes have an influence over particle size and crystallinity (Murat et al. 2010). In *Magnetospirilla*, the magnetosomes are aligned in a single chain oriented along the longitudinal cell axis. Cryoelectron tomography studies have shown the existence of a filamentous structure, responsible for organizing the magnetosome crystals (Komeili et al. 2006; Scheffel et al. 2006; Katzmann et al. 2010).

6.4 What Is Magnetite Doing in the Human Brain?

Several areas of the cerebrum, the dentate nucleus, the basal ganglia, and areas of the midbrain could have high iron content (Hallgren and Sourander 1958). However, samples of these areas showed magnetic particles at a similar level to those of the cerebral cortex. We know that magnetite crystals allow bacteria to orient themselves with respect to the Earth's magnetic field and allow animals, such as bees, birds, and fish, to navigate by compass direction. We do not know why the magnetite is present in the human brain; we only know that it is there. Ferromagnetic crystals interact over a million times more intensively with the external magnetic field than do diamagnetic or paramagnetic materials like deoxyhemoglobin, ferritin, or hemosiderin.

The fundamental question is: what is the mechanism through which the weak geomagnetic fields are perceived by organisms that are able to precipitate crystals of a ferromagnetic mineral such as magnetite? Could these crystals use their motion in a variety of ways to "translate" the geomagnetic field into signals that can be processed by the nervous system? In bacteria, the answer is simple: the magnetite crystals orient the bacteria as a function of the local magnetic field. Magnetite found in animals guides them through a biological compass, but it is unclear why the magnetite is present in humans.

The presence of biological membranes bounding the magnetite implicates some kind of mechanical coupling of each compass-like magnetite particle to a mechanoreceptor. This may allow the particle position to be monitored by a unique sensory organelle. As observed in bacteria, cells produce magnetite when needed. Forms of advanced physical "intelligence" can directly tap into this information if they have a crystalline network within their brain cavity. In nature, DNA (proteins) transforms DNA functions through piezoelectric crystal lattice structures converting electromagnetic oscillations to mechanical vibrations and vice versa. Studies with exogenously administered electromagnetic fields have shown that both transcription (RNA synthesis) and translation (protein synthesis) can be induced by electromagnetic fields. In bones, in fact, direct current may produce osteogenesis (bone formation) and bacteriostasis affecting adenosine triphosphate (ATP) generation, protein synthesis, and membrane transport.

6.4.1 Electromagnetic Representation

In the human brain, pyramidal cells are present and arranged in layers in the cortex of the two cerebra. The pyramidal cells may act as electro-crystal cells immersed in extracellular tissue fluids. They could operate in the fashion of a liquid crystal oscillator in response to different light commands, or light pulses, which in turn change the orientation of every molecule and atom within the body. Electron impulses from a neuron generate a weak amperage magnetic field

activating ultrathin crystals or liquid crystal in the pyramidal cell. On flexing, this ultrathin crystal becomes a piezoelectric oscillator, producing a circular polarized light pulse that travels throughout the body, or a transverse photonic bundle of energy.

Mechanical stress produces a piezoelectric signal from the collagen in bones. The signal is biphasic, switching polarity with each stress-and-release. Signals are rectified by apatite and collagen junctions. The strength of the signal tells the bone cells how strong the stress is, and its polarity tells them what direction it comes from. Osteogenic (bone forming) cells, which have been shown to have a negative potential, would be stimulated to grow more bone, while those in the positive area would stop producing bone matrix and be resorbed when needed. If bone growth and resorption are part of one process, the electrical signal acts as an analogue code to transfer information about stress to the cells and trigger the right response. Hence, stress is converted into an electrical signal. An interesting property of semiconductor diode junctions may be observed when current is run though the diode in forward bias, i.e., when there is a good current flow across the barrier. Some of the energy is turned into light and emitted from the surface and is therefore known as light-emitting diodes (LEDs). Bone has a LED that requires an outside source of light before an electric current can make it release its own light, and the light it emitted at an infrared frequency is invisible to us, but consistent. By applying a few microamperes of external current thereby triggering biologically generated electric currents, it may be possible to regenerate the spinal cord, optic nerve, bone, or entire limbs naturally or influence developing embryos.

6.4.2 A Role for Memory

Banaclocha (2005, 2007) and Banaclocha et al. (2010) suggested that in addition to electrical, molecular, and synaptic communication within the neocortex, there is a magnetic interplay between neuronal and astroglial networks consistent with the statistical mechanics of neocortical interaction (Ingber 1984). This may explain memory and cerebral computation. According to this hypothesis, neural activity-associated magnetic fields (NAAMFs) generated in neocortical minicolumns can, over time, determine the intensity and orientation of the static magnetic fields in neighboring astrocytes. This results in the generation of specific 3-D magnetic structures that in combination with attractor states may constitute the basis of short-term memory and other cognitive functions. According to this hypothesis, exposure to electromagnetic fields will modulate the ion channels' membrane conductance through interactions with extracellular or membrane-bound proteins. Biomagnetite may thus play a key role in the transduction of magnetic signals produced within the neocortex itself. Since magnetite crystals are synthesized and distributed in the human brain in a specific and controlled form, NAAFs may drive the distribution and organization of biomagnetite nanoparticles (single domain and/or superparamagnetic) in neuronal membranes in a nonrandom crystal distribution over the neuronal

surface. Each neuron might have a specific biomagnetite hallmark, depending on its activity and connectivity, when alternating magnetic fields associated with each neutron activity drive the magnetite distribution in a nonrandom way. The biomagnetite distribution in the neocortical astroglial network would store long-term information and would generate 3-D magnetic constructs of sufficient intensity to affect magnetite nanoparticles localized in adjacent neuronal membranes. Self-organization of the astroglial magnetic field may work as a complex and dynamic physical actractor driving and modulating spontaneous neuronal activity in the neocortex (Cossart et al. 2003; Beggs and Plenz 2004; MacLean et al. 2005). This may explain some cognitive functions as the result of the magnetic properties that arise naturally as a consequence of the cytoarchitectonic organization of biomagnetite in the neocortex. Consequently, creativity, imagination, thinking, and dreams would arise when magnetically memorized information in the astroglial biomagnetite network drive feed-forward coherent and synchronized neuronal activities in the membranes. The integration and self-organization of multiple astroglial magnetic fields may store external information in the long term.

6.5 Conclusions

The discovery of magnetite nanoparticles and the study of their physical properties using geochemical methodology opened new horizons in the neurosciences. Biomagnetite may be a shared phenomenon in bacteria, animals, and the human brain where it serves to detect magnetic signals. Magnetite in the brain may well be one of the mechanistic components retained during the evolution of the species in order to identify and transduce the magnetic fields generated in the cerebral neocortex. This may give credence to the hypothesis of nongenetically transmitted heredity. It is possible that the magnetite nanoparticles distributed in the membrane of neurons play a role in reception, transduction, and storage of information arriving in the neocortex.

References

Banaclocha MAM (2005) Magnetic storage of information in the human cerebral cortex: a hypothesis for memory. Int J Neurosci 115:329–347

Banaclocha MAM (2007) Neuromagnetic dialogue between neuronal minicolumns and astroglial network: a new approach for memory and cerebral computation. Brain Res Bull 73:21–27

Banaclocha MAM, Bokkon I, Banaclocha HM (2010) Long-term memory in brain magnetite. Med Hypotheses 74:254–257

Beggs JM, Plenz D (2004) Neuronal avalanches are diverse and precise activity patterns that are stable for many hours in cortical slice cultures. J Neurosci 24:5216–5229

Blakemore RP (1975) Magnetotactic bacteria. Science 190:377–379

Cossart R, Aronov D, Yuste R (2003) Attractor dynamics of network UP states in the neocortex. Nature 423:3924–3929

Devouard B, Posfai M, Hua X, Bazylinski DA, Frakel RB, Busek PB (1998) Magnetite from magnetotactic bacteria: size distribution and twinning. Am Mineral 83:1387–1398

Dobson J (2001) Nanoscale biogenic iron oxides and neurodegenerative disease. FEBS Lett 496:1–5

Dobson J, Grassi P (1996) Magnetic properties of human hippocampal tissue-evaluation of artefact and contamination sources. Brain Res Bull 39:255–259

Faivre D, Zuddas P (2006) An integrated approach to determine the origin of magnetite nanoparticles. Earth Planet Sci Lett 243:53–60

Faivre D, Zuddas P (2007) Mineralogical and isotopic properties of biogenic nanocrystalline magnetites. In: Schüler D (ed) Magnetoreception and magnetosomes in bacteria. Springer, Heidelberg

Faivre D, Menguy N, Guyot F, Lopez O, Zuddas P (2005) Morphology of nanomagnetite crystals: implications for formation conditions. Am Mineral 90:1793–1800

Frankel RB, Blakemore RP (1991) Iron biominerals. Plenum Press, New York

Hallgren B, Sourander P (1958) The effect of age on the non-haemin iron in the human brain. J Neurochem 3:41–51

Hautot D, Pankhurst QA, Khan N, Dobson J (2007) Preliminary evaluation of nanoscale biogenic magnetite in Alzheimer's disease brain tissue. Proc R Soc Lond B 207(Suppl):1–5

Hedges RW (1985) Inheritance of magnetosome polarity in magnetotropic bacteria. J Theor Biol 112:607–608

Ingber L (1984) Statistical mechanics of neocortical interactions deviation of short-term memory capacity. Phys Rev A 29:3346–3358

Katzmann E, Scheffel A, Gruska M, Plitzko JM, Schüler D (2010) Loss of the actin-like protein MamK has pleiotropic effects on magnetosome formation and chain assemblage in *Magnetospirillum gryphiswaldense*. Mol Microbiol 77:208–224

Kirschvink JL, Kobayashi-Kirschvink A, Woodford BJ (1992) Magnetite biomineralization in the human brain. Proc Natl Acad Sci USA 89:7683–7687

Kobayashi A, Yamamoto N, Kirschvink J (1997) Studies of inorganic crystals in biological tissue: magnetite in human tumor. J Jpn Soc Powder Powder Metall 44:294–300

Komeili A, Li Z, Newmann DK, Jensen GJ (2006) Magnetosomes are cell membrane invaginations organized by the actin-like protein MamK. Science 311:242–245

MacLean JN, Watson BO, Aaron GB, Yuste R (2005) Internal dynamics determine the cortical response to thalamic stimulation. Neuron 48:811–823

Mann S, Frankel RB, Blakemore RP (1984) Structure, morphology and crystal growth of bacterial magnetite. Nature 310:405–407

Murat D, Quinlan A, Vali H, Komeili A (2010) Comprehensive genetic dissection of the magnetosome gene island reveals the step-wise assembly of a prokaryotic organelle. Proc Natl Acad Sci USA 107:5593–5598

Nanney DL (1985) Heredity without genes: ciliate explorations of clonal heredity. Trends Genet 1:295–298

Scheffel A, Gruska M, Faivre D, Linaroudis A, Plitzko JM, Schüler D (2006) An acidic protein aligns magnetosomes along a filamentous structure in a magnetotactic bacteria. Nature 440:110–115

Chapter 7
Chemometrics and Medical Geochemistry: A Brief Tutorial

Robyn E. Hannigan

Abstract Chemometrics – the science of extracting information from chemical systems using multivariate and mathematics methods – when applied to geochemical and human health data can reveal unique relations. As a tutorial for chemometric analysis of geochemical data and linked medical data, this chapter presents a brief survey of approaches that can be used to reveal new insights into the interdependencies of geochemistry and human health.

Keywords Chemometrics • Multivariate statistics • Statistical modeling • Data visualization

7.1 Introduction

Chemometric techniques are commonly used in analytical chemistry and are typically applied to experimental design and method development. More recently chemometrics has been applied to solve descriptive and predictive questions using chemical system properties to understand the underlying relations and structure of biological systems. Applications of chemometrics to geochemistry are limited to multivariate statistical analysis of geochemical data and are rarely applied to understand the linkages between geochemical and biological systems.

The use of statistical approaches to evaluate geochemical data in the context of human health, or any context, requires the development of falsifiable hypotheses and an understanding that statistically significant is not the same thing as geologically significant (Vermeesch 2009). When developing a testable hypothesis, we most often begin with a null hypothesis (H_o), phrased in the language of "no effect"

R.E. Hannigan (✉)
Department of Environmental, Earth, and Ocean Sciences, University of Massachusetts Boston, Boston, MA, USA
e-mail: Robyn.Hannigan@umb.edu

P. Censi et al. (eds.), *Medical Geochemistry: Geological Materials and Health*, DOI 10.1007/978-94-007-4372-4_7,

(e.g., Se concentrations in groundwater are not associated with human health effects in the local population), and an alternative hypothesis (H_a), phrased in the language of "effect" (e.g., Se concentrations in groundwater are associated with human health effects in the local population). We then use statistical methods, most often univariate, to accept or reject our null hypothesis. While this approach works just fine in simple systems, where questions are obvious and where effect and sample sizes are homogenous across the data, this approach becomes unwieldy when dealing with interaction effects between geochemical and medical variables, multiple colinearity, lack of *a priori* knowledge about the system interactions, and heterogeneity in variance across the sample set.

While application of chemometric approaches in medical geochemistry are absolutely appropriate and often the only methods that will reveal meaningful causative relations between the two systems, there are precautions we must take and assumptions we must make. This chapter is a simple summary of some approaches that can be used to test complex null hypotheses to identify statistically, medically, and geologically significant relations among geochemical and human biological data. This tutorial is not, however, exhaustive or prescriptive.

7.2 Methods

The data used in this tutorial are compiled both from the literature and from the author's research and are presented here for teaching purposes only. Chemometric approaches discussed below were done in SPSS 20.0, Minitab 16.0, and Statistica 10. This tutorial assumes the reader is proficient at data quality assurance and quality control procedures and that all data to be used have been vetted for quality and geological relevance.

7.3 Results and Discussion

7.3.1 Univariate Assessment of Significance

Geochemists rarely have the opportunity to design experiments. We operate at the mercy of natural processes, and when working in the field of medical geochemistry, we most often are evaluating relations between human health and geochemistry in a reactive rather than proactive manner. There are advantages and disadvantages to this condition. The advantage is that we have *a priori* knowledge of the human health impacts (e.g., volcanic ash leading to development of breathing disorders in exposed individuals) as well as *a priori* knowledge of the underlying geological processes (e.g., overproduction of groundwater for irrigation led to increased selenium concentrations which increased the selenium concentrations in produce and ultimately impacted human health). This *a priori* knowledge allows us to

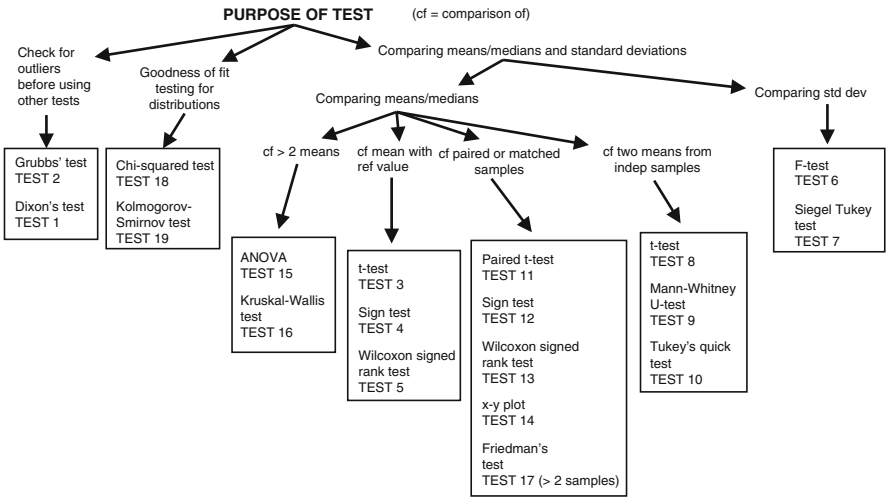

Fig. 7.1 Univariate significance tests to explore relations among data. Tests 1 and 2 assume normally distributed data. For non-normal or multiple outliers, use outlier generation modeling (Davies and Gather 1993)

develop hypotheses that are testable and based on solid scientific understanding (H_o: The concentration of Se in groundwater has not changed since pumping began; H_a: The concentration of Se in groundwater has changed since pumping began). We can use simple univariate approaches to test the null hypothesis. The data, in this example, are Se concentrations in groundwater, measured quarterly, just prior to and since pumping began. Using a simple flow chart (Fig. 7.1), we must first test the Se data for outliers, then check the Se data for normality. In this dataset there are no data gaps (Table 7.1) (e.g., dates without Se measurement).We also assume that the analytical precision and accuracy are sufficient to retain these data (e.g., no bias). When data gaps occur, you may use a number of chemometric approaches to "fill in" these gaps such as imputation or interpolation (Adèr 2008).

Testing our hypothesis that Se concentration in the groundwater has not changed since pumping began, we will look at a subset of Se concentrations and test for outliers (Table 7.2).

By eye, we suspect that the Se measurement taken 9 months prior to the start of pumping is an outlier. We cannot remove this point based on our bias alone. First we must confirm that the data are normal. Using the Kolmogorov-Smirnov normality test, the data are normally distributed ($p > 0.10$, $\alpha = 0.05$). We can then use Dixon's Q outlier test to see if the suspect Se concentration (23 $\mu g\ L^{-1}$) is an outlier for the whole dataset or just within the pre-pump data. For the whole dataset, the Q value is 0.154 which is less that the critical value for Q (95% confidence, $n = 9$; 0.493) so 23 is not an outlier. Looking only at the pre-pump data, we see that the Q value is 0.579 which is still less than the Q_{crit} for four samples ($\alpha = 0.05$, $Q_{crit} = 0.829$). So, like it or not, we have to keep that point in our dataset.

Table 7.1 Groundwater data used in this case study

Sample #	Time since pumping (months)	Precip (cm)	Planting group (1 = fallow, 2 = planted)	Se ($\mu g\ L^{-1}$)	U ($\mu g\ L^{-1}$)	Mo ($\mu g\ L^{-1}$)	DOC ($mg\ L^{-1}$)	Nitrate ($mg\ L^{-1}$)	Silica ($mg\ L^{-1}$)
S1	−60	1.00	1	2.00	0.11	9.38	1.61	0.01	0.01
S2	−57	1.00	1	8.00	0.05	8.93	1.90	0.01	0.01
S3	−54	2.00	2	6.00	0.14	8.93	1.88	0.03	0.02
S4	−51	2.00	2	6.00	0.02	7.33	1.93	0.07	0.06
S5	−48	5.00	2	4.00	0.15	7.81	3.30	0.01	0.02
S6	−45	1.00	1	3.00	0.04	7.58	2.95	0.02	0.02
S7	−42	1.00	1	12.00	0.00	6.49	3.21	0.00	0.02
S8	−39	1.00	1	20.00	0.01	7.48	2.79	0.03	0.02
S9	−36	5.00	2	18.00	0.08	8.22	2.72	0.02	0.11
S10	−33	5.00	2	8.00	0.01	7.23	0.94	0.01	0.01
S11	−30	5.00	2	12.00	0.00	7.86	1.67	0.01	0.04
S12	−27	1.00	1	8.00	0.05	7.63	1.64	0.01	0.07
S13	−24	1.00	1	6.00	0.57	9.10	1.52	0.01	0.01
S14	−21	0.00	1	2.00	0.06	8.57	1.23	0.03	0.01
S15	−18	2.00	2	4.00	0.13	8.82	0.91	0.04	0.01
S16	−15	0.00	2	4.00	0.05	10.36	0.87	0.02	0.02
S17	−12	1.00	2	4.00	0.05	8.63	1.62	0.04	0.05
S18	−9	1.00	1	23.00	0.30	9.24	1.54	0.04	0.05
S19	−6	0.00	1	8.00	0.08	9.53	1.51	0.01	0.05
S20	−3	0.00	1	12.00	0.04	9.88	0.73	0.02	0.08

(continued)

Table 7.1 (continued)

Sample #	Sr ($\mu g\ L^{-1}$)	Ba ($\mu g\ L^{-1}$)	Ca ($mg\ L^{-1}$)	Eh (volts)
S1	3.70	1.87	34.58	420
S2	3.45	9.50	45.60	430
S3	6.14	9.67	36.90	510
S4	8.64	6.31	48.32	620
S5	9.28	7.45	44.38	620
S6	13.02	7.36	25.85	590
S7	10.22	4.70	40.80	650
S8	14.99	7.29	52.85	420
S9	16.57	10.26	37.18	380
S10	24.37	5.47	47.33	420
S11	26.51	6.66	44.02	550
S12	28.10	7.85	61.39	610
S13	10.93	5.35	50.95	520
S14	12.81	5.44	54.94	700
S15	13.88	6.76	65.89	680
S16	20.41	7.11	48.86	770
S17	19.89	8.25	55.27	620
S18	21.99	8.92	60.53	580
S19	24.15	7.84	65.25	520
S20	26.71	8.46	61.91	550

(continued)

Table 7.1 (continued)

Sample #	Time since pumping (months)	Precip (cm)	Planting group (1 = fallow, 2 = planted)	Se ($\mu g\ L^{-1}$)	U ($\mu g\ L^{-1}$)	Mo ($\mu g\ L^{-1}$)	DOC ($mg\ L^{-1}$)	Nitrate ($mg\ L^{-1}$)	Silica ($mg\ L^{-1}$)
S21	0	5.00	2	35.00	0.14	9.47	0.62	0.02	0.09
S22	3	6.00	2	67.00	0.10	8.16	1.02	0.02	0.06
S23	6	10.00	2	90.00	0.17	6.66	0.90	0.04	0.05
S24	9	5.00	1	92.00	0.69	8.57	0.77	0.01	0.00
S25	12	2.00	1	101.00	0.30	11.37	1.74	0.01	0.07
S26	15	0.00	1	150.00	0.06	8.74	0.78	0.03	0.11
S27	18	0.00	2	150.00	0.14	9.40	0.73	0.03	0.14
S28	21	2.00	2	270.00	0.00	7.69	0.69	0.01	0.00
S29	24	2.00	2	300.00	0.00	8.36	1.53	0.01	0.01
S30	27	1.00	1	290.00	0.03	7.11	1.45	0.02	0.04
S31	30	1.00	1	250.00	0.00	8.38	1.66	0.02	0.00
S32	33	2.00	1	300.00	0.03	7.64	2.53	0.01	0.01
S33	36	0.00	2	350.00	0.03	8.18	2.57	0.02	0.01
S34	39	5.00	2	350.00	0.04	7.41	1.01	0.01	0.05
S35	42	5.00	2	400.00	0.08	7.69	1.62	0.01	0.02
S36	45	2.00	1	500.00	0.04	9.59	1.47	0.01	0.02
S37	48	0.00	1	600.00	0.04	8.55	1.37	0.03	0.02
S38	51	1.00	1	800.00	0.07	8.55	1.69	0.00	0.03
S39	54	7.00	2	900.00	0.07	8.93	1.68	0.01	0.03
S40	57	6.00	2	1,200.00	0.08	9.76	1.57	0.02	0.09

(continued)

Table 7.1 (continued)

Sample #	Sr ($\mu g\ L^{-1}$)	Ba ($\mu g\ L^{-1}$)	Ca ($mg\ L^{-1}$)	Eh (volts)
S21	29.37	8.28	50.86	550
S22	19.43	19.37	34.80	230
S23	32.11	13.21	54.31	180
S24	26.32	5.87	93.67	280
S25	22.17	10.11	63.23	410
S26	20.08	8.08	69.05	580
S27	32.86	19.90	48.37	610
S28	52.08	21.30	57.12	890
S29	44.60	47.30	47.11	760
S30	74.40	54.10	62.08	650
S31	76.00	32.10	57.15	730
S32	52.30	30.20	68.88	620
S33	79.30	32.00	57.11	830
S34	49.30	53.80	56.10	920
S35	74.30	81.10	97.37	950
S36	59.60	71.60	85.26	970
S37	84.30	36.70	90.40	970
S38	72.40	14.30	93.98	1,100
S39	69.10	51.70	112.56	1,150
S40	52.30	105.50	86.83	1,020

Time since pumping (months) is negative if prior to pumping, positive after pumping started. Precipitation measured at the site of groundwater sample collection *DOC* dissolved organic carbon

Table 7.2 Subset of Se concentration data used for testing for outliers

Se ($\mu g\ L^{-1}$)	4	**23**	8	12	35	67	90	92	101
Time since pumping began (months)	−12	**−9**	−6	−3	0	3	6	9	12

Suspected outlier shown in bold

Since we know the selenium data are normally distributed and that none of these data are outliers, we can proceed to hypothesize about the impact of pumping on groundwater Se since we suspect that pumping led to increased Se in the groundwater translating to increased Se in the produce grown using these waters and subsequently to human health effects.

To test whether pumping changed groundwater Se concentrations, we must make sure we have a balanced dataset. Ideally, we want as many measurements of Se before pumping as we have after. If this were not the case, we could not proceed with our evaluation of the data. For the purposes of this tutorial, let us assume that we have normally distributed data extending, quarterly, 5 years prior to pumping and to the present which is 5 years after pumping (including the first year) (Table 7.1).

To test that there is a difference, post-pumping, in Se concentrations in the groundwater, we can perform a *t*-test (unpaired because the samples are not the same ones tested pre- and post-pumping, two-tailed because we do not want to introduce bias in assuming that Se concentrations are higher post-pumping). Our results show that the mean Se concentrations are significantly different pre- and post-pumping ($t = 5.112$; $p < 0.0001$). Also we find that the standard deviations in mean Se concentration pre- and post-pump are statistically different meaning that our whole dataset is, in fact, non-normal. We found, above, that a subset (Table 7.2) was normally distributed but do not ever assume that the state of a subset translates to the entire dataset any more than you would assume that your sample data represent the entire population of samples that could be tested. Since we found a significant difference in means but also found the data were not normal (standard deviation of the means were statistically different), we could use a corrected *t*-test: unpaired *t*-test – Welch corrected. This also identifies the mean difference pre- and post-pumping, but the non-normal distribution of the data is a violation of the assumption of not only the normality of mean required by the *t*-test but also the normality of the variance about the mean assumption. So we must turn to a nonparametric means comparison statistic so that the violation of the assumptions of normality does not bias our results and lead us to draw conclusions that are incorrect (accepting a false null). A nonparametric test for significant differences between means is the Mann-Whitney *U* test. Again we choose the two-tailed probability value for this test. The means are statistically significantly different pre- and post-pumping ($p < 0.0001$). But, can we say that pumping is the cause of this difference?

To evaluate this we need *a priori* knowledge of the system. What other factors can change groundwater Se concentrations in the region we are studying? Water–rock interactions can lead to increased Se concentrations in groundwater that are weathering bedrock high in Se (e.g., marine shales and mudstones). This will also lead to increases in other metals such as U, Mo, and dissolved organic carbon

(DOC). Se can also be oxidized by nutrients such as nitrate. So, groundwater redox state matters with respect to Se concentrations as well. Thus, we have to consider what factors might affect groundwater redox. Irrigation pumping is one of them as is groundwater-surface water interaction which can be measured by changes in groundwater recharge rate and stream baseflow as well as water table depth. In addition to natural processes such as increased storm intensity and increased recharge, human activities can also impact Se concentrations in the groundwater through activities such as ash deposition from coal power station introduced into soil and therefore interacting with precipitation during infiltration, Se in manure introduced as fertilizer in soils, and waste water from landfills infiltrating into the groundwater. As you can see from the simple scenario we began with, statistical analyses of geochemical data alone become quite complicated rather quickly. We have to turn from univariate statistics to multivariate statistics in order to evaluate the impact of both natural and human impacts on groundwater Se concentrations before we can ascribe them to irrigation pumping alone.

7.3.2 Multivariate Approaches to Evaluating Relations Among Data

As geochemists we have inherent *a priori* knowledge of our geological setting and the potential natural causes for changes in elemental composition of groundwater. If our groundwater is interacting with a marine shale that has high concentrations of Se, then we should also see high concentrations of other metals known to be enriched in these sedimentary rocks. For example, we should see increased concentrations of U and Mo in our groundwater, and assuming that the ground waters are reducing, we should also see high concentrations of sulfide and dissolved DOC. In an almost perfect world, such as we are in for the purposes of this tutorial, we have measured values of U, Mo, and DOC for all of our samples. If the groundwater is oxidized or the aquifer is a sandstone or limestone, we should see low concentrations of Se, U, and Mo and high concentrations of Ba, Sr, and Ca (if a carbonate) or Si (if a sandstone). If Se is being oxidized by nitrate introduced from surface water interactions, then we should see differential oxidation of Se compared to other redox sensitive metals. Lastly, if Se is being introduced from pollution or from soil amendments, we should see Se concentrations increase during times of agricultural activity and decline during fallow seasons. Of course the above are oversimplifications but provide a framework for our next set of statistical tests.

We will assume, here, that the aquifer is a Miocene black shale. Therefore, we can assume that some of the Se in the groundwater is from weathering of this material. We can test for seasonality in our data with respect to Se concentrations using two factors: fallow/growing season and precipitation. We would label our data as group 1 (fallow) and group 2 (growing) and use measured mean quarterly precipitation values (Table 7.1). We now can build our hypotheses. Again, we need

to be certain all of our data are normally distributed. We now have the following scalar variables: Se, Mo, U, DOC, nitrate, silica, Sr, Ba, Ca, redox potential (Eh), and two nominal factors: Pre- and post-pumping and growing season. A univariate test for normality of all of the scalar values shows that none of the scalar data are normally distributed. So we need to transform the data for normality. There are numerous approaches we can take to do this (Draper and Cox 1969; Cox and Small 1978). Natural log transformation normalized several metals (Se, U, Mo, Sr, Ca) as well as redox potential (Eh). However, several analytes remained non-normally distributed. Since not all of the scalar variables could be normalized using mathematical transformations, we can rank the data (highest to lowest within a given variable), and this normalizes the data. We will use non-normally distributed original data very rarely and only when using robust statistical tests (those that can tolerate outliers and violations in the assumptions of normality). The majority of our analyses will use ranked data.

So now let us explore whether there is any relation between Se in groundwater and growing season. To do this we could use the univariate approach as above but since we have precipitation data and precipitation data covaries with growing season (lower in the fallow seasons), we have to consider that precipitation and growing season are covariates. So we need to perform a multivariate analysis of variance (MANOVA) and include precipitation as a covariate. We will use a generalized linear model MANOVA with planting group as a fixed factor (two levels) and precipitation as a covariate. The model will produce information regarding the probability that the variance in Se is due to the planting season ($p = 0.798$) or due to precipitation ($p = 0.197$). The interaction of planting group and precipitation on Se is not significant ($p = 0.109$). So the hypothesis that planting season and/or precipitation have no effect on groundwater Se is retained. Since we now know this, we can further explore the geochemical controls on Se concentration.

We can use the ranked data to evaluate relations among our scalar variables using a Spearman rank correlation. Significant ($p < 0.05$) relations were found between Sr and Se ($r = 0.846$), between Se and Ba ($r = 0.832$), between Ca and Se ($r = 0.622$), and between Eh and Se ($r = 0.910$). These relations do not suggest a linear relation but reflect interdependence between Se and these other parameters. Recall that we know the bedrock is Miocene black shale and we hypothesized that Se increases in groundwater could be attributed to water-rock interactions. We found no relation between Se and other "black shale"-associated metals such as Mo or U. We did find a relation between the "carbonate" metals Sr, Ba, and Ca and with Eh. This suggests that Se concentrations are related to redox potential and that, perhaps, there is a source of Sr, Ba, and Ca mixing with the groundwater and equilibrating under oxidized conditions. Could it be that surface water, with a carbonate character, could be mixing with the groundwater? If that were happening, could Se be being oxidized by nitrate from these waters? There is a weak negative relation between nitrate and Eh (90% confidence, $r = -0.279$, $p = 0.082$) which means that as Eh increases (oxidized environment) the nitrate concentrations are declining which may reflect some unique redox chemistry for nitrite and perhaps that the nitrogen in the system is from the bedrock itself (e.g., Morrison et al. 2012).

While the correlations are informative, we should also rely on geochemical data visualization techniques to evaluate the dataset. If we knew the major anion and cation chemistry of the groundwater we would use piper diagrams to classify the water types. In this example, however, we do not have this information. So we can use a multivariate statistical visualization to establish these relations. In this case we will use factor analysis with principal component extraction. This is not a robust method and so we will perform this analysis on our ranked data. We select varimax rotation for the solution to maximize the variance of the squared loadings which really means that we are trying to minimize complexity in our model and do so by making large loadings larger and small loadings smaller. In our model we find that four factors account for 77% of the total variance in the dataset which is very good considering that the data are ranked. As a geochemist what this means is that the linear relations of analytes to these four factors can be used to reveal the underlying structure of the data. We can use this structure to evaluate geochemical processes responsible for the structure. Looking at how the variables relate to factors (Fig. 7.2), we find that Se, Sr, Ba, Ca, and Eh are more strongly associated with factor 1 than other factors. We can say that these variables "define" factor 1. Factor 2 is defined by U, Mo, and DOC. Factor 3 is defined by nitrate and silica, and factor 4 is defined by precipitation. Given these relations, we can ascribe meaning to these four factors as, for example, factor 1, inorganic water/rock interaction; factor 2, organic water/rock interaction; factor 3, nutrient chemistry; and factor 4, recharge/infiltration. Since factor 4 shows no relation to Se, we can consider the possibility that Se is not being introduced from precipitation and soil-water interactions.

We can also, given the relations to factor 1, consider, more strongly, the role of aquifer-groundwater interactions and changes in oxidation on Se concentrations. Using the factor loadings, which range from -1 to $+1$ and interpreted the same way we interpret a correlation coefficient, we can graphically explore the relation between variables and factors (Fig. 7.2). When using loadings to explore data structure, the sign of the loading matters. The results of our factor analysis also present some questions for us to evaluate. First is that Eh correlates with factor 1 in the same "direction" as Se, Sr, Ba, and Ca. We expect that since Se is redox sensitive, Eh and Se would be related, and when we refer back to our correlation analysis, Se and Eh were strongly positively correlated meaning that as Eh increases (water becomes more oxidized), Se concentrations increase. This makes some sense but why is there no relation, in our correlation results or factor analysis, between DOC, U, and Mo with Eh? One possibility is that the variances are non-normal in all of our analytes, and though we ranked our data, this does not remove the impact of non-equal variances in our variables. Regardless, let us proceed since we now have some idea of the processes governing Se concentrations which appear to be a combination of water-rock interaction and redox.

Recall that, in our example (Table 7.1), our aquifer is a marine shale but that we might also have to consider groundwater-surface water interactions that could lead to increased Sr, Ba, and Ca in the groundwater. The factor loadings for Se and these other metals in factor 1 allude to the potential fact that factor 1 is not only water-rock interaction but also surface-groundwater interaction. One way for us to evaluate this

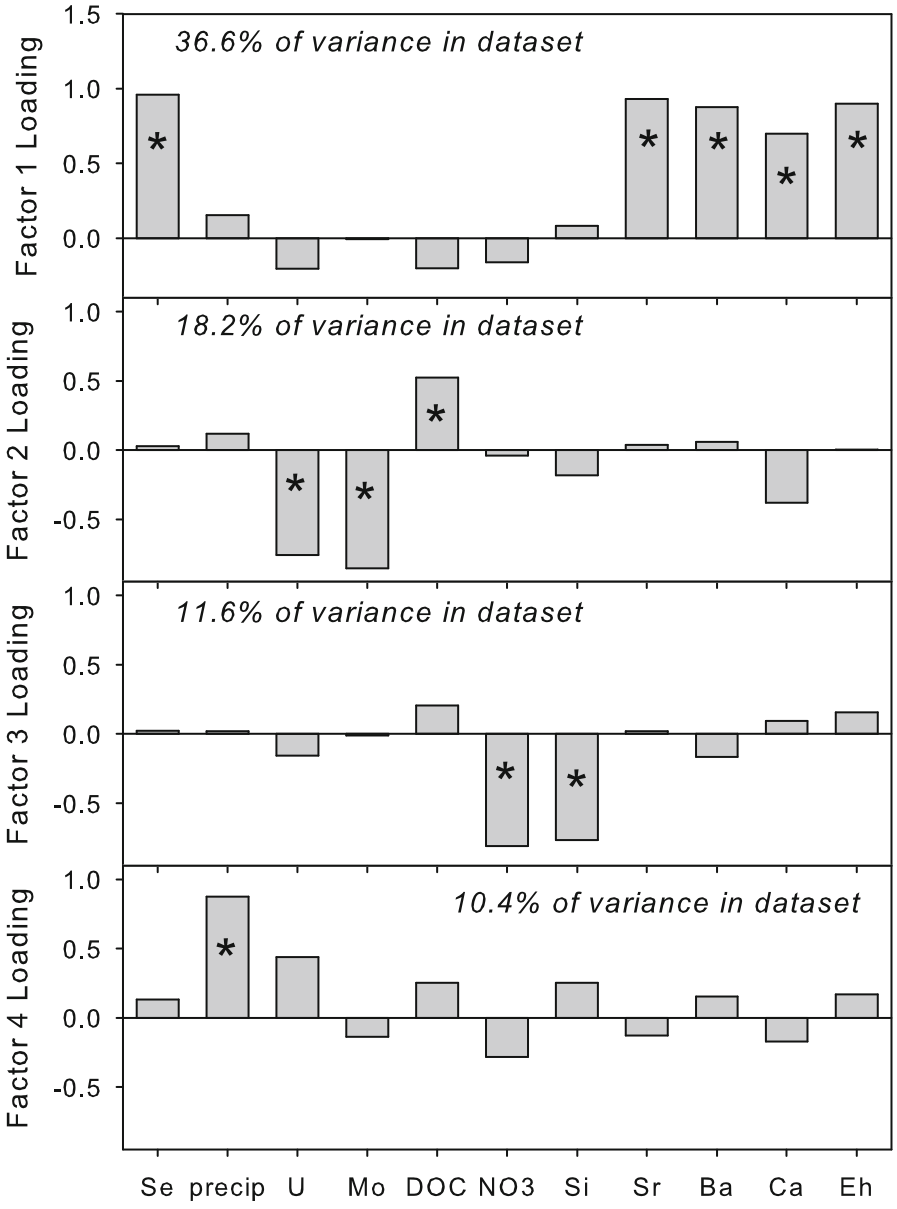

Fig. 7.2 Factor loadings for variables in our groundwater dataset. * Identifies variables that are strongly associated with a particular factor. How these variables relate to factors allows us to ascribe meaning to the factors with respect to processes accounting for variance in our data

hypothesis is to look at the relations among our samples in factor space (Fig. 7.3a). Remember that our overarching goal is to evaluate a link between irrigation, Se concentrations in groundwater, and human health impacts. So here we will evaluate the relation between irrigation and Se by plotting factor 1 and 3 scores (trace metals and nutrients). These relations are intriguing. Prior to pumping, the groundwater had lower Se and other metals and higher concentrations of nitrate/silica. Mann-Whitney U results show that there is no statistically significant difference in nitrate or silica concentrations before and after pumping. So we may have to retain our null hypothesis that there is no relation between Se in groundwater and surface water interactions. But, we also can look at factor 4 which is precipitation and see what we can find (Fig. 7.3b). Alas there are no real relations revealed here either. So if we turn to factor 2 which is "redox," what do we see (Fig. 7.3c)? Not much. The factor analysis results show that factor 2, like factors 3 and 4, do separate pre- and post-pumping samples and so we could ascribe meaning to this in that factors 2, 3, and 4 are associated with "pumping" in some way. But, does this mean that Se concentrations are related to pumping?

We can, based on the above, be confident that Se concentrations are related to pumping. The processes influencing this relation remain obscure. To add confidence to our analyses, we can use linear discriminant function analysis, using our raw data, which will use the linear relations of the variance of our sample dataset to "classify" samples as pre- and post-pumping. We will do this by setting aside a randomly selected subset (using a random number generator) of the data to "train" or develop the classification model. Using the data from 15 pre-pump and 15 post-pump, we enter each variable in a stepwise manner so that we can identify the variables that are most critical to correctly classifying samples to pre- and post-pumping. Training samples were classified to pre- and post-pumping group with 90% accuracy (cross-validated). The results also provide equations that allow us to classify "unknowns" and so we use the equations (Eqs. 7.1 and 7.2) to classify the randomly selected samples we set aside above using our discriminant function. Most statistical packages have the classification of unknowns using a "training model" option so you do not have to mathematically solve the equations for unknowns.

$$\begin{aligned}\text{Pre-pumping group} = {} & -89.08 - 0.07\,\text{Se} + 3.03\,\text{precip} - 44.93\,\text{U} \\ & + 15.60\,\text{Mo} + 12.70\,\text{DOC} + 215.98\,{\text{NO}_3}^{1-} + 5.35\,\text{Si} \\ & + 0.34\,\text{Sr} + 0.31\,\text{Ba} + 0.40\,\text{Ca} - 1.75\,\text{Eh} \end{aligned} \tag{7.1}$$

$$\begin{aligned}\text{Post-pumping group} = {} & -102.98 - 0.08\,\text{Se} + 3.98\,\text{precip} - 43.85\,\text{U} \\ & + 16.51\,\text{Mo} + 10.17\,\text{DOC} + 223.44\,{\text{NO}_3}^{1-} + 53.17\,\text{Si} \\ & + 0.51\,\text{Sr} + 0.31\,\text{Ba} + 0.26\,\text{Ca} + 16.30\,\text{Eh} \end{aligned} \tag{7.2}$$

The classification success for our randomly selected "unknown" samples was 100%. When looking at the coefficients in the equations, we see that the most

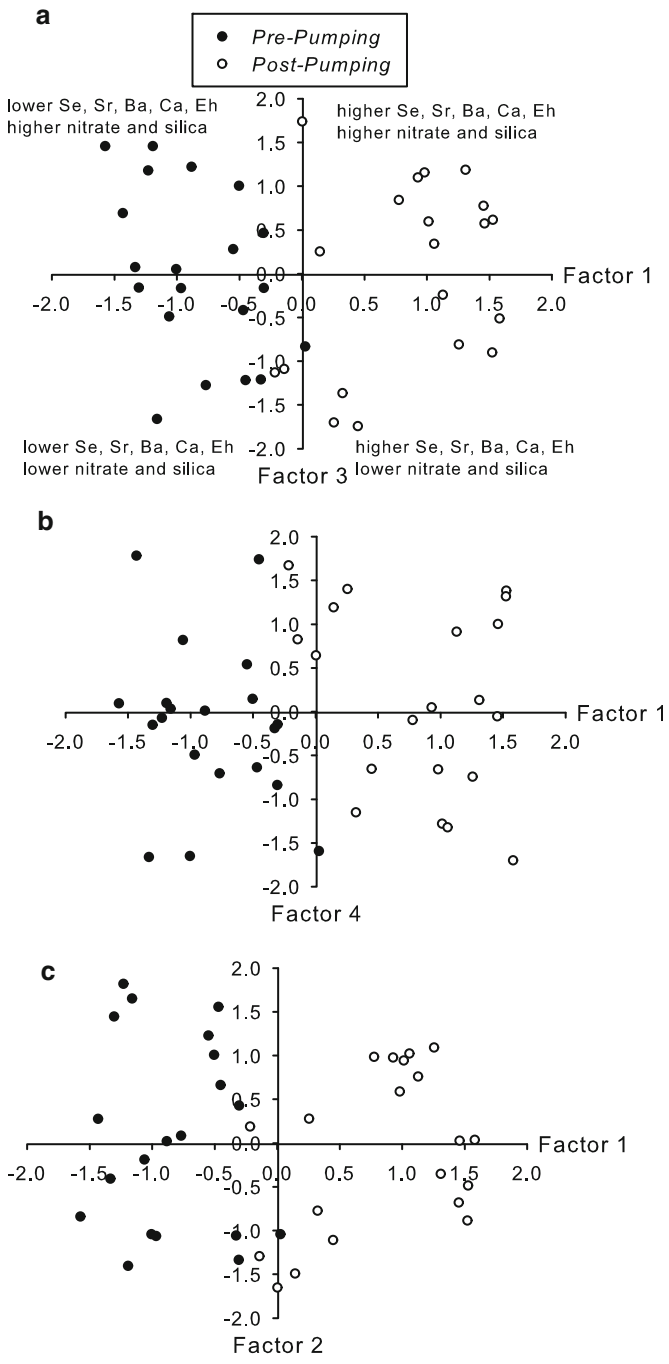

Fig. 7.3 Factor loadings of samples identified as pre- (*closed circle*) and post- (*open circle*) pumping. (**a**) factor 1 vs. factor 3, (**b**) factor 1 vs. factor 4, and (**c**) factor 1 vs. factor 2. These results show that the factors accounting for variance in the data do separate the two sample types

important variables for classification to pre- or post-pumping are those that are strong on one function but not another. Silica and Eh are good examples of this with these results suggesting that pumping most directly impacted these two variables. This then further confirms our supposition that groundwater pumping and associated changes in water–rock interaction and redox conditions influenced Se concentrations.

In the above statistical approaches, we see a number of ways to "skin" the cat. We can, with a great deal of confidence say that the groundwater chemistry did change once irrigation pumping began and that the changes in chemistry are related to changes in redox and water-rock interactions. So now that we have found out a great deal about the processes influencing groundwater chemistry, can we link the Se, and so the irrigation pumping, to human health impacts?

7.3.3 Exploring Human Health Data in the Context of Geochemical Data

In our example we have a relatively complete geochemical dataset (Table 7.1). We will now introduce the human health data associated with the population who are eating the produce grown on fields that are irrigated with the high Se groundwater. In this case, as in many cases, we do not have "pre-"irrigation health data and so cannot look for trends in the data as we could in the geochemical data. We have serum Se concentrations as well as other blood test results (creatinine, albumin, etc), and we have information, from surveys, about their lifestyle and other factors that might influence blood Se such as diet and smoking (Table 7.3). We are now mixing scalar data (concentrations) with ordinal data (vegetarian vs. mixed diet). The first thing we need to establish is whether the "exposed" population has higher serum Se than the normal population (41.7 $\mu g\ L^{-1}$ to 158.2 $\mu g\ L^{-1}$; (Lockitch 1989)). Using a hypothetical median value of 99.95 $\mu g\ L^{-1}$, we will use a univariate nonparametric Wilcoxon rank sum test (since serum Se is non-normal) and compare the mean of our population to the hypothetical median of 99.95. The results indicate that the mean serum Se of our population is significantly different from the hypothetical median ($p = 0.0043$). Knowing this we also want to explore whether any of the other serum parameters are significantly different from "normal." White blood cell count (WBC), a biomarker of kidney function, and creatinine, a biomarker for cardiac function, are normally distributed and so we can use a parametric *t*-test to compare to the hypothetical mean for these analytes. No significant difference from "normal" was found for hemoglobin (15.22 g dL^{-1} vs. 15.5 g dL^{-1}; $p = 0.0821$) or serum albumin (42.1 $\mu g\ L^{-1}$ vs. 42 $\mu g\ L^{-1}$; $p > 0.9999$). There is a significant difference in WBC (5.91×10^9 cells L^{-1} vs. 7.55×10^9 cells L^{-1}; $p < 0.0001$) and serum creatinine (99.4 $\mu g\ L^{-1}$ vs. 75 $\mu g\ L^{-1}$; $p < 0.0001$).

We first need to test for a relation between serum Se and the health effects in our population. We also have "yes"/"no" data from the patients (self-reported) about whether they eat a diet high in locally grown vegetables (at least 1 serving per day) and whether they have been diagnosed with cardiac or kidney disorders. We also

Table 7.3 Human health data

Patient #	Se ($\mu g\ L^{-1}$)	Veg diet ($1 \leq 1$ meal per day, $2 = 1+$ meal per day)	Cardiac issues ($1 =$ cardiac issue, $2 =$ no cardiac issue)	Kidney issues ($1 =$ no kidney issues, $2 =$ kidney issues)	Smoker ($1 \leq 0.5$ pack/day, $2 \geq 0.5$ pack/day)
P1	87.45	1	1	1	1
P2	94.73	1	1	1	1
P3	338.39	2	1	1	1
P4	342.53	2	1	1	2
P5	315.78	2	2	1	1
P6	319.15	2	1	1	1
P7	51.69	1	1	1	1
P8	64.47	1	2	1	1
P9	286.02	2	2	1	2
P10	299.89	2	2	1	1
P11	260.38	2	1	1	1
P12	48.37	1	1	1	1
P13	278.43	2	1	1	1
P14	377.36	2	1	2	1
P15	327.61	2	2	2	1
P16	75.54	2	1	2	2
P17	112.17	1	1	1	1
P18	89.23	1	1	1	2
P19	96.53	1	1	1	2
P20	53.65	1	1	2	2

Patient #	Hemoglobin ($g\ dL^{-1}$)	WBC ($\times 10^9$ cells L^{-1})	Creatinine ($\mu g\ L^{-1}$)	Albumin ($\mu g\ L^{-1}$)
P1	15.40	8.5	97	38
P2	16.90	6.0	91	51
P3	16.10	7.4	98	44
P4	13.90	6.3	154	45
P5	16.10	3.3	98	42
P6	13.00	3.5	140	33
P7	16.30	5.1	129	43
P8	15.60	6.4	97	42
P9	14.20	6.3	97	41
P10	14.80	8.2	83	44
P11	14.70	5.8	78	41
P12	15.70	6.5	96	46
P13	14.90	7.1	91	45
P14	16.40	7.8	101	40
P15	14.40	3.5	80	42
P16	14.90	7.1	90	40
P17	15.00	5.5	81	43
P18	17.10	5.4	89	43
P19	14.70	6.2	86	40
P20	15.40	4.2	98	43

(continued)

Table 7.3 (continued)

Patient #	Se ($\mu g\ L^{-1}$)	Veg diet ($1 \leq 1$ meal per day, $2 = 1+$ meal per day)	Cardiac issues ($1 =$ cardiac issue, $2 =$ no cardiac issue)	Kidney issues ($1 =$ no kidney issues, $2 =$ kidney issues)	Smoker ($1 \leq 0.5$ pack/day, $2 \geq 0.5$ pack/day)
P21	112.03	1	1	2	2
P22	271.82	2	1	1	2
P23	342.60	2	2	2	1
P24	113.01	1	1	1	1
P25	94.69	1	1	1	1
P26	92.17	1	1	1	2
P27	128.44	1	1	1	2
P28	67.98	1	1	1	1
P29	71.69	1	1	1	1
P30	114.12	1	2	1	1
P31	107.25	1	1	1	2
P32	315.34	2	1	1	1
P33	358.43	2	2	2	1
P34	45.34	1	1	1	1
P35	82.20	1	1	1	1
P36	82.21	1	1	1	1
P37	207.55	1	2	1	1
P38	284.79	2	2	1	2
P39	310.10	2	2	2	1
P40	373.22	2	2	2	1

Patient #	Hemoglobin ($g\ dL^{-1}$)	WBC ($\times 10^9$ cells L^{-1})	Creatinine ($\mu g\ L^{-1}$)	Albumin ($\mu g\ L^{-1}$)
P21	14.10	6.0	126	41
P22	14.60	6.7	90	43
P23	16.60	7.1	90	45
P24	13.90	3.6	102	39
P25	16.20	7.5	100	49
P26	16.00	4.1	123	43
P27	15.50	6.1	93	41
P28	16.40	4.5	89	43
P29	14.30	4.8	93	38
P30	14.80	6.6	86	40
P31	16.20	9.5	85	44
P32	14.50	3.7	97	42
P33	14.30	6.6	97	42
P34	15.10	4.7	87	40
P35	16.50	6.1	119	42
P36	16.10	4.1	103	40
P37	14.50	4.4	84	42
P38	14.40	4.8	127	44
P39	14.90	10.6	94	40
P40	14.50	4.7	117	40

Concentrations of Se, hemoglobin, creatinine, and albumin were measured in serum samples

have data on whether they are smokers (>0.5 pack/day). In this population we will assume that none of the population is exposed to metals through their workplace and that all are males and are between 35 and 45 years of age and are all Caucasians. We make these assumptions, for our case, as we do not want confounding variables of gender, ethnicity, or occupation. However, in real cases you will likely have to deal with these issues and so we include "smoking" as a lifestyle variable that can confound relations between Se in the groundwater and health effects on our study population. We first, then, need to exclude smoking as a covariate to cardiac and kidney health end points. Covariates are variables that account for the effect of a variable that is observable but difficult to control. We know that smoking is linked to low-level Se exposure and to outcomes such as cancer (Goodman et al. 2001). We will use ordinal logistic regression with serum Se as the response and the model variables of "high-vegetable diet" and "smoker" and setting "smoker" as a factor with two levels (1 smoker, 2 nonsmoker). Our results indicate that being a smoker does impact serum Se levels (estimated coefficient = 0.261, $p = 0.663$). The model also shows that there is sufficient evidence to conclude that at least one of the estimated coefficients (diet and/or smoker) is different from zero ($G = 40.467$, $p = 0.000$). Though the results suggest that smoking may be a confounding variable in our case study, the ordinal regression also indicated that the predictive capacity of the model is moderate (Kendall's Tau-a = 0.46, Goodman-Kruskal Gamma = 0.65, Somer's $D = 0.46$). So we can conclude that being a smoker does influence serum Se concentrations and so must retain smoking as a covarying factor in any of the models we develop to test whether there is a relation the cardiac or kidney health of the population that consumes a high proportion of the vegetables grown using the contaminated groundwater.

To test whether serum Se concentrations are associated with health effects, we will test whether Se has any predictive power on these responses while keeping diet and smoking in the model as covariates. We will use a partial least squares model for this. Including only serum Se as a predictor, the R^2 for cardiac issues is 0.233 and for kidney issues is 0.106. Though weak, these values are significant ($p = 0.038$) at the 95% confidence level. If we model cardiac and kidney effects as a response to interactions between serum Se, smoking, and diet, the model is no longer significant ($p = 0.190$) though serum Se is still most strongly associated with these two health outcomes (62% of variance in cardiac and kidney issues is attributable to serum Se).

We can be reasonably confident that serum Se is associated, to a moderate extent, with the cardiac and kidney health outcomes of our population. We can further explore the data using factor analysis to see whether those people with cardiac and/or kidney problems load high on a factor that accounts for the variance in serum Se. We have to code our data as follows: 0, no cardiac or kidney issues; 1, cardiac only; 2, kidney only; and 3, kidney and cardiac issues. We will use ranked serum Se, diet, smoker, and ranked blood chemistry as variables. Four factors are required to account for 81% of the variance in the data. Interestingly serum Se and diet correlated with factor 1 (0.911 and 0.926, respectively). Factor 2 is associated with serum hemoglobin, WBC, and albumin. Factor 3 is associated with serum creatinine, and factor 4 is associated with smoking. Removal of the serum data (hemoglobin,

WBC, creatinine, albumin) results in three factors explaining 100% of the variance, but each factor (serum Se, diet, and smoking) accounts for an equal share of the variance (∼33%) and so these results mean very little. Given that we have shown, statistically, that there is a relation between serum Se and health effects, we can, for now, move on to testing our larger hypothesis.

7.3.4 Chemometrics and Combined Geochemical and Human Health Data

Thus far, we have treated the geochemical data in isolation from the human health data. Recall that we have established, statistically, that:

(a) Mean groundwater Se concentrations are different pre- and post-pumping.
(b) Planting season and precipitation are not related to groundwater Se.
(c) Groundwater Se concentrations are influenced by redox and water-rock interaction.
(d) There appears to be another water source (oxidizing, high in Sr, Ba, and Ca) mixing with the groundwater.
(e) Serum Se concentrations are different from "normal."
(f) Albumin and hemoglobin are "normal."
(g) Creatinine and white blood cell count are not normal.
(h) Smoking influences serum Se concentrations.
(i) Serum Se is related to cardiac and/or kidney effects.

While the above analyses are significant, we have not addressed their power yet. Statistical significance tells us how sure we are that the difference or relation exists. It gives us confidence that our results are different from what would be expected just by chance. Significance protects us from committing a type I error, rejecting a true null hypothesis. But what protects us from committing a type II error, accepting a false null hypothesis? Statistical power is the probability of retaining a false null hypothesis and is most closely associated with sample size. If your sample size is too small, you may get a significant statistical result, but the result will have little power and so you may retain a false null hypothesis and commit a type II error. So, for all of our tests thus far, what is the power?

One approach to assessing power is a simple power analysis for ANOVA. We have, for pre- and post-pumping, for planting season, and other metrics, only two levels. We have 30 groundwater samples (15 pre- and 15 post-pumping) and 40 patients (21 with low-vegetable diet, 19 with high-vegetable diet, etc.). We will use GPower (Faul 2012) to calculate the power of our statistics. We used Mann-Whitney tests to evaluate differences in means between groups (groundwater Se, pre- and post-pumping; serum Se, diet; etc.). Using a two-tailed approach to power tests and using rank data (normalized), setting our effect size to large (0.50), our α at 0.05, and entering in the number of samples per "group," we find the following:

- With only 15 samples pre-pumping and 15 post-pumping, our power is only 25% meaning our probability of committing a type II error (β) is 75%. So though we found a significant difference in groundwater Se pre- and post-pumping, the statistic has little power and so we cannot reject the null hypothesis. Even if we open our confidence from 95 to 80%, we still do not have power.
- When comparing cardiac/kidney health and serum Se, we also have no power despite having significant results and so cannot conclude, with any power, that serum Se is associated with the two health end points.
- When comparing smoking or diet to serum Se, we also lack power and so cannot reject our null hypothesis that these two factors are not related to serum Se concentrations.

Since our sample sizes are too small to provide power, based on the post hoc power tests, what sample size would we need to have both significance and power in our statistical analyses? Performing an a priori power test, 2 tailed with an effect size of 0.5 (large), retaining α at 0.05, and power at 95%, we would need 42 samples per group. This would, then, require us to have at least 84 samples if samples were evenly distributed between groups. Ideally you would perform an *a priori* power test prior to beginning your sample collection, but in our case we "inherited" data that was collected for other purposes. So, do we abandon chemometrics and simple say that we cannot conclude anything? No. But we now have to use our geochemical knowledge to evaluate the statistics. For example, our statistical analyses suggested that groundwater Se is influenced by oxidation and that differences in concentrations pre- and post-pumping could be attributed to mixing of oxidized water with reducing groundwater. Our statistical analyses alluded to the relation between serum Se and diet, as well as smoking, and also between serum Se and health effects. What we now must attempt is to leverage statistical "visualization" techniques to explore these relations.

7.3.5 Path Analysis and Structural Equation Modeling

Path analysis is an extension of multiple regressions and is a statistical approach that allows us to visualize the magnitude and significance of hypothesized cause connections between sets of variables. Here we will explore the use of a specific type of path analysis, structural equation modeling (SEM) using Statistica 10. SEM is a general, but powerful, multivariate statistical technique that allows us to evaluate the relative influence of measured and unobserved (latent) variables on one and other. Specific to our example we are able, through SEM, to evaluate the direct and indirect effects of groundwater Se and diet on health. We are, therefore, using SEM as a "causative" model where we hypothesize relations among variables and test the causal model using a linear equation system.

In our SEM we will define a series of variables as follows: exogenous latent variables (oval shapes on PATH diagram with arrows out only) are those that

are only independent variables and are unobserved but have measured (manifest) variables that serve to "define" them. You can think of this as a "factor" in factor analysis where our measured variables "load" on a factor. In SEM, the measured (manifest) variables "load" on latent variables. In our case study, we have a few such exogenous latent variables. First we have time which we assign the manifest variable of "months since pumping" as we assume that only the months since pumping matter in our study but cannot be sure this is the only time factor. Second we have a bundled variable of precipitation and planting season. These are the only 2 "environmental" variables that we have shown have an independent relation to time and other manifest variables. So we call this latent exogenous variable, in our model, Env Var. We also have an exogenous health-related variable comprised of creatinine and white blood cell count as these are not associated with other manifest variables, so we will define another exogenous latent variable as "other health factors." In the case of all of these exogenous latent variables, we are not assuming that the manifest variables associated with them are the only variables accounting for their contribution to relations among our data but that these variables represent possible independent, unobserved variables that may contribute to the variance in our dataset.

Next we define our endogenous (dependent and independent) latent variables (oval shapes on PATH diagram, arrows in and/or out). In the case of endogenous latent variables, we can have multiple relations within our model and so can be independent as well as dependent. Since these are latent they are still like factors and are not directly observed but are associated with manifest variables. We know from our previous statistical analyses that serum creatinine and serum WBC are associated with kidney and cardiac health, but these two measures are not the only possible serum indicators of health effects so we define an endogenous latent variable "serum chem" associated with the measured creatinine and WBC. Our last endogenous latent variable is "kidney/cardiac health" which is associated with the measured health scores for our study subjects. Since these scores are "self-reported," they are not a direct measure of health and so this variable is defined as a latent variable. Next we have the variables that define redox (U, DOC, Mo, Eh, nitrate), WRI (water-rock interaction; Si, Ca, Sr, Ba), and other health variables (serum hemoglobin and serum albumin). Lastly we have manifest variables that are not latent such as diet (high or low vegetable), smoker, groundwater Se, and serum Se.

Once our variables are defined, we then construct a path diagram (Fig. 7.4) that shows the directional relations between our variables that we wish to test. Here we do not include covariance among variables but you can include covariance in SEM models. As you can see from our path model, we have defined, based on our statistical tests above, direct and indirect relations among variables. For example, SEM allows us to test whether time has a direct effect on groundwater Se (arrow from time to GW [Se]) or if time indirectly relates to groundwater Se by first affecting redox which then directly affects groundwater Se. In our analyses above, we could only test for direct relations. With SEM we can test for both direct and indirect relations. The model presented here was run using standardized residuals (difference between the measured and estimated function)

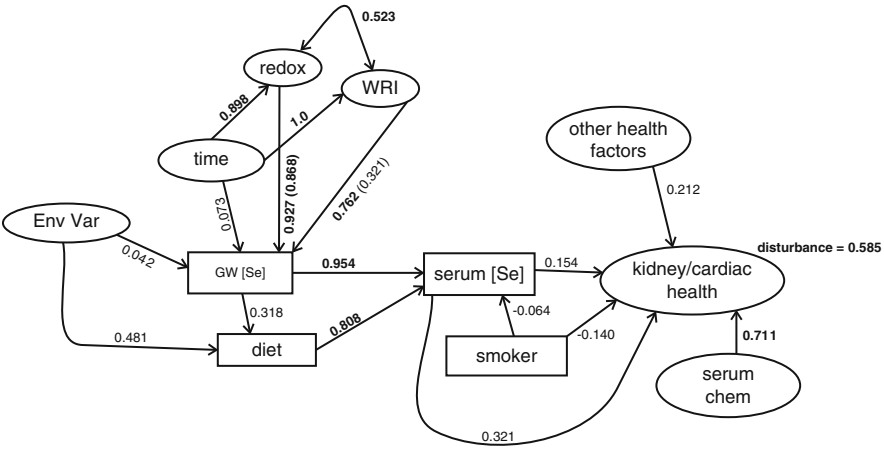

Fig. 7.4 Path diagram for the structural equation model that explores relations among latent and manifest environmental and health variables. Estimates in *bold* are significant at $\alpha = 0.05$. Values in parentheses are estimates of relations when allowing for covariance of WRI and redox

and also included exploration of autocorrelation of residuals and correlations among latent variables. The model also allowed for correlations among the disturbances (error path of measured variable on each latent variable).

Before we discuss the results, there are a few key points regarding SEM that must be discussed. First is that you can construct multiple path diagrams changing the relations (direct/indirect, covariance, etc.) and compare the fit of the models using the reported Akaike's information criterion (AIC) statistic. Each SEM will report a chi-square-maximum likelihood (χ^2_{ML}) statistic. The χ^2_{ML} is a discrepancy measure that compares sample covariance with implied model covariance computed from model structure and all model parameters. In general, the reported χ^2_{ML} should be close to the degrees of freedom of the model. In the model we developed the χ^2_{ML} was 283.71 ($p = 0.00$), and the degrees of freedom for the model was 174. A higher AIC statistic is favored when selecting a model. The model presented here had an AIC of 11.326. If we remove many of the variables and simply have a path from time to groundwater Se to serum Se to health the AIC is 1.759. Clearly, the model presented here is better as it reflects the complexity of our data.

Recall that our overarching goal is to evaluate whether pumping of an aquifer increased groundwater Se and if this high Se groundwater, used for irrigation, impacted human health. Our results (Fig. 7.4) are complex but quite informative. The unobserved environmental variable does not strongly relate to either groundwater Se ($R^2 = 0.042$) or to diet ($R^2 = 0.481$). The moderate, but not significant, relation between diet and groundwater Se is expected given that the environmental variable is linked to the planting season. Similarly, our unobserved health factor variable does not directly relate to kidney/cardiac health ($R^2 = 0.212$). The lack of relation between these unobserved variables and our directly measured variables does not

mean that there is not a lurking variable out there but simply means that the variance in precipitation and planting season does not, collectively, related to groundwater Se and, similarly, that the variance in serum hemoglobin and albumin does not relate directly to kidney/cardiac health.

What is very interesting is that, from our previous statistical tests, we concluded that time directly influences groundwater Se. Our SEM results show that this is not the case ($R^2 = 0.073$). Rather time directly influences redox ($R^2 = 0.898$) and water-rock interaction (WRI; $R^2 = 1.0$) and that these, in turn, influence groundwater Se ($R^2 = 0.927$ and $R^2 = 0.762$, respectively). Eh is positively correlated with WRI variables Ba, Sr, and Ca and so some of the contribution of WRI to groundwater Se may be overestimated without allowing for interaction effects between these two latent variables. When we rerun the model allowing for covariance between redox and WRI (Fig. 7.4), we see that 52% of the variance in both is accounted for by their covariance and that redox remains a strong predictor of groundwater Se, but WRI is no longer a strong predictor. The χ^2_{ML} and AIC of this model is 264.138, and the AIC is 6.773. Despite the fact that covariance between redox and WRI does significantly change the relation between WRI and groundwater Se, the model fit itself is not better and so we will retain our original model with the understanding that the relation between redox and WRI does effect groundwater Se. So from our model we know that time accounts for approximately 90% of the variance in redox which then accounts for 93% of the variance in groundwater Se. Seven percent of the variance in groundwater Se is unaccounted for or can be attributed to WRI.

Diet is not directly related to environmental factors such as precipitation, planting season, or groundwater Se which suggests that if diet is related to serum Se ($R^2 = 0.880$), then some other source of Se must link diet and groundwater Se since groundwater Se is directly related to serum Se ($R^2 = 0.954$). Recall that diet is approximated by the self-reported amount of vegetables eaten per day. We have no data on whether these estimates are accurate, what other dietary components that may be associated with groundwater (e.g., beef from cattle drinking the water), or if the people are truly eating locally grown produce. Our SEM results suggest that there is a "lurking" variable, one that has an important effect on serum Se through diet that is not among the included variables. Our results clearly show that groundwater Se is the best predictor of serum Se and that serum Se is not a good predictor of kidney or cardiac health. Serum creatinine and WBC, however, are good predictors of health ($R^2 = 0.711$). There appears to be error correlation within the kidney/cardiac health variable caused by the covariance of these two variables since the disturbance is significant (0.585). This is likely induced by the fact that kidney and cardiac health are binary-coded variables and so non-normality of variance may lead to a type 2 error, but the chance is 58.5%.

Overall SEM revealed interesting relations between our variables. The SEM results suggest we should retain our null hypothesis that pumping has not changed groundwater Se concentrations as the effect is indirect. Rather we should rephrase our null hypothesis and test whether pumping has changed groundwater redox and/or water-rock interactions and then test if changes in redox and/or water-rock interaction could be related to changes in groundwater Se. If we test the null

hypothesis that there was no change in redox, for example, due to pumping, we would, based on the SEM results, reject this hypothesis and retain our alternate hypothesis that pumping did change redox. We hypothesized that diet has no effect on serum Se concentrations. This null should be rejected based on the SEM results. Can we say that groundwater Se led to changes in diet which led to serum Se changes? No because both diet and groundwater Se are directly related to serum Se, according to our SEM results, and the relation between groundwater Se and diet to serum Se is indirect. So this suggests another source of Se to the population living in this region. As to whether serum Se is unrelated to kidney/cardiac problems, this appears to be supported and so we would retain this null. Serum creatinine and WBC are directly related to these health effects but are unrelated to serum Se. So perhaps what we need to evaluate is what the missing source of Se is, and how this might be directly linked to kidney/cardiac health.

7.4 Conclusion

The above case study is not meant to be an exhaustive presentation of all statistical tests that could be applied to test hypotheses in the case of a post hoc (after the fact) evaluation of existing data. It is important to note that this case is not a real case based on real data collected to test the hypotheses we have been testing. This is a case study of using data, compiled for other studies, and evaluating hypotheses in a post hoc manner. Also this is a case study presenting a series of approaches that are what the author would do for such a study and is neither exhaustive or prescriptive. Statistics are tools and like other tools you need to select the one that is best for the job. If you have a nail to put in a wall, a hammer is the best choice but a wrench will often suffice.

Acknowledgements I would like to thank all of my chemometrics students, past and present, for listening to me babble on about this stuff. Also I thank L. T. and C. M. for providing data for this chapter. I also thank "OnTheHub" for providing access, at an affordable price, to various and sundry statistical software packages.

References

Adèr HJ (2008) Chapter 13: missing data. In: Adèr HJ, Mellenbergh GJ (eds) Advising on research methods: a consultant's companion. Johannes van Kessel Publishing, Huizen

Cox DR, Small NJH (1978) Testing multivariate normality. Biometrika 65:263–272

Davies L, Gather U (1993) The identification of multiple outliers. J Am Stat Assoc 88:782–792

Draper NR, Cox DR (1969) On distributions and their transformation to normality. J R Stat Soc Ser B (Methodol) 31:472–476

Faul F (2012) Gpower 3.1. Retrieved 10 July 2012. http://www.psycho.uni-duesseldorf.de/abteilungen/aap/gpower3/download-and-register

Goodman GE, Schaffer S, Bankson DD, Hughes MP, Omenn GS (2001) Predictors of serum selenium in cigarette smokers and the lack of association with lung and prostate cancer risk. Cancer Epidemiol Biomarkers Prev 10:1069–1076

Lockitch G (1989) Selenium: clinical significance and analytical concepts. Crit Rev Clin Lab Sci 27:483–541

Morrison SJ, Goodknight CS, Tigar AD, Bush RP, Gil A (2012) Naturally occurring contamination in the mancos shale. Environ Sci Technol 46:1379–1387

Vermeesch P (2009) Lies, damned lies, and statistics (in geology). Eos Trans Am Geophys Union 90:443

Chapter 8
Dust, Metals and Metalloids in the Environment: From Air to Hair

Gaetano Dongarrà, E. Tamburo, and D. Varrica

Abstract Billions tons of particulate matter, made up of inorganic and organic compounds, are released every year into the atmosphere, from both anthropogenic and natural sources. The latter, which include geogenic material from erosion, agriculture, sea spray and volcanic activity, account for about 97% of the total mass of particles. The contribution of anthropogenic sources, about 3%, is more pronounced in industrialised and also in urban areas, where vehicular traffic is one of the most important sources. When examining the health impact, in addition to mass level and size, two other main characteristics of particulate matter need to be considered: its nature and chemical composition. These parameters appear intrinsically related to one another. Presence, abundance and behaviour of trace metals in air are also closely related to atmospheric particulate matter, as most metals in the lower atmosphere are present in association with particles. Most of these aspects are presented and discussed in this present chapter as only a better knowledge of atmospheric particulate matter, its composition, metal content and some implications on the human health, may aid to select correct actions and appropriate control strategies.

Keywords Air pollution • Metals and metalloids in environment • Trace metals speciation • Particulate matter • Hair analysis

G. Dongarrà (✉) • E. Tamburo • D. Varrica
Dip. Scienze della Terra e del Mare (DiSTeM) Department, Università di Palermo,
Via Archirafi, 36 90123 Palermo, Italy
e-mail: gaetano.dongarra@unipa.it

P. Censi et al. (eds.), *Medical Geochemistry: Geological Materials and Health*, DOI 10.1007/978-94-007-4372-4_8,

8.1 Introduction

The American Environmental Protection Agency (EPA) has recently reported on the risk of inhaling $PM_{2.5}$ fine particles (EPA 2005). The Final EPA Staff Paper, recommending stronger particle pollution standards, concluded that, in the USA, meeting existing $PM_{2.5}$ standards will prevent at least 15,000 premature deaths, 75,000 cases of chronic bronchitis, 10,000 hospital admissions for respiratory and cardiovascular disease and hundreds of thousands of occurrences of aggravated asthma. Similar concerns are present in Europe where it is estimated a loss in statistical life expectancy of over 8 months due to $PM_{2.5}$ in air, equivalent to 3.6 million life years lost annually (CEC 2005). Even with effective implementation of current policies, this will only reduce to around 5.5 months (equivalent to 2.5 million life years lost or 272,000 premature deaths). Aerosol particles of less than 2.5 μm are also receiving worldwide attention, owing to their potential greater negative consequences on public health, especially on that part of population living in urban areas influenced by high traffic density or industrial activities. Recent human activities have created, through nanotechnologies, nano-sized particles much smaller than $PM_{2.5}$ and characterised by larger and more reactive exposed surface areas. These are the most dangerous particles because our immune system, which developed to protect itself against larger particles, does not capture the smallest ones and therefore has no efficient mechanisms for removing them. It has been estimated that each of our breath contains roughly 5×10^7 million particles 50 nanometres (nm) or less in dimension and that, during an average day, we inhale over 10^{12} such particles (Buseck and Adachi 2008). All this gives emphasis to the risk of inhaling particulate matter and points to the obvious potential for uptake of contaminants of different nature. For these reasons, monitoring of PM, mainly PM_{10} and $PM_{2.5}$, has become a crucial part of public health policy measurements and regulations in many countries around the world. However, air quality policies are typically based only on the mass of these size fractions and do not take into account their chemical composition. This constitutes an important point of weakness of current policies when examining the health impact, in addition to mass level and size, two other main characteristics of particulate matter need to be considered: its nature and chemical composition. Thus, this manuscript, which is part of a lecture held at Capo Granitola, Trapani (Italy), during the "Summer School on Medical Geochemistry. Effects on Health of Geological Material Exposure. The geochemical approach", focuses on the still-evolving knowledge about atmospheric particulate matter, its composition, its metal content and some implications on the environment.

8.2 What Do We Mean for Particulate Matter (PM)?

In the specialised literature, there is a certain degree of inconsistency over the use and meaning of the term "particulate matter" especially with regard to the distinction between particulate matter and aerosol. Here are some examples.

Airborne particulate matter (PM) is a complex mixture of solid and liquid particles of primary and secondary origin, which contain a wide range of inorganic and organic components (Wiseman and Zereini 2010). *Airborne particulate matters (PM) are aerodispersed systems of solid and liquid particles with different sizes, forms and chemical compositions* (Spurny 2000). *Aerosols are small particles of solid or liquid ranging in size from clusters of a few molecules to about 20 μm in radius* (Berner and Berner 1996). *Whereas an aerosol is technically defined as a suspension of fine solid or liquid particles in a gas, commonly usage refers to the aerosol as the particulate component only* (Seinfeld and Pandis 1998). *Solid particles and liquid droplets* – write Gierè and Querol (2010) – *are collectively referred to as particulates or particulate matter (PM). In contrast, the term aerosol refers to both the PM and the gas in which it is suspended.* For sake of clearness, in this chapter, the term "particulate matter" will be used to indicate only the solid fraction of aerosol.

8.3 Where Does It Come From?

Airborne particulate matter comes from different sources and processes, and therefore, everywhere in the lower troposphere, there is a mixture of solid particles of different origin. On a global scale, between 3.4 and 12 billion tons of particulate matter, made up of inorganic and organic compounds, are released every year into the atmosphere, from both anthropogenic and natural sources (Houghton et al. 1996; Andreae and Rosenfeld 2008; Durant et al. 2010). There are many other estimates existing in the literature (Junge 1979; Nriagu 1979; Chester 2000), and even the large range indicated above is affected by considerable uncertainties associated to all the flux sizes, especially regarding sea salt emission into the atmosphere. The number of particles and mass concentrations is also highly variable, both in time and space, covering the ranges 10^{+2} to 10^{+5} cm^{-3} and 1–100 $\mu g\ m^{-3}$, respectively (Pöschl 2005). The global atmospheric concentrations are strongly geographically dependent and decrease exponentially with height with a profile described by

$$N(h) = N(0)e^{-h/z} \tag{8.1}$$

with h (km) the altitude above ground in kilometres and z (km) the scale height (z may vary from 10 to 6 in continental and urban air, respectively). During winter, z may reduce to 2 in continental air (Hess et al. 1998). Particulate matter originates from a variety of natural and man-made sources and enters the atmosphere mainly by means of the following processes: (l) sea salt formation caused by bursting and evaporation of bubbles at the sea surface, (2) ascent of particles produced by mechanical alteration of rocks, (3) windblown desert dust, (4) vo1canic eruptions, (5) dispersal of plant fragments and pollens, (6) fossil fuel and biomass combustion, (7) residues from man's activities produced by mechanical destruction or transformation of solid materials, (8) road dust resuspension by

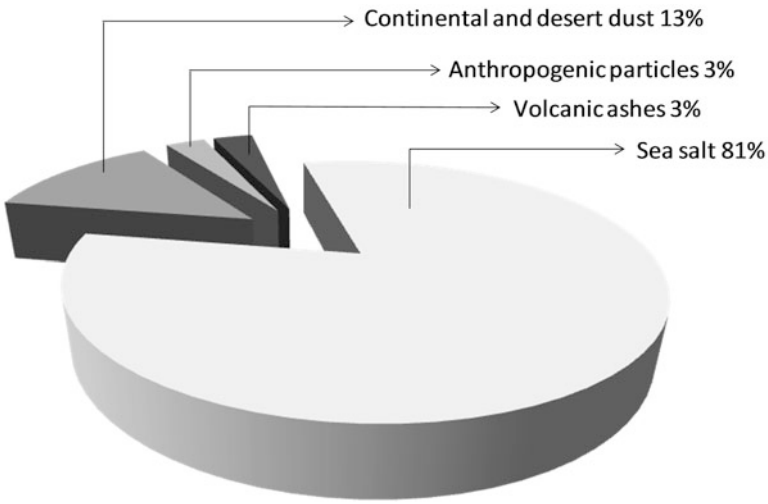

Fig. 8.1 Estimates on the percentage of particulate matter introduced into the atmosphere from natural and anthropogenic sources. Sea salt and mineral dust exhibit the largest contribution. Man-made source accounts for about 3% of the total mass of particulate

automotive traffic and (9) reactions between gaseous emissions and among solid, liquid and gas components of the atmosphere. Of course, anyone may individuate more specific sources attributable to the above categories. It is commonly accepted that airborne particles of natural origin considerably exceed the anthropogenic ones, with the geogenic and biogenic airborne particles accounting for more than 90% of the total mass of particles (Fig. 8.1). The contribution of anthropogenic sources, although to a lesser extent, is more pronounced in industrialised and also in urban areas, where vehicular traffic is one of the most important sources. However, it is worth noting that it is not as simple as it seems to distinguish what is really of natural origin from what is anthropogenic. Even this aspect of particulate matter should be further studied as suggested by Andreae and Rosenfeld (2008) who write: *Natural source processes are not always easily distinguished from anthropogenic ones. Vegetation fires, for example, have existed on Earth since the evolution of land plants some 400 million years ago, but at present the vast majority of biomass fires are caused by humans, and therefore pyrogenic aerosols must be considered as mostly anthropogenic. In a similar way, mineral dust aerosols have been mobilized in vast amounts from the Earth's deserts throughout geological history, but the human-caused destabilization of soils in arid and semi-arid regions has clearly increased dust fluxes in many regions.* Similar considerations were formulated by Rasmussen (1998).

8.4 Size and Toxicological Definitions

The grain size of airborne particulate matter is very often related to the amount of energy spent during its formation process: the higher the energy – the smaller the particle formed, and the lower the energy – the larger the particle (Breysse and Lees 2006). Dust particles of our interest are usually in the size range from below 1 μm to less than 100 μm in diameter. However, as airborne particles have irregular shapes, each specific fraction of PM is categorised according to the aerodynamic equivalent diameter (AED) of the particles. AED is defined as the diameter of a hypothetical sphere of density 1 g cm^{-3} having the identical settling velocity in calm air as the particle in question. Being a function of particle diameter, density and shape, AED determines the transport and removal rate of particles in air: coarse particles have a short atmospheric lifetime and are quickly removed from the atmosphere by gravitational settling, while the smaller ones, with submicron size, can have lifetimes of several weeks. From a toxicological viewpoint, AED determines the efficiency of particles to penetrate and deposit at different sites in the lung. Also in this case, it is not difficult to find several types of classifications of airborne particles among different specialists who deal with such a subject. With regard to human exposures by inhalation, some size-dependent particulate fractions (Fig. 8.2), based on the penetration of these particles in the various regions of the respiratory tract, have been defined in CEN (1993) and also described by Nieboer et al. (2005) as follows:

Inhalable or inspirable particulate fraction (AED < 100 μm) is that fraction of total airborne particles that enters the body through the nose and/or mouth during breathing and settle in the extrathoracic airways (mouth, larynx and pharynx). Particles with aerodynamic diameter >50 μm, because of gravity, do not have a

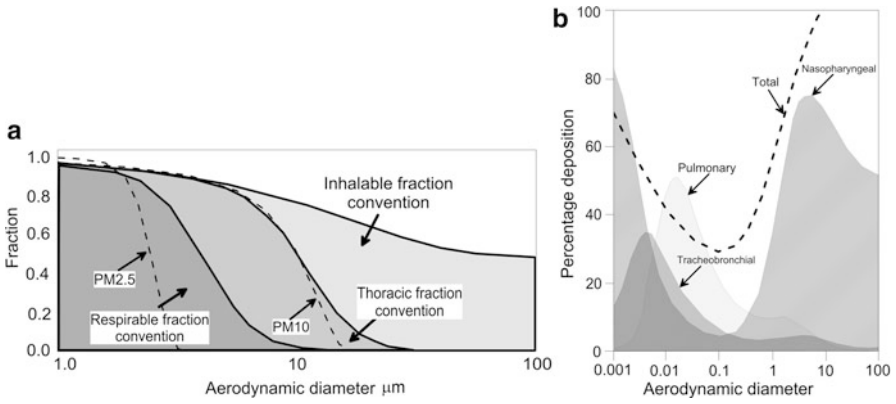

Fig. 8.2 Classification (**a**) and particle deposition (**b**) within the different human regions of the respiratory airways as a function of the aerodynamic diameter (Figures modified from Marconi 2003; ICRP 1994 and Vincent 2007)

long atmospheric lifetime and settle with a terminal velocity >7 cm s^{-1} (WHO 1999). This fraction is relevant to health effects anywhere in the respiratory tract, such as rhinitis, nasal cancer and systemic effects.

Thoracic particulate fraction (the PM_{10} fraction) is the inhaled particle component which penetrates the airways of the lung (the region below the larynx). This fraction includes coarse (AED 10–2.5 μm), fine (AED < 2.5 μm) and ultrafine (AED < 0.1 μm) particles. It is relevant for asthma, bronchitis and lung cancer.

Respirable particulate fraction ($PM_{2.5}$ fraction) indicates the inhaled particles that deeply penetrate into the human respiratory system, beyond the alveolar region of the lung, where the gas exchange takes place and where settling at the surface of bronchi may occur. It is potentially related to the development of chronic diseases as pneumoconiosis and emphysema.

Ultrafine fraction (UF), which has a cut-off of 0.1 μm, accounts for a small proportion of the total mass level, but the particles are small enough to pass into the bloodstream and because of their larger reactive surface area may induce severe damages.

8.5 Nature and Chemical Composition

To define the chemical composition of airborne particulate matter, we like to recall the expression used by Pöschl (2005) who properly emphasised the complexity of airborne PM: "air particulate matter can be pictured as the result of an exploded pharmacy, comprising just about any non- or semivolatile chemical compound occurring in the biosphere, hydrosphere, and lithosphere, or released by human activity". Nevertheless, it is possible to distinguish airborne particles in inorganic, carbonaceous, primary and secondary, depending on their nature and their formation process, no matter whether they are coming from natural or anthropogenic sources (Fig. 8.3).

Inorganic particles include mineral dust, sea spray-derived compounds, ammonium sulphates and nitrates. The composition of airborne mineral dust generally resembles the global composition of Earth's crust, even though it may be strongly influenced by local lithology and phenomena as windblown dust from arid and semiarid regions (i.e. Saharan outbreaks in Europe and windblown from Gobi desert in China). The main crustal minerals that make up a significant proportion of the total mass of particulate are, therefore, feldspars, quartz, clay minerals, carbonates, gypsum and halite. Oxides of various elements are also present. Sea salt makes a dominant contributor to particulate matter concentrations, especially close to the continental coasts, where "whitecaps" break generating droplets of seawater that after evaporation produce airborne salt particles. They contain primarily sodium, magnesium, chloride and sulphate ions. Having a residence time in air of about 3 days, sea salts can be advected over a long distance, further away from the coast, for hundreds of kilometres. Just to give an idea, the annual average sea

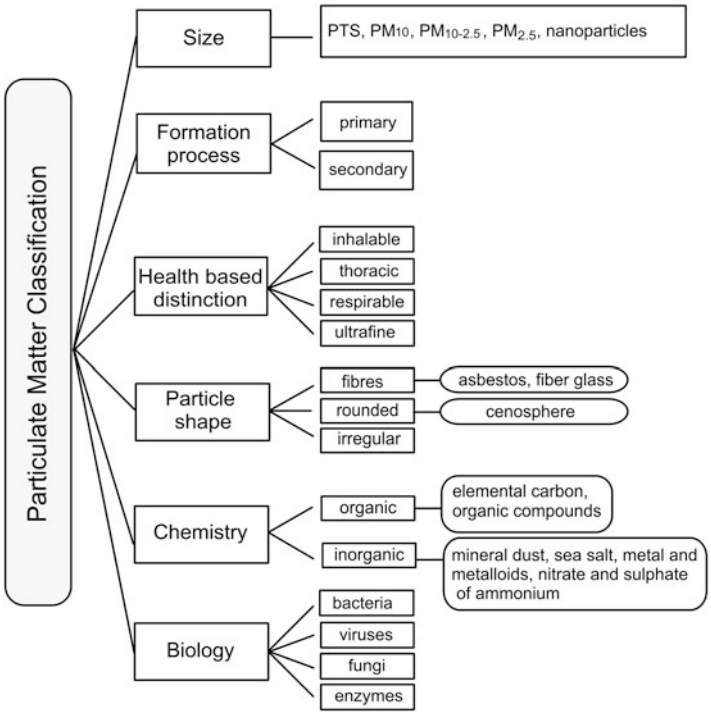

Fig. 8.3 Particulate matter classification according to physical, chemical and biological characteristics

salt concentration above the European continent has been estimated in the range 0.3–13 $\mu g\ m^{-3}$ (Manders et al. 2010). Carbonaceous particulate matter consists of a complex mixture of elemental carbon (often called soot) and hundreds of organic molecules, prevalently generated by natural and anthropogenic biomass burning, by fossil fuel combustion and dispersal of vegetable and animal biological materials.

Primary particles are those emitted directly as particles into the atmosphere. Secondary particles are formed in the atmosphere by gas-to-particle conversion process: primary gaseous emissions that condense in the atmosphere, gas-phase photochemical reactions of hydrocarbons, ozone and nitrogen oxides, yielding secondary organic compounds, oxidation of sulphur and nitrogen oxides forming the strong sulphuric and nitric acids that subsequently react with ammonia to give solid ammonium sulphate and ammonium nitrate or with solid particles of $CaCO_3$ and NaCl to form $CaSO_4$ and $NaNO_3$:

$$2NH_{3(g)} + H_2SO_{4(l)} \rightarrow (NH_4)_2SO_{4(s)} \tag{8.2}$$

$$NH_{3(g)} + HNO_{3(l)} \rightarrow NH_4NO_{3(s)} \tag{8.3}$$

$$2NaCl_{(s)} + H_2SO_{4(l)} \rightarrow Na_2SO_{4(s)} + 2HCl_{(l)} \tag{8.4}$$

$$CaCO_{3(s)} + H_2SO_{4(l)} \rightarrow CaSO_{4(s)} + CO_{2(g)} + H_2O_{(l)} \quad (8.5)$$

$$NaCl_{(s)} + HNO_{3(l)} \rightarrow NaNO_{3(s)} + HCl_{(l)} \quad (8.6)$$

$$CaCO_{3(s)} + 2HNO_{3(l)} \rightarrow Ca(NO_3)_{2(s)} + CO_{2(g)} + H_2O_{(l)} \quad (8.7)$$

Nitrates, sulphates, ammonium salts and inorganic and organic carbon are the most abundant species in the $PM_{2.5}$ fraction. However, not all the particles dispersed in air are isotropic, but many of them, especially the secondary ones, may exhibit a different composition from the surface through the core. To calculate a global-scale average chemical composition of airborne particulate matter is a meaningless exercise as it depends on the source of provenance, on the grain size of particles, and it also exhibits a composition influenced by climatic and meteorological conditions, and therefore, it is highly variable in spatial–temporal terms. However, some general considerations can be drawn from the vast literature existing on the subject. Here, we report some relevant results achieved by Putaud et al. (2004, 2010) who have reviewed data on chemical characteristics of particulate matter, from more than 60 natural background, rural, near-city, urban and kerbside sites across Europe. Among their major conclusions we have to mention are:

- No common relationship between PM mass levels and PM chemical composition has been recognised for all the study sectors of Europe.
- Mineral dust and sea salt are the prevailing components of the coarse fraction of particulate matter ($PM_{10–2.5}$).
- Mineral dust is also a major constituent of PM_{10}.
- Sea salt was observed in PM_{10} as well as in $PM_{2.5}$.
- Both PM_{10} and $PM_{2.5}$ are generally made up of organic matter (OM), SO_4^{2-} and NO_3^- ions.
- OM and black carbon (BC) as well as NH_4^+, NO_3^- and non-sea salt SO_4^{2-} contribute more to the fine fraction.
- The contribution of mineral dust to all PM size fractions is more important in Southern Europe whereas the marine contribution to PM_{10} is larger in Northwestern Europe. The contributions of SO_4^{2-} and NO_3^- to PM_{10} do not vary much across Europe, compared to the gradients observed when moving from rural to kerbside sites within each sector.

8.6 Trace Metals and Metalloids

Metals and metalloids (M&M) play an important role in sustaining life on our planet, and without them, life could not exist. Similar to the other stable chemical elements, they cannot be destroyed but migrate from an environment to another according to their biogeochemical cycle. Sometimes, their pathway is controlled by the biological activity, as in the case of methylation of Hg. All the M&M present

in the periodic table may be found in the atmosphere as solid metal particles or attached to the surface of other pre-existing particles, as fine liquid droplets or as vapours and as organic and inorganic compounds. However, they are essentially associated with airborne particulate matter, and even though they are present at only trace levels (ppb), they may pose a hazard to human health because of their potential exposure impacts.

There is a wide range of sources and release mechanisms for trace M&M into the atmosphere. The most extensive natural sources are related to the crustal material, eroded from the Earth surface, and to volcanic activity. Together they account for about 80% of all the natural sources, with the remaining contributions furnished by biogenic sources and forest fires (Nriagu 1990). Important anthropogenic sources of M&M to atmosphere are fossil fuel combustion, municipal waste incineration, industrial activity, buildings construction and vehicular traffic through exhaust and no-exhaust emissions. The relative importance of each release source will differ from site to site, but, excluding specific workplaces, the major impact is expected in metropolitan areas where static and mobile pollution sources introduce large amounts of metals and non-metals into the environment modifying the background chemistry of the airborne particulate matter. Generally, human activities release metals and metalloids proportionally more abundant in fine particles than in larger particles. This does not seem to be related to the chemical properties of the elements involved, but the explanation should be looked for mostly in the condensation process of moderately volatile elements on pre-existing small particles having greater surface-to-volume ratio than larger particles.

The residence time of metals in air, independent of their origin, is closely related to the size of particles in which they are bound. Therefore, while soil-derived metals are of little environmental concern because of their association with coarse particle sizes, smaller-sized heavy metals, which remain in suspension for days or even weeks, may have adverse health effects.

As an example, Fig. 8.4 depicts the comparison of metallic element concentrations in road dust (<20 μm) and particulates PM_{10} and $PM_{2.5}$ collected at suburban and urban sites in Palermo (Italy).

Similar trace metal concentrations, however, may be observed in most cities which agree with analogous socio-economic activities. Al and Fe, accounting for about 70–80% of the total trace elements, are, among the analysed elements, the most abundant (in the range 11,000–27,000 ppm and 3,000–32,000 ppm, respectively) in all the different grain sizes and at both sampling sites, with Al concentrations more prevalent at suburban site than at the urban site, while the contrary occurs for Fe. To these elements, add in urban PM_{10} and $PM_{2.5}$ Ba, Cu and Zn, with concentrations varying from 1,000 to 2,000 ppm. Co and U are the less present elements in all the specimens. Li, a typical crustal element, differs significantly from the coarser road dust to PM, being two orders of magnitude more abundant in road dust. Cr, Mn, Mo, Ni, Pb and Sb, trace elements known to be mainly emitted by anthropic processes, show higher concentrations in urban samples. It has to be noted that elements of definite crustal origin (Co, Fe, Li, Mn, Sr and U) are not enriched with respect to local soil. Ba, Pb, As and Cr had enrichment

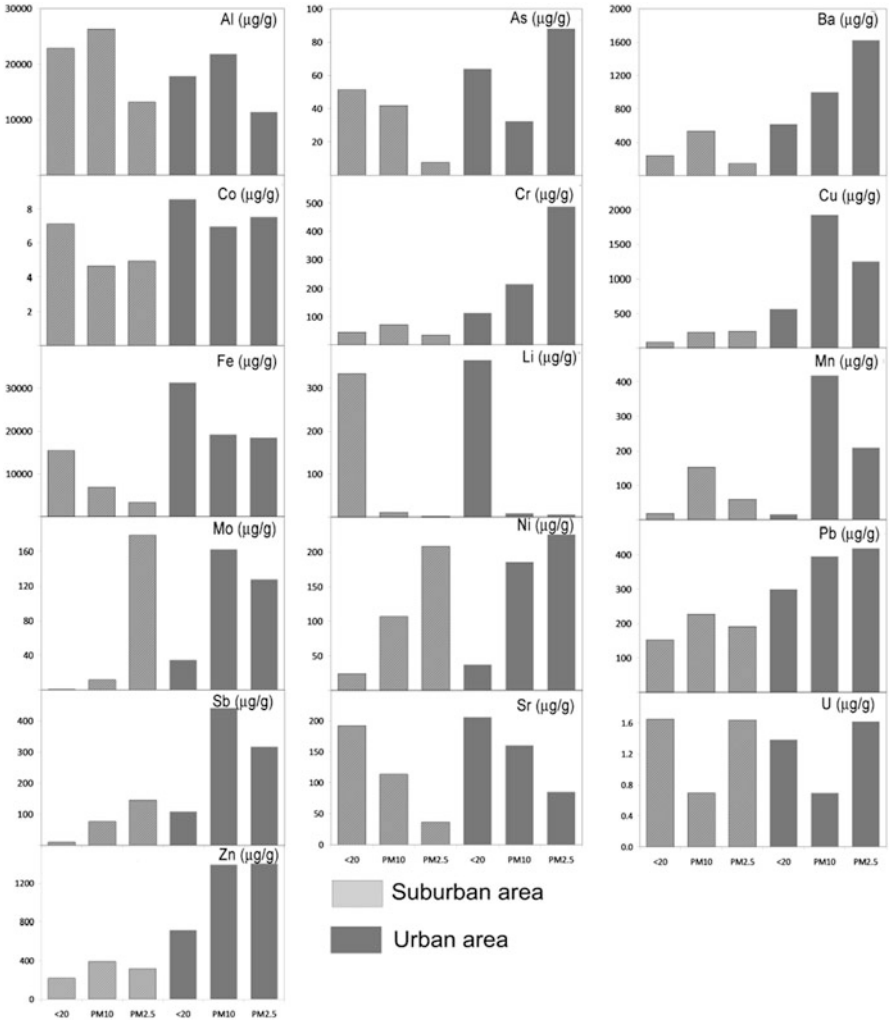

Fig. 8.4 Comparison of metallic element concentrations in road dust (<20 μm) and particulates PM_{10} and $PM_{2.5}$ collected at suburban and urban sites in Palermo (Italy). Data for PM_{10} and $PM_{2.5}$ from Dongarrà et al. (2007, 2010)

factor (EF) values of <100, and Cu and Mo EF values fell in the range 100–1,000 (for the meaning of enrichment factor, see Sect. 8.7.1). The highest EF value was observed for Sb (EF > 1,000).

Among the trace elements predominantly found in road dust and known to be hazardous to human health, lead (Pb) has been for decades the toxic metal of greatest concern. It may be reassuringly to know that in the last 15 years, because of the phasing-out of lead in gasoline, a continuous decrease in lead concentrations has been observed in airborne particulate matter, although it is still present (Fig. 8.5).

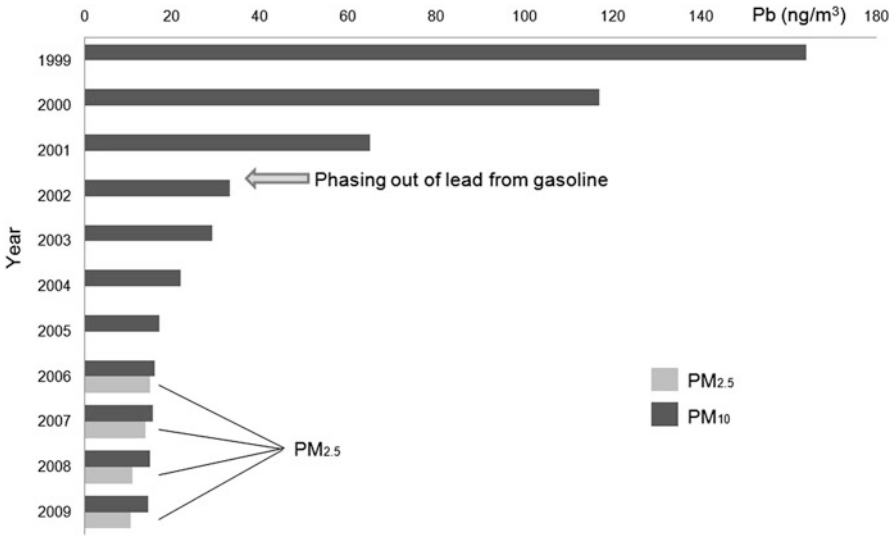

Fig. 8.5 Continuous decrease of lead concentrations ($\mu g\ m^{-3}$) in PM_{10} monitored in Palermo from 1999 to 2009. Lead concentrations in $PM_{2.5}$ for the last 3 years are also reported for comparative purposes

8.7 Fingerprint Tracers in Determining Dust, Metal and Metalloid Sources

8.7.1 Elemental Tracers

Source identification and apportionment of pollutants is paramount in air quality management. In apportionment studies to distinguish the source of particulate matter and the origin of M&M in atmosphere, certain trace elements are commonly used as characteristic indicators of natural or anthropogenic sources. Typical rare earth element (REE) patterns have been used as markers to trace atmospheric deposition of particulate matter (Dongarrà and Varrica 1998; Chiarenzelli et al. 2001). REEs identify a particular rock type and may be used as markers to determine from which geological source or geographical area airborne particulate matter might come. The underlying assumption is that the soil rock system has a unique composition regarding the REE, a condition which is not always true. Dongarrà et al. (2003) employed chondrite-normalised REE patterns in dust samples and Nerium oleander leaves from the town of Messina (Italy) to document that the main mineral components in leaves and dust had a common crustal origin and, as a consequence, they ascertain the anthropogenic nature of some M&M (Au, Br, Cd, Cu, Mo, Pb, Pd, Pt, Sb and Zn) found significantly in excess with respect to the baseline represented by the average continental Earth's crust.

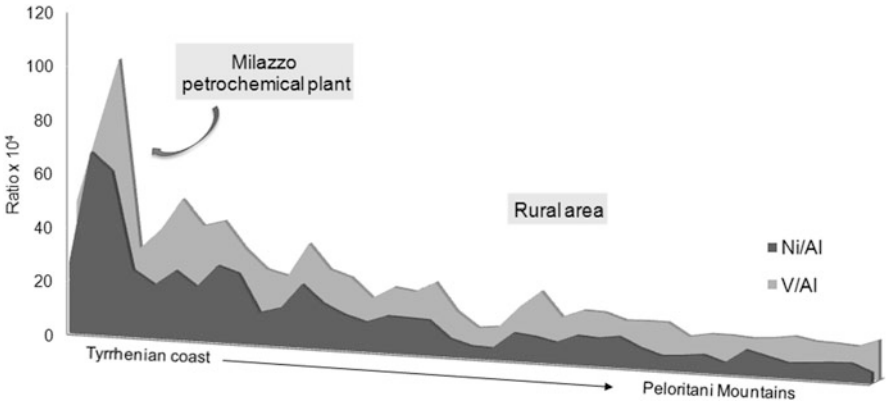

Fig. 8.6 Variations of Ni/Al and V/Al ratios along a transect from the Tyrrhenian coast of Sicily to the Peloritani Mountains

Ni and V (Fig. 8.6) are tracers of high-temperature combustion processes as those occurring in oil and coal burning and/or oil-refining industries (Dongarrà et al. 1995). This is due to their concentration in fossil fuels where they, present as petroporphyrins or as salts of organic acids, can reach levels two order of magnitude higher than other trace metals. Incidentally, the abundance of vanadium in oils derives from the marine organism, *Ascidia gemmata,* able to accumulate in its vanadocytes large amounts of vanadium, in the form of hemovanadin, as high as one million times the amount occurring in seawater. Selenium and arsenic can be tracers of coal combustion (Plant et al. 2005) when a significant contribution of natural sources (soils enriched in sulphide minerals) can be ruled out.

For a long time, due to the combustion of Pb-alkyl additives in gasoline, the presence of lead in air has been interpreted as a strong evidence of environmental pollution caused by automobile exhaust emissions. From the phasing-out of lead from gasoline and the consequent significant reduction in emission of this element, interest in other possible chemical markers of automotive traffic has been extended to vehicular non-exhaust sources, such as tire wear, brake wear, engine corrosion and catalytic converters. For this scope, Cu, Mo and Sb, in combination, may in some cases be used as a fingerprint to trace traffic-related emissions (Fig. 8.7).

Monitoring of these elements in PM_{10} and $PM_{2.5}$ in urban areas has revealed a direct relationship of both their concentrations and enrichment factors with the mass levels of particulate matter and also showed Cu/Sb ratios compatible with the same ratio in brake wear and linings and quite different from that one in crustal material (Sternbeck et al. 2002; Gomez et al. 2005; Smichowski 2008; Dongarrà et al. 2009). Pt, Pd and Rh belong to a new generation of metallic pollutants of atmosphere as the introduction of catalytic converters in cars has lead to an increase of these elements in the lower troposphere, especially along roadsides in areas affected by intensive vehicle traffic (Zereini and Alt 2000 and articles therein). Although Pt, Pd and Rh deposition due to emissions from catalytic converters is still limited, besides

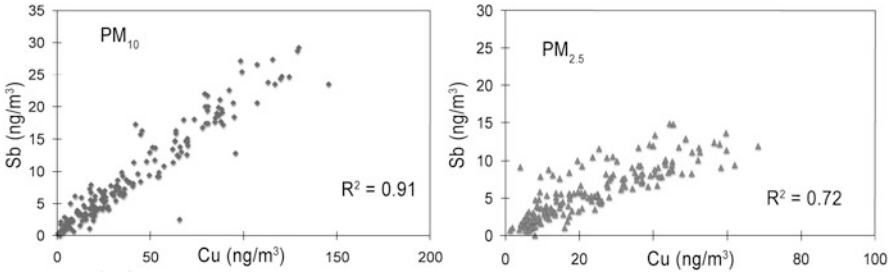

Fig. 8.7 New tracers of metal pollution derived from vehicular traffic. Relationships between Sb and Cu concentrations in PM_{10} and $PM_{2.5}$ collected at Palermo. Typical Cu/Sb ratios are also reported for comparative purposes: brake wear 2–4, PM_{10} 4.0, $PM_{2.5}$ 4.4; road dust (<20 μm) 14; continental crust 83

to have a significant impact on the urban environment, it has been demonstrated that their concentrations in airborne particulate matter may be robust indicators of motor vehicle emissions.

Comparison of elements in the atmosphere with those present in any other natural source leads to the enrichment factor EF defined as

$$\mathrm{EF}_X = \frac{\left(\frac{X}{\mathrm{Ref}}\right)_{\mathrm{atm}}}{\left(\frac{X}{\mathrm{Ref}}\right)_{\mathrm{source}}} \tag{8.8}$$

where *X* is the element of interest and Ref is the reference element; *atm* indicates the analysed particulate matter while *source* is regarding the average concentrations of X and Ref in the source of comparison. Generally, Ref is chosen among elements of definitely natural origin (e.g. Al, Si, Sr, Sc, Ti if the reference source is the Earth's crust and Na for a comparison with seawater). Applications of EFs may be amply found in literature, but it is important more important to recall the caution needed in its use because of the intrinsic limits and the several factors that affect its variance. According to the above algorithm, an element is considered geogenic when its enrichment factor is around 1, while any value over one should denote an enrichment of X in the analysed sample. Reimann and De Caritat (2000) indicated some shortcomings of EFs that must be accurately evaluated before drawing conclusions from the computed EFs as (a) the variable composition of local substrates compared to the average crust, (b) the great variability in trace element contents of rocks of even similar bulk composition (Güllü et al. 2005), (c) the fractionation of elements during their transfer from the natural source to the atmosphere and (d) the impact of biogeochemical processes. Varrica et al. (2000) also indicated the experimental error in analytical determinations as a further factor that may increase the variance of the enrichment factor. Nevertheless, when properly used, the EF constitutes a valid tool to trace the provenance of some elements.

8.7.2 Isotopic Signatures

Particles occurring as dust in the atmosphere contain chemical elements that generally retain the isotopic composition of their source. When naturally occurring and anthropogenically introduced elements have significantly different isotope ratios, the circumstance provides a convenient approach for studying and tracing the sources and pathways of dust and metal pollution in atmosphere. This method has been widely used with Pb, Sr and Nd. More specifically, Sr and Nd isotopes ($^{87}Sr/^{86}Sr$ and $^{143}Nd/^{144}Nd$, respectively) have been used for mineral dust source identification as they allow the distinction of dust generated from young volcanic areas and old continental shields as well as to distinguish dust from different source regions (Grousset and Biacaye 2005; Lahd Geagea et al. 2008). In this study, the researchers, by combining data on Nd isotopes and backward trajectory, recognised in either western Libya or northern Mauritania the main source areas of Saharan dust which frequently deposits over Europe.

Similarly, isotope ratios of lead ($^{206}Pb/^{207}Pb$, $^{208}Pb/^{207}Pb$) in particulate matter of geogenic origin are different from those of lead released into the atmosphere by anthropogenic activities. Thus, an effective discrimination between natural and man-made Pb inputs has been assisted, for the last decades, by measurement of variations in Pb-isotope ratios. An overview of literature published on the use of Pb isotopic analyses of different environmental matrices, including atmospheric dust, has been recently furnished by Komárek et al. (2008). However, with the phasing-out Pb added as an anti-knock compound in gasoline, the possibility of using lead radiogenic isotopes to demonstrate the anthropogenic input of this metal into the atmosphere has been drastically reduced. Nevertheless, they still have the potentiality to trace significant transboundary atmospheric transport or to trace the atmospheric dispersal of Pb in mining areas. For example, Pb-isotope ratios have been successfully used by Erel et al. (2002, 2006) to deduce that Pb in atmospheric aerosols sampled in Jerusalem (Israel) originated from Turkey, Egypt and Eastern Europe. Doucet and Carignan (2001) proved that even Pb from dust originating from Sahara contributes significantly to the isotopic composition of Pb in atmospheric particles that reach Europe.

8.7.3 Speciation of Trace Metals in the Environment

It is the accurate knowledge of the chemical form of a metal (or metalloid) that provides information on its possible biological implications. Unfortunately, the term “speciation” has assumed in the chemical terminology a number of different meanings. One, prevalently employed in soil science, is regarding to which soil phase the metals are bound. The considered soil phases are generally categorised as follows: (a) exchangeable metals, (b) metals bound to carbonates, (c) metals

bound to iron and manganese oxides, (d) metals bound to organic matter and (e) metals in residual fraction (Tessier et al. 1979). This is because the distribution of an element among different mineralogical phases profoundly affects its mobility and availability and may help in understanding some aspects of its biogeochemical cycle. In fact, a labile fraction of the particle-bound metals is considered to be more readily available to living organisms than a resistant fraction. Heal et al. (2005) showed that in urban atmospheres, the water-soluble form is the dominant fraction of $PM_{2.5}$-bound heavy metals. Example of such studies may be found in Smichowski et al. (2005), Manno et al. (2006), Samontha et al. (2007), Rao et al. (2008) and Feng et al. (2009).

Another meaning of the term speciation is concerning specific form of an element defined as to isotopic composition, electronic or oxidation state and/or complex or molecular structure (Templeton et al. 2000). This second approach is relevant not only because the toxicity of some elements depends greatly on oxidation state (Cr^{+6} and As^{+3} are much more toxic than Cr^{+3} and As^{+5}) but also as the chemical form of an element may be a fingerprint in the process of source identification and apportionment in PM investigations (Huggins et al. 2000). Only a few studies have been conducted to this end. Up to now, one of the best and most powerful ways to investigate chemical speciation in solids is the x-ray absorption spectroscopy technique (XAS) which provides information on the oxidation state and local structural environment that surrounds the absorbing atom, allowing the recognition of natural and anthropogenic sources which contribute to the presence of some metal species into ambient air. XAS (divided in EXAFS and XANES) can be used regardless of the crystalline and noncrystalline form of the sample (Penner-Hahn 1999).

Wang et al. (2007) obtained the XANES spectra of Cr, Mn, Cu and Zn in PM_{10} and $PM_{2.5}$ samples collected in Shanghai. Their main conclusion was that the analysed samples exhibited similar speciation patterns independently of particle size. Varrica et al. (2013) carried out XAS analysis on samples of wheel rims dust, road dust and atmospheric particulate matter. They revealed that the specimens contained an admixture of Sb(III) and Sb(V) oxides in different relative abundance, compatible with a scenario where road traffic heavily contributes to the total content of Sb in urban atmosphere (Fig. 8.8).

8.7.4 Why Do We Concern So Much for M&M in Air?

The risk of health problems associated with exposure to metals and metalloids present in airborne particulate matter has been the target of a large number of toxicological and epidemiological studies (Goldoni et al. 2006; Kawata et al. 2007; Lippmann et al. 2006). Although, until now, it is difficult to make firm conclusions attributing, in absolute manner, to specific components of PM the responsibility for the observed negative health consequences, some metal particles seem to be able

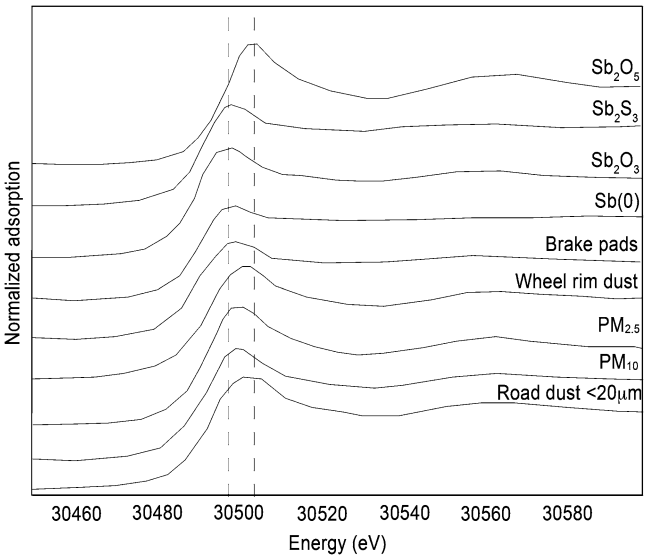

Fig. 8.8 Comparison of K-edge XANES spectra of particulate matter PM_{10} $PM_{2.5}$ and road dust (<20 μm) collected in Palermo with samples of brake linings, wheel rim dust and reference compounds

to cross the cell membrane affecting biochemical mechanism. Methylate forms of Hg can cause neurotoxicity; lead is known to induce toxic effects on the central nervous system, especially in children; an excess of copper may cause toxicity to liver cells; accumulation of aluminium in critical parts of brain seems to be involved in Alzheimer's disease; and a number of metals, such as Be, Cd, Cr and Ni, are considered human carcinogens (Nordberg and Cherian 2005). The toxic effects of metals may act on specific target organs or induce specific functional changes. Much of the damage produced by toxic metals derives from the formation of oxidative free radicals, such as hydroxyl radical ($HO^{\bullet}$), superoxide radical ($O_2^{\bullet -}$) or hydrogen peroxide (H_2O_2), which induce various modifications to DNA bases, enhances lipid peroxidation and alters calcium and sulfhydryl homeostasis (Ercal et al. 2001; Valko et al. 2005). Free radicals (sometimes named reactive oxygen species, ROS) have a much greater reactivity with intracellular nucleophiles than molecular oxygen from which they are derived with the complicity of metals. Mechanisms involving the Fenton reaction, generation of the superoxide radical and the hydroxyl radical appear to be involved for a large number of metals:

Fenton and Haber – Weiss-like reactions of metals

$$Me^{n+} + H_2O_2 \rightarrow M^{(n+1)+} + OH^- + {}^{\bullet}OH \tag{8.9}$$

$$O_2^{\bullet -} + H_2O_2 \leftrightarrow OH^- + {}^{\bullet}OH + O_2 \tag{8.10}$$

further propagation

$$RH_{(lipids,\ proteins,\ DNA)} + OH^{\bullet} \rightarrow R^{\bullet}{}_{(lipids,\ proteins,\ DNA)} + H_2O \tag{8.11}$$

$$R^{\bullet}{}_{(lipids,\ proteins,\ DNA)} + O_2 \rightarrow ROO^{\bullet} \tag{8.12}$$

$$ROO^{\bullet} + RH_{(lipids,\ proteins,\ DNA)} \rightarrow ROOH + R^{\bullet}{}_{(lipids,\ proteins,\ DNA)} \tag{8.13}$$

Metals can also increase the acidity of the blood which, in turn, affects calcium homeostasis provoking calcium to be drawn from bones. Furthermore, M&M can stimulate or increase allergic reactions and compete with other essential trace metals for biochemical bond sites.

Toxic metals and metalloids would tend to accumulate if there were no mechanisms or routes devoted to excrete them from our body. Major routes for excretion are the kidney and liver, while less important with respect to reduction of the total body burden are the biological fluids saliva, tears and urine as well as tissues such as nails and hair. Nevertheless, these last minor routes allow non-invasive methods to assess people's exposure to toxic M&M. Hair, more than nails, has been employed in evaluating past and continuous exposure to high levels of metals (Bache et al. 1991; Ashraf et al. 1994; Batzevich 1995; D'Ilio et al. 2000; Lee et al. 2000; Violante et al. 2000; Chojnacka et al. 2005, 2006a, b, 2010a; Sanna et al. 2008; De Prisco et al. 2010). Although several justified critical points still exist such as interpretation of results of hair analyses (Nowak and Chmielnicka 2000; Sanna et al. 2003, 2011; Chojnacka et al. 2006b, 2010a, b; Kempson and Lombi 2011), here, we wish showing how environmentalists could benefit of the latent capacity of such tool in identifying areas which require attention for the potential exposure of resident populations to metals and also to ascertain occupational exposure. Dongarrà et al. (2012) demonstrated the capacity of human hair to uptake metals from the surrounding environment providing a comparison of the trace elements content in human scalp hair from young individuals living in several areas of Sicily characterised by different environmental conditions. The metal profiles in hair samples collected from different areas appeared to be consistent with the geographical situation of major sources of contamination, i.e., volcanic and mine areas, industrial zones and rural environment. Figure 8.9 shows the significant differences in lead and arsenic between the town of Palermo and Pace del Mela and Antillo, respectively. Pace del Mela is a small town in northeastern Sicily (Italy) on the Tyrrhenian coast in the province of Messina. This is an area of high environmental risk, due to the presence of the large petrochemical industry of Milazzo; Antillo is a small country town in the mineralised area of the southeastern sector of the Peloritani Mountains (northeastern Sicily, Italy). This area is site of polymetallic mineralisation where large-scale mining was practised in the past. Figure 8.9 also shows the higher content of vanadium in hair samples from

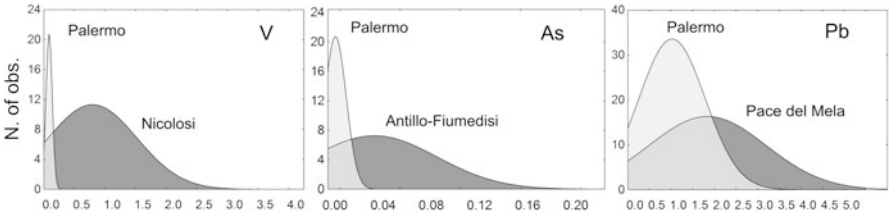

Fig. 8.9 Differences in vanadium, arsenic and lead concentrations ($\mu g\ g^{-1}$) in hair samples of young students collected at Palermo, Nicolosi (Etna volcano), Antillo–Fiumedinisi (mining area) and Pace del Mela (industrial area)

young people living in Nicolosi (southern flank of Mt. Etna), probably due to the high content of vanadium in local groundwaters used for irrigation and human consumption.

8.8 Conclusions

We have presented some arguments concerning the study of airborne particulate matter, some well known and some others that deserve more deep attention, although we are confident that:

- Many questions remain unanswered.
- Other questions have triggered more questions.
- Many important questions have yet to be asked.

But that is the core of research.

References

Andreae MO, Rosenfeld D (2008) Aerosol–cloud–precipitation interactions. Part 1. The nature and sources of cloud-active aerosols. Earth Sci Rev 89:13–41

Ashraf W, Jaffar M, Mohammad D (1994) Trace metal contamination study on scalp hair of occupationally exposed workers. Bull Environ Contam Toxicol 53:516–523

Bache CA, Lisk DJ, Scarlett JM, Carbone LG (1991) Epidemiologic study of cadmium and lead in the hair of ceramists and dental personnel. J Toxicol Environ Health 34:423–431

Batzevich VA (1995) Hair trace element analysis in human ecology studies. Sci Total Environ 164:89–98

Berner EK, Berner RA (1996) Global environment: water, air and geochemical cycles. Prentice Hall, Old Tappan, p 376

Breysse P, Lees PSJ (2006) Particulate matter. The Johns Hopkins University http://ocw.jhsph.edu/courses/PrinciplesIndustrialHygiene/PDFs/Lecture4.pdf. Accessed 30 May 2012

Buseck PR, Adachi K (2008) Nanoparticles in the atmosphere. Elements 4:389–394

CEC (2005) Communication from the Commission to the Council and the European Parliament. Thematic Strategy on air pollution. Commission of the European Communities

CEN (1993) Workplace atmospheres. Size fraction definitions for measurement of airborne particles European Committee for Standardization, British Standard Institute, Great Britain, BS EN 481:1993

Chester R (2000) Marine geochemistry. Blackwell Publishing, New York, p 506

Chiarenzelli J, Aspler L, Dunnet L (2001) Multi-element and rare earth element composition of lichens, mosses and vascular plants from the central Barrenlands, Nunavut, Canada. Appl Geochem 16:245–270

Chojnacka K, Górecka H, Chojnacki A, Górecki H (2005) Inter-element interactions in human hair. Environ Toxicol Pharmacol 20:368–374

Chojnacka K, Górecka H, Chojnacki A, Górecki H (2006a) The effect of age, sex, smoking habit, hair color on the composition of hair. Environ Toxicol Pharmacol 22:52–57

Chojnacka K, Górecka H, Górecki H (2006b) The influence of living habits and family relationships on element concentrations in human hair. Sci Total Environ 366:612–620

Chojnacka K, Michalak I, Zieńliska A, Górecka H, Górecki H (2010a) Inter-relationship between elements in human hair: the effect of gender. Ecotoxicol Environ Saf 73:2022–2028

Chojnacka K, Zieńliska A, Dobrzanski HGZ, Górecki H (2010b) Reference values for hair minerals of Polish students. Environ Toxicol Pharmacol 29:314–319

D'Ilio S, Violante N, Senofonte O, Caroli S (2000) Occupational exposure of goldsmith workers of the area of Rome to potentially toxic metals as monitored through hair analysis. J Microchem 67:343–349

De Prisco PP, Volpe MG, Petitto F, Palladino C, Saturnino C, Capasso A, Di Stasio M, De Prisco R (2010) Level of essential and toxic metals in urban adolescents hair: preliminary study. Biomed Res 21:131–140

Dongarrà G, Varrica D (1998) The presence of heavy metals in air particulate at Vulcano island (Italy). Sci Total Environ 212:1–9

Dongarrà G, Ottonello D, Sabatino G, Triscari M (1995) Use of lichens in detecting environmental risk and in geochemical prospecting. Environ Geol 26:139–146

Dongarrà G, Sabatino G, Triscari M, Varrica D (2003) The effects of anthropogenic particulate emissions on roadway dust and Nerium oleander leaves in Messina (Sicily, Italy). J Environ Monit 5:766–773

Dongarrà G, Manno E, Varrica D, Vultaggio M (2007) Mass levels, crustal component and trace elements in PM10 in Palermo, Italy. Atmos Environ 41:7977–7986

Dongarrà G, Manno E, Varrica D (2009) Possible markers of traffic-related emissions. Environ Monit Assess 154:117–125

Dongarrà G, Manno E, Varrica D, Lombardo M, Vultaggio M (2010) Study on ambient concentrations of PM_{10}, $PM_{10-2.5}$, $PM_{2.5}$ and gaseous pollutants. Trace elements and chemical speciation of atmospheric particulates. Atmos Environ 44:27–34

Dongarrà G, Varrica D, Tamburo E, D'Andrea D (2012) Trace elements in scalp hair of children living in differing environmental contexts in Sicily (Italy). Environ Toxicol Pharmacol 34: 160–169

Doucet FJ, Carignan J (2001) Atmospheric isotopic composition and trace metal concentration as revealed by epiphytic lichens. Atmos Environ 35:3681–3690

Durant AJ, Bonadonna C, Horwell CJ (2010) Atmospheric and environmental impacts of volcanic particulates. Elements 6:235–240

EPA (2005) Final staff paper recommends stronger particle pollution standards. http://yosemite.epa.gov/opa/admpress.nsf/d9bf8d9315e942578525701c005e573c/7a82ddc6d0b37f65852570310065bdfc. Accessed 30 May 2012

Ercal N, Gurer-Orhan H, Aykin-Burns N (2001) Toxic metals and oxidative stress part I: mechanisms involved in metal-induced oxidative damage. Curr Top Med Chem 1:529–539

Erel Y, Axelrod T, Veron A, Mahrer Y, Katsafados P, Dayan U (2002) Transboundary atmospheric lead pollution. Environ Sci Technol 36:3230–3233

Erel Y, Dayan U, Rabi R, Rudich Y, Stein M (2006) Trans boundary transport of pollutants by atmospheric mineral dust. Environ Sci Technol 40:2996–3005
Feng XD, Dang Z, Huang WL, Yang C (2009) Chemical speciation of fine particle bound trace metals. Int J Environ Sci Technol 6:337–346
Gierè R, Querol X (2010) Solid particulate matter in the atmosphere. Elements 6:215–222
Goldoni M, Caglieri A, Poli D, Vettori M, Corradi M, Apostoli P, Mutti A (2006) Determination of hexavalent chromium in exhaled breath condensate and environmental air among chrome plating workers. Anal Chim Acta 562:229–235
Gomez DR, Ginè MF, Sánchez Bellato AC, Smichowski P (2005) Antimony: a traffic-related in the atmosphere of Buenos Aires, Argentina. J Environ Monit 7:1162–1168
Grousset FE, Biacaye PE (2005) Tracing dust sources and transport patterns using Sr, Nd and Pb isotopes. Chem Geol 222:149–167
Güllü G, Doğan G, Tuncel G (2005) Atmospheric trace element and major ion concentrations over the eastern Mediterranean Sea: identification of anthropogenic source regions. Atmos Environ 39:6376–6387
Heal MR, Hibbs LR, Agius RM, Beverland IJ (2005) Total and water-soluble trace metal content of urban background PM_{10}, $PM_{2.5}$ and black smoke in Edinburgh, UK. Atmos Environ 39: 1417–1430
Hess M, Koepke P, Schult I (1998) Optical properties of aerosols and clouds. Bull Am Meteorol Soc 79:831–844
Houghton JT, Meira Filho LG, Callander BA, Harris N, Kattenberg A, Maskell K (1996) Climate change 1995. The Science of Climate Change, Contribution of working Group I to the second Assessment Report of the Intergovernmental Panel on Climate Change, Cambridge University Press, Cambridge
Huggins FE, Shah N, Huffman GP, Robertson JD (2000) XAFS spectroscopic characterization of elements in combustion ash and fine particulate matter. Fuel Process Technol 65–66:203–218
ICRP (1994) International Commission on Radiological Protection: human respiratory model for radiological protection. Ann ICRP 24:1–300
Junge C (1979) The importance of mineral dust as an atmospheric constituent. In: Morales C (ed) Saharan dust. Wiley, New York, pp 243–266
Kawata K, Yokoo H, Shimazaki R, Okabe S (2007) Classification of heavy metal toxicity by human DNA microarray analysis. Environ Sci Technol 41:3769–3777
Kempson IM, Lombi E (2011) Hair analysis as a biomonitor for toxicology, disease and health status. Chem Soc Rev 40:3915–3940
Komárek M, Ettler V, Chrastný V, Mihaljevič M (2008) Lead isotopes in environmental sciences: a review. Environ Int 34:562–577
Lahd Geagea M, Stille P, Gauthier-Lafaye F, Millet M (2008) Tracing of industrial aerosol sources in an urban environment using Pb, Sr, and Nd isotopes. Environ Sci Technol 42:692–698
Lee WC, Lee MJ, Lee SM, Kim JS, Bae CS, Park TK (2000) An observation on the mercury contents of scalp hair in the urban residents of South Korea. Environ Toxicol Pharmacol 8: 275–278
Lippmann M, Ito K, Hwang J-S, Maciejczyk P, Chen L-C (2006) Cardiovascular effects of nickel in ambient air. Environ Health Perspect 114:1662–1669
Manders AMM, Schaap M, Querol X, Albert MFMA, Vercauteren J, Kuhlbusch TAJ, Hoogerbrugge R (2010) Sea salt concentrations across the European continent. Atmos Environ 44:2434–2442
Manno E, Varrica D, Dongarrà G (2006) Metal distribution in road dust samples collected in an urban area close to a petrochemical plant at Gela, Sicily. Atmos Environ 40:5929–5941
Marconi A (2003) Materiale particellare aerodisperso: definizioni, effetti sanitari, misura e sintesi delle indagini ambientali effettuate a Roma. Ann Ist Super Sanita 39:329–342
Nieboer E, Thomassen Y, Chashchin V, Odland JO (2005) Occupational exposure assessment of metals. J Environ Monit 7:411–415
Nordberg M, Cherian MG (2005) Biological responses of elements. In: Selinus O (ed) Essential of medical geology. Elsevier Academic Press, San Diego

Nowak B, Chmielnicka J (2000) Relationship of lead and cadmium to essential elements in hair, teeth, and nails of environment exposed people. Ecotoxicol Environ Saf 46:265–274
Nriagu JO (1979) Global inventory of natural and anthropogenic emissions of trace metals to the atmosphere. Nature 279:409–411
Nriagu JO (1990) Global metal pollution. Environment 32:7–33
Penner-Hahn JE (1999) X-ray absorption spectroscopy in coordination chemistry. Coord Chem Rev 190–192:1101–1123
Plant JA, Kinniburg DG, Smedley PL, Fordyce FM, Klinck BA (2005) Arsenic and selenium. In: Holland HD, Turekian KK (eds) Treatise on geochemistry, vol 9. Elsevier Ltd, Amsterdam, pp 17–66
Pöschl U (2005) Atmospheric aerosols: composition, transformation, climate and health effects. Angew Chem Int Ed 44:7520–7540
Putaud JP, Raes F, Van Dingenen R et al (2004) A European aerosol phenomenology – 2: chemical characteristics of particulate matter at kerbside, urban, rural and background sites in Europe. Atmos Environ 38:2579–2595
Putaud JP, Van Dingenen R, Alastuey A et al (2010) A European aerosol phenomenology – 3: Physical and chemical characteristics of particulate matter from 60 rural, urban, and kerbside sites across Europe. Atmos Environ 44:1308–1320
Rao CRM, Sahuquillo A, Lopez Sanchez JF (2008) A review of the different methods applied in environmental geochemistry for single and sequential extraction of trace elements in soils and related materials. Water Air Soil Pollut 189:291–333
Rasmussen PE (1998) Long-range atmospheric transport of trace metals: the need for geosciences perspectives. Environ Geol 33:96–108
Reimann C, De Caritat P (2000) Intrinsic flaws of element enrichment factors (Efs) in environmental geochemistry. Environ Sci Technol 34:5084–5091
Samontha A, Waiyawat W, Shiowatana J, McLarenb RG (2007) Atmospheric deposition of metals associated with air particulate matter: fractionation of particulate-bound metals using continuous-flow sequential extraction. Sci Asia 33:421–428
Sanna E, Liguori A, Palmas L, Renata Soro M, Floris G (2003) Blood and hair lead levels in boys and girls living in two Sardinian towns at different risks of lead pollution. Ecotoxicol Environ Saf 35:248–252
Sanna E, Floris G, Vallascas E (2008) Town and gender effects on hair lead levels in children from three Sardinian towns (Italy) with different environmental backgrounds. Biol Trace Elem Res 124:52–59
Sanna E, De Micco A, Vallascas E (2011) Evaluation of association between biomarkers of lead exposure in Sardinian children (Italy). Biol Trace Elem Res 143:1383–1392
Seinfeld JH, Pandis SN (1998) Atmospheric chemistry and physics: from air pollution to climate change. Wiley, New York
Smichowski P (2008) Antimony in the environment as a global pollutant: a review on analytical methodologies for its determination in atmospheric aerosols. Talanta 75:2–14
Smichowski P, Polla G, Gómez D (2005) Metal fractionation of atmospheric aerosols via sequential chemical extraction: a review. Anal Bioanal Chem 381:302–316
Spurny KR (2000) Aerosol chemistry and its environmental effects. In: Spurny KR (ed) Aerosol chemical processes in the environment. Lewis Publishers, Boca Raton/London/New York/Washington, DC
Sternbeck J, Sjödin A, Andréasson K (2002) Metal emissions from road traffic and the influence of resuspension-results from two tunnel studies. Atmos Environ 36:4735–4744
Templeton DM, Ariese F, Cornelis R, Danielsson LG, Muntau H, Van Leeuwen HP, Łobiński R (2000) Guidelines for terms related to chemical speciation and fractionation of elements. Definitions, structural aspects, and methodological approaches (Iupac Recommendations 2000). Pure Appl Chem 72:1453–1470
Tessier A, Campbell PGC, Bisson M (1979) Sequential extraction procedure for the speciation of particulate trace metals. Anal Chem 51:844–851

Valko M, Morris H, Cronin MTD (2005) Metals, toxicity and oxidative stress. Curr Med Chem 12:1161–1208

Varrica D, Aiuppa A, Dongarrà G (2000) Volcanic and anthropogenic contribution to heavy metal content in lichens from Mt. Etna and Vulcano island (Sicily). Environ Pollut 108:153–162

Varrica D, Bardelli F, Dongarrà G, Tamburo E (2013) Speciation of Sb in airborne particulate matter, vehicle brake linings, and brake pad wear residues. Atmos Environ 64:18–24

Vincent JH (2007) Aerosol sampling: science, standards, instrumentation and applications. Wiley, New York

Violante N, Senofonte O, Marsili G, Meli P, Soggiu ME, Caroli S (2000) Human hair as a marker of pollution by chemical elements emitted by a thermoelectric power plant. J Microchem 67: 397–405

Wang Y, Li A, Zhan Y, Wei L, Li Y, Zhang G, Xie Y, Zhang J, Zhang Y, Shan Z (2007) Speciation of elements in atmospheric particulate matter by XANES. J Radioanal Nucl Chem 273:247–251

WHO (1999) Air quality guidelines for Europe, 2nd edn. WHO Regional Office for Europe, Copenhagen, 1999

Wiseman CLS, Zereini F (2010) Airborne particulate matter: sources, composition and concentration. In: Zereini F, Wiseman CLS (eds) Urban airborne particulate matter origin, chemistry, fate and health impacts. Springer, Berlin/Heidelberg, pp 1–2, 26, part I

Zereini F, Alt F (2000) Anthropogenic platinum-group-element emissions: their impact on man and environment. Springer, Berlin/Heidelberg/New York

Chapter 9
Metal Geochemistry of a Brackish Lake: Étang Saumâtre, Haiti

Alex Eisen-Cuadra, Alan D. Christian, Emmanis Dorval, Bryanna Broadaway, Josi Herron, and Robyn E. Hannigan

Abstract Étang Saumâtre (also known as Lac Azuéi, Lago del Fondo, or Yainagua) is a brackish lake located in eastern Haiti. Sources of irrigation and drinking water for the surrounding communities in Thomazeau, Ganthier, and Fond Parisien are freshwater springs and shallow wells tapping the complex fractured aquifer system surrounding Étang Saumâtre. In some groundwater samples, we found concentrations of trace metals exceeding World Health Organization guideline values. Lake sediment trace metal concentrations were also high. For example, chromium (Cr) ranged from 26.24 to 198.44 mg/kg, exceeding the USEPA sediment quality guideline value for heavily polluted. High concentrations of potentially toxic trace metals in both lake sediments and groundwater suggest that the population relying on this lake for drinking water, irrigation, and subsistence fishing may be at risk for metal-induced health effects. By understanding the geochemical behavior of redox-sensitive trace metals such as Cr, in the context of limnology and long-term fate and transport within the system, our results provide unique insights into the

A. Eisen-Cuadra (✉)
Department of Chemistry, University of Massachusetts Boston, Boston, MA, USA
e-mail: alexeisencuadra@gmail.com

A.D. Christian
Department of Biology, University of Massachusetts Boston, 100 Morrissey Blvd, Boston, MA 02125-3393, USA

E. Dorval
Dorval Initiative de Recherche Ecologique and Consultation, c/o Librerie La Lumiere Rue Baussan # 34, Port-au-Prince, Haiti

B. Broadaway • R.E. Hannigan
Department of Environmental, Earth, and Ocean Sciences, University of Massachusetts Boston, 100 Morrissey Blvd, Boston, MA 02125-3393, USA
e-mail: Robyn.Hannigan@umb.edu

J. Herron
Department of Biology, University of Great Falls, 1301 20th Street South, Great Falls, MT, USA

P. Censi et al. (eds.), *Medical Geochemistry: Geological Materials and Health*, DOI 10.1007/978-94-007-4372-4_9,

geochemical controls on remobilization of redox metals from the sediments and the potential impact of future environmental change on the sediment and water quality in this system.

Keywords Trace elements • Redox chemistry • Groundwater • Drinking water • Closed-basin • Sediment geochemistry • Transition metals

9.1 Introduction

Anthropogenic activities and global change phenomena continue to have significant impacts on the geochemical cycling of trace metals (Xu et al. 2011; Doney et al. 2009; Gąsiorowski and Sienkiewicz 2010). In recent decades, surface water quality of many lakes, rivers, and coastal oceans around the world has worsened in part due to land-use practices and changes in the hydrologic balance (Li et al. 2009; Carpenter et al. 1998; Liu et al. 2003). Hydrologically, closed-basin lakes are particularly susceptible to changes in land use and climate. Closed-basin lake sediments record changes in both land use and land cover as well as larger-scale changes in climate and act as sinks for both dry and wet deposition (Galloway et al. 2008; Smith et al. 2011). In these lakes, input is primarily from precipitation, runoff (overland flow) and groundwater, and output is solely through evaporation. Since these lakes are evaporitic, their salinity is maintained by input–output relationships. As land use and climate changes occur, input may exceed output leading to freshening and, as such, to changes in metal speciation. Interactions between sediments and lake water, as well as groundwater, have the potential to remobilize materials deposited years prior, making the lake-sediment-groundwater interface a critical zone for evaluating trace metal mobility patterns. As trace metal mobility directly impacts bioavailability, it is crucial to understand the dynamics of such processes and evaluate the potential consequences they may have on human health.

Trace metals such as arsenic (As), chromium (Cr), copper (Cu), lead (Pb), and zinc (Zn) are deposited through dry and wet deposition. Important sources include anthropogenic effluent and emissions, mineral weathering processes, and the washing of soil particles transported in runoff from the terrestrial watershed (Salbu and Steinnes 1995). Trace metal concentrations vary depending on the natural abundance, intensity of precipitation events, and land-use practices in the region. Additionally, sedimentary particles are an important consideration because their affinity to adsorb trace metals varies depending on the surface area, grain size, specific gravity, magnetic properties, etc. (Horowitz 1991). Trace metals accumulate within lake sediment over time, thereby providing a temporal record of land use/climate change. Since sediment quality guidelines specific to trace metal concentrations have been developed, we are able to use these guidelines to retrospectively evaluate changes in the lake ecosystem.

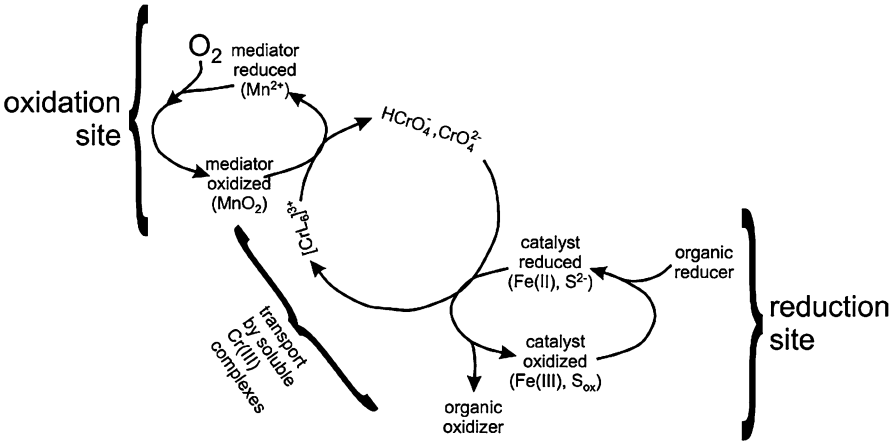

Fig. 9.1 The sedimentary redox cycle of Cr (Adapted from Kotaś and Stasicka 2000)

Sediment quality guidelines provide a basis for identifying contaminants of concern in aquatic ecosystems and predicting adverse effects on aquatic and human life (MacDonald et al. 2000). Toxic trace metals can bioaccumulate and pose significant threats to human health. If toxic trace metals from polluted sediment are resuspended via changes in redox conditions, dredging, storms, etc., it can impact many species that live in the lake (USEPA 2012a). Hence, sediment quality guidelines allow researchers to compare results from multiple systems to better predict health outcomes (Ingersoll et al. 2001; Edward 2006).

While a number of potentially toxic trace metals are evaluated in this chapter, we focus much of our discussion on Cr. Cr accumulation in groundwater, lake water, and sediments is expected to correlate with mineral weathering processes, natural environmental inputs from the region, and anthropogenic activities (Farmer and Lovell 1986; Jordão et al. 1997). Cr may be deposited in sediment via precipitation of $Cr(OH)_3(s)$, in aerosol form through atmospheric deposition, as aqueous $Cr^{2+/3+}$ in runoff, or as aqueous or solid $Cr^{2+/3+}$ or Cr^{6+} through waste disposal or in leachate from various urban, industrial, and agricultural activities (Luo et al. 2010; Salbu and Steinnes 1995). Once in system, metal addition, absorption, desorption, dissolution, substitution, etc. are expected to follow traceable paths with respect to a given set of redox conditions, divalent metals, pH, Eh, temperature, and availability of elements involved in the cycling of Cr, such as Fe- and Mn-oxyhydroxides (Fig. 9.1).

Cr is a redox-sensitive trace metal with varying toxic effects depending on the oxidation state. It is most commonly found in the environment as Cr(III) and Cr(VI) (Schüring 2000). These two species are significantly different in physicochemical properties and biochemical reactivity. Cr(III) is typically found as an oxide, $((FeCr)_2O_3)$ (Salbu and Steinnes 1995), and is more stable in reducing environments

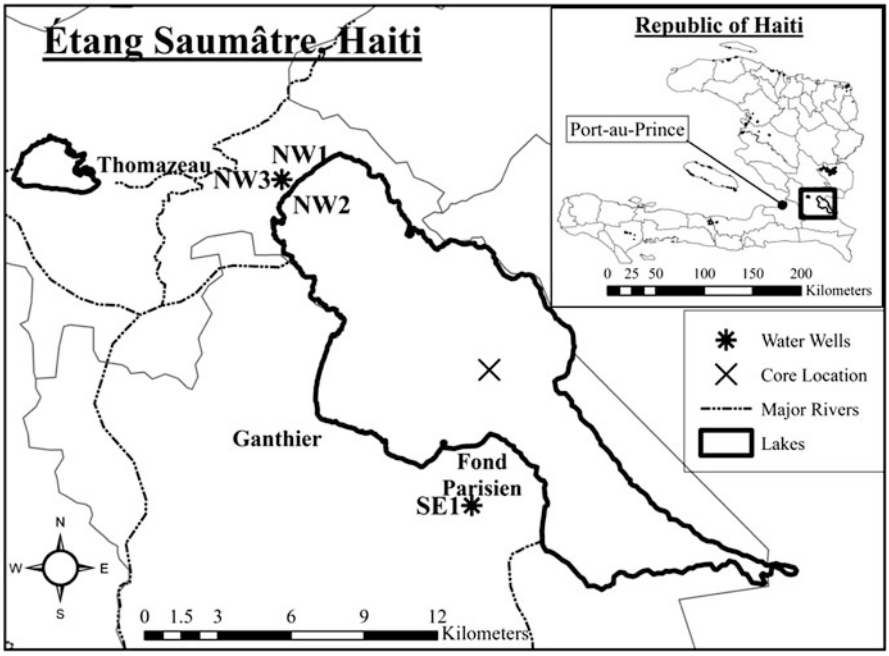

Fig. 9.2 Map of Étang Saumâtre, Haiti (latitude = 18.5975° and longitude = −72.0147222°) and the groundwater (*) and lake sediment (X) sampling site. *Note*: some groundwater samples taken from water wells used by the local inhabitants (NW1, NW2, and NW3) are in close proximity to each other and thus indicated by a single *asterisk*

than Cr(VI) (Langard and Schrauzer 1984). Cr may enter the human body under physiological conditions through inhalation and ingestion, followed by uptake in the gastrointestinal tract, and under pathological conditions via skin absorption (Langard and Schrauzer 1984). Rates of uptake depend on the valence state, water solubility, pH, and length of exposure. Hence, understanding the controls on Cr cycling and the potential for redox transformations within environmental systems is crucial when considering potential effects on human health (Fendorf et al. 2000).

9.1.1 Setting

This chapter focuses on Étang Saumâtre (Fig. 9.2), an alkaline brackish lake located in eastern Haiti, ~45 km from the capitol Port-au-Prince. The lake lies in a pull-apart basin in the Enriquillo-Plantain Garden Fault Zone (Mann et al. 1983; Calais et al. 2010) and is approximately 21.8 km in length, 10.2 km at its widest, and 25 m at its deepest. Étang Saumâtre is the largest lake in Haiti and provides crucial ecosystem goods and services to the Haitian population, especially to the regional inhabitants.

Étang Saumâtre is actively fished, supporting the dietary needs of local communities and sustaining important economic niches through the sale of fish on local markets (Dorval, pers. comm., 2011). Haitians as a whole reportedly suffer from a lack of protein in their diet, and in response, a plan to enlarge Haitian fisheries was suggested to help increase the consumption of high-quality protein (Sebrell et al. 1959). During a sample collection trip in 2011, a local community leader reported a steady decline of catch at Étang Saumâtre in recent years (personal communication, May 28, 2011).

Land use/land cover varies around the lake. The mountains that surround Étang Saumâtre are mainly limestone, and they are actively mined in the southeastern subbasin for building materials to construct homes and other infrastructures (Hadden and Minson 2010). This mining activity, and the denudation associated with it, leads to increased surface runoff during precipitation events. In the northwestern subbasin, water is pumped from the lake to local farms and used for livestock as well as irrigation of crops such as onions, coffee, garlic, and sugarcane. Due to the land use in this area, runoff is more likely to contain agrochemicals and other potential contaminants associated with farming.

Sources of irrigation and drinking water for the surrounding communities of Thomazeau, Ganthier, and Fond Parisien include freshwater springs and shallow groundwater tapped by hand-dug wells. The aquifer system in this region is complex and fractured, comprised of quaternary sands and clays underlain by fractured limestone. Due to enhanced intensity and frequency of storms, lake levels have been increasing to the extent that many formally habitable areas are now permanently or seasonally flooded leading to displacement of the local population. Additionally, several homes that were built by nongovernmental organizations to house Haitians displaced from Port-au-Prince as a result of the January 12, 2010 earthquake are now permanently flooded and uninhabitable (Dorval, pers. comm., 2011).

Deforestation makes the region more vulnerable to hurricanes and tropical storms due to less protection against strong winds, floods, and mud slides (Bueno et al. 2008). Trace metal mobility may be concurrently augmented, likely resulting in worse sanitation conditions due to limited water supplies and contaminated water from floods, placing even greater demand on an already stressed public health system. Energy and food security are also at greater risk, and fisheries and coral reef habitats will likely transform as a result of salinity, temperature, and pH variations.

9.1.2 Temporal Changes in Land Use/Land Cover and Climate

Land use and land cover have changed over the past century in the region surrounding Étang Saumâtre, and climate change also has impacted this system. Using the sediment record of the lake, it may be possible to evaluate the long-term impacts of these changes on sediment and water quality and in so doing develop an understanding of the potential impacts on human health. Exposure to high

concentrations of contaminant trace metals affects survival, fecundity, reproductive success, and growth of aquatic organisms. Changes in the bioavailability of trace metals and biomagnification of these contaminants can lead to harmful impacts on human health. A several thousand year record of Lake Miragoane, Haiti, documented various deleterious impacts on vegetation and lake level fluctuations in Haiti due to human activities and climate influences (Higuera-Gundy et al. 1999). Using lake sediment and groundwater trace metals, our data elucidate the impact of regional land use/land cover changes on the lake system, specifically the impact of these changes on the geochemical fate of potentially toxic trace metals.

Reconstruction of the environmental history of Étang Saumâtre requires accurate age dating of the sediments. Using age dating techniques (^{137}Cs and ^{210}Pb), the delivery and deposition of potentially toxic trace metals over time can be evaluated. Changes in precipitation and anthropogenic activities in the watershed related to agriculture, sewage runoff, deforestation, etc. will likely result in changes in trace metal and terrestrial organic matter input. Deforestation and enhanced storm intensities are expected to increase surface runoff and accelerate erosion. This enhances the delivery of allochthonous material to the lake such as soil nutrients, organic matter, and inorganic matter – ultimately changing the composition of the lake sediment (Rosenmeier et al. 2004).

Given that we expect trace metal concentrations to track, to some extent, changes in land use and climate, we can use their concentrations to retrospectively evaluate changes in sediment quality and elucidate potential hazards. A comparison of sediment trace metal concentrations to accepted sediment quality guidelines (SQG) can be used as a reference (Giesy and Hoke 1990; MacDonald et al. 2000; Luo et al. 2010). Based on these guidelines, we can classify "time periods" as non-polluted, moderately polluted, or heavily polluted.

Since the bioavailability and toxicity of trace metals is governed, to a large extent, by redox chemistry, we use a redox-sensitive rare earth element (REE), cerium (Ce), to reconstruct the redox history of the sediments (McLennan 1989). The relative abundance of Ce relative to its neighbors lanthanum (La) and praseodymium (Pr) is based on the degree of oxygenation of the water column as well as the sediment pore waters. Under reducing conditions, Ce^{3+} will behave similarly to the other trivalent REE, but under oxidizing conditions, Ce^{4+} will precipitate from solution through adsorption onto organic particulates and/or Fe- and Mn-oxyhydroxides. As a result, oxidized waters show a relative depletion in Ce defined as the cerium anomaly (Holser 1997; Schroder and Grotzinger 2007). Varying redox conditions in groundwater and changes in lake circulation (e.g., down welling) may lead to changes in local nutrient and oxygen gradients, which could affect coagulation of clays, leading to differential complexation of the REE, ultimately influencing $(Ce/Ce^*)_N$, ± 0.1, where $(Ce/Ce^*)_N = (Ce_N/0.5^*(La_N + Pr_N))$, normalized ($N$) to the upper continental crust (UCC) (Taylor and McLennan 1985).

9.2 Methods

9.2.1 Sample Collection

We collected groundwater and sediment samples around and within Étang Saumâtre, Haiti, respectively (Fig. 9.2). Four groundwater samples were collected from hand-pumped wells in polypropylene containers in May 2010. Three groundwater samples were from adjacent sites in the northwestern sub-basin, and one groundwater sample was from a well of the western side of the southeastern sub-basin (Fig. 9.2). Groundwater samples were filtered through 0.45-μm filters and acidified to pH < 2 using ultrapure trace metal grade HNO_3.

In May 2011, a sediment core from the central sub-basin of the lake (Fig. 9.2) was collected using a 50.00 cm length × 5.95 cm diameter cylinder sleeve, with an Uwitec Corer, equipped with hammer action and automatic core catcher to preserve stratification. After collection, the sediment core was sliced in field into 1-cm sections and dried under ambient temperature. Sediment samples were placed into individually labeled and sterilized Whirl-Paks® and shipped to the laboratory under the United States Department of Agriculture Animal and Plant Health Inspection Service permit number: P330-10-00064. Samples were shipped within 1 week and arrived approximately 3 weeks later. Upon arrival, samples were immediately stored at −15°C. Samples were heated at 65°C for 24 h prior to preparation for analysis. Dried sediment samples were stored in new sterilized Whirl-Paks® and stored in the dark until analysis.

9.2.2 Analytical Methods

All analyses were performed at the University of Massachusetts Boston Environmental Analytical Facility. After sediment samples were dried at 65°C for 24 h, and prior to all analyses, sediment samples were ground into a homogenous powder. For trace metal and REE analysis, samples were acid digested following standard methods (Hannigan and Sholkovitz 2001). In brief, 50.0-mg samples were digested at 70°C for 48 h in 4 mL of 3:1 ultrapure trace metal grade HNO_3 to pure plasma H_2O_2. Samples were dried at 70°C and then resuspended in 4 mL of ultrapure trace metal grade HNO_3, capped and digested again at 70°C for 24 h. Samples were dried at 70°C and resuspended in 1 mL of ultrapure trace metal grade HNO_3 and brought to a final volume of 50 mL (gravimetrically) with ∼18.2 MΩ-cm water. Trace metal concentrations were quantified by external calibration internal standardization using USGS SDO-1 (Ohio Devonian Oil Shale) and spiked with an internal standard, i.e., 20 ppb ^{115}In (Nassef et al. 2006). Samples were analyzed by inductively coupled plasma mass spectrometry (ICP-MS; PerkinElmer ELAN DRC II).

Method detection limits (MDL) are calculated for trace metals in sediment. MDL is defined as “the minimum concentration of a substance that can be measured and

reported with 99% confidence that the analyte concentration is greater than zero" (USEPA 2012b). MDLs are calculated by taking the standard deviation of the seven standard sample MDLs and multiplying them by the student *t*-value. In this case, for seven samples, and six degrees of freedom, the *t*-value at a 99% confidence interval equals 3.143.

$$\text{MDL} = (\text{Standard deviation})\,(t - \text{value}) = (\text{Standard deviation})\,(3.143)$$

The calculated MDL for As, Cr, Cu, Pb, and Zn were 0.008, <0.001, 0.007, 0.005, and <0.001 mg/kg, respectively.

Radiometric age dating of bulk sediment samples was made based on a constant rate of supply model. Samples were analyzed by gamma spectroscopy using a CANBERRA WELL Germanium Detector equipped with CANBERRA Genie 2000 MCA microprocessor (Zhu and Olsen 2009). Each sample was counted until percent error dropped below 10% and representative peak analysis reports could be generated (Schelske et al. 1994).

All maps were made with ArcGIS 9, all statistical analyses were conducted using Minitab 16, and all figures were made with SigmaPlot 11.0.

9.3 Results and Discussion

9.3.1 Radioisotope Dating

Sediment core age dating was calculated based upon radiocesium (^{137}Cs) major (28.50 cm) and minor (10.50 cm) peaks and the date of sediment core collection, 2011.4667 C.E = 0.00 cm. ^{137}Cs is present in the global environment due to atomic bomb testing since 1954, peaking around 1962/1963, as well as the 1986 Chernobyl disaster (Kendall and McDonnell 1998; Robbins and Edgington 1975). The rate of sedimentation for the central sub-basin = 0.59 cm/year (Fig. 9.3).

Sediment focusing in this area of the basin precluded use of ^{210}Pb for dating; thus, we relied on ^{137}Cs for reconstruction of the changes in geochemistry. A sediment core (~753 cm in length) from Lake Miragoâne, Haiti, was dated using multiple techniques at different depths, e.g., ^{210}Pb, organic ^{14}C, and carbonate ^{14}C (Binfordll and Dorsey 1991). Based on corrected ages, this sediment core has an average rate of sedimentation equal to ~0.05 cm/year. The differences between our sedimentation rates and theirs may reflect different age dating techniques, the length of each respective core, different locations, a general increase in the rate of sedimentation in recent years, etc. For example, the rate of sedimentation of the sediment core from Binfordll and Dorsey 1991 between 22 and 8 cm is equal to ~0.25 cm/year. This suggests that recent changes over the past 20 years associated with land use/land cover and climate may have occurred, such that a constant rate of supply model may not be appropriate over long time periods.

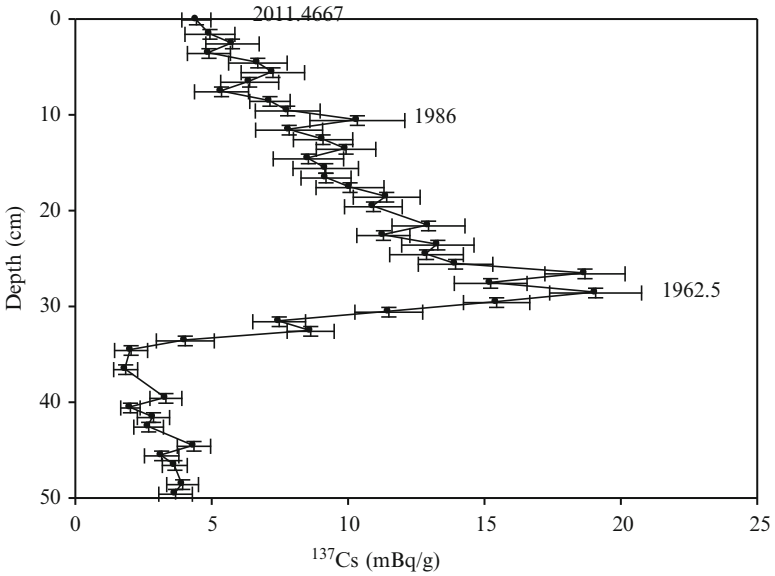

Fig. 9.3 ^{137}Cs depth profile of the central sub-basin sediment core. ^{137}Cs peaks occur due to atomic bomb testing peaking around 1962/1963 and the 1986 Chernobyl disaster. The relation between ^{137}Cs and depth is linearly expressed as $y = -1.7032x + 2{,}009.1$, with an $R^2 = 0.9663$

Over the past 50 years, the Earth's surface has warmed ~0.5°C (IPCC 2007), which is expected to have intensified the global water cycle by ~4% because warmer air can absorb and redistribute a greater amount of water (Durack et al. 2012; Allen and Ingram 2002. Proxies of this phenomena are expected to be most notable in the trade-wind belts, 18–26°, where evaporation is highest and relative humidity is lowest (Sharp 2007). An increase in precipitation may increase sediment deposition rates due to weathering processes and increased runoff (Salbu and Steinnes 1995).

9.3.2 Sediment Quality Analysis

We measured five trace metals (As, Cr, Cu, Pb, and Zn) and interpret the deposition in each sediment core section. The highest concentrations of our five target trace metals occur toward the top of the sediment core (more recently), whereas lower concentrations and greater stability occur toward the bottom of the core (Fig. 9.4). The average concentration of trace metals As, Cr, Cu, Pb, and Zn across all sections of the core ranged from 0.88, 70.11, 10.65, 2.02, to 9.03 mg/kg, respectively (Fig. 9.4). Maximum trace metal concentration values for all analytes are at least double their respective minimum concentration values.

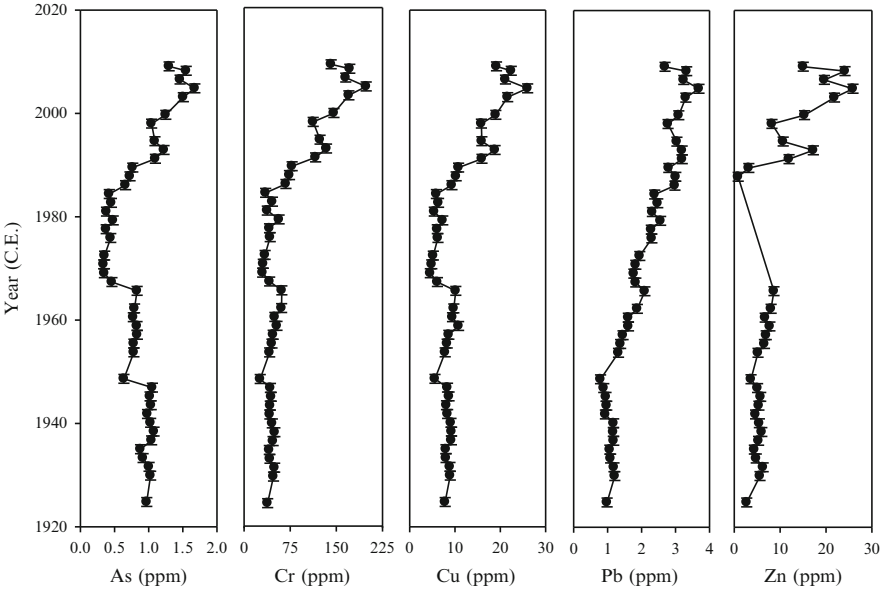

Fig. 9.4 Sediment profile of selected trace metals [As, Cr, Cu, Pb, and Zn (ppm)] since ~1925. For the trace metals presented here, $n = 43$, except Zn ($n = 32$) because only 32 samples had detectable levels

Three of the five elements, As, Pb, and Zn, fall within the non-polluted concentration range throughout the sediment cores' captured history (Figs. 9.4 and 9.5; Table 9.1). For all three of these elements, the highest concentrations occur toward the top of the core suggesting an increase in depositional flux in recent years. Pb concentrations have been steadily increasing since ~1950, which is a common trend observed in sediment cores throughout the world (Li et al. 2012; Fagel et al. 2010). The observation of increasing Pb concentrations is attributed to an increase in fossil fuel combustion, but isotopic Pb data is needed to more pointedly determine the source of pollution.

Meanwhile, the remaining two elements, Cu and Cr, had noteworthy sediment core concentrations. Cu had increasing concentrations from the bottom to the top of the core, which generally falls under the non-polluted range except for a brief time around 2004 (Fig. 9.4; Table 9.1). In 2004, Cu briefly enters the moderately polluted index but then shifts back to the non-polluted index.

Cr concentrations are within the moderately polluted index for the 1920s to 1990s sections. However, since 1990, Cr deposition in the lake has increased to levels above the heavily polluted sediment threshold value (USEPA Guideline Values; Table 9.1). Furthermore, between 2003 and 2008, Cr concentrations are two times higher than the USEPA guideline value for heavily polluted sediment. Cr concentrations at these elevated levels are known to have deleterious effects on aquatic life and may translate into nocuous impacts on human health (Langard and Schrauzer 1984; Nriagu and Nieboer 1988).

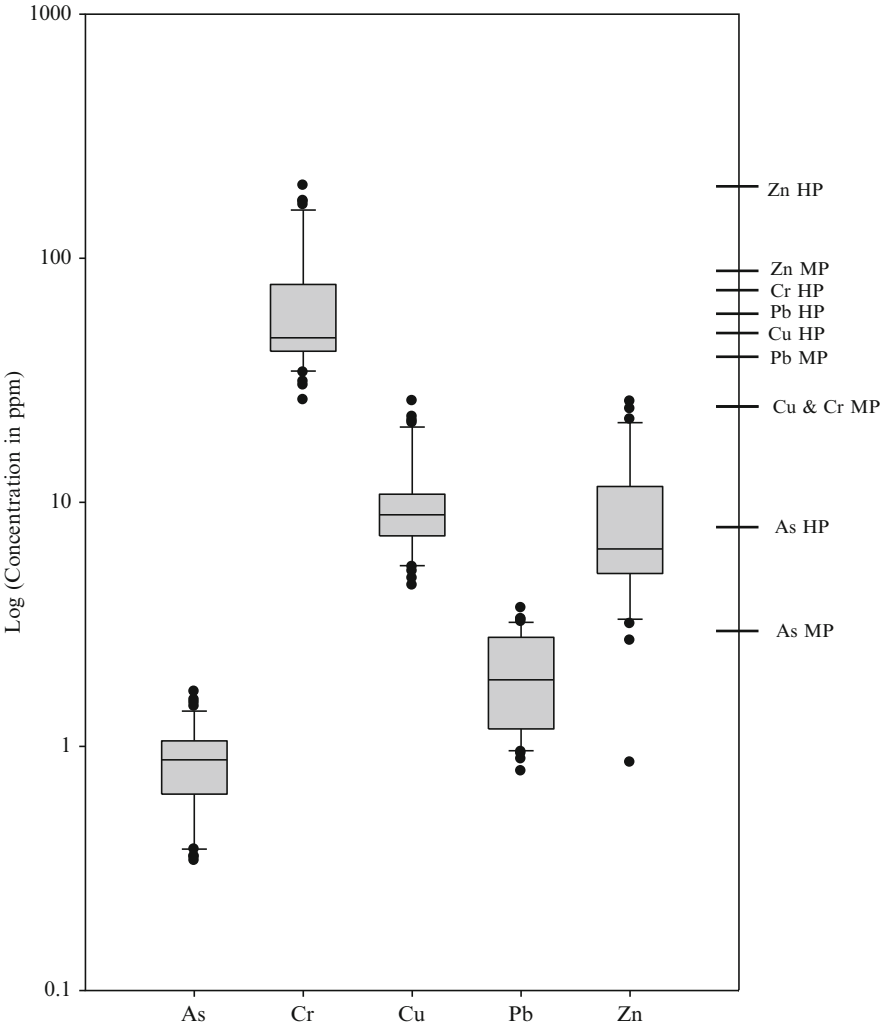

Fig. 9.5 Box and Whisker plot of As, Cr, Cu, Pb, and Zn. USEPA sediment quality guideline values proposed (Giesy and Hoke 1990) are displayed on the right *y*-axis. *HP* heavily polluted, *MP* moderately polluted

Table 9.1 USEPA sediment quality guideline values proposed by Giesy and Hoke (1990) *for selected trace metals*

SQG USEPA	As (ppm)	Cr (ppm)	Cu (ppm)	Pb (ppm)	Zn (ppm)
Non-polluted	<3	<25	<25	<40	<90
Moderately polluted	3–8	25–75	25–50	40–60	90–200
Heavily polluted	>8	>75	>50	>60	>200

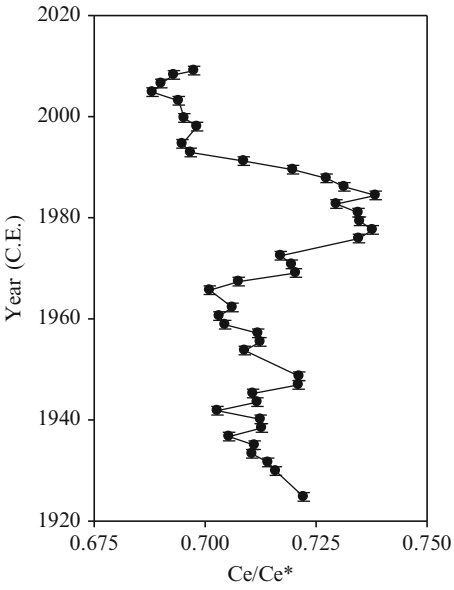

Fig. 9.6 Down column Ce/Ce*. Negative cerium anomalies are typical of sediments deposited under anoxic conditions (Kakuwa and Matsumoto 2006)

9.3.3 Redox Chemistry of Lake Sediment

Because Cr appears to be the element of most immediate concern, understanding Cr cycling and the potential for redox transformations is essential to determining possible effects on human health because the bioavailability and toxicity of trace metals are largely controlled by redox chemistry (Fendorf et al. 2000). The majority of the REE does not have redox chemistry with the exception of Ce and Eu (McLennan 1989).

The anomalous separation of Ce from the other REE can reveal the redox conditions in sediment and during early diagenesis (Holser 1997). Ce, La, and Pr were normalized to the UCC (Taylor and McLennan 1985), and the Ce/Ce* was calculated for each section in the sediment core (Fig. 9.6) (Hannigan and Sholkovitz 2001).

Ce/Ce* remains within a narrow range (<0.075) throughout the sediment core (Fig. 9.6). The fluctuating pattern of Ce/Ce* may imply a system with specific sources dominating during particular periods (e.g., storm-enhanced aerosol deposition) such that the sediments are inheriting the observed pattern. All of the Ce/Ce* values are below 1, i.e., negative cerium anomaly, which is typical of sediments deposited under anoxic conditions such that Cr is expected to follow the redox chemistry of Fe(III) and Mn(IV) oxides. This is confirmed to a significant extent by correlating the depositional fluxes over the entire sediment core (Fig. 9.7).

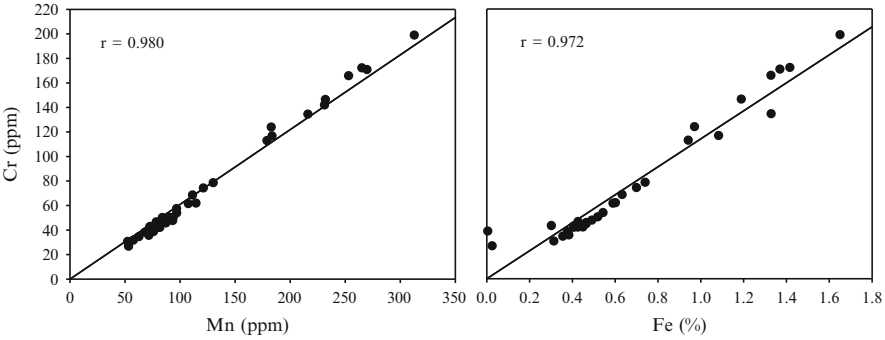

Fig. 9.7 Mn (ppm) and Fe (%) versus Cr (ppm) of Étang Saumâtre lake sediment. Strong linear correlations exist between Cr and Mn, and Cr and Fe, suggesting that Cr deposition is largely controlled by the sedimentary cycling of Mn, Fe (Fig. 9.1) and the given redox conditions

9.3.4 Water Quality Analysis

As, Cr, and Pb had concentrations exceeding WHO guideline values for some hand-dug groundwater wells (NW1, NW2, NW3, and SE1) from the Étang Saumâtre region (Fig. 9.8). Concentrations of As were variable depending on the sample location: below detection limit at SE1, approximately equal to WHO guidelines at NW2 and 3, and double WHO guidelines at NW1 (Fig. 9.8). Cr concentrations were variable across the wells ranging from concentrations approximately equal to guideline concentrations at NW2, to concentrations more than fivefold greater than the guideline concentrations at NW3 and SE1, and to concentrations more than an order of magnitude higher than WHO guidelines at NW1 (Fig. 9.8). Pb is approximately equal to the WHO guideline value at NW1, is sevenfold larger than the guideline value at well SE1, and is below detection at wells NW2 and 3.

The groundwater wells in our study are within village limits and are left uncapped. The water is used for drinking, livestock, and irrigation of crops. By evaluating long-term changes of sediment and water quality, we can monitor the fate of toxic trace metals and predict/prevent the potentially deleterious impacts they may have on human health by informing communities and developing management plans based on the given results. These results coupled with the recent increase in the contaminant trace metal loading of sediment imply that the lake system is changing. This transformation is effecting the deposition and mobility of contaminant trace metals and may have the unintended consequence of altering the trace metal distribution in and around the lake and within water sources.

Drinking water is an influential determinant of health by preventing and controlling waterborne diseases (WHO 2012). The potential risk of chronic As, Cr, and Pb exposure in the Étang Saumâtre region places the communities using these water wells in need of cleaner water and appropriate screening (Kazi et al. 2009). Arsenicosis may develop over a period of 20 years and may be reversible if arsenic

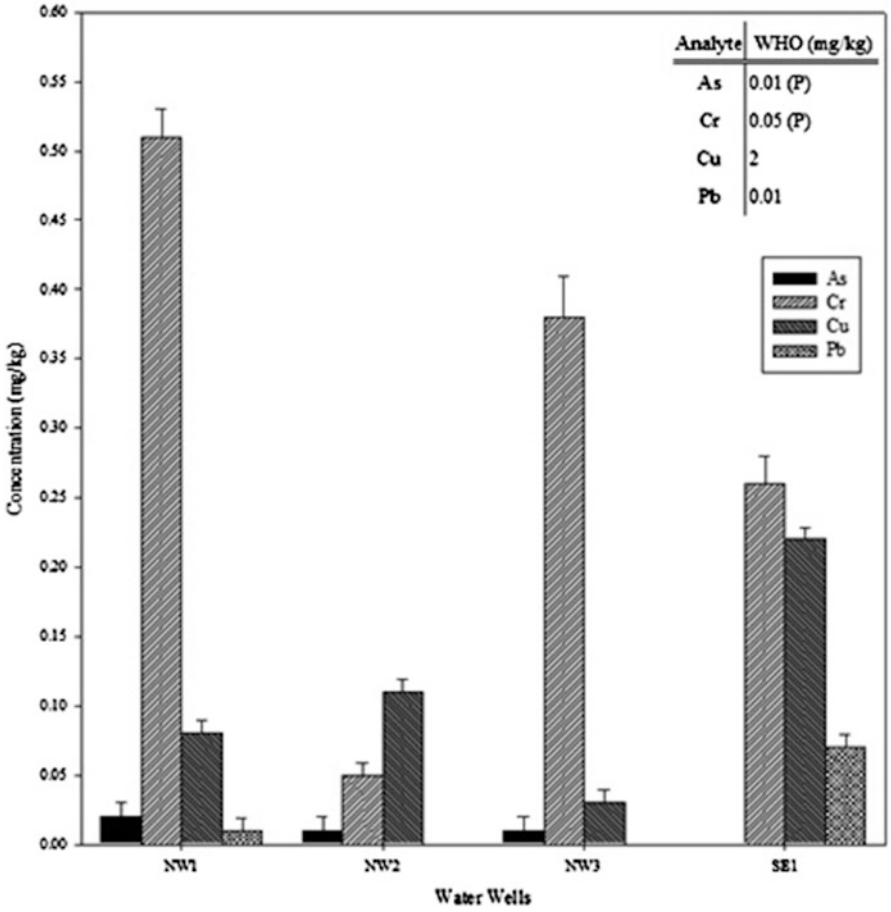

Fig. 9.8 Select elemental composition (As, Cr, Cu, Pb) of groundwater from the water wells surrounding Étang Saumâtre, Haiti, with World Health Organization Guidelines for Drink-Water Quality at the *top right of figure*. (*P*) = provisional guideline value, as there is evidence of a hazard, but the available information on health effects is limited. (*C*) = concentrations of the substance at or below the health-based guideline value may affect the appearance, taste, or odor of the water, leading to consumer complaints. Analytes below detection were omitted from the respective figure

ingestion ceases at an early stage of development (Atkins 2006). Symptoms in the beginning stages of arsenic poisoning can include the appearance of dark spots on the skin, to a hardening of the skin into a tumorlike rounded mass, often occurring on the palms, soles, and torso (Kazi et al. 2009). Pb has been well recognized for scores of toxic effects (Dieter 2011; WHO 2012).

Cr exposure has been linked to a variety of clinical problems such as increased incidence of respiratory cancer, skin allergies, perforation of the nasal septum, asthma, bronchitis, pneumonitis, and inflammation of the larynx and liver (Nriagu

and Nieboer 1988; Kotaś and Stasicka 2000). Cr skin exposure effects include skin allergies, dermatitis, dermal necrosis, dermal corrosion, hypersensitivity, etc. (Kotaś and Stasicka 2000). While more specific mechanisms are needed, Cr toxicity is generally thought to arise due to its redox chemistry. For example, Cr freely diffuses across cell membranes and may disrupt biological processes by acting as an oxidizing agent and by forming free radicals during the reduction of Cr(VI) to Cr(III) inside cells (Kotaś and Stasicka 2000). Additionally, Cr may act as a metal center and form chelate and coordination complexes with organic ligands that interfere with metalloenzyme systems (Kotaś and Stasicka 2000; Langard and Schrauzer 1984). Consequently, Cr(VI) is considered to be 100 times more toxic to humans than Cr(III) (Pais and Jones 1997). Changes in the redox conditions of groundwater and lake water and changes in lake circulation (e.g., down welling) can influence local nutrient and oxygen gradients that may alter the oxidation state of Cr and cause a serious epidemic.

9.4 Conclusion

The communities depending on Étang Saumâtre and its resources, for drinking water, irrigation, and subsistence fishing, may be at risk of metal-induced health effects. The environmental history of Étang Saumâtre and the potential impact of future environmental change on the sediment and water quality are presented. Cr concentrations increase shortly after 1980, indicating that recent changes may be anthropogenically derived. Cr concentrations prior to this time period fell into the moderately polluted index. This may suggest that the natural environment has elevated Cr concentrations and anthropogenic activities such as deforestation and agriculture may have augmented the mobility of Cr from erosion and storm intensity increases. Ce anomalies typical of sediments deposited under anoxic conditions help elucidate the controls on Cr mobility of the given system. Hence, it can be concluded that the deposition of Cr follows the chemistry of Fe and Mn and its geochemical fate can be monitored over time. Cr contamination should be a major concern for communities living in this region. Potential sources of Cr still need to be narrowed, and public awareness must be increased. Translations of these results into French and Creole are currently underway. This chapter provides vital baseline data for monitoring the future impact of natural and anthropogenic changes on sediment quality, and drinking and irrigation water, with respect to potentially toxic trace metals in the region of Étang Saumâtre, Haiti.

Further research is needed to determine the extent to which land-use practices have contributed to changes in trace metal loading. This research is ongoing and will incorporate the use of x-ray diffraction, stable isotope chemistry, and other methods to determine how the delivery and deposition of organic matter has been altered due to land-use practices and climate. Additional interests include how Cr sediment chemistry records dynamic land use and population changes occurring in

the region as well as natural geologic and climatic events. Along with quantifying the relation between Cr and the redox chemistry of Fe(III) and Mn(IV) oxides in groundwater and lake water. Any disturbance of the ecosystem may exacerbate the health of the communities living in this region. It is critical, therefore, that as part of the broader research focused on sediment and water quality, an assessment of the impact of land use and climate change in terms of water quality and ability to sustain a productive fishery continues.

Acknowledgements This research was funded, in part, by NSF 0959666 (Hannigan and Christian), NSF 1062374, and by a UMass President's Science and Technology grant (Hannigan). Additional support was provided by the Department of Environmental, Earth, and Ocean Sciences at UMass, Boston.

References

Allen MR, Ingram WJ (2002) Constraints on future changes in climate and the hydrologic cycle. Nature 419(6903):224–232

Atkins PW (2006) Shriver and Atkins inorganic chemistry. Oxford University Press, Oxford

Binfordll MW, Dorsey KT (1991) Reconstruction of Caribbean climate change over the past 10,500 years. Nature 352:29

Bueno R et al (2008) The Caribbean and climate change: the costs of inaction. Tufts University, Medford. Accessed, 10(09). http://ase.tufts.edu/gdae/Pubs/rp/Caribbean-full-Eng.pdf

Calais E et al (2010) Transpressional rupture of an unmapped fault during the 2010 Haiti earthquake. Nat Geosci 3(11):794–799

Carpenter SR et al (1998) Nonpoint pollution of surface waters with phosphorus and nitrogen. Ecol Appl 8(3):559–568

Dieter H (2011) Drinking water toxicology in its regulatory framework. In: Treatise on water science. Elsevier, Oxford, pp 377–415

Doney SC et al (2009) Ocean acidification: the other CO_2 problem. Mar Sci 1:169–192

Durack PJ, Wijffels SE, Matear RJ (2012) Ocean salinities reveal strong global water cycle intensification during 1950 to 2000. Science 336(6080):455–458

Edward R (2006) Calculation and uses of mean sediment quality guideline quotients: a critical review. Environ Sci Technol 40(6):1726–1736

Fagel N et al (2010) Geochemical evidence (C, N and Pb isotopes) of recent anthropogenic impact in south-central Chile from two environmentally distinct lake sediment records. J Quatern Sci 25(7):1100–1112

Farmer J, Lovell M (1986) Natural enrichment of arsenic in Loch Lomond sediments. Geochim Cosmochim Acta 50(9):2059–2067

Fendorf S, Wielinga BW, Hansel CM (2000) Chromium transformations in natural environments: the role of biological and abiological processes in chromium(VI) reduction. Int Geol Rev 42(8):691–701

Galloway JN et al (2008) Transformation of the nitrogen cycle: recent trends, questions, and potential solutions. Science 320(5878):889–892

Gąsiorowski M, Sienkiewicz E (2010) 20th century acidification and warming as recorded in two alpine lakes in the Tatra Mountains (South Poland, Europe). Sci Total Environ 408(5): 1091–1101

Giesy JP, Hoke RA (1990) Freshwater sediment quality criteria: toxicity bioassessment. In: Baudo R, Giesy J, Muntau H (eds) Sediments: chemistry and toxicity of in-place pollutants. Lewis Publishers, Chelsea, pp 265–348

Hadden RL, Minson SG (2010) The geology of Haiti: an annotated bibliography of Haiti's geology, geography and earth science. Army Geospatial Center, Alexandria, DTIC Document
Hannigan RE, Sholkovitz ER (2001) The development of middle rare earth element enrichments in freshwaters: weathering of phosphate minerals. Chem Geol 175(3–4):495–508
Higuera-Gundy A et al (1999) A 10,300 14C yr record of climate and vegetation change from Haiti. Quatern Res 52(2):159–170
Holser WT (1997) Evaluation of the application of rare-earth elements to paleoceanography. Palaeogeogr Palaeoclimatol Palaeoecol 132(1–4):309–323
Horowitz AJ (1991) Primer on sediment-trace element chemistry. 2
Ingersoll CG et al (2001) Predictions of sediment toxicity using consensus-based freshwater sediment quality guidelines. Arch Environ Contam Toxicol 41(1):8–21
IPCC (2007) The physical science basis. Contribution of working group I to the fourth assessment report of the intergovernmental panel on climate change. Cambridge University Press, Cambridge/New York, 996 p
Jordão CP, Pereira JL, Jham GN (1997) Chromium contamination in sediment, vegetation and fish caused by tanneries in the State of Minas Gerais, Brazil. Sci Total Environ 207(1):1–11
Kakuwa Y, Matsumoto R (2006) Cerium negative anomaly just before the Permian and Triassic boundary event – the upward expansion of anoxia in the water column. Palaeogeogr Palaeoclimatol Palaeoecol 229(4):335–344
Kazi TG et al (2009) The correlation of arsenic levels in drinking water with the biological samples of skin disorders. Sci Total Environ 407(3):1019–1026
Kendall C, McDonnell JJ (1998) Isotope tracers in catchment hydrology. Elsevier Science, Amsterdam
Kotaś J, Stasicka Z (2000) Chromium occurrence in the environment and methods of its speciation. Environ Pollut 107(3):263–283
Langard S, Schrauzer GN (1984) Biological and environmental aspects of chromium. Biol Trace Elem Res 6(6):539–539
Li S et al (2009) Water quality in the upper Han River basin, China: the impacts of land use/land cover in riparian buffer zone. J Hazard Mater 165(1–3):317–324
Li HB et al (2012) Lead contamination and source in Shanghai in the past century using dated sediment cores from urban park lakes. Chemosphere 88(10):1161–1169
Liu SM et al (2003) Nutrients in the Changjiang and its tributaries. Biogeochemistry 62(1):1–18
Luo W et al (2010) Ecological risk assessment of arsenic and metals in sediments of coastal areas of northern Bohai and Yellow Seas, China. AMBIO: J Hum Environ 39(6):367–375
MacDonald DD, Ingersoll C, Berger T (2000) Development and evaluation of consensus-based sediment quality guidelines for freshwater ecosystems. Arch Environ Contam Toxicol 39(1):20–31
Mann P et al (1983) Development of pull-apart basins. J Geol 91:529–554
McLennan SM (1989) Rare earth elements in sedimentary rocks; influence of provenance and sedimentary processes. Rev Mineral Geochem 21(1):169–200
Nassef M et al (2006) Determination of some heavy metals in the environment of Sadat industrial city. In: Proceeding of the 2nd environmental physics conference, Cairo University, Egypt, 2006, pp 145–152
Nriagu JO, Nieboer E (1988) Chromium in the natural and human environments. Wiley-Interscience, New York
Pais I, Jones JB (1997) The handbook of trace elements. CRC Press, Boca Raton
Robbins JA, Edgington DN (1975) Determination of recent sedimentation rates in Lake Michigan using Pb-210 and Cs-137. Geochim Cosmochim Acta 39(3):285–304
Rosenmeier MF et al (2004) Recent eutrophication in the Southern Basin of Lake Petén Itzá, Guatemala: human impact on a large tropical lake. Hydrobiologia 511(1):161–172
Salbu B, Steinnes E (1995) Trace elements in natural waters. CRC Press, Boca Raton
Schelske CL et al (1994) Low-background gamma counting: applications for 210 Pb dating of sediments. J Paleolimnol 10(2):115–128

Schroder S, Grotzinger J (2007) Evidence for anoxia at the Ediacaran-Cambrian boundary: the record of redox-sensitive trace elements and rare earth elements in Oman. J Geol Soc 164(1):175

Schüring J (2000) Redox: fundamentals, processes, and applications. Springer, Heidelberg

Sebrell WH et al (1959) Appraisal of nutrition in Haiti. Am J Clin Nutr 7(5):538–584

Sharp Z (2007) Principles of stable isotope geochemistry. Pearson Education, Upper Saddle River

Smith S et al (2011) Anthropogenic sulfur dioxide emissions: 1850–2005. Atmos Chem Phys 11(3):1101–1116

Taylor SR, McLennan SM (1985) The continental crust: its composition and evolution. Blackwell Scientific Publications, Oxford

USEPA (2012a) Basic information – contaminated sediments

USEPA (2012b) Method detection/quantitation and calibration forum on environmental measurements. Office of the Science Advisor, US EPA

WHO (2012) WHO drinking-water quality. WHO

Xu L et al (2011) Sediment records of Sb and Pb stable isotopic ratios in Lake Qinghai. Microchem J 97(1):25–29

Zhu J, Olsen CR (2009) Beryllium-7 atmospheric deposition and sediment inventories in the Neponset River estuary, Massachusetts, USA. J Environ Radioact 100(2):192–197

Chapter 10
Trace Element Composition of Modern Human Bone

Thomas H. Darrah, M. Ellen Campbell, Jennifer J. Prustman-Pfeiffer, Robert J. Poreda, and Robyn E. Hannigan

Abstract The utilization of trace elements in medical, biological, anthropological, and/or geographic provenance studies of human biominerals requires an understanding of trace element incorporation into human bones. While the majority of research has focused on the incorporation of a select group of elements (F, Sr, Pb, K, Mg, Zn, and Na), little information exists on the abundance and incorporation of most geologically significant trace and rare earth elements, specifically those that may have a utility for geographic provenance studies. Because trace element patterns vary according to geological processes, the chemical composition of different geographic areas are often distinguishable. As a result, trace elements may be useful for dietary or forensic geographic provenance studies. However, trace element incorporation into bone depends also upon dietary and metabolic processes in addition to the chemical composition of an individual's geographic domicile. We use ICP-MS analyses for 38 trace elements in cortical bone tissues of 58 patients who underwent hip replacement surgery to investigate trace and rare earth element incorporation into modern human bones. We develop a standard system for the evaluation of trace elements including incorporation coefficients (Ki) and ratios of incorporation (Ri) that allow comparison of the levels of incorporation for various

T.H. Darrah (✉)
Division of Earth and Ocean Sciences, Nicholas School of the Environment, Duke University, 207A Old Chemistry Building, Box 90227, Durham, NC 27708, USA
e-mail: thomas.darrah@duke.edu

M.E. Campbell • R.E. Hannigan
Department of Environmental, Earth, and Ocean Sciences, University of Massachusetts Boston, 100 Morrissey Blvd, Boston, MA 02125-3393, USA

J.J. Prustman-Pfeiffer
Department of Autopsy Pathology, University of Rochester Medical Center, 601 Elmwood Ave, Box 626, Rochester, NY 14642, USA

R.J. Poreda
Department of Earth and Environmental Sciences, University of Rochester, 227 Hutchison Hall, Rochester, NY 14627, USA

P. Censi et al. (eds.), *Medical Geochemistry: Geological Materials and Health*, DOI 10.1007/978-94-007-4372-4_10,

trace elements and develop systematics to determine which elements are controlled by metabolic activity as opposed to dietary or environmental factors. Elements that are not strongly affected by metabolic activity (e.g., oxyanions, REEs, Ba, U, and Th) may be directly linked to geographic location or dietary inputs. We find that trace element incorporation occurs systematically according to predictable physiochemical parameters including ionic radius, valence state, and solubility. Ratios of incorporation (Ri) values for trace element concentrations in bone quantify the relative deviation for each trace element from the theoretical geological standard for average soil composition of the continents (UCC).

Keywords Bone • Trace elements • Element incorporation • Metals and metabolism

10.1 Introduction

Bone tissue is a composite biomineral consisting of an organic collagen matrix and inorganic hydroxyapatite (HAP) ($Ca_{10}(PO_4)_6(OH)_2$). Bone mineralization, including new bone formation and repair, is a dynamic process in which bone minerals are continuously formed and remodeled throughout an individual's life (Boskey and Pleshko Camacho 2007; Glimcher 2006; LeGeros 2002). Several types of bone cells regulate bone mineral formation. Initially, osteoblasts synthesize an organic collagen network or matrix. Following the formation of the collagen matrix, the osteoblasts stimulate calcification of inorganic bone minerals from the body's calcium and phosphate saturated extracellular fluids (Glimcher 2006; Skinner 2005). Under normal homeostatic conditions, extracellular fluids are supersaturated with respect to Ca and inorganic PO_4. In fact, mineralization would occur if not for the presence of nucleation inhibitors (LeGeros and LeGeros 1984). The osteoblasts are thought to induce crystallization by reducing inhibitors of nucleation and creating high surface area bone nano-crystals, bone crystal nuclei, or crystallites (Glimcher 1998, 2006; LeGeros and LeGeros 1984; Roberts et al. 1992).

The formation of bone crystal nuclei, while biologically regulated by osteoblasts, is an inorganic chemical process that requires elemental supersaturation of the bone nuclei to induce inorganic crystal formation (Mann 2001; Pasteris et al. 2008). The chemical composition of the nano-crystals (or bone crystal nuclei) is often distinctly different from mature bone minerals with calcium levels well below stoichiometric Ca to P ratios (Ca:P < 1.67) in these high surface area crystallites (Eppell et al. 2001; Pasteris et al. 2008; Rey et al. 1995a, b; 1990; Roberts et al. 1992; Tong et al. 2003). As bone crystals mature, Ca concentrations approach stoichiometric HAP composition (Ca:P ~ 1.67) depending upon the total amount of total trace element substitution (Glimcher 2006; Rey et al. 1989, 1995a, b, 1990).

Following the deposition of bone minerals, osteoblasts mature into osteocytes. Osteocytes reside within the mineral matrix and control bone minerals activities in concert with other osteocytes and the extracellular fluid. Osteocytes encourage bone deposition by contact with osteoblasts (Glimcher 2006), while osteoclast

cells dissolve and/or resorb existing bone tissue in the process termed remodeling. Following bone tissue resorption, osteoblast cells form new bone minerals on the existing collagen matrix. Research suggests the entire human skeleton is replaced in approximately 5–10 years (Boskey and Pleshko Camacho 2007; Glimcher 2006; Mann 2001).

The majority of bones (including the femoral head) consist of both trabecular and cortical bone tissue. Cortical bone tissue is strong, dense, and compact, and provides structural integrity, while trabecular bone is low density and spongy, and is more metabolically active (Agerbaek et al. 1991; Boonen et al. 1997; Marcus 1991; Tidswell et al. 2008). In humans, cortical bone tissue remodels on the order of decades (25–30 years) (Christoffersson et al. 1984; Gerhardsson et al. 1993; Weisskopf and Myers 2006), while estimates of trabecular bone remodeling rates are 2–3 or 2–5 years based on osteon density (Boonen et al. 1997; Dorsey et al. 2006; Glimcher 1998) and workplace exposure to lead (Christoffersson et al. 1984). Remodeling rates also vary with age, diet, health, and metabolic rate (Boonen et al. 1997).

Bone minerals, specifically bioapatites (HAP), serve as a reservoir of bioavailable minor and trace elements and a store of the body's inorganic elements (P (80% by weight), Ca (99% by weight), Mg (50% by weight), and trace metals up to 99%) (Glimcher 2006; Pasteris et al. 2008; Skinner 2005). Trace element replacement in bone can reach parts per million for specific trace elements such as Na, Mg, K, Sr, and Pb (LeGeros and LeGeros 1984; Skinner 2005). Bone tissue (HAP) does not simply function as a chemical storage reservoir for inorganic elements, but also releases elements to the bloodstream on demand through bone remodeling and interaction with biological fluids (Berglund et al. 2000; Glimcher 2006; Pasteris et al. 2008).

Biological and bone research has predominantly focused on specific inorganic components of bone chemistry, e.g., Ca, Mg, Zn, F, Sr, P, CO_3, and Pb (Ericson et al. 1991; Grynpas 1993; Nielsen 2004; Rey et al. 1995a, b; Spadaro and Gullino 2005; Spadaro et al. 1970). Increased dietary concentrations of Sr (to ~170 ppm) and F (to 1 ppm) increase their concentrations in serum and extracellular fluid and hence increase bone Sr and F levels. Increased Sr and F concentrations stimulate bone mineral formation by enhancing osteocyte metabolism and improving bone mineral density (e.g., Grynpas 1993), while high concentrations of Sr, Pb, and F have deleterious effects on osteocyte activity and bone crystal quality (Carmouche et al. 2005; Grynpas and Marie 1990; Puzas et al. 1992). However, very little is known about the incorporation of other trace elements and rare earth elements (REEs) into human bone tissues.

In order to understand trace element and REE incorporation into human bone tissues, we compare bone compositions to "natural abundance," i.e., the composition of soils from which plants and animals take their nutrients. Rochester, NY (current study area) soil chemistry falls within the normal range for upper continental crust (UCC), a common geological standard with well-established geochemical composition. Figure 10.1 shows the natural abundance of trace and rare earth elements for the theoretical UCC standard (Rudnick and Gao 2003; Taylor and McLennan 1995).

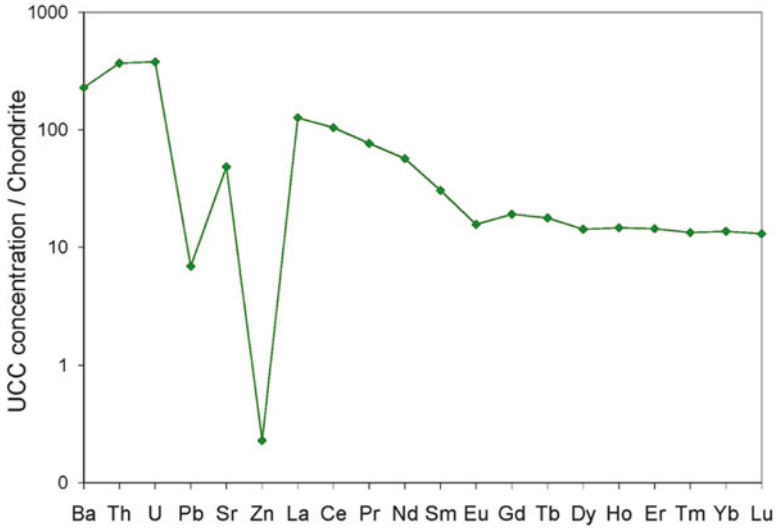

Fig. 10.1 Relative abundance of trace and rare earth elements in upper continental crust (UCC) normalized to chondrite (or bulk earth) composition. Bone elemental composition is normalized to UCC or chondrite to correct for natural variations in absolute elemental abundance

Because bone mineralization is essentially an inorganic process, bone mineral composition reflects the chemical environment of the body at the time of bone mineralization (Beard and Johnson 2000; Goodman et al. 2004; Hoogewerff 2008) in an analogous manner to trace metal substitution in geological samples. For example, the chemical composition of seawater determines the composition of marine carbonates ($CaCO_3$) (Stoll and Schrag 1998; Stoll et al. 1999) with small but predictable variations because of changes in temperature (Lea et al. 2000; Rosenthal et al. 2006; Sosdian et al. 2006) and changes in CO_3 saturation (Lea et al. 2000; Rosenthal et al. 2006). The "environment of mineralization" for biominerals, specifically human bone tissue, differs from purely inorganic geological minerals because bone is a composite mineral formed on an organic collagen matrix. The chemical composition of bone minerals is a complex function of (1) the effects on chemical species during biopurification of food sources, (2) digestive and metabolic processes occurring within the body, (3) exposure to naturally occurring trace elements present in ingested food and drinking water, and (4) anomalous trace element concentrations from specific anthropogenic activities (e.g., inhalation of air particulate matter from power plants and vehicle exhaust, ingestion or injection of medicines and other medical chemicals, and various types of exposure to workplace contaminants) (Darrah 2009; Darrah et al. 2009a).

To establish which trace elemental parameters correlate with geologic and/or dietary inputs and may be applied to forensic geographic provenance, anthropological, paleodietary, and/or modern dietary studies, we require a systematic understanding of the trace element incorporation process from initial utilization of nutrients in local soils, through the food chain to the ultimate incorporation of trace elements into human bone. The current study seeks to determine (1) the degree

of biopurification for geologically relevant trace elements, relating bone chemistry to geographic and/or dietary inputs; (2) a method to evaluate elemental depletion resulting from biopurification to relate bone composition to geological inputs via a set of normalization coefficients; (3) which elements are not affected by variable metabolic and/or biological processing and therefore can be related to geographic and/or dietary inputs; and (4) a method to correct for bone concentration variations related to differences in metabolic rate.

10.2 Methods

10.2.1 Analytical Methods

Bone samples include the femoral heads of 58 patients resident to upstate New York. Bone mineral trace element (e.g., Sr, Ba, Cd, Ag), transition metal (e.g., Ti, Fe, Zn, Cu), rare earth element (REE), and heavy element (Pb, Th, U) composition for cortical bone tissue for each femoral head were established by solution-based inductively coupled plasma-mass spectrometry (ICP-MS) using the conditions presented in Table 10.1 and presented elsewhere (Darrah 2009; Darrah et al. 2009b; Sprauten et al. 2012).

10.2.2 Elemental Ratios

In order to discern changes in element composition for bone, the abundance of each element is normalized to stoichiometric bone Ca to provide a coefficient of incorporation (Ki):

$$\mathrm{Ki(X)} = \frac{\text{molar [X]}}{\text{molar [Ca]}}, \quad \text{where molar [Ca] equals } 39.90\% \tag{10.1}$$

Table 10.1 Solution based ICP-MS instrument operating conditions

Thermo X7 ICP-MS	
Spray chamber	Cyclonic; glass expansion IsoMist temperature 20°C
Cones	Nickel
Plasma gas	15 L/min
Nebulizer gas flow rate	0.95–1.06 L/min optimized daily
Lens voltage	7.2 V
RF power	1,300 W
Dwell time	25 ms
Sweeps	10
Replicates	3
Scan mode	Peak hop

Ki for each element is shown relative to [X]/[Ca] of the designated UCC standard, times a factor of 1,000 to reflect the average range of element incorporation, to provide a ratio of incorporation (Ri_{Ca}):

$$\text{Relative incorporation (w.r.t Ca)} = \text{RiCa} = 1,000^{*}\left[\frac{\text{Ki(X)}_{\text{BONE}}}{([\text{X}]/[\text{Ca}])_{\text{UCC}}}\right], \quad (10.2)$$

where [X] = is the molar concentration of a trace element (e.g., Sr, Ba, Zn, Pb) for bone and UCC, respectively, and [Ca] is the molar concentration of Ca in stoichiometric bone and UCC, respectively.

To identify changes in element composition of bone related to an individual's metabolic rate, the composition of each element is normalized to measured Zn concentrations, a known metabolically controlled element. The [X]/Zn ratio for each element, relative to [X]/Zn of the UCC standard, times a factor of 1,000, provides a ratio of incorporation that corrects for metabolic variation (Ri_{Zn}):

$$\text{Relative incorporation (w.r.t. Zn)} = \text{Ri}_{\text{Zn}} = 1,000^{*}\left[\frac{([\text{X}]/[\text{Zn}])_{\text{Bone}}}{([\text{X}]/[\text{Zn}])_{\text{UCC}}}\right] \quad (10.3)$$

UCC is a widely accepted standard with universal applicability that reflects average continental composition (where most humans live) (Rudnick and Gao 2003; Taylor and McLennan 1995). UCC also accurately reflects the local trace element signature of the local (Rochester) environment. Other normalizations may prove suitable for other geological areas.

10.3 Statistical Treatment of Data

Statistical parameters were calculated using SPSS vs. 20. Statistical comparisons of datasets employed two sample *t*-tests and Mann-Whitney tests, at 95% confidence interval, unless otherwise noted.

10.4 Results and Discussion

10.4.1 Concentrations and Relative Abundance

Table 10.2 shows a statistical summary of mean and median concentrations, standard deviations, and 95% confidence intervals (CI) for (a) transition metals, (b) trace elements and heavy metals, and (c) rare earth elements (REEs) in cortical tissues. Trace element and REE concentrations for each patient and UCC, all normalized to chondrite, are shown in Fig. 10.2a, while in Fig. 10.2b the bone concentrations are normalized to UCC, and Fig. 10.2c plots the concentration distributions for each element.

Table 10.2 Statistical summary of (a) transition metal, (b) trace element and heavy metal, and (c) rare earth element concentrations in cortical tissue samples of 58 patients resident to Rochester

Rochester patients									
(a) Transition metals	Sc (ppb)	Ti (ppb)	V (ppb)	Cr (ppb)	Mn (ppb)	Fe (ppm)	Co (ppb)	Cu (ppm)	Mo (ppb)
Mean	169.85	379.04	18.09	624.60	101.05	102.82	297.07	2.17	22.74
Median	176.20	392.20	16.37	629.00	88.41	108.30	311.70	1.44	19.04
St Dev.	33.47	71.16	8.39	158.90	53.87	19.93	57.69	4.49	20.17
Range	73.6, 249.4	191.8, 513.3	3.7, 50.1	200.4, 992	10.8, 301.9	43.0, 127.4	121.1, 371.5	0, 31.8	7.2, 159.0
95% CI	161.1, 178.7	360.3, 397.8	15.9, 20.3	582.8, 666.4	86.9, 115.2	97.6, 108.1	281.9, 312.2	1.0, 3.3	17.4, 28.0

(b) Trace elements	Al (ppb)	Zn (ppm)	Cd (ppb)	Sr (ppm)	Ba (ppm)	Pb (ppb)	Th (ppb)	U (ppb)
Mean	833.60	124.33	44.60	61.70	2.93	3,558.00	1.67	2.82
Median	709.90	125.60	25.30	58.62	2.60	2,961.00	1.13	1.25
St Dev.	524.80	24.32	103.50	20.00	1.68	2,292.00	1.39	4.03
Range	195.4, 3,469	58.1, 166.0	4.0, 801.8	21.4, 115.9	0.5, 9.2	68.0, 9,530	0.4, 5.4	0, 19.9
95% CI	695.6, 971.6	117.9, 130.7	17.3, 71.8	56.4, 67.0	2.5, 3.4	2,955, 4,160	1.3, 2.0	1.8, 3.9

(c) REEs	La (ppb)	Ce (ppb)	Pr (ppb)	Nd (ppb)	Sm (ppb)	Eu (ppb)	Gd (ppb)	Lu (ppb)
Mean	91.80	193.10	44.20	41.50	11.26	1.02	413.00	4.07
Median	23.90	48.20	12.10	12.20	3.46	0.75	8.00	3.98
St Dev.	336.70	640.50	157.80	154.70	50.55	0.91	930.00	1.06
Range	4.7, 2,559	12.0, 4,786	2.8, 1,198	4.0, 1,183	1.0, 387.5	0.4, 6.9	2.0, 4,875	1.5, 7.5
95% CI	3.3, 180.4	24.7, 361.5	2.7, 85.6	0.8, 82.1	0, 24.5	0.8, 1.3	169, 658	3.8, 4.3

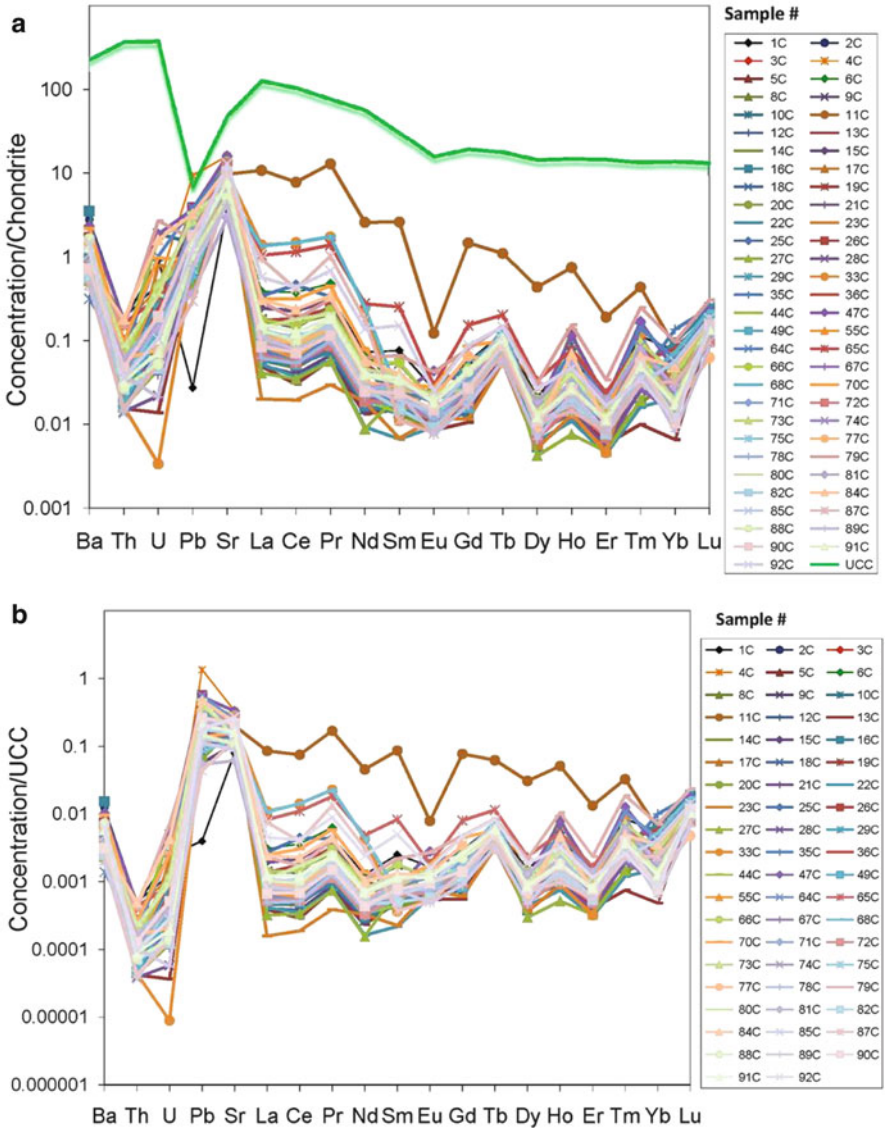

Fig. 10.2 (**a**) Spider plot of trace element (Ba, Th, U, Pb, Sr, Zn) and rare earth element (La through Lu) concentrations in cortical bone samples of 58 patients, and upper continental crust (UCC), normalized to chondrite. All elements except Zn occur at much lower concentrations in human bone than in UCC, although Pb and Sr approach UCC values. (**b**) Spider plot of trace element (Ba, Th, U, Pb, Sr, Zn) and rare earth element (La through Lu) concentrations in cortical bone samples of 58 patients, normalized to upper continental crust (UCC). The pattern of rare earth elements (REEs) normalized to UCC is relatively flat, although REEs are depleted by approximately 2–4 orders of magnitude in bone relative to UCC. Trace elements Ba, Th, and U are significantly depleted, while Pb, and Sr approach UCC levels and Zn occurs in the same range

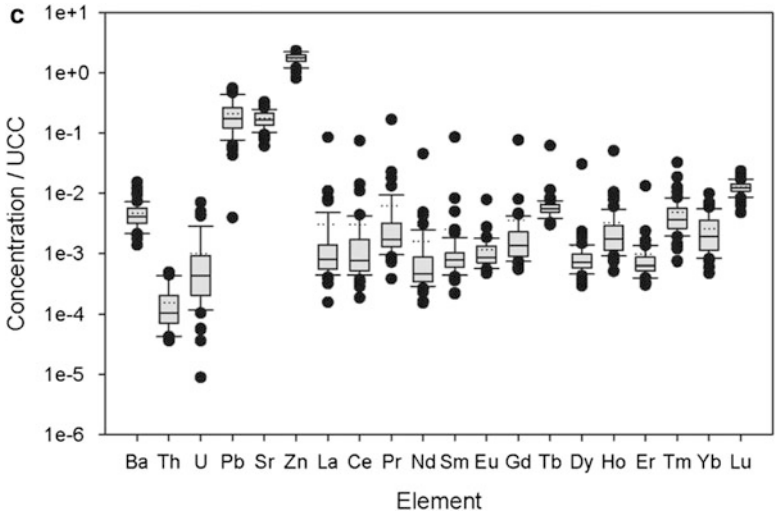

Fig. 10.2 (continued) (**c**) Box plot of trace element (Ba, Th, U, Pb, Sr, Zn) and rare earth element (La through Lu) concentrations in cortical bone samples of 58 patients, normalized to upper continental crust (UCC). For each element, the 50th percentile is shown by a *grey filled box*, with a line indicating the median value. 90th percentiles are indicated by T-bars, while outliers are marked as dots. *Dotted lines* indicate mean values

The majority of trace and rare earth elements are significantly depleted relative to UCC, with the exception of Sr and Pb, which have bone concentrations approaching UCC levels, and Zn, which occurs at approximately equal abundance in UCC and human bone. However, ratios of all trace elements to Ca are much lower in bone than in UCC.

10.4.2 Coefficients of Incorporation to Calcium (Ki)

We calculate molar ratios of each element to calcium (Ki) in the bone tissues of each patient. Table 10.2 shows mean Ki and standard deviation for (a) transition metals and (b) trace elements. Ki values range from 10^{-4} (Zn) to 10^{-8} (REEs), showing the variability of element fractionation during biopurification.

Previous research has determined that changes in metabolic rates can affect the rate of biomineral formation (e.g., Boonen et al. 1997) and trace metal incorporation into bone (Hoogewerff 2008). In order to investigate the effects of metabolism on element incorporation, we plot element ratios to calcium (Ki) against Zn concentration (Figs. 10.3 and 10.4). Because metabolic and homeostatic processes regulate Zn concentration, abundance of Zn in bone does not correlate with dietary intake (Ezzo 1994; Hoogewerff 2008). Instead, Zn concentrations indicate metabolic (Ezzo

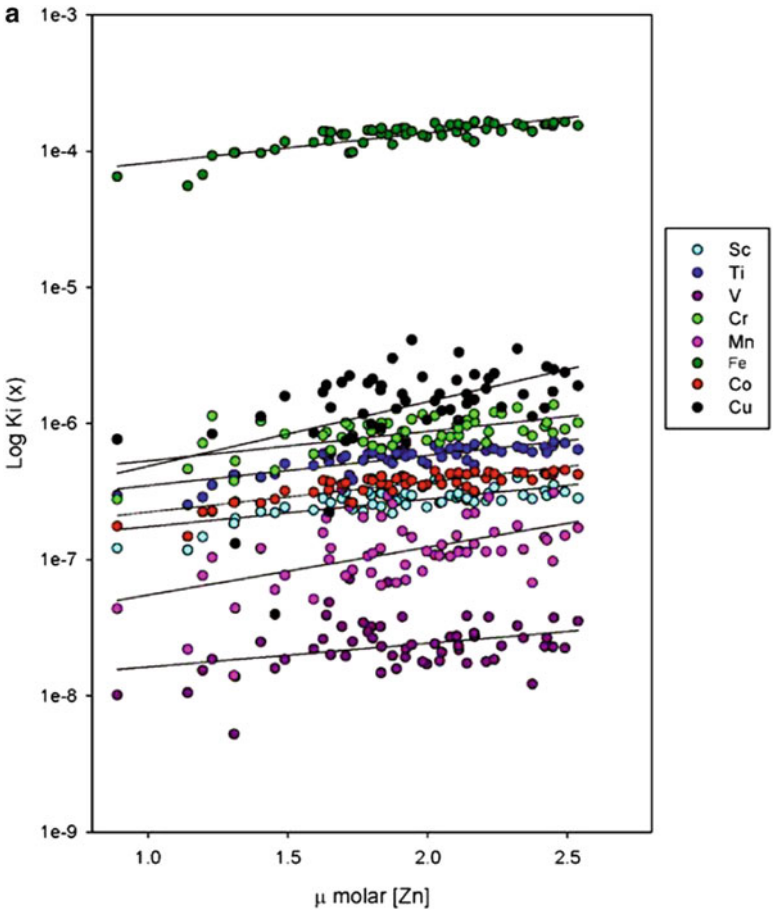

Fig. 10.3 (**a**) Incorporation coefficients (Ki) of transition metals vs. zinc concentration for 58 patients. Ki = [X]/[Ca]. Best fit slopes, intercepts, and r^2 values for linear regressions are listed in Table 10.2. Sc, Ti, Fe, and Co have r^2 values >0.5, are interpreted as indicating a significant degree of metabolic control on incorporation into bone. Cr has an r^2 value of 0.34, which may indicate a lower degree of metabolic regulation. Ki values for these five elements vs. Zn are shown individually in (**b**–**f**)

1994) and bone formation rates (Jamieson et al. 2006). Zn is the most abundant bio-essential trace metal in mammals (Ezzo 1994) and is metabolically regulated as a metalloenzyme cofactor in bone formation, cell formation, and other biological processes (Ezzo 1994; Hoogewerff 2008; Jamieson et al. 2006).

Trace element Ki values are plotted vs. Zn (Fig. 10.4a) and vs. Lu (Fig. 10.4b). Pearson correlations between trace element abundance and Zn concentrations estimate the degree of metabolic control for each element. Ratios for five transition metals (Sc, Ti, Fe, Co, and Cr) have r^2 values that indicate a correlation, with relative

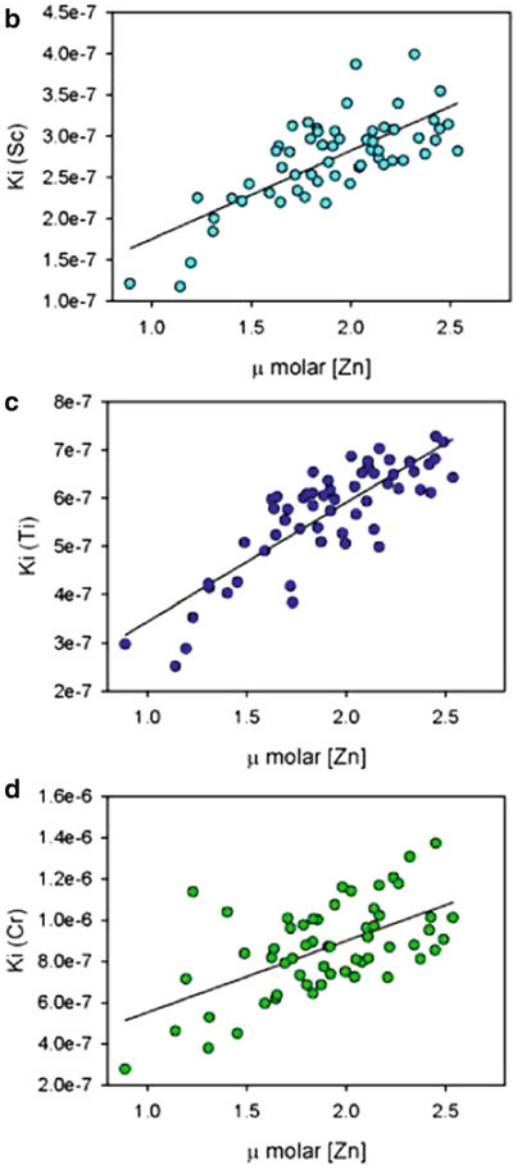

Fig. 10.3 (continued)

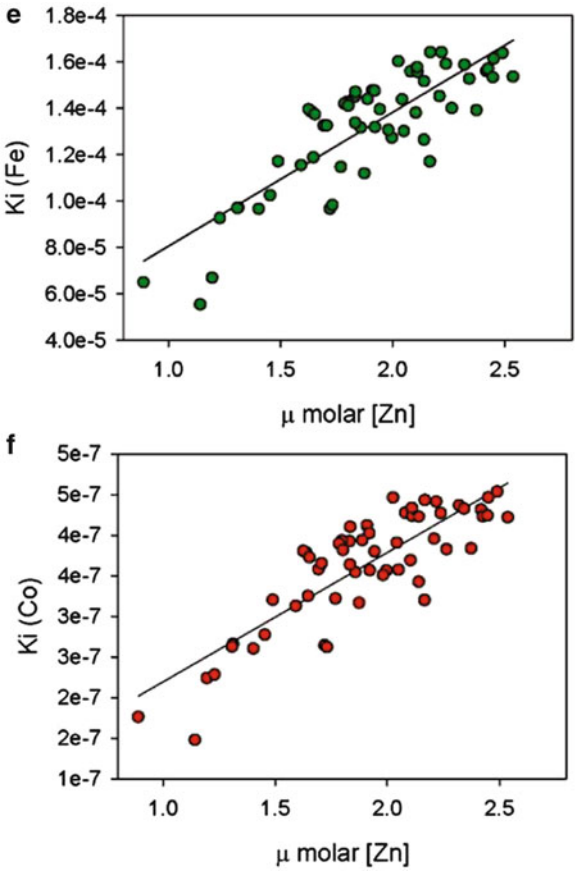

Fig. 10.3 (continued)

abundance increasing with increasing [Zn]. This positive correlation suggests that metabolic processes affect the degree of incorporation for these transition metals, whereas r^2 values of <0.25 for V, Mn, and Cu indicate an absence or very low degree of metabolic regulation. Among other trace elements and heavy metals (Fig. 10.4a), only Sr correlates with Zn concentration ($r^2 = 0.41$), indicating some degree of metabolic control on Sr concentration. Ratios for other trace elements have very low r^2 values (<0.05) that indicate no significant metabolic control. Because Lu has the highest field strength among REEs, it may act as a potential proxy for total bone mineral content (i.e., Lu most strongly prefers solid crystal phase among REEs) (Hirano and Suzuki 1996). Pearson correlations for all transition, trace, and heavy metals yield r^2 values <0.05, indicating a complete lack of covariance to Lu and no correlation to bone mineral content (Figs. 10.4 and 10.6; Table 10.2).

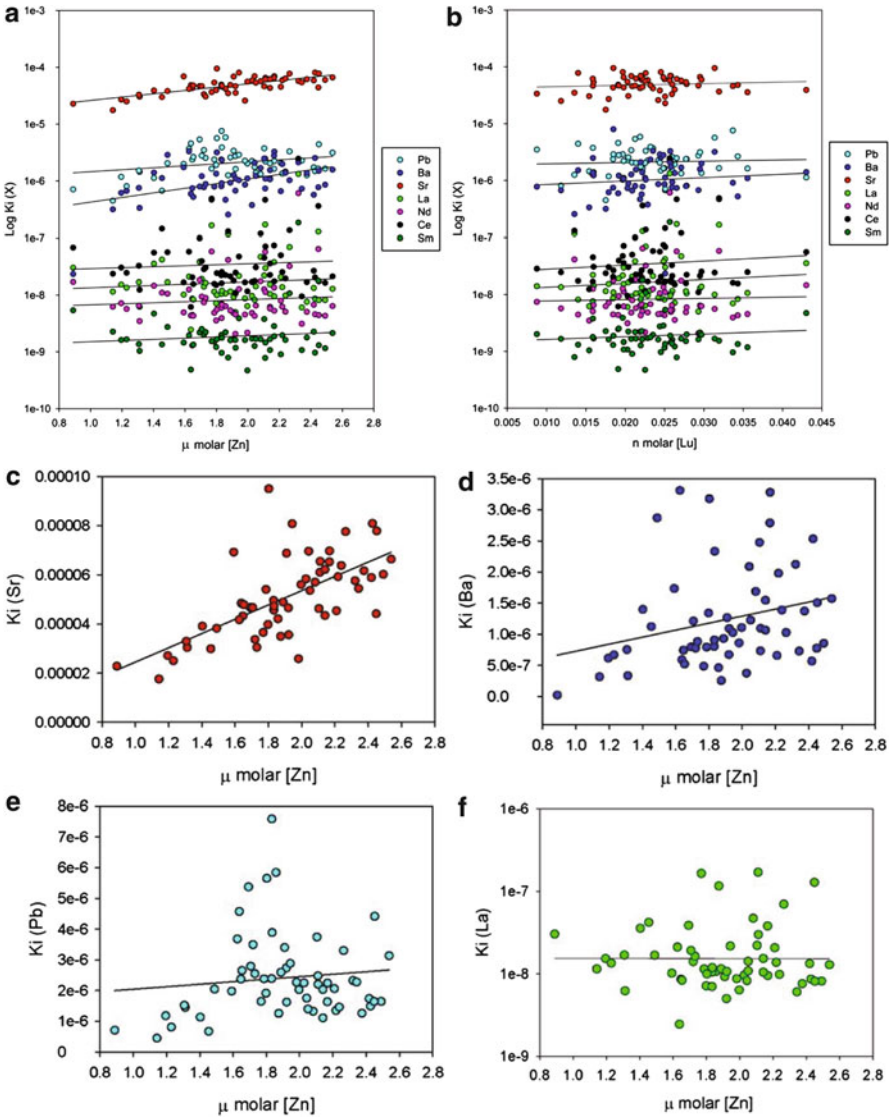

Fig. 10.4 (**a**, **b**) Incorporation coefficients (Ki) for trace elements and REEs for 58 patients vs. (**a**) metabolically controlled Zn concentration, [Zn], and (**b**) the REE lutetium, [Lu]. Ki = [X]/[Ca]. Best fit slope, intercept, and r^2 values are listed in Table 10.2. Only Sr, with an r^2 value of 0.41, is indicated to be metabolically regulated. (**c**–**f**) Incorporation coefficients (Ki) vs. metabolically controlled Zn concentration for 58 patients. (**c**) Sr ($r^2 = 0.41$); (**d**) Pb ($r^2 = 0.01$); (**e**) Ba ($r^2 = 0.04$); and (**f**) La ($r^2 = 0.005$). Ki = [X]/[Ca]. Best fit slope and intercept are listed in Table 10.2. Strontium abundance correlates with Zn, indicating metabolic regulation. Ba, Pb and La have low correlation with Zn, indicating a lack of metabolic regulation and suggesting that their variability can be attributed to dietary and/or environmental inputs

10.4.3 Ratios of Incorporation (Ri)

We calculate Ri_{Ca} according to Eq. 10.2. In order to correct for potential metabolic influence on element concentrations, Ri values are also calculated as ratios to Zn (Ri_{Zn}), according to Eq. 10.3. Mean Ri values, standard deviations, and 95% confidence intervals for Sr, Ba, Pb, La, Ce, Nd, Sm, and Zn are shown in Table 10.3 for (a) Ri_{Ca} cortical bone tissues and (b) Ri_{Zn} cortical bone tissues.

Figure 10.5 shows distributions of Ri_{Ca} for several trace and rare earth elements in cortical bone samples. Ratios of incorporation decrease with increasing ionic radius for elements of the same oxidation state (Fig. 10.5). Figure 10.6a–d shows Ri_{Ca} values for Pb, Ba, Zn, and La vs. Ri_{Ca} (Sr). While Sr abundance covaries with Zn indicating metabolic regulation, Pb, Ba, and La abundance do not. Ri_{Ca} values are compared to molar [Lu], with Pb, Ba, Zn, and Sr plotted as examples (Fig. 10.7a–d). Lu is the highest field strength REE and is used as a proxy for total mineral content. Trace elements (except for other REEs) do not covary with [Lu], indicating a lack of correlation for specific trace elements with total mineral content. Ri_{Zn} values for Pb, Ba, and La are plotted against Ri_{Zn} (Sr) in Fig. 10.8a–d. Corrected for metabolic effects, comparison of Ri_{Zn} values shows no correlations with Sr or consistent incorporation related to metabolic rate except for extreme La and Ba in some OA patients that may relate to bone disease and/or diet.

We compare trace element compositions of bone from 58 Rochester residents to the composition of upper continental crust (UCC), to find relations that could be used for geographical provenance studies. Before geographic domain can be assigned to humans based on their bone compositions, we need to understand how trace element abundances are altered from their soil sources through the food chain and in the human body.

Upper continental crust (UCC) serves as a proxy for "natural abundance" and also characterizes soils in the greater Rochester area. We find significant differences between bone concentrations and UCC, with most elements strongly depleted in bone. Trace element depletion from UCC to human bone is achieved by a combination of processes: (1) biopurification in the food chain: as nutrients progress through the food chain, most elements become progressively depleted, while bio-essential nutrients are concentrated, e.g., Ca and Zn (Balter 2004; Burton and Price 1999; Burton et al. 1999; Ezzo 1994), and (2) human biopurification *in vivo*: physiological processes (e.g., digestion, metabolism) that result in preferential biological selection for certain elements during digestion and ionic transport across biological membranes (Ezzo 1994; Nielsen 2004). For example, as elements are transported across the digestive membrane, Ca is preferred to Sr, and Sr is preferred to Ba, i.e., Ca/Sr and Sr/Ba increase (Nielsen 2004).

In order to relate bones to geographical areas, we need to identify systematic variations between bone compositions and dietary (geological) sources. We find that element abundances in bone are not simply a function of the ratio of total inorganic bone mineral content relative to organic collagen matrix. None of the trace element

Table 10.3 Statistical summaries of molar ratios to calcium for the 58 Rochester resident patients, where mean molar ratio to calcium equals the estimated incorporation coefficient (Ki), for (a) transition metals, (b) trace elements, and (c) rare earth elements (REEs)

(a) Transition metals	Sc	Ti	V	Cr	Mn	Fe	Co	Cu
Estimated Ki	3.80E−07	7.95E−07	3.57E−08	1.21E−06	1.85E−07	1.85E−04	5.06E−07	3.42E−06
Std dev.	7.48E−08	1.49E−07	1.65E−08	3.07E−07	9.85E−08	3.58E−05	9.83E−08	7.10E−06
Best fit slope	1.07E−07	2.47E−07	6.17E−09	3.46E−07	7.41E−08	1.60E−07	1.60E−07	1.07E−06
Best fit intercept	6.88E−08	9.64E−08	1.38E−08	2.06E−07	−4.24E−09	5.99E−08	5.99E−08	−4.35E−09
r^2	0.550	0.690	0.070	0.343	0.224	0.710	0.706	0.223
(b) Trace elements	Zn	Ba	Pb	Sr	La	Nd	Sm	Ce
Estimated Ki	1.91E−04	2.14E−06	1.72E−06	7.07E−05	6.64E−08	2.89E−08	7.52E−09	1.38E−07
Std dev.	3.73E−05	1.23E−06	1.11E−06	2.29E−05	2.43E−07	1.08E−07	3.38E−08	4.59E−07
Best fit slope		1.05E−11	6.36E−12	4.56E−10	1.16E−12	−4.53E−08	1.61E−13	2.23E−12
Best fit intercept		4.10E−08	1.63E−06	−5.28E−06	−9.75E−08	5.35E−13	−1.47E−08	−1.79E−07
r^2		0.043	0.012	0.410	0.023	0.026	0.026	0.027

Best fit slope, intercept, and r^2 values relate to linear regressions for Ki(X) plotted against metabolically regulated zinc concentration (Figs. 10.4 and 4.4)

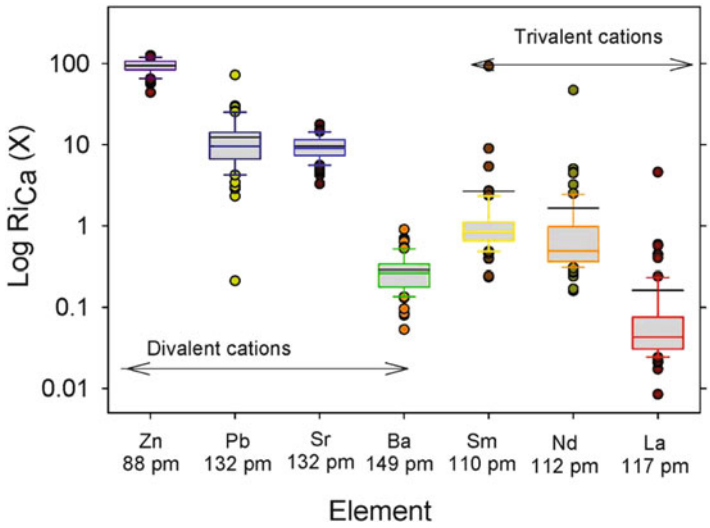

Fig. 10.5 Ratios of incorporation to calcium (Ri_{Ca}) of trace and rare earth elements in cortical bone samples. Ionic radius increases from left to right (Zn to Ba). Ratios of incorporation decrease with increasing ionic radius with elements of the same oxidation state. Molar ratios to calcium decrease in comparison to UCC as ionic radius increases. Note that atomic number increases from La to Nd to Sm, but ionic radius decreases because of La contraction

concentrations (except other REEs) had significant correlation with [Lu], which we use as a proxy for total inorganic bone mineral content because of its high field strength. This indicates that there are additional controls on the incorporation of trace elements and transition metals such as dietary or biological processing. Our results for trace element concentrations in bone indicate significant effects of biopurification processes and metabolic regulation on bone chemistry. For elements that are biopurified systematically according to physiochemical parameters and for which this process can be quantified (e.g., by Ri_{Ca} values), bone chemistry may be correlated to the chemical composition of an individual's geographic provenance. However, metabolic regulation *in vivo* also affects some trace elements, which complicates their relation between inputs and bone.

10.4.4 Metabolic Regulation of Trace Elements and Transition Metals

Metabolic processes, rather than dietary inputs, control Zn concentration in human bone (Ezzo 1994; Hoogewerff 2008; Jamieson et al. 2006). Using coefficients of incorporation (Ki = [X]/[Ca]) for transition metals and trace elements, we find that Sr and the transition metals Sc, Ti, Co, Fe, and Cr correlate with [Zn], indicating

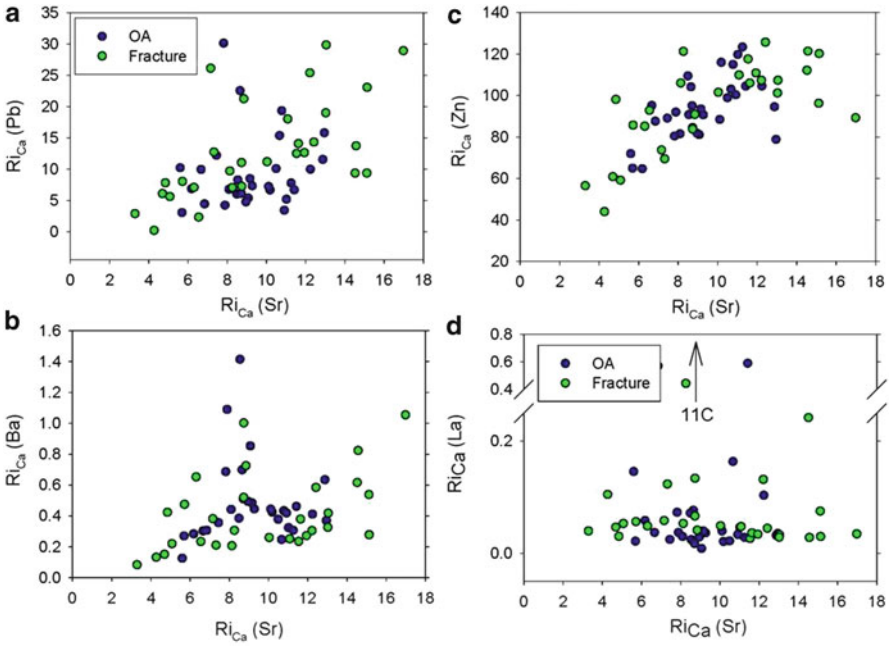

Fig. 10.6 Ri_{Ca} values for cortical tissue samples of 58 patients. (**a**) Pb vs. Sr; (**b**) Ba vs. Sr; (**c**) Zn vs. Sr; and (**d**) La vs. Sr. Ri_{Ca} = molecular ratios to Ca normalized to UCC × 1,000. Pb and Zn abundance appear to co-vary with Sr. Ba concentrations have two trends. One trend shows Ba co-varies with Sr, while the second shows an relative increase in Ba w.r.t. Sr. Several osteoarthritic individuals have increased REE concentration (La) relative to Sr. REE concentrations in bone do not co-vary with Sr or other minor element concentrations

metabolic regulation of these elements (Figs. 10.3 and 10.4). Ba, Pb, REEs, and the transition metals V and Mn do not correlate with Zn, and we conclude that they are not metabolically regulated.

The correlation of Ki (Sr) with [Zn] is much lower than the slopes for correlated transition metals, indicating that Sr concentrations in bone are not as strongly influenced by variations in individuals' metabolic rates. This is consistent with previous research showing that Sr is a useful indicator of paleodiet (Ezzo 1994) and geographical provenance (Burton et al. 2003) and with observations of increased Sr concentration in bone tissues of both rats and human patients with increased dietary exposure to Sr (Dahl et al. 2001; Grynpas et al. 1996).

Transition metals have long and well-established biological and metabolic functions related to their diverse coordination chemistries. The roles of hemoglobin Fe in oxygen transport (e.g., Eguchi and Saltman 1984), Zn in bone and cell formation (Ezzo 1994; Jamieson et al. 2006) and insulin regulation (Bentley et al. 1976), Cr for cholesterol regulation (e.g., Preston et al. 1976), and Co complexes in vitamin B12 (e.g., Hush and Woolsey 1974) are a few examples of the roles that

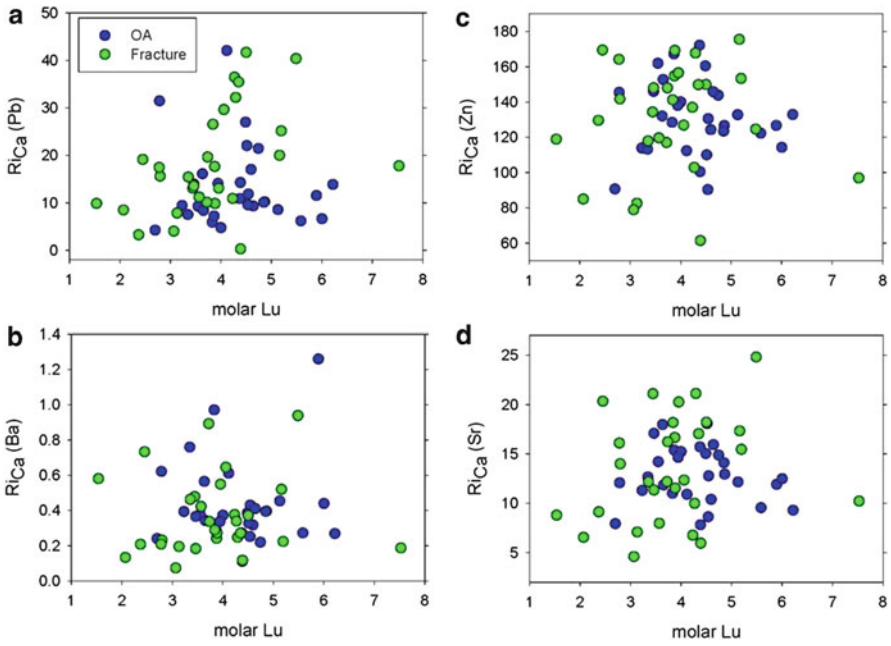

Fig. 10.7 Ri_{Ca} values for cortical tissue. (**a**) RiCa Pb vs. Lu; (**b**) RiCa Ba vs. Lu; (**c**) RiCa Zn vs. Lu; and (**d**) RiCa Sr vs. Lu. Ri_{Ca} = molecular ratios to Ca normalized to UCC × 1,000. Elemental concentrations do not appear to co-vary with Lu concentration indicating that abundance of these elements in bone is not expected to be a simple function of bone mineral content

transition metals play in biological and metabolic processes. These known processes may account for the correlations with metabolism (Zn) that we observe for Fe, Cr, and Co. These metals and Sc and Ti, which correlate with Zn, may also be selected for during bone cellular processes, as for Zn.

Our results are consistent with previous research suggesting metabolic control of most transition metal concentrations in human bones (Hoogewerff 2008). The r^2 values for Ki (V) and Ki (Mn) with [Zn] are low, indicating an absence or very low degree of metabolic control. The indicated lack of metabolic control for V is consistent with previous research showing that bone V concentrations increase in rats treated with V-based drugs (Facchini et al. 2006). The lack of metabolic regulation of V and Mn may result from their complex coordination chemistries. Both elements may occur as oxyanions (e.g., MnO_5^{3-} or VO_4^{3-}) as opposed to other transition metals that occur in cationic form.

V and Mn, which do not appear to be metabolically regulated, may be useful for geographical provenance or paleodietary studies relating bone compositions to dietary inputs. Metabolic regulation of the other transition metals suggests that they will not correlate to geological or dietary inputs without a method of correcting for

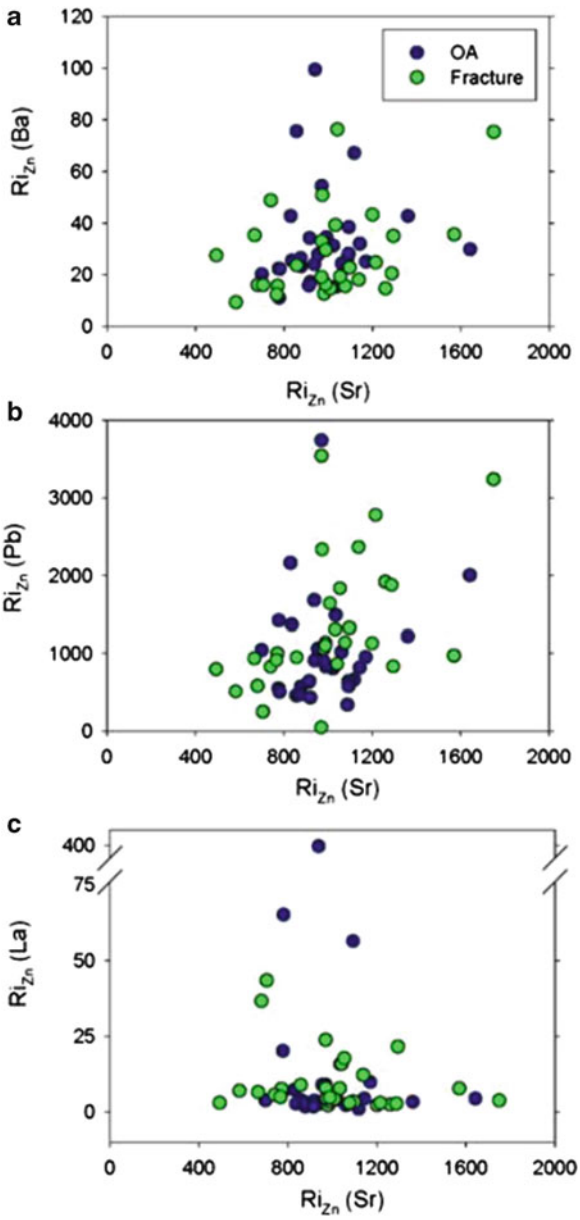

Fig. 10.8 Ratios of incorporation to zinc (Ri_{Zn}) values for cortical tissue samples of 58 patients. (**a**) Ba vs. Sr; (**b**) Pb vs. Sr; and (**c**) La vs. Sr. Ri_{Zn} = molecular ratios to Zn normalized to UCC × 1,000 (Eq. 10.3). Corrected for metabolic effects, Ba, Pb, and La show no correlation with Sr, indicating that concentrations of these elements are not controlled by biological processes, and may reflect dietary and anthropogenic inputs, or disease-related effects

variation between individual metabolic rates. We apply a correction for metabolic rate by normalizing to Zn (Ri_{Zn}, Eq. 10.3). These Ri_{Zn} values act as coefficients for metabolically regulated incorporation of Sr and the transition metals Sc, Ti, Co, Fe, and Cr.

Table 10.4 Estimated ratio of incorporation (Ri) values for each element to calcium (Ri(Ca)) normalized to UCC × 1,000, and zinc (Ri(Zn)), normalized to UCC × 1,000, where: (a) (Ri(Ca)) in cortical bone tissue; (b) (Ri(Ca)) in trabecular bone tissue; (c) (Ri(Zn)) in cortical bone tissue; and (d) (Ri(Zn)) in trabecular bone tissue

(a) RiCa cortical	Zn	Sr	Pb	Ba	La	Nd	Sm
Mean	131.43	13.23	15.70	0.40	0.23	2.23	3.49
Std dev.	25.71	4.29	10.12	0.23	0.84	8.31	15.68
95% CI	124.7, 138.2	12.1, 14.4	13.0, 18.4	0.34, 0.46	0.076, 0.165	0.774, 1.526	0.99, 1.88
X/Ca in UCC	1.45E−03	5.35E−03	1.10E−04	5.36E−03	2.89E−04	1.30E−05	2.15E−06

(b) RiCa trabecular	Zn	Sr	Pb	Ba	La	Nd
Mean	99.20	8.56	11.10	0.46	0.44	6.93
Std dev.	27.68	3.70	9.80	0.34	1.63	24.44
95% CI	91.9, 106.5	7.6, 9.5	8.5, 13.7	0.37, 0.56	0.12, 0.34	1.86, 5.76
X/Ca in UCC	1.45E−03	5.35E−03	1.10E−04	5.36E−03	2.89E−04	1.30E−05

(c) RiZn cortical	Sr	Pb	Ba	La	Ce	Nd
Mean	100.07	4.86	0.14	0.29	1.40	0.06
Std dev.	25.18	2.87	0.45	0.86	0.83	0.21
95% CI	93.5, 106.7	4.1, 5.6	0.02, 0.25	0.07, 0.52	0.64, 1.45	0.008, 0.117
X/Zn in UCC	3.68	0.08	3.69	0.20	0.42	0.42
(d) RiZn trabecular	Sr	Pb	Ba	La	Ce	Nd
Mean	96.24	5.27	10.66	11.66	0.97	0.31
Std dev.	29.34	4.12	13.36	11.10	2.36	0.50
95% CI	80.0, 94.67	4.2, 6.3	6.2, 9.3	0.12, 0.33	0.23, 0.87	0.12, 0.33
X/Zn in UCC	3.68	0.08	3.69	0.2	0.42	0.42

10.5 Biopurification of Non-metabolic Elements

10.5.1 Trace Elements and Transition Metals

Biopurification processes in humans occur through biologically selective membranes, e.g., the digestive membrane. Gastrointestinal processes select Ca over Sr during diffusion across digestive membranes into the blood (Nielsen 2004). The digestive membrane concentrates Zn into the blood, and metalloprotenetic selection concentrates Zn into osteoblast cells during bone formation (Ezzo 1994). Biopurification causes Ca/Sr to increase from soil → plants → herbivores → carnivores (Balter 2004; Burton et al. 1999, 2003; Ezzo 1994). By comparing the compositions of human bone to the NIST 1486 SRM, which is composed of cow bone meal, we find that elemental ratios of Sr/Ca and Ba/Ca are more than an order of magnitude higher in cow bone. While it is unclear if this relates to herbivorous dietary inputs or is the result of cows' ruminant digestion and metabolism, it clearly

reveals differences in trace element incorporation between species at different levels of the food chain.

Dietary preferences will affect nutrient inputs and bone trace element concentrations. This study does not attempt to correlate dietary preferences (e.g., vegetarian and/or meat selection) with bone trace element concentrations. However, for Rochester residents, Ri_{Ca} values for alkaline earths, REEs, and most transition metals appear to occur in relatively narrow ranges (Table 10.3), which suggests biological regulation of trace element incorporation into bone.

Little is known about how biopurification alters the relative concentrations of trace elements other than Sr, Ba, and Zn. Our ratios of elemental incorporation (Ri_{Ca}) evaluate the degree of fractionation during the biopurification processes for each trace element. Assuming that biopurification works as a simple box model with UCC nutrient inputs, biopurification processes, and bone composition outputs, Ri_{Ca} for each trace element is the coefficient of biopurification (depletion) with respect to a UCC soil source. This coefficient acts as a correction factor to relate bone concentrations to dietary or geologic inputs, at least for elements that metabolic activity does not significantly alter.

We find that Ri_{Ca} values decrease with increasing ionic radius for elements of equal oxidation state, i.e., trace elements (2^+) and REEs (3^+) (Fig. 10.5). This indicates that trace element incorporation responds to the physiochemical parameters (ionic radius, charge) of each element. HREEs (e.g., Lu, Dy) are preferentially transported across the digestive membrane and during other biological processes because of increased solubility of HREEs relative to LREEs (e.g., La, Ce, Pr) (Hirano and Suzuki 1996). Our results are consistent with this and indicate that these selective processes affect incorporation of trace elements into bone.

10.5.2 Rare Earth Elements

Biopurification processes significantly reduce the incorporation of REEs in human bones relative to Ca (Figs. 10.2b and 10.5). REEs are more depleted relative to UCC in bones than other trace elements with limited or no biological functions (Sr, Ba). Fractionation between REEs incorporated into bone is minimal, based on the approximately flat pattern of bone concentrations normalized to UCC (Fig. 10.2b). Small variations between the bone tissue samples and UCC include (1) an enrichment of about 12% in the heavy REE Lu; and (2) a "zigzag" pattern (as opposed to a smooth pattern), for heavy REEs (HREE).

1. The Lu enrichment may result from increased solubility of REEs with increasing atomic number in biological fluids (e.g., Hirano and Suzuki 1996), allowing Lu to be easily transported across biologically selective membranes such as the gastrointestinal membranes. Another possibility is that the field strength, defined as the charge to ion radius ratio (Z/R_{ion}), increases with atomic number or decreasing ionic radius. As a result, Lu may incorporate into the bone crystal with

a stronger bond than La (i.e., higher partition coefficient between mineral and fluid (Kd)) resulting in preferential incorporation of HREEs compared to light REEs (LREEs) into bone. Both possibilities are consistent with the increase in Ri_{Ca} values with increasing atomic number throughout the REE suite (Fig. 10.5).
2. The zigzag pattern in REE concentration normalized to UCC may reflect a systematic inaccuracy in the quantification of NIST 1486 SRM for the low-concentration HREEs or analytical difficulties in measuring REEs at bone concentrations. Future work may explore alternative analytical methods to analyze REE patterns such as oxygen dynamic reaction cells and/or column chemistry to remove major elements prior to analysis of REEs.

Despite low concentrations of REEs in bone relative to Rochester UCC soils, REE concentrations may provide the best fingerprint for geographical provenance because they have minimal metabolic regulation, based on a lack of correlation to Zn concentrations. Their trace element patterns in bone may accurately record the relative concentrations (e.g., La/Dy, Lu/Dy, Ba/Dy) of geological or dietary inputs.

10.6 Conclusion

We use trace element concentrations in the bone tissues of 58 Rochester residents to identify differences between human bones and the composition of their geological source of nutrients (UCC). We find that element abundances in bone are not simply a function of the ratio of total inorganic bone mineral content relative to organic collagen matrix. Our results for trace element concentrations in bone indicate significant effects of biopurification processes and metabolic regulation.

Using coefficients of incorporation ($Ki = [X]/[Ca]$) for transition metals and trace elements, we find that Sr and the transition metals Sc, Ti, Co, Fe, and Cr correlate with metabolically regulated [Zn]. The concentration of these elements varies as a result of biologically and metabolic processes and does not preserve geological or dietary input ratios in bone. A correction factor, normalized to Zn, attempts to correct for variations in an individual's metabolic rate to determine elemental variations from UCC. While Sr is metabolically regulated, bone Sr concentrations are not as greatly affected by variations in individuals' metabolic rates as the transition metals. This is consistent with previous research showing that Sr is a useful indicator of paleodiet and geographical provenance.

Ba, Pb, Al, REEs, and the transition metals V and Mn do not correlate with [Zn], and we conclude that they are not metabolically regulated. These elements may be useful for geographic provenance and paleodietary studies, even if their total abundance is significantly altered with respect to UCC. Even non-metabolically regulated element compositions of bone are not simply a function of environmental or dietary intakes but rather significantly altered by biopurification processes. After dietary intake, metabolic activity controls incorporation along with the rate of diffusion of ionic species across biological selective membranes. The use of

trace elements for geographic provenance requires a correction for the relative incorporation of each trace element compared to the theoretical UCC standard. We find that physiochemical properties including ionic radius and the charge to ionic radius ratio (Z/R_{ion}) control trace element incorporation. There is a clear association between decreasing incorporation of trace elements and increasing ionic radius for elements of the same valence state.

References

Agerbaek MO, Eriksen EF, Kragstrup J, Mosekilde L, Melsen F (1991) A reconstruction of the remodeling cycle in normal human cortical iliac bone. Bone Miner 12:101–112

Balter V (2004) Allometric constraints on Sr/Ca and Ba/Ca partitioning in terrestrial mammalian trophic chains. Oecologia 139:83–88

Beard BL, Johnson CM (2000) Strontium isotope composition of skeletal material can determine the birth place and geographic mobility of humans and animals. J Forensic Sci 45:1049–1061

Bentley G, Dodson E, Dodson G, Hodgkin D, Mercola D (1976) Structure of insulin in 4-zinc insulin. Nature 261:166–168

Berglund M, Akesson A, Bjellerup P, Vahter M (2000) Metal-bone interactions. Toxicol Lett 112–113:219–225

Bergquist BA, Blum JD (2007) Mass-dependent and -independent fractionation of Hg isotopes by photoreduction in aquatic systems. Science 318:417–420

Blum JD, Bergquist BA (2007) Reporting of variations in the natural isotopic composition of mercury. Anal Bioanal Chem 388:353–359

Boonen S, Aerssens J, Dequeker J, Nicholson P, Cheng XG, Lowet G, Verbeke G, Bouillon R (1997) Age-associated decline in human femoral neck cortical and trabecular content of insulin-like growth factor I: potential implications for age-related (type II) osteoporotic fracture occurrence. Calcif Tissue Int 61:173–178

Boskey A, Pleshko Camacho N (2007) FT-IR imaging of native and tissue-engineered bone and cartilage. Biomaterials 28:2465–2478

Burton JH, Price TD (1999) Evaluation of bone strontium as a measure of seafood consumption. Int J Osteoarchaeol 9:233–236

Burton JH, Price TD, Middleton WD (1999) Correlation of bone Ba/Ca and Sr/Ca due to biological purification of calcium. J Archaeol Sci 26:609–616

Burton JH, Price TD, Cahue L, Wright LE (2003) The use of barium and strontium abundances in human skeletal tissues to determine their geographic origins. Int J Osteoarchaeol 13:88–95

Carmouche JJ, Puzas JE, Zhang X, Tiyapatanaputi P, Cory-Slechta DA, Gelein R, Zuscik M, Rosier RN, Boyce BF, O'Keefe RJ, Schwarz EM (2005) Lead exposure inhibits fracture healing and is associated with increased chondrogenesis, delay in cartilage mineralization, and a decrease in osteoprogenitor frequency. Environ Health Perspect 113:749–755

Christoffersson JO, Schutz A, Ahlgren L, Haeger-Aronsen B, Mattsson S, Skerfving S (1984) Lead in finger-bone analysed in vivo in active and retired lead workers. Am J Ind Med 6:447–457

Dahl SG, Allain P, Marie PJ, Mauras Y, Boivin G, Ammann P, Tsouderos Y, Delmas PD, Christiansen C (2001) Incorporation and distribution of strontium in bone. Bone 28:446–453

Darrah TH (2009) Inorganic trace element composition of modern human bones: relation to bone pathology and geographical provenance, Earth and Environmental Sciences. University of Rochester, Rochester, p 183

Darrah T, Poreda R, Campbel E, Prutsman-Pfieffer J, Hannigan R (2009a) The incorporation of Gd in human bone from medical contrast imaging. Geochim Cosmochim Acta 73:A262–A262

Darrah TH, Prutsman-Pfeiffer JJ, Poreda RJ, Campbell ME, Hauschka PV, Hannigan RE (2009b) Incorporation of excess gadolinium into human bone from medical contrast agents. Metallomics 1:479–488

Dorsey CD, Lee BK, Bolla KI, Weaver VM, Lee SS, Lee GS, Todd AC, Shi WP, Schwartz BS (2006) Comparison of patella lead with blood lead and tibia lead and their associations with neurobehavioral test scores. J Occup Environ Med 48:489–496

Eguchi LA, Saltman P (1984) The aerobic reduction of Fe(III) complexes by hemoglobin and myoglobin. J Biol Chem 259:4337–4338

Eppell SJ, Tong WD, Katz JL, Kuhn L, Glimcher MJ (2001) Shape and size of isolated bone mineralites measured using atomic force microscopy. J Orthop Res 19:1027–1034

Ericson JE, Smith DR, Flegal AR (1991) Skeletal concentrations of lead, cadmium, zinc, and silver in ancient North American Pecos Indians. Environ Health Perspect 93:217–223

Ezzo JA (1994) Zinc as a paleodietary Indicator: an issue of theoretical validity in bone-chemistry analysis. Am Antiq 59:606–621

Facchini DM, Yuen VG, Battell ML, McNeill JH, Grynpas MD (2006) The effects of vanadium treatment on bone in diabetic and non-diabetic rats. Bone 38:368–377

Gerhardsson L, Attewell R, Chettle DR, Englyst V, Lundstrom NG, Nordberg GF, Nyhlin H, Scott MC, Todd AC (1993) In-vivo measurements of lead in bone in long-term exposed lead smelter workers. Arch Environ Health 48:147–156

Ghosh S, Xu YF, Humayun M, Odom L (2008) Mass-independent fractionation of mercury isotopes in the environment. Geochem Geophys Geosyst 9:Q03004

Glimcher MJ (1998) The nature of the mineral phase in bone: biological and clinical implications. In: Avioli LV, Krane SM (eds) Metabolic bone disease and clinically related disorders, 3rd edn. Academic, San Diego

Glimcher MJ (2006) Bone: nature of the calcium phosphate crystals and cellular, structural, and physical chemical mechanisms in their formation. In: Sahai N, Schoonen MAA (eds) Medical mineralogy and geochemistry, Reviews in mineralogy and geochemistry. Mineralogical Society of America, Washington, DC, pp 223–282

Goodman A, Jones J, Reid J, Mack M, Blakey M, Amarasiriwardena D, Burton P, Coleman D (2004) Isotopic and elemental chemistry of teeth: implications for places of birth, forced migration patterns, nutritional status, and pollution. In: Blakey ML, Rankin-Hill L (eds) The New York African burial ground skeletal biology final report. Howard University, Washington, DC, pp 216–265

Grynpas MD (1993) Age and disease-related changes in the mineral of bone. Calcif Tissue Int 53:S57–S64

Grynpas MD, Marie PJ (1990) Effects of low-doses of strontium on bone quality and quantity in rats. Bone 11:313–319

Grynpas MD, Hamilton E, Cheung R, Tsouderos Y, Deloffre P, Hott M, Marie PJ (1996) Strontium increases vertebral bone volume in rats at a low dose that does not induce detectable mineralization defect. Bone 18:253–259

Hirano S, Suzuki KT (1996) Exposure, metabolism, and toxicity of rare earths and related compounds. Environ Health Perspect 104:85–95

Hoogewerff J (2008) Introduction to the use and limits of elemental and isotopic analysis for the forensic provenancing of unidentified human remains. In: Proceedings of the American Academy of forensic science 60th annual scientific meeting, AAFS, Washington, DC, 2008

Hush NS, Woolsey IS (1974) Optical and electron-spin resonance-spectra of cobalt complexes related to vitamin-B12. J Chem Soc Dalton Trans 1:24–34

Jamieson JA, Taylor CG, Weiler HA (2006) Marginal zinc deficiency exacerbates bone lead accumulation and high dietary zinc attenuates lead accumulation at the expense of bone density in growing rats. Toxicol Sci 92(1):286–294

Lea DW, Pak DK, Spero HJ (2000) Climate impact of late quaternary equatorial Pacific sea surface temperature variations. Science 289:1719–1724

LeGeros RZ (2002) Properties of osteoconductive biomaterials: calcium phosphates. Clin Orthop Relat Res 395:81–98

LeGeros RZ, LeGeros JP (1984) Phosphate minerals in human tissue. In: Nriagu JO (ed) Phosphate minerals. Springer, New York, pp 351–395

Mann S (2001) Biomineralization: principles and concepts in bioinorganic materials chemistry. Oxford University Press, New York, p 198
Marcus R (1991) Skeletal aging – understanding the functional and structural basis of osteoporosis. Trends Endocrinol Metab 2:53–58
Nielsen SP (2004) The biological role of strontium. Bone 35:583–588
Pasteris JD, Wopenka B, Valsami-Jones E (2008) Bone and tooth mineralization: why apatite? Elements 4:97–104
Preston AM, Dowdy RP, Preston MA, Freeman JN (1976) Effect of dietary chromium on glucose-tolerance and serum-cholesterol in guinea-pigs. J Nutr 106:1391–1397
Puzas JE, Sickel MJ, Felter ME (1992) Osteoblasts and chondrocytes are important target-cells for the toxic effects of lead. Neurotoxicology 13:783–788
Rey C, Collins B, Goehl T, Dickson IR, Glimcher MJ (1989) The carbonate environment in bone-mineral – a resolution-enhanced Fourier-Transform Infrared-Spectroscopy Study. Calcif Tissue Int 45:157–164
Rey C, Shimizu M, Collins B, Glimcher MJ (1990) Resolution-enhanced Fourier-Transform Infrared-Spectroscopy Study of the environment of phosphate ions in the early deposits of a solid-phase of calcium-phosphate in bone and enamel, and their evolution with age. 1. Investigations in the V4 PO4 domain. Calcif Tissue Int 46:384–394
Rey C, Hina A, Tofighi A, Glimcher MJ (1995a) Maturation of poorly crystalline apatites: chemical and structural aspects in vivo and in vitro. Cells Mater 5:345–356
Rey C, Miquel JL, Facchini L, Legrand AP, Glimcher MJ (1995b) Hydroxyl-groups in bone-mineral. Bone 16:583–586
Roberts JE, Bonar LC, Griffin RG, Glimcher MJ (1992) Characterization of very young mineral phases of bone by solid-state P-31 magic angle sampling spinning nuclear-magnetic-resonance and x-ray-diffraction. Calcif Tissue Int 50:42–48
Rosenthal Y, Lear CH, Oppo DW, Linsley BK (2006) Temperature and carbonate ion effects on Mg/Ca and Sr/Ca ratios in benthic foraminifera: *Aragonitic* species *Hoeglundina elegans*. Paleoceanography 21:14
Rudnick RL, Gao S (2003) Composition of the continental crust. Treatise Geochem 3:1–64
Skinner HCW (2005) Biominerals. Mineral Mag 69:621–641
Sosdian S, Gentry DK, Lear CH, Grossman EL, Hicks D, Rosenthal Y (2006) Strontium to calcium ratios in the marine gastropod *Conus ermineus*: growth rate effects and temperature calibration. Geochem Geophys Geosyst 7:Q11023
Spadaro D, Gullino ML (2005) Improving the efficacy of biocontrol agents against soilborne pathogens. Crop Prot 24:601–613
Spadaro JA, Becker RO, Bachman CH (1970) The distribution of trace metal ions in bone and tendon. Calcif Tissue Res 6:49–54
Sprauten M, Darrah TH, Campbell ME, Hannigan R, Cvancarova M, Beard C, Haugnes H, Peterson D, Fossa SD, Oldenburg J, Travis LB (2012) Impact of long-term serum Platinum-concentrations on neuro- and ototoxicity in cisplatin-treated survivors of testicular cancer. J Clin Oncol 30(3):300–307
Stoll HM, Schrag DP (1998) Effects of quaternary sea level cycles on strontium in seawater. Geochim Cosmochim Acta 62:1107–1118
Stoll HM, Schrag DP, Clemens SC (1999) Are seawater Sr/Ca variations preserved in quaternary foraminifera? Geochim Cosmochim Acta 63:3535–3547
Taylor SR, McLennan SM (1995) The geochemical evolution of the continental crust. Rev Geophys 33:241–265
Tidswell HK, Innes JF, Avery NC, Clegg PD, Barr ARS, Vaughan-Thomas A, Wakley G, Tarlton JF (2008) High-intensity exercise induces structural, compositional and metabolic changes in cuboidal bones – findings from an equine athlete model. Bone 43:724–733
Tong W, Glimcher MJ, Katz JL, Kuhn L, Eppell SJ (2003) Size and shape of mineralites in young bovine bone measured by atomic force microscopy. Calcif Tissue Int 72:592–598
Weisskopf MG, Myers G (2006) Cumulative effect of lead on cognition – is bone more revealing than blood? Neurology 67:1536–1537

Index

P. Censi et al. (eds.), *Medical Geochemistry: Geological Materials and Health*, DOI 10.1007/978-94-007-4372-4,